USGS
science for a changing world

DOE/ID-22194

Prepared in cooperation with the U.S. Department of Energy

Hydraulic Characteristics of Bedrock Constrictions and an Evaluation of One- and Two-Dimensional Models of Flood Flow on the Big Lost River at the Idaho National Engineering and Environmental Laboratory, Idaho

Scientific Investigations Report 2007–5080

U.S. Department of the Interior
U.S. Geological Survey

View looking downstream through the site 2 constriction in the Big Lost River, about 2.5 miles downstream of the diversion dam, Idaho National Engineering and Environmental Laboratory, Idaho (photograph taken on May 31, 2006). Measured flow was 10 m^3/s on May 31, 2006. Water-surface elevation for this flow was measured on July 11, 2006.

Cover: View looking downstream through the site 2 constriction in the Big Lost River, about 2.5 miles downstream of the diversion dam, Idaho National Engineering and Environmental Laboratory, Idaho (photograph taken on July 19, 2000).

Hydraulic Characteristics of Bedrock Constrictions and an Evaluation of One- and Two-Dimensional Models of Flood Flow on the Big Lost River at the Idaho National Engineering and Environmental Laboratory, Idaho

By Charles Berenbrock, Joseph P. Rousseau, and Brian V. Twining

Prepared in cooperation with the
U.S. Department of Energy

Scientific Investigations Report 2007–5080

U.S. Department of the Interior
U.S. Geological Survey

U.S. Department of the Interior
DIRK KEMPTHORNE, Secretary

U.S. Geological Survey
Mark D. Meyers, Director

U.S. Geological Survey, Reston, Virginia: 2007

For sale by U.S. Geological Survey, Information Services
Box 25286, Denver Federal Center
Denver, CO 80225

For more information about the USGS and its products:
Telephone: 1-888-ASK-USGS
World Wide Web: http://www.usgs.gov/

Suggested citation:
Berenbrock, C., Rousseau, J.P., and Twining, B.V., 2005, Hydraulic characteristics of bedrock constrictions and an evaluation of one- and two-dimensional models of flood flow on the Big Lost River at the Idaho National Engineering and Environmental Laboratory, Idaho: U.S. Geological Survey Scientific Investigations Report 2007-5080, 206 p.

Contents

Contents—Continued

Figures

Figures—Continued

Figures—Continued

Tables

Conversion Factors and Datums

Conversion Factors

Multiply	By	To obtain
acre-foot (acre-ft)	1,233	cubic meter
cubic foot per second (ft^3/s)	0.02832	cubic meter per second
foot (ft)	0.3048	meter
foot (ft)	30.48	centimeter
foot per mile (ft/mi)	0.1894	meters per kilometer
inch (in.)	2.54	centimeter
inch per year (in/yr)	25.4	millimeter per year
mile (mi)	1.609	kilometer
pound (lb)	0.4536	kilogram
pound per foot-second [lb/)ft-s)]	14.594	Watt per square meter
square foot (ft^2)	0.0929	square kilometer
square mile (mi^2)	2.590	square kilometer
Watt per square meter (W/m^2)	1.0	meter-Newton per second per square meter

Temperature in degrees Fahrenheit (°F) may be converted to degrees Celsius (°C) as follows:

°C=(°F-32)/1.8

Datums

Vertical coordinate information is referenced to the North American Vertical Datum of 1988 (NAVD88).

Horizontal coordinate information is referenced to the North American Datum of 1983 (NAD83).

Elevation, as used in this report, refers to distance above the vertical datum.

A note about units used in this report: English units (ft-lb-s) are used for measures of elevation, vertical and horizontal distance, volumetric flow rate, flow velocity, flow depth, and stream power. SI units (m-kg-s) are used for measures of volumetric flow rate and particle size. Both types of units are used to facilitate comparisons with earlier work, to preserve the integrity of the original field-surveyed data, and to provide consistency between field survey units and topographic map units that were used in this and earlier cited studies.

Hydraulic Characteristics of Bedrock Constrictions and an Evaluation of One- and Two-Dimensional Models of Flood Flow on the Big Lost River at the Idaho National Engineering and Environmental Laboratory, Idaho

By Charles Berenbrock, Joseph P. Rousseau, and Brian V. Twining

Abstract

A 1.9-mile reach of the Big Lost River, between the Idaho National Engineering and Environmental Laboratory (INEEL) diversion dam and the Pioneer diversion structures, was investigated to evaluate the effects of streambed erosion and bedrock constrictions on model predictions of water-surface elevations. Two one-dimensional (1-D) models, a fixed-bed surface-water flow model (HEC-RAS) and a movable-bed surface-water flow and sediment-transport model (HEC-6), were used to evaluate these effects. The results of these models were compared to the results of a two-dimensional (2-D) fixed-bed model [Transient Inundation 2-Dimensional (TRIM2D)] that had previously been used to predict water-surface elevations for peak flows with sufficient stage and stream power to erode floodplain terrain features (Holocene inset terraces referred to as BLR#6 and BLR#8) dated at 300 to 500 years old, and an unmodified Pleistocene surface (referred to as the saddle area) dated at 10,000 years old; and to extend the period of record at the Big Lost River streamflow-gaging station near Arco for flood-frequency analyses. The extended record was used to estimate the magnitude of the 100-year flood and the magnitude of floods with return periods as long as 10,000 years.

In most cases, the fixed-bed TRIM2D model simulated higher water-surface elevations, shallower flow depths, higher flow velocities, and higher stream powers than the fixed-bed HEC-RAS and movable-bed HEC-6 models for the same peak flows. The HEC-RAS model required flow increases of 83 percent [100 to 183 cubic meters per second (m^3/s)], and 45 percent (100 to 145 m^3/s) to match TRIM2D simulations of water-surface elevations at two paleoindicator sites that were used to determine peak flows (100 m^3/s) with an estimated return period of 300 to 500 years; and an increase of 13 percent (150 to 169 m^3/s) to match TRIM2D water-surface elevations at the saddle area that was used to establish the peak flow (150 m^3/s) of a paleoflood with a return period of 10,000 years. A field survey of the saddle area, however, indicated that the elevation of the lowest point on the saddle area was 1.2 feet higher than indicated on the 2-ft contour map that was used in the TRIM2D model. Because of this elevation discrepancy, HEC-RAS model simulations indicated that a peak flow of at least 210 m^3/s would be needed to initiate flow across the 10,000-year old Pleistocene surface.

HEC-6 modeling results indicated that to compensate for the effects of streambed scour, additional flow increases would be needed to match HEC-RAS and TRIM2D water-surface elevations along the upper and middle reaches of the river, and to compensate for sediment deposition, a slight decrease in flows would be needed to match HEC-RAS water-surface elevations along the lower reach of the river.

Differences in simulated water-surface elevations between the TRIM2D and the HEC-RAS and HEC-6 models are attributed primarily to differences in topographic relief and to differences in the channel and floodplain geometries used in these models. Topographic differences were sufficiently large that it was not possible to isolate the effects of these differences on simulated water-surface elevations from those attributable to the effects of supercritical flow, streambed scour, and sediment deposition.

Introduction

The Big Lost River in southeastern Idaho flows onto the Idaho National Engineering and Environmental Laboratory (INEEL) and the Eastern Snake River Plain southeast of Arco, Idaho (fig. 1) and northward across the INEEL where it terminates in a series of playas and sinks. Flow in the river is extensively regulated to provide water for irrigation in the Big Lost River valley. Mackay Reservoir, a 38,500 acre-ft capacity reservoir (Williams and Krupin, 1984, p. 72) northwest of Mackay and about 45 mi upstream of the INEEL (fig. 1), and many large diversion channels are used to store and deliver irrigation water throughout the growing season. Although flooding at the INEEL is rare, it is important to accurately define these rare flood events so that planners and managers can evaluate the effects that flooding may have on facilities at the INEEL.

In 1996, the U.S. Geological Survey (USGS) completed a study for the U.S. Department of Energy (DOE) to estimate the 100-year peak flow for the Big Lost River at the INEEL. In that study, flow data from a streamflow-gaging station near Arco, upstream of the INEEL, were evaluated to estimate flood-flow frequency using a three-parameter log-Pearson Type III distribution as outlined in Guidelines for Determining Flood Flow Frequency, Bulletin #17B (Interagency Advisory Committee on Water Data, 1982). The resulting estimates for the 100-year flood for the Big Lost River near Arco produced very high levels of uncertainty at the upper and lower 95-percent confidence limits. The log-Pearson Type III analysis resulted in a computed 100-year peak flow of 5,480 ft^3/s with upper and lower 95-percent confidence limits of 11,600 and 3,150 ft^3/s, respectively (Kjelstrom and Berenbrock, 1996)[1]. The large uncertainty was attributed primarily to interference effects caused by upstream flow regulation on recorded peak flows at the streamflow-gaging station near Arco, Idaho.

To circumvent the influence of flow regulation on peak-flow measurements at the Big Lost River streamflow-gaging station near Arco, Kjelstrom and Berenbrock (1996) subsequently estimated the 100-year peak flow near Arco by adding flows estimated from flood-frequency curves for the Big Lost River at the Howell Ranch streamflow-gaging station (85 years of record; upstream of flow-regulation interference effects), and from Lower Cedar Creek (16 years of record; upstream of flow-regulation interference effects) to flows estimated using a regional-regression model applied to 22 ungaged subbasins in the Big Lost River drainage basin. Combined flows were routed downstream to Arco, and Dawdy's (1979) equation was used to calculate channel infiltration losses. Channel infiltration losses between Arco and the INEEL boundary were not subtracted from the 100-year peak flow estimate at Arco because these losses were assumed to be offset by runoff from local drainages between Arco and the INEEL. The resulting estimate for the 100-year peak flow using this approach was 7,260 ft^3/s. Upper and lower confidence limits for this estimate were not provided.

In 1999, the Bureau of Reclamation published a study of the Big Lost River (Ostenaa and others, 1999) that also included estimates of the 100-year peak flow at the INEEL. These estimates were derived from a combination of paleohydrologic data, streamflow-gaging data, and the results of a two-dimensional (2-D) numerical model that was used to simulate flood elevations for different assumed peak flows. Radiocarbon dating of buried charcoal remnants in terrace deposits adjacent to the main channel of the Big Lost River was used to establish the minimum age of floodplain terrain features that might be susceptible to inundation and erosion in the event of a large flood. The 2-D model was used to determine the flow needed to overtop and erode these dated surfaces. Long-term preservation of these surfaces was used as evidence that floods would need to exceed a limiting discharge for overtopping and erosion of these surfaces to occur. The age of the surface was used to define the minimum return period for the overtopping flood. These data were incorporated with data from the streamflow-gaging station near Arco to extend the period of record available for flood-frequency analysis. The resulting estimate of the 100-year peak flow was 2,910 ft^3/s, with upper and lower 97.5 percent confidence limits of 3,270 and 2,386 ft^3/s, respectively (Ostenaa and others, 1999, p. 53). The 1999 Bureau of Reclamation estimate for the 100-year peak flow is 40 percent lower than the regional-regression model estimate presented in the 1996 USGS study by Kjelstrom and Berenbrock (1996).

In 2000, the USGS conducted another study (Hortness and Rousseau, 2002) to reevaluate the approach used by Kjelstrom and Berenbrock (1996) to estimate the 100-year peak flow. In this study, the 100-year peak flow at the Howell Ranch streamflow-gaging station, derived from a log-Pearson Type III analysis based on 93 years of flow record, was routed downstream and the magnitude of this flow was adjusted to account for gains and losses in streamflow based on regression models of flow attenuation between the Howell Ranch gaging station and Mackay Reservoir, between Mackay Reservoir and Arco, and between Arco and the INEEL diversion dam. The resulting estimate using this approach was 3,750 ft^3/s, with upper and lower 95-percent confidence limits of 6,250 and 1,300 ft^3/s, respectively. Uncertainty estimates using this approach were determined by pooling the upper and lower 95-percent confidence limits for each of the three regression models with the uncertainty limits for the log-Pearson Type III analysis at the Howell Ranch gaging station.

[1]These values were revised in 2000 to correct an error in the earlier computations and to include additional data obtained since the 1996 study (n=47). Revised values are 4,990 ft^3/s for the 100-year peak flow, 9,590 ft^3/s for the upper 95-percent confidence limit, and 3,030 ft^3/s for the lower 95-percent confidence limit for the period 1947 through 1961, and 1965 through 2000 (n=51).

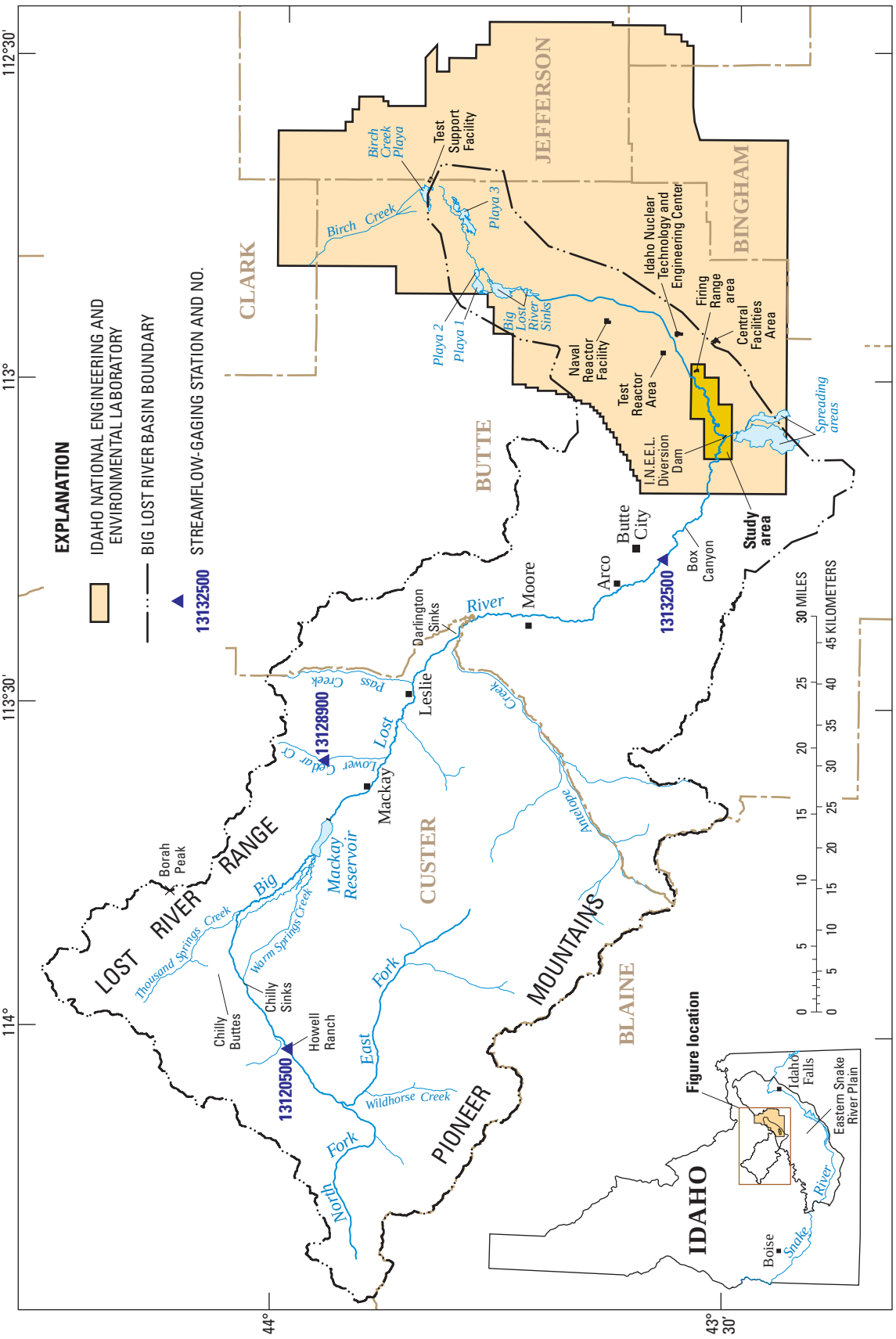

Figure 1. Location of the Big Lost River Basin and the Idaho National Engineering and Environmental Laboratory, Idaho.

In the 2-D model simulations conducted by Bureau of Reclamation, overtopping of dated surfaces was used as the basis for assigning a magnitude and minimum return period for paleofloods with sufficient stream power to erode the dated surfaces. These modeling efforts and their associated geomorphologic studies were a pioneering contribution to understanding the hydraulics of flood flow on the Big Lost River and to bridging data limitations to estimate the magnitude of floods with return periods that are much longer than the existing historic record will support.

In this study, the effect of bedrock constrictions and streambed scour on simulated water-surface elevations are evaluated. Bedrock constricts flow in the river at three locations in the study area. A field reconnaissance in 1999 indicated that the depth of the alluvial fill in the channel bed in some of these constrictions is as much as 4 ft. If this fill is erodible, as was suggested by the ease with which steel rods were driven into the channel bed to determine depth of fill, then the through-flow or discharge capacity of the constrictions for a given stage quite likely increases as flow increases, thus lowering the water surface below those simulated under conditions that assume a fixed-bed configuration. Visual evidence of bed scour inside the constrictions is readily apparent (cover photograph) indicating that flow velocities and shear stresses are sufficient to erode the channel at flows that historically have been less (70 m^3/s) than current estimates [205 m^3/s (Kjelstrom and Berenbrock, 1996); 82 m^3/s (Ostenaa and others, 1999); and 106 m^3/s (Hortness and Rousseau, 2002)] of the 100-year peak flow.

Purpose and Scope

Earlier computer models used to analyze flooding on the Big Lost River did not account for scouring of the channel bed during flood events. Both the USGS one-dimensional (1-D) implementation (Kjelstrom and Berenbrock, 1996) of the Water-Surface PROfile (WSPRO) model and the Bureau of Reclamation's two-dimensional (2-D) implementation (Ostenaa and others, 1999) of the Transient Inundation 2-Dimensional (TRIM2D) model (Walters and Casulli, 1998) assumed that the channel bed remained stable during all flows. In natural streams high flows are likely to scour the channel bed, particularly in areas where water is forced to flow through narrow constrictions at high velocities. Backwater effects that produce higher hydraulic gradients across the constrictions, and thus higher flow velocities with greater potential to scour the streambed locally, accompany higher flows in the constrictions. Scouring, particularly within the constrictions, increases the cross-section area available for flow, reducing or limiting the accumulation of backwater that would result from a given flow. Because streambed scour was not accounted for in the earlier TRIM2D model simulations, predictions of water-surface elevations may have underestimated the amount of flow needed to overtop and erode floodplain surfaces that were used to date paleofloods with return periods of 300 to 500 years and 10,000 years. These simulated flows along with their associated return periods were used to compute the magnitude of floods with return periods greater than 100 years and as long as 10,000 years (Ostenaa and others, 1999).

The purposes of the current study, the results of which are reported here, were (1) to evaluate the effects of channel constrictions and streambed scour and sediment deposition on simulated water-surface elevations in a reach of the Big Lost River downstream of the INEEL diversion dam, and (2) to compare these simulated water-surface elevations to those of the TRIM2D model that were used to determine the magnitude of peak flows needed to overtop and erode inset channel terraces dated at a minimum of 300 to 500 years old, and an unmodified Pleistocene surface dated at 10,000 years old.

Specific objectives of this study included:

1. Determining the effects of channel constrictions on flow velocities and backwater;

2. Determining water-surface elevations resulting from the separate and combined effects of changes in flow regime and streambed scour and sediment deposition during periods of high flow, and comparing these elevations to those estimated by Ostenaa and others (1999) for paleofloods with return periods of 300 to 500 years and 10,000 years; and

3. Determining flow velocities and stream powers associated with peak flows capable of overtopping and eroding floodplain terrain features that were used to establish paleoflood return periods of 300 to 500 years and 10,000 years in the study by Ostenaa and others (1999).

The scope of this study included:

1. Excavation of the river channel upstream, downstream, and within the confines of three key bedrock constrictions to determine depth to bedrock and composition of the alluvial fill;

2. Characterization of the armored surface layer in selected reaches of the river to determine the susceptibility of the streambed to scour;

3. High resolution definition of the channel and floodplain geometry to support 1-D modeling of flow through a reach of the river that includes all three bedrock constrictions of interest;

4. A field topographic survey of the land-surface elevations near the "saddle area" to determine the lowest elevation of the unmodified 10,000-year old Pleistocene surface;

5. Development of two 1-D flow models to simulate water-surface elevations and backwater effects at peak flows of 50, 100, 150, 187, and 200 m^3/s using the:

    (a) Current streambed elevation of the channel bed (HEC-RAS); and

(b) Streambed elevation under conditions of maximum possible scour (HEC-6);

6. Comparison of the results of the 1-D models (HEC-RAS and HEC-6) to those of the 2-D model (TRIM2D) that were used by the Bureau of Reclamation to establish the magnitude of paleofloods with minimum return periods of 300 to 500 years and 10,000 years (Ostenaa and others, 1999).

Description of Study Area

The Big Lost River is on the northwestern side of the Eastern Snake River Plain (fig. 1). The upper portion of the Big Lost River drainage basin trends northwest to southeast and is bordered by mountains along its northern, western, and southern boundaries. Southeast of Arco, Idaho, the Big Lost River flows onto the broad, undulating Eastern Snake River Plain, a northeast-trending structural basin about 200 mi long and 50 to 70 mi wide. Most of the INEEL overlies extensively fractured and highly permeable Holocene and Pleistocene basalt lava flows that are covered by a thin veneer of eolian and sedimentary deposits. As a result, all flow from the Big Lost River onto the Eastern Snake River Plain either evaporates or infiltrates into the ground. The Big Lost River terminates in a series of interconnected playas and the Big Lost River sinks near the northern end of the INEEL.

The Big Lost River drains about 1,410-mi^2 upstream of the USGS gaging station near Arco. The upper basin is mostly mountainous with a relatively flat, elongated valley varying in width between 2 and 10 mi. Elevations range from about 5,300 ft on the valley floor near Arco to more than 12,600 ft in the Lost River Range (fig. 1). The mean basin elevation is about 7,700 ft and the mean basinwide precipitation is about 20 in/yr. The mean elevation of the valley floor is about 6,000 ft and the mean precipitation over the valley floor is about 10 in/yr. Precipitation on the mountains, in the form of snow, supplies most water in the valley.

Mackay Reservoir, 30 mi upstream of Arco and 45 mi upstream of the boundary of the INEEL, stores water from the Big Lost River for irrigation. Before reaching the plain, most water stored in the reservoir and most tributary inflow between the reservoir and Arco are diverted for irrigation or lost by infiltration through the streambed. During many years, little or no flow is recorded at streamflow-gaging station 13132500, Big Lost River near Arco. When the water supply is adequate, the Big Lost River flows onto the INEEL and terminates in a series of playas in the northern part of the INEEL (fig. 1). A diversion dam (fig. 1) on the INEEL is used to route water away from the main channel of the Big Lost River to a series of interconnected spreading areas to prevent flooding of several downstream facilities—the Idaho Nuclear Technology and Engineering Center (INTEC), the Test Reactor Area (TRA), and the Naval Reactor Facility (NRF).

The study area covers a 1.9 mi reach that extends upstream of the Pioneer weir and canal diversion structures to a point about 2.3 mi downstream of the INEEL diversion dam (fig. 2). In the study area, the Big Lost River is an ephemeral stream with broad, sweeping meanders that typically are incised less than 20 ft into the surficial sediments and subcropping basalts (fig. 3).

The river channel is constricted at three points within the study area (fig. 2). At these constrictions, the river narrows considerably (45 to 27 ft at site 1; 57 to 17 ft at site 2; and 53 to 46 ft at site 3) and is confined by nearly vertical walls cut into basalt. At the site 2 constriction (cover photograph), the narrowest point of the river in the study area, the Big Lost River is less than 20 ft wide and more than 20 ft deep. At sites 1 and 3 constrictions, basalt subcrops also confine the river, but the constrictions at these sites are 10 to 30 ft wider than the constriction at site 2.

Streambed material in the study area consists of sand, pebbles, cobbles, and boulders, with lesser amounts of silt and clay-size material. The streambed is armored with lightly-cemented pebbles and cobbles except inside and near the constrictions. Bed material at the constriction sites consists of silts and very-fine to coarse sands containing pebbles dispersed in lenticular sand lenses. Large boulders, some up to several feet in diameter, are present in the streambed immediately upstream and downstream of the constrictions and probably originated from basalt breaking off the nearly vertical sides of the constrictions. Boulders and large cobble-size materials are conspicuously absent inside the constrictions. Trench excavations, (see section "Description of Trench Excavations") uncovered no evidence of buried boulder accumulations inside the constrictions, and no evidence of cementation of the channel fill underlying the armored surface layer in the study area. Alluvial deposits are considerably thicker near the modern-day Big Lost River floodplain. These deposits were derived from streams and deposited as channel, overbank, eolian, and lacustrine deposits (fig. 3) (Kuntz and others, 1994; Geslin and others, 1999).

Vegetation in the study area primarily is sagebrush and grass. Vegetation density increases near the river. Sparse stands of cottonwood and juniper grow along the river banks. Most of these trees are now dead because of infrequent streamflow and a range fire that occurred in May 2000.

Several man-made features are within or adjacent to the study area. The INEEL diversion dam is about 2 mi upstream of the study area (fig. 2). The diversion dam is a low to moderate height (about 25 ft high across the Big Lost River channel) earthen berm that was constructed in 1958 and enlarged in 1984 to divert water from the main channel of the Big Lost River to a series of off-channel depressions known locally as the spreading areas. The purpose of the diversion dam is to reduce the risk of flooding on downstream facilities along the Big Lost River. The combined storage capacity of the spreading areas is about 50,000 acre-ft.

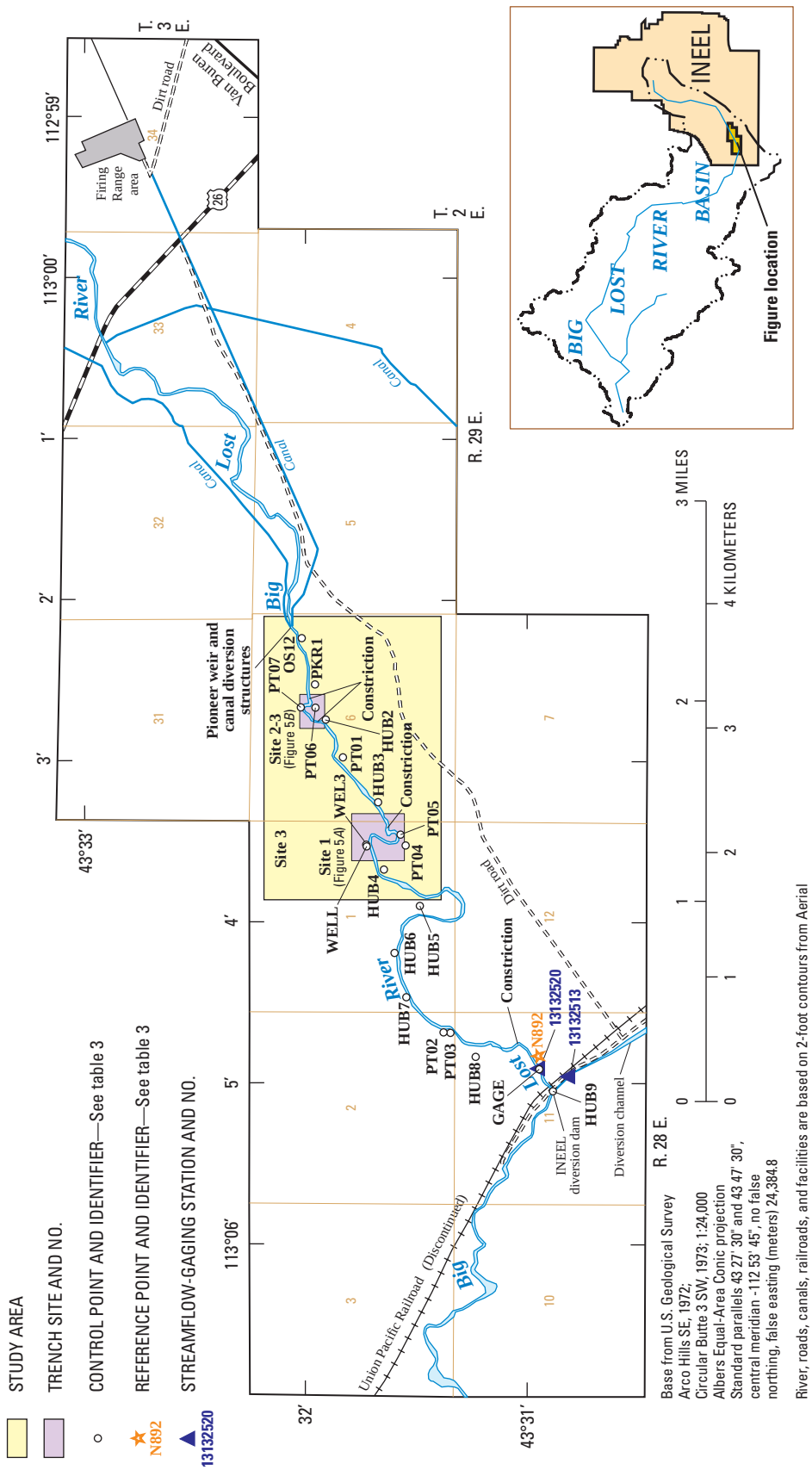

Figure 2. General location of study area, constrictions, trench sites, reference points, control points, and streamflow-gaging stations on the Big Lost River, Idaho National Engineering Environmental Laboratory, Idaho.

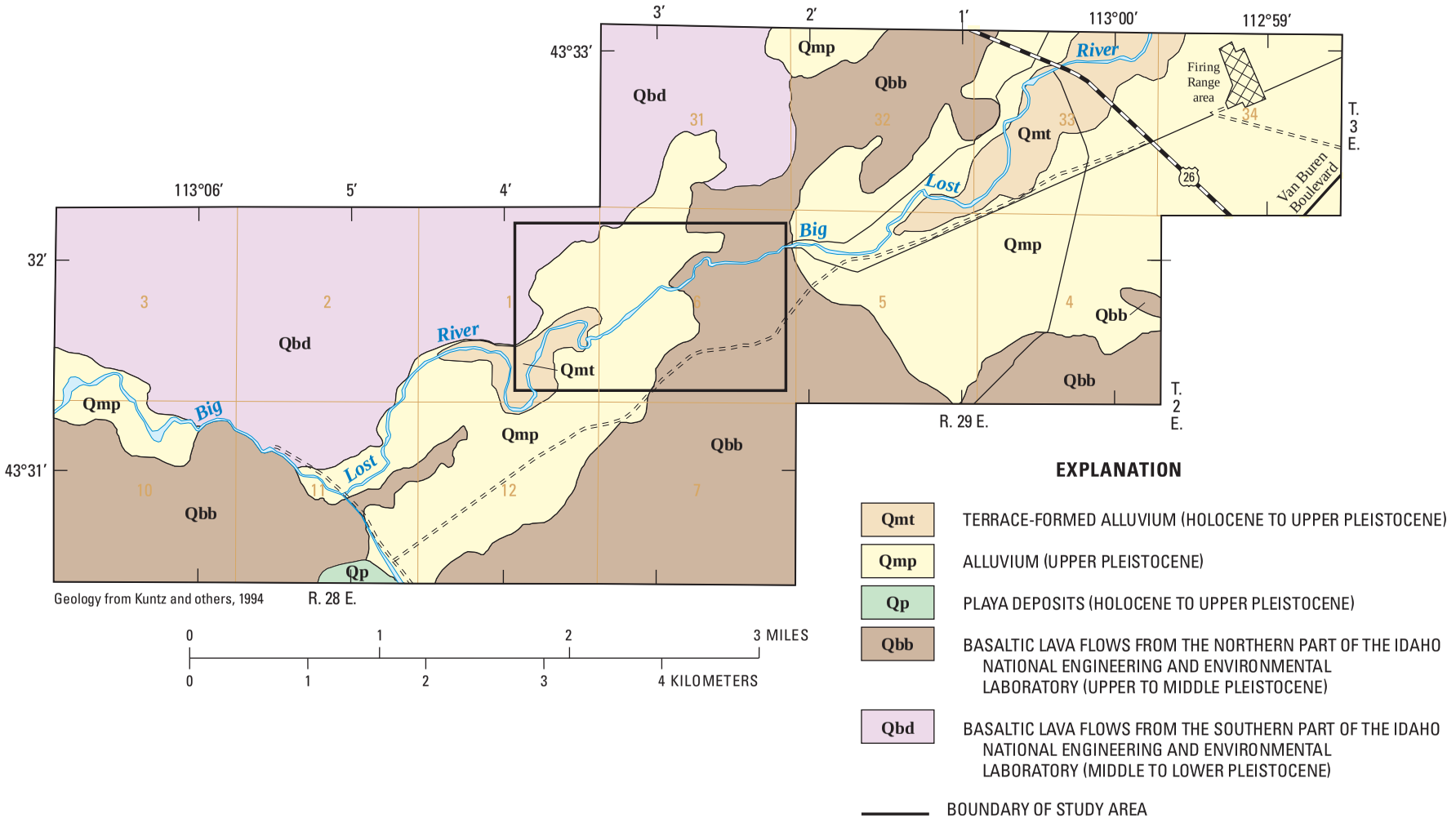

Figure 3. Generalized geology in the vicinity of the study area, Idaho National Engineering and Environmental Laboratory, Idaho.

Two culverts, with manually operated control valves, are used to regulate flow through the diversion dam. The culverts are corrugated circular steel, 6 ft in diameter and about 150 ft long. With the gated control valves completely open, the combined open-culvert through-flow capacity is about 1,200 ft^3/s (Berenbrock and Doyle, 2003, p. 17-18). All flows in excess of 1,200 ft^3/s are automatically routed into a diversion channel that conveys the water away from the main river channel into the spreading areas. Additional regulation of downstream flow is accomplished by closing the gated control valves which forces more water to flow from the main channel into the diversion channel. Another pair of circular corrugated culverts is immediately downstream of the diversion dam under an abandoned railroad crossing. These culverts are about 6 ft in diameter and about 75 ft long, with no control devices.

During the early 1940s, farmers constructed a wooden bridge (Brenda Pace, Bechtel BWXT Idaho, oral commun., 2004) with cement wingwalls across the basalt constriction at site 2, about 3.6 mi downstream of the INEEL diversion dam. The wingwalls were placed on basalt above the erodible banks leading into the constriction and are the only remaining remnants of the bridge (cover photograph).

A concrete weir with twin control structures was constructed at the downstream end of the study area to divert water to canals on both sides of the river. The weir, control structures, and canals were constructed for irrigation before the inception of the INEEL in 1949, and have since been abandoned. The weir has deteriorated and mostly fallen apart. The control structures also have deteriorated but probably could channel water to the adjoining canals; however, the canals have been filled in at their heads and have been breached in many other places to prevent water from flowing in them. The canal north of the river is about 20 mi long, intersects the TRA, goes around the NRF, and ends at playa 1. The canal south of the river is about 5 mi long, intersects the Firing Range area, and ends at the river upstream of INTEC. These canals generally parallel the river downstream (figs. 1 and 2).

Previous Investigations

Many studies of the water resources of the Big Lost River have been conducted over the past 100 years. Earlier investigators primarily were concerned with base flows, mean annual runoff, and basin yield. Wright (1903) reported on the effects of irrigation on gains and losses in the Big Lost River. Stearns and others (1938) estimated surface- and ground-water outflows from the Big Lost River Basin as part of a study of the geology and ground-water resources of the Eastern Snake River Plain. Crosthwaite and others (1970) estimated surface-water outflows from 44 subbasins in the Big Lost River Basin.

Several other reports describe flooding or the probability of flooding in the Big Lost River Basin. The U.S. Army Corps of Engineers (1967) reported on the extent of flooding along the Big Lost River in 1967 and on antecedent conditions in the basin leading up to the flood event. The U.S. Army Corps of Engineers (1991) also presented information on flood mitigation options available for the Big Lost River Basin. Carrigan (1972), Druffel and others (1979), Nobel (1980), and Koslow and Van Haaften (1986) examined the probable hydrologic effects of flooding arising from a hypothetical failure of Mackay Dam. Estimates of the attenuated peak flow resulting from a failure of Mackay Dam ranged from 45,000 ft^3/s (Koslow and Van Haaften, 1986) to about 54,000 ft^3/s (Druffel and others, 1979) 45 mi downstream at the western boundary of the INEEL. Rathburn (1989) presented evidence for a late Pleistocene glacial-lake-outburst paleoflood with an estimated flow of between 2 and 4 million ft^3/s in the Box Canyon area between Arco and the INEEL.

Lamke (1969) developed stage-discharge relations for the spreading-area diversion channel and the lower reaches of the Big Lost River on the INEEL. Bennett (1986) used the step-backwater computations model WSPRO to determine stage-discharge relations in the diversion channel and flow to the spreading areas. Berenbrock and Kjelstrom (1998) developed the first floodplain map of the Big Lost River at the INEEL using results from WSPRO. In the report for that study, Berenbrock and Kjelstrom indicated that their analysis should be considered preliminary and that additional data and a 2-D model would be needed to accurately estimate the extent of flooding. In refining the WSPRO model, Downs and others (1999) doubled the number of cross sections, and added three additional cross sections in the reach of the river between the INEEL diversion dam and Highway 26. Data for these additional cross sections were obtained from 2-ft topographic contour maps. Model simulation results from Downs and others (1999) were not compared to those of Berenbrock and Kjelstrom (1998) because different flows were used to define the extent of flooding.

Ostenaa and others (1999) developed a 2-D surface-water flow model (TRIM2D) for the study area to determine flow conditions needed to produce overtopping and erosion of Holocene floodplain terrain features (inset terraces) that were presumed to be at least 300 to 500 years old and an unmodified Pleistocene surface estimated to be 10,000 years old. The grid for this model consisted of 2,800 columns and 1,519 rows or about 4.2 million cells; only about 2.5 million cells were active and the remaining cells were dry (inactive). The size of each computational cell was 2 m (6.56 ft) long by 2 m wide (2×2m).

The study by Ostenaa and others (1999) determined that a flood flow only slightly larger than 110 m^3/s (3,884 ft^3/s) would initiate flow across an unmodified Pleistocene surface referred to as the “saddle area” north of the site 1 constriction (fig. 4); and that a flow of 150 m^3/s (5,297 ft^3/s) would severely erode this feature. Ostenaa and others (1999, p. 31) considered a flood of this magnitude to be the maximum flood flow since the late Pleistocene. Their study also indicated that

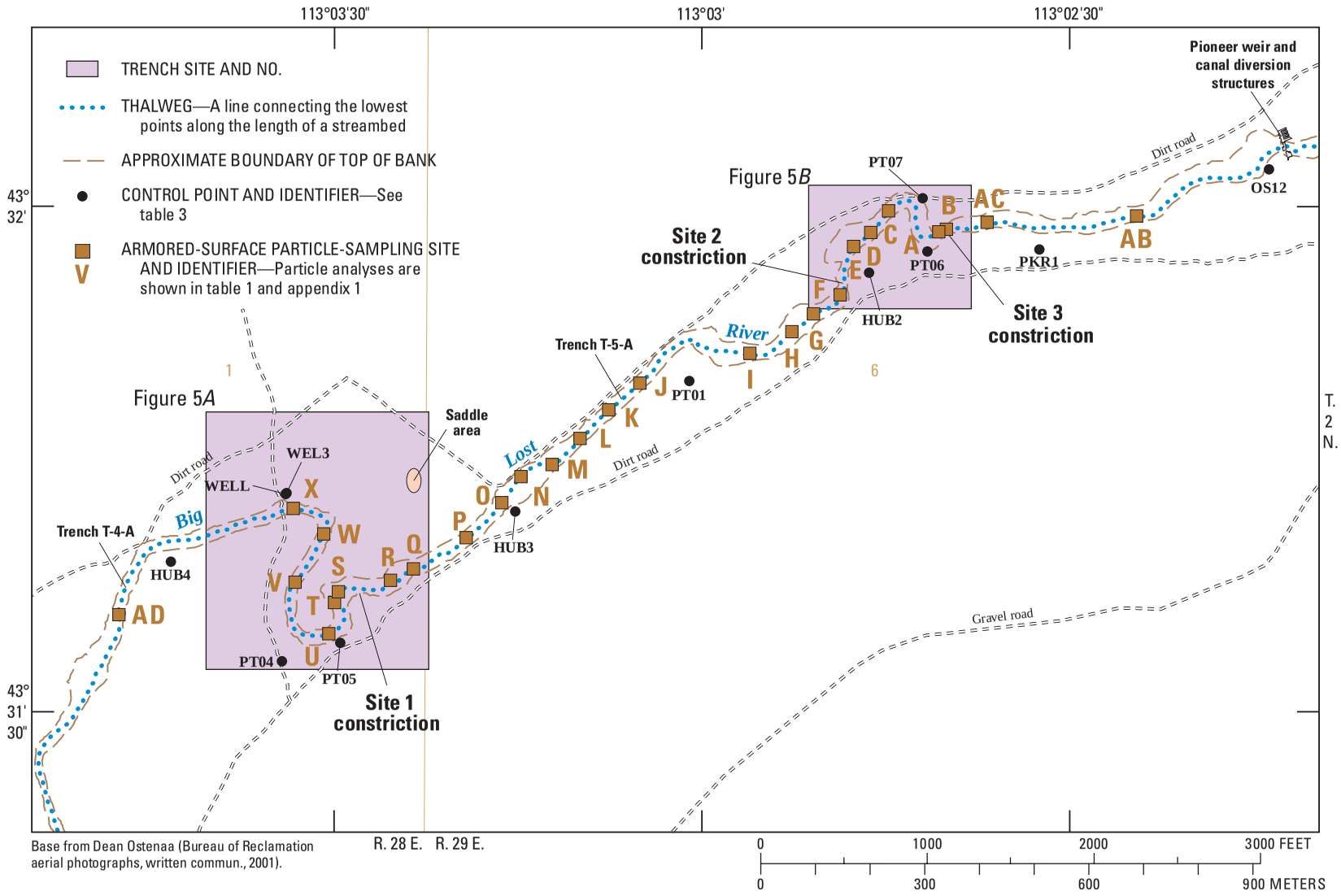

Figure 4. Location of the study area, constrictions, control points, surface-particle sampling sites, and trenches T-4-A and T-5-A on the Big Lost River upstream of the Pioneer diversion structures, Idaho National Engineering and Environmental Laboratory, Idaho.

a flow of 100 m^3/s (3,531 ft^3/s) was not sufficient to overtop the saddle area, but was sufficient to overtop and erode inset terraces, upstream and downstream of the saddle area, dated at 300 to 500 years old. The study by Ostenaa and others also included a simulated flood flow of 70 m^3/s (2,472 ft^3/s), which is approximately equivalent to the largest recorded peak flow [70.8 m^3/s (2,500 ft^3/s)] (Kjelstrom and Berenbrock, 1996; O'Dell and others, 2002, p. 194) on the Big Lost River near the Arco gaging station (13132500). Model simulation of this flow by Ostenaa and others (1999) using TRIM2D indicated that values of stream power were great enough to cause substantial erosion and modification of the river channel. At sites 1 and 2 constrictions, the resultant stream power was about 100 W/m^2 for a peak flow of 70 m^3/s (2,471 ft^3/s) (Ostenaa and others, 1999, appendix D, figs. D-25 and D-26). Stream powers of this magnitude can easily scour the sand-silt streambed at the sites 1 and 2 constrictions as demonstrated in the HEC-6 sediment-transport model simulations presented in the section "HEC-6 Simulation Results" of the current report. At the site 3 constriction, the stream power was about 25 W/m^2 and probably is great enough to scour the fine-grain channel fill at this location.

Streambed and Channel Characterization

In 2000, field data were collected to characterize the susceptibility of the armored surface layer and underlying streambed sediments to scour, and to define the cross-section geometry of the channel and floodplain for use in a 1-D surface-water flow model (HEC-RAS) and a 1-D surface-water flow and sediment-transport model (HEC-6). In 2001, two additional streambed sites, sites 4 and 5, were trenched and sampled.

Sampling of Armored Surface Layer

The armored surface layer was sampled at 30 locations between the INEEL diversion dam and the Pioneer diversion structures (labeled A through AD in figs. 4, 5*A*, and 5*B*). Armoring is not present everywhere in the study reach and is conspicuously absent immediately upstream, downstream, and within the three bedrock constrictions evaluated in this study. Sites selected for sampling included locations within channel-controlled and constriction-controlled sections of the river. Channel-controlled sections are defined as sections of the river that are dominated by friction and are not substantially affected by backwater. Constriction-controlled sections are defined as sections of the river that are strongly affected by backwater and minimally affected by friction. The hydraulic characteristics that distinguish channel-controlled from constricted-controlled sections, as defined in this study, are described in the section "Hydraulics of the Study Reach."

The armored surface layer was sampled using a method described by Wolman (1954) to determine the size distribution of sediments along the surface of the streambed. Lag deposits on gravel-bed streambeds commonly are larger in size than the underlying channel fill. These lag deposits tend to armor or protect the streambed from erosion under low- to moderate-flow conditions. Sampling consisted of measuring the intermediate axis of 100 individual rocks picked randomly from the channel bed at nominal 1-ft spacings on the basis of a grid system. Grid dimensions used in this study were 10×10 ft. After measuring, a particle-size distribution was developed to examine the range in particle size. The counting method gives a size distribution based on the number of rocks sampled. Particle-count size distributions are presented in appendix 1 (at back of report) and summarized in table 1. The median size (d_{50}) of particles from the streambed ranged from 6.21 to 48.7 mm, and generally d_{50} decreased downstream.

A plot of the d_{50} distribution of particle sizes from the upstream end to the downstream end of the study area is presented in figure 6. Ternary diagrams of the particle-size distribution of materials composing the armored surface layer are also shown in figure 6. The armored surface layer is composed predominately of granule- to cobble-size material (2 to 64 mm) with a large proportion of this material in the pebble- to cobble-size range (16 to 64 mm). This particle-size distribution for the armored surface layer (Folk, 1980) indicates that the river would be classified as a gravel-bed river.

Trench Excavation and Channel-Fill Sampling

Five sites along the Big Lost River were selected for trenching and sampling of the channel fill to determine the grain-size distribution of sediments beneath the armored surface layer (figs. 4, 5*A*, and 5*B*). Sediment samples were collected from trenches oriented perpendicular and parallel to the channel, or on terraces immediately adjacent to the channel. Twenty-two trenches were excavated at sites 1, 2, and 3. Excavations were made at these sites in both channel-controlled and constriction-controlled sections of the river. Sites 4 and 5 are in channel-controlled sections of the river. Site 4 provides information on the upstream boundary of the sediment-transport model, and site 5 provides channel-fill information in the reach between sites 1 and 2. Two trenches were excavated at sites 4 and 5.

A backhoe was used to excavate sediments to be sampled and to expose streambed depositional features. The trenches at each site were excavated to the top of basalt or to the capacity of the backhoe tractor, about 8 to 12 ft depending on the backhoe used. The backhoe was used to retrieve sediment samples from depths greater than about 4 ft. The objective of trenching was to provide a composite representation of the grain-size distribution of the channel fill below the armored surface layer, determine the degree of sediment consolidation, and determine the depth to bedrock where possible.

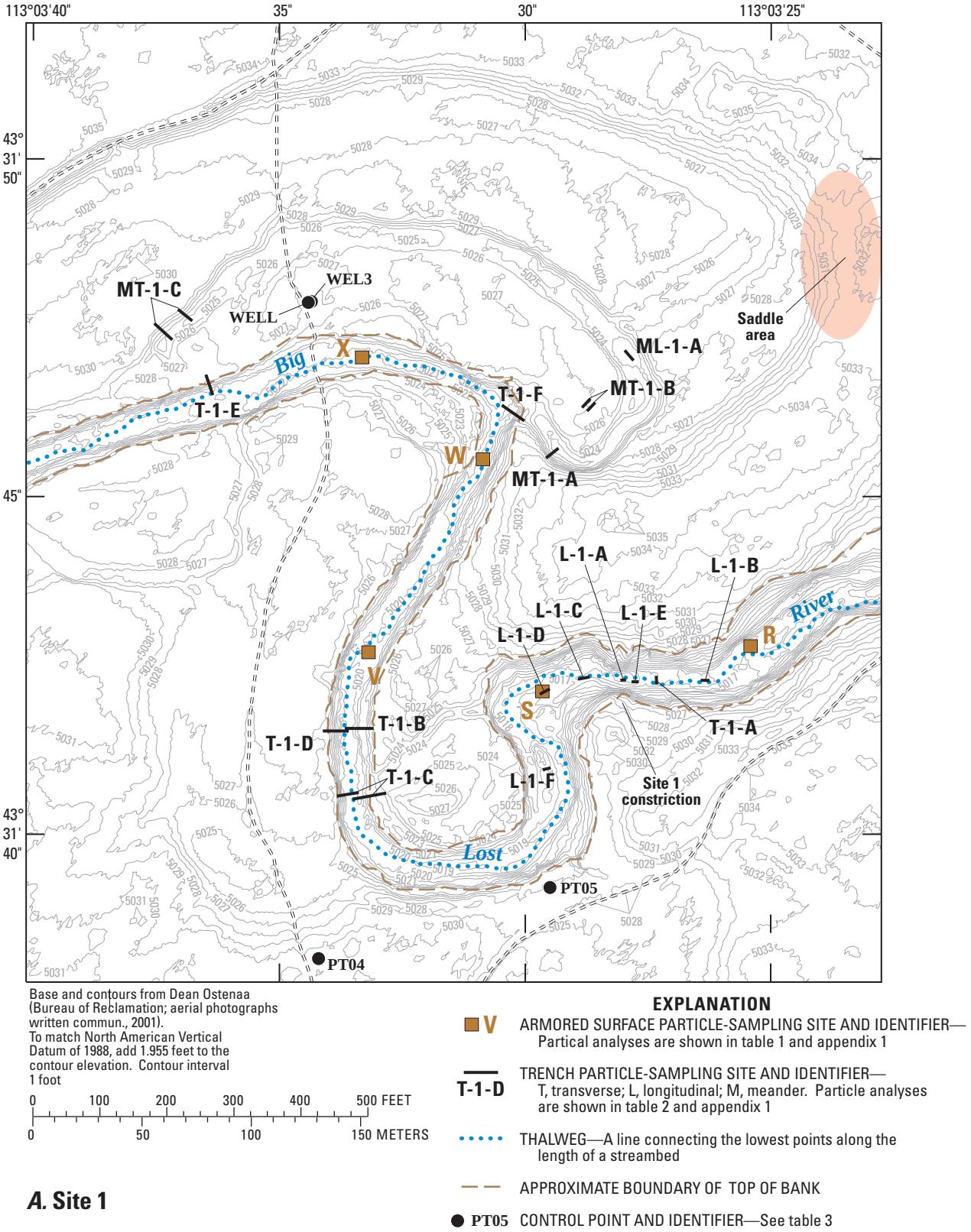

***A.* Site 1**

Figure 5. Location of particle-sampling sites at sites 1, 2, and 3 on the Big Lost River, Idaho National Engineering and Environmental Laboratory, Idaho.

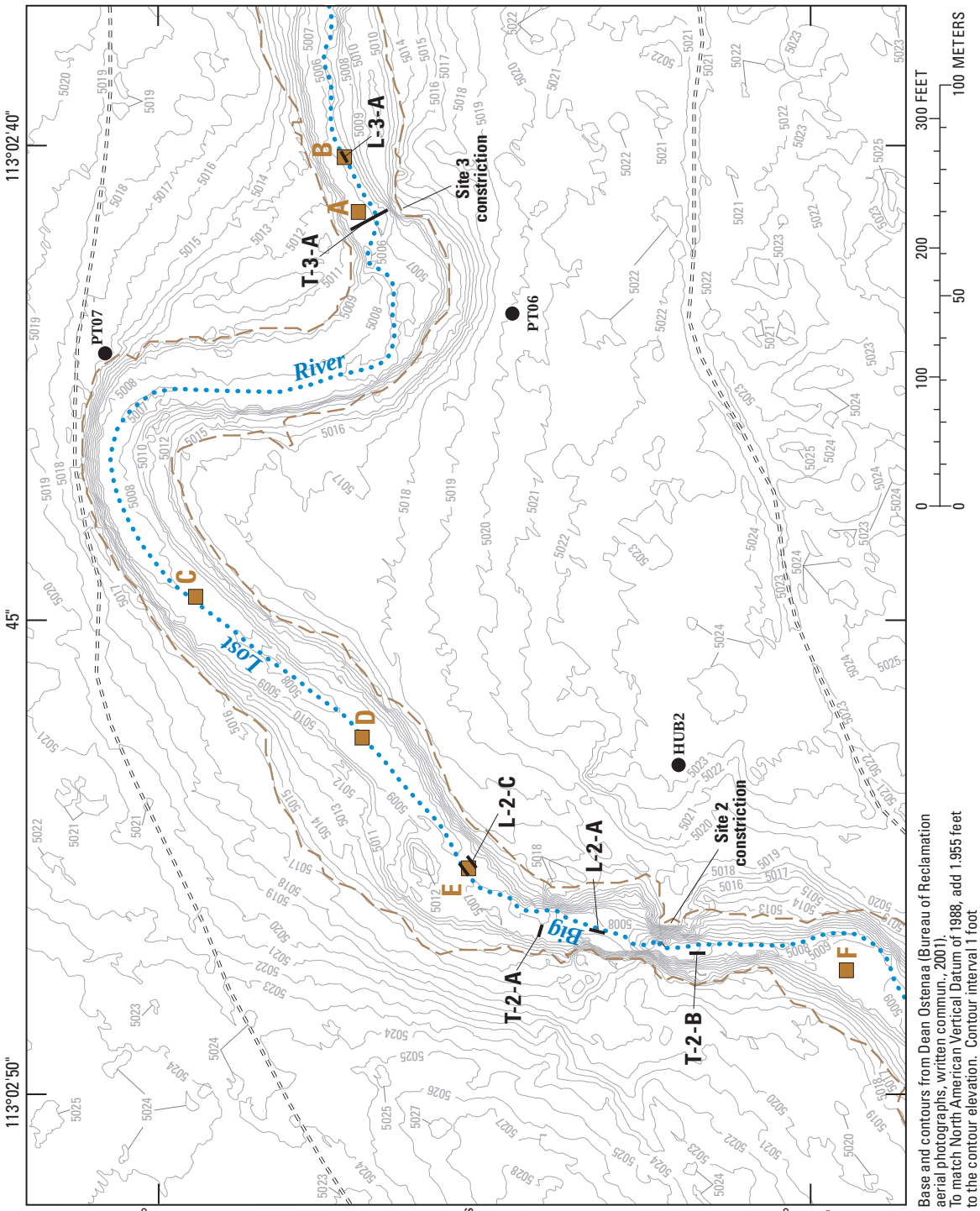

***B.* Sites 2 and 3**

Figure 5.—Continued.

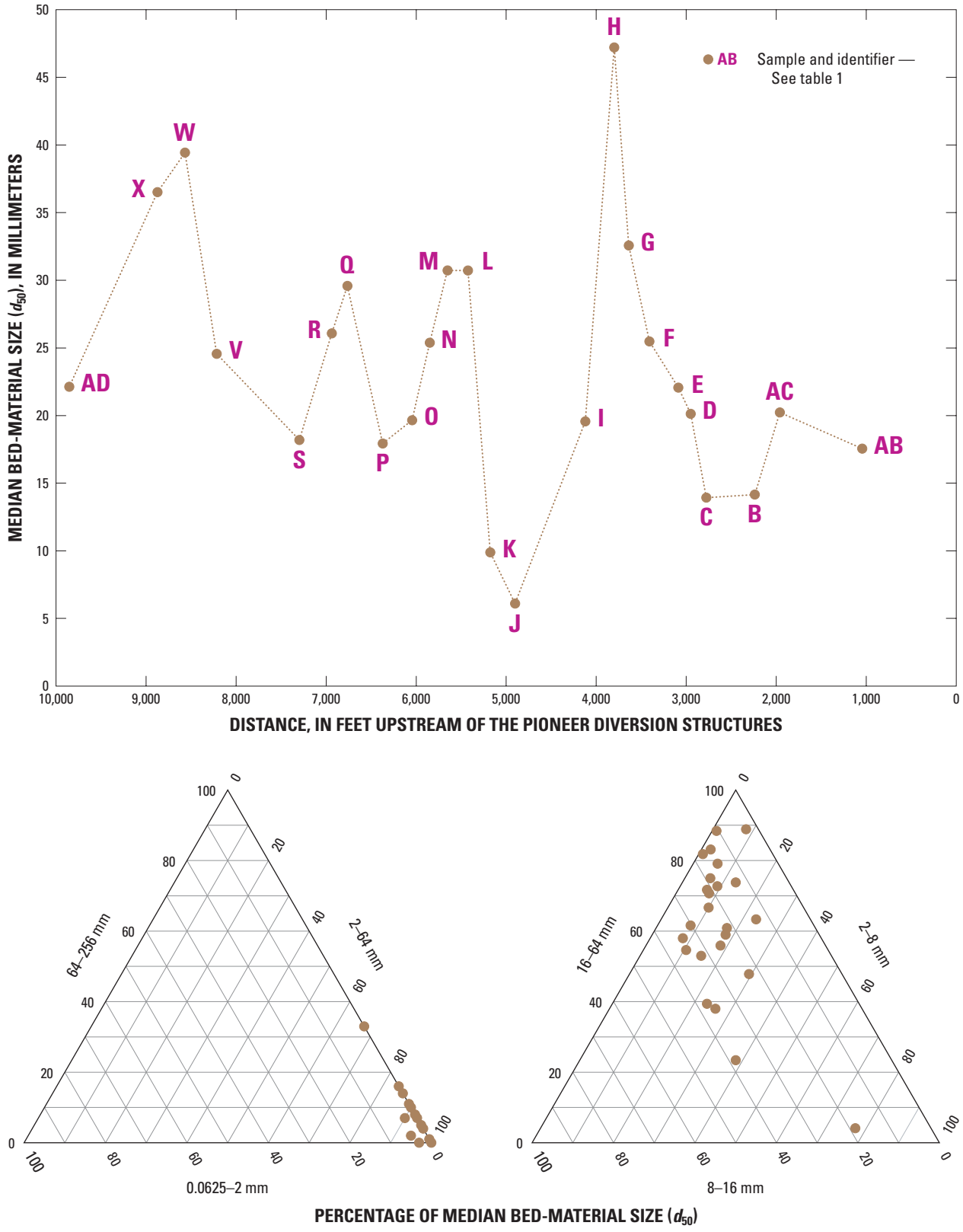

Figure 6. Median size (d_{50}) and ternary size distribution of selected samples collected from the armored surface layer on the Big Lost River upstream of the Pioneer diversion structures, Idaho National Engineering and Environmental Laboratory, Idaho.

Table 1. Particle-size characteristics of samples collected from the armored surface layer at selected sites on the Big Lost River upstream of the Pioneer diversion structures, Idaho National Engineering and Environmental Laboratory, Idaho.

[Location of sampling sites is shown in figures 4 and 5; and fig. 1-1 of appendix 1. Particle-size data are shown in appendix 1. **Particle-size diameter**: The letter *d* with numerical subscript denotes the particle diameter of the sample for which the percentage by count is finer than the designated diameter size. For example, d_{65} = 21.9 is the diameter of particles for which 65 percent of the sample is finer than 21.9 mm. ft, ft; mm, millimeter]

Sampling site identification No.	Distance upstream of Pioneer diversion structures (ft)	Particle-size diameter (mm)						Geometric standard deviation (mm) (σ_g)
		$d_{15.9}$	d_{35}	d_{50}	d_{65}	$d_{84.1}$	d_{90}	
A[1]	2,220	8.42	12.5	16.7	20.3	27.3	30.0	1.80
B	2,210	7.24	10.5	14.2	17.3	21.4	23.3	1.72
C	2,770	7.52	10.4	13.9	17.7	24.5	29.0	1.80
D	2,940	8.24	12.9	20.1	25.3	33.2	40.5	2.01
E	3,070	12.7	17.8	21.9	27.5	40.2	45.4	1.78
F	3,400	11.4	19.8	25.4	30.1	38.5	44.1	1.84
G	3,630	11.9	23.7	32.5	40.7	52.4	56.1	2.10
H	3,800	16.9	38.8	47.2	61.3	80.3	91.1	2.18
I	4,110	8.38	14.8	19.5	27.4	48.2	53.1	2.40
J	4,920	3.87	5.11	6.21	7.34	9.20	11.0	1.54
K	5,160	4.65	7.61	9.71	11.7	24.2	32.5	2.28
L	5,410	20.5	26.8	30.7	35.3	44.3	47.3	1.47
M	5,640	18.4	26.2	30.7	36.1	45.6	53.6	1.57
N	5,850	9.95	15.4	25.5	41.7	55.5	68.0	2.36
O	6,060	8.53	15.9	19.7	27.2	54.1	59.2	2.52
P	6,360	5.96	11.3	18.0	29.5	47.1	63.0	2.81
Q	6,760	11.6	20.6	29.6	37.7	55.3	64.1	2.18
R	6,930	12.4	20.9	25.9	34.4	48.1	51.3	1.97
S	7,280	8.61	13.2	18.2	22.1	38.8	48.1	2.12
T[2]	7,380	14.8	22.5	29.2	38.2	50.3	55.1	1.84
U[1]	7,580	16.9	35.6	44.7	53.1	66.1	74.1	1.98
V	8,200	11.2	18.4	24.5	30.7	39.2	43.1	1.87
W	8,550	9.78	22.1	39.5	46.7	62.8	67.1	2.53
X	8,850	17.2	26.5	36.5	46.2	62.1	67.2	1.90
Y	19,300	6.41	7.78	8.88	9.69	11.9	12.7	1.36
Z	19,500	14.7	29.6	43.2	50.2	65.1	77.1	2.10
AA	20,100	16.7	34.3	48.7	58.7	77.5	82.1	2.15
AB	1,040	10.1	14.7	17.6	21.9	26.3	31.1	1.61
AC	1,950	10.9	16.2	20.2	24.6	34.3	38.1	1.77
AD	10,200	5.67	15.6	22.2	26.8	50.3	59.5	2.98

[1]Sampled gravel bar.

[2]Sampled narrow chute of channel between bedrock in middle of channel.

The elevations of the streambed and the top of bedrock, where encountered, were surveyed at each trench site. Samples collected from the trenches were stored in buckets and bags and were labeled and recorded in a field book for later analysis. Each trench was given an identifier that corresponded to the site number and the trench designation within the site preceded by the letter T or L, corresponding to transverse or longitudinal, to describe the trench orientation in relation to the alignment of the stream channel; or the designation ML (meander longitudinal) or MT (meander transverse) to describe trenches excavated on a meander-scarred terrace adjacent to the active channel upstream of the site 1 constriction. At many of the trench sites stratified sedimentary layers were encountered and were individually sampled. The labeling scheme for these sites included a numerical designation to distinguish between individual layers and their sampling depths (table 2).

Table 2. Particle-size characteristics from sieve analysis of trench samples used in the HEC-6 model at sites 1 through 5 on the Big Lost River upstream of the Pioneer diversion structures, Idaho National Engineering and Environmental Laboratory, Idaho.

[**Sampling site identification No.**: Location of sampling sites is shown in figures 4 and 5. Letters 'L' or 'T' correspond to longitudinal or transverse to describe the trench orientation in relation to the alignment of the stream channel. Particle-size data are shown in appendix 2. **Particle-size diameter**: The letter *d* with numerical subscript denotes the particle-size diameter of the sample for which the percentage by count is finer than the designated diameter size. For example, d_{65} = 42.9 indicates that 65 percent of the sediment by weight is finer than 42.9. ft, ft; mm, millimeter; –, no data]

Sampling site identification No.	Distance upstream of Pioneer diversion structures (ft)	Sample depth (ft)	Particle-size diameter (mm)						Geometric standard deviation (mm) (σ_g)
			$d_{15.9}$	d_{35}	d_{50}	d_{65}	$d_{84.1}$	d_{90}	
SITE 1									
L-1-A1	7,140	1.0-5.5	1.28	9.87	22.3	42.9	108	149	9.19
L-1-B1	7,010	0.0-3.0	.76	2.58	8.52	16.5	34.6	43.4	6.75
L-1-C1	7,200	0.0-3.0	1.04	8.80	18.7	32.4	47.0	52.7	6.72
L-1-D1	7,270	0-1.0	.47	2.59	7.85	15.8	29.4	37.9	7.87
L-1-D2	7,270	1.0-1.5	.23	.29	.33	.37	.44	.46	1.37
L-1-D3	7,270	1.5-5.5	1.15	4.31	14.8	35.7	91.3	134	8.93
L-1-DC1	7,270	1.0-1.5	.08	.14	.20	.38	1.22	1.90	3.92
L-1-DC2	7,270	5.5	.07	.17	.52	1.13	2.48	3.23	6.03
L-1-DC3	7,270	3.5-4.0	.22	.48	.91	1.66	4.22	5.35	4.35
L-1-E1	7,120	0-4	.17	.44	1.27	4.14	27.3	68.0	12.7
T-1-A1	7,090	0-0.75	.21	.29	.33	.37	.44	.47	1.45
T-1-A2	7,090	0.75-4.0	.49	3.62	13.8	25.6	43.7	50.3	9.44
T-1-B1	8,080	[1]0.0-1.5	2.36	15.9	34.2	50.1	107	148	6.74
T-1-B2	8,080	[1]1.5-2.5	.28	.48	.60	.73	.95	1.15	1.84
T-1-B3	8,080	[1]2.5-4.0	.92	4.71	14.8	22.8	38.7	46.7	6.49
T-1-C1	7,960	[2]0.0-2.5	.08	.16	.31	.64	1.61	2.22	4.57
T-1-C2	7,960	[2]2.5-5.0	.26	.30	.34	.38	.45	.47	1.32
T-1-C3	7,960	[2]5.0-5.5	.07	.12	.15	.18	.24	.35	1.84
T-1-C4	7,960	[2]5.5-7.5	.88	17.0	26.2	36.4	49.6	54.5	7.51
T-1-C5	7,960	[2]7.5-10.0	3.17	21.5	35.5	44.1	58.1	63.2	4.28
T-1-C6	7,960	[1]1.0-3.0	.77	8.69	15.1	28.4	45.5	51.6	7.69
T-1-C7	7,960	[1]3.0-3.75	.12	.17	.21	.28	0.41	.46	1.85
T-1-C8	7,960	[1]3.75-5.5	.88	8.80	26.9	39.5	53.6	58.9	7.80
T-1-D1	8,050	[2]2.5-3.5	1.25	5.21	12.1	24.5	44.0	50.6	5.93
T-1-D2	8,050	[2]8.0	.30	.42	.54	.66	.84	.90	1.67
T-1-D3	8,050	[2]3.5-4.5	1.03	3.96	5.88	8.59	13.1	14.9	3.57
T-1-D4	8,050	[2]9.0-11.0	.70	5.30	12.5	21.0	37.6	45.8	7.33
T-1-D5	8,050	[2]8.0	.26	.31	.37	.43	.60	.76	1.52
T-1-DCLAY2	8,050	[3]6.0	.09	.27	.53	.98	2.06	3.10	4.84
T-1-E1	9,100	4.0-5.0	.64	5.05	10.8	19.0	35.9	44.5	7.49
SITE 2									
L-2-A1	3,190	0-0.7	0.18	0.28	0.34	0.42	0.75	1.19	2.04
L-2-A2	3,190	0.7-2.0	.39	1.14	1.93	2.69	4.09	5.46	3.22
L-2-A3	3,190	2.0-3.5	.51	.63	.74	.88	1.31	1.63	1.61
L-2-A4	3,190	3.5-4.5	.28	.56	1.10	2.69	8.08	11.9	5.39
L-2-B1	3,280	0-0.5	.16	.26	.32	.39	.51	.83	1.78
L-2-B2	3,280	0.5-2.5	.30	.41	.51	.64	.85	.93	1.69
L-2-B3	3,280	2.5-4.5	.53	1.74	4.26	14.8	28.2	35.6	7.26
L-2-C1	3,070	0-0.5	.73	3.65	6.66	9.92	14.9	19.1	4.51
L-2-C2	3,070	0.5-1.0	.36	.57	.70	.87	1.68	2.63	2.17
L-2-C4	3,070	2.0-2.5	.35	.99	1.64	2.73	6.61	9.33	4.35
T-2-A1	3,140	0.0-0.5	.23	.29	.34	.39	.46	.49	1.41
T-2-A2	3,140	0.5-2.0	.28	.33	.38	.44	.71	.98	1.60
T-2-A3	3,140	2.0-3.5	.51	.90	1.77	5.22	18.6	25.7	6.02
T-2-A4	3,140	3.5-4.5	.59	1.43	4.67	10.7	33.9	43.0	7.60
T-2-A5	3,140	4.5-7.7	.15	.27	.34	.43	.78	1.08	2.25
T-2-A6	3,140	6	.07	.13	.17	.22	.39	.48	2.32

Table 2. Particle-size characteristics from sieve analysis of trench samples from sites 1 through 5 on the Big Lost River upstream of the Pioneer diversion structures, Idaho National Engineering and Environmental Laboratory, Idaho.—Continued

[**Sampling site identification No**.: Location of sampling sites is shown in figures 4 and 5. Letters 'L' or 'T' correspond to longitudinal or transverse to describe the trench orientation in relation to the alignment of the stream channel. Particle-size data are shown in appendix 2. **Particle-size diameter**: The letter *d* with numerical subscript denotes the particle-size diameter of the sample for which the percentage by count is finer than the designated diameter size. For example, d_{65} = 42.9 indicates that 65 percent of the sediment by weight is finer than 42.9. ft, ft; mm, millimeter; –, no data]

Sampling site identification No.	Distance upstream of Pioneer diversion structures (ft)	Sample depth (ft)	Particle-size diameter (mm)						Geometric standard deviation (mm) (σ_g)
			$d_{15.9}$	d_{35}	d_{50}	d_{65}	$d_{84.1}$	d_{90}	
SITE 3									
L-3-A1	2,220	0-1.5	0.66	4.63	9.32	15.4	26.0	30.5	6.26
L-3-A2	2,220	0-1.5	.75	3.90	8.40	15.1	26.2	30.9	5.91
L-3-A3	2,220	1.5-1.6	.86	4.75	8.07	11.5	19.2	23.8	4.73
L-3-A4	2,220	1.5-1.6	.21	.71	1.72	3.75	10.3	13.8	7.03
L-3-A5	2,220	1.6-1.8	.15	.28	.39	.55	1.16	1.90	2.78
L-3-A6	2,220	1.6-1.8	.07	.11	.20	.75	2.92	4.02	6.66
L-3-A7	2,220	1.8-2.9	.13	.30	.49	1.58	3.85	5.16	5.41
L-3-A8	2,220	1.8-2.9	.58	1.00	1.66	3.18	9.24	12.6	4.00
L-3-A9	2,220	2.9-4.0	.73	2.02	4.38	8.39	15.2	20.9	4.55
L-3-A11	2,220	4.0	.11	.16	.20	.24	.42	0.53	1.98
L-3-A12	2,220	4.0	1.37	2.99	4.79	7.34	12.2	14.2	2.98
T-3-A1	2,270	1.5-1.75	.54	.70	.86	1.09	1.68	1.92	1.77
T-3-A2	2,270	1.75-2.25	.26	.31	.36	.42	.54	.73	1.45
T-3-A3	2,270	2.25-4.0	.58	1.50	2.60	4.87	12.5	16.7	4.65
T-3-A4	2,270	0-1.5	.38	1.95	4.25	7.60	14.2	19.7	6.12
SITE 4									
T-4-A1	9,840	1.0-5.0	1.20	6.16	13.9	27.8	87.3	130.0	8.53
SITE 5									
T-5-A1	4,960	0.0-5.0	0.93	5.43	12.3	23.1	42.4	49.4	6.75
T-5-A2	4,960	5.0	.10	.19	.31	.49	1.1	1.58	3.34

[1]Depth is measured from top of left bank where sample was taken.

[2]Depth is measured from top of right bank where sample was taken.

[3]Depth is measured from the streambed in the center of the channel where sample was taken.

Coarse-Grained Particle-Size Analysis

Grain-size analyses were conducted at the USGS Core Library in the Central Facilities Area (CFA) at the INEEL. The methods and procedures used for the grain-size analyses are outlined in the American Society of Testing Material's (ASTM) Manual on Test Sieving Methods (1985), the USGS Vancouver Sediment Laboratory's Quality Control and Quality Assurance Plan (Daniel J. Gooding, U.S. Geological Survey, written commun., 2000), and the American Society of Civil Engineers (ASCE) Manual on Sedimentation (1975).

Seventy-five sediment samples were collected from 24 trenches in the study area. Sixty-four of these samples (table 2) were used to classify sediment sizes that were used in the HEC-6 model. Samples from the meander-scarred terrace were not used for this purpose. Most samples were placed into bags, but some were collected in buckets to ensure representative sampling of the larger-size materials. Particles greater than (>) the opening of a 0.0625 mm sieve and less than (<) the opening of a 4 mm sieve are considered large-grained and are composed of very fine sands to very coarse sands (>0.0625 – <4 mm), pebbles (>4 – <64 mm), cobbles (>64 – <256 mm), and boulders (>256 mm). Particles less than 0.0625 mm are classified as fine-grained silts and clays. The samples were analyzed using the dry-sieve method described in the aforementioned references to determine the percent-finer-than and the cumulative percent-finer-than fractions, and the characteristic particle sizes.

The first step in the analysis was to dry the samples thoroughly and obtain a gross weight. All samples were open-air dried in trays for a minimum of 24 hours. Samples that contained semi-consolidated, or aggregated, fine-grained particles were oven dried to assist with moisture removal.

Large-volume bucket samples were split using a mechanical sample splitter to reduce the sample size to an appropriate volume for sieving. Particles greater than 64 mm were too large for the splitter and were hand split and placed into separate bins. Hand-split samples were weighed separately from the finer fraction and the weights added back to the cumulative weight of the sample to calculate weight percentages for each size fraction. Bagged sample volumes were small enough that they did not need to be split and the entire sample was run through the sieves. Aggregated fine-grained particles were broken apart using a mortar and pestle prior to sieving.

After drying and splitting, the samples were poured over the largest sieve (256 mm openings) and set in a mechanical shaker, which was then operated for 10 minutes (American Society of Civil Engineers, 1975, p. 412). Sieve sizes ranged from 256 to 0.0625 mm and were partitioned into 10 size classifications, ranging from silt and clay (<0.0625 mm) to boulder (>256 mm).

After shaking, each sieve containing sediments was weighed and the tare weights of the sieves subtracted from the combined weight of the retained sample and sieve. Results were entered into a spreadsheet programmed to (1) calculate the percent-finer-than fraction, cumulative percent-finer-than fraction, and the characteristic particle sizes, and (2) graph the cumulative percent-finer-than fraction and the distribution of sediment sizes. Particles ranged in size from about 100 to less than 0.0625 mm. Particles less than 0.0625 mm were collected in a closed sieve pan at the bottom of the sieve stack and were weighed.

If any residual aggregated particles were found after sieving, this was noted in the remarks column of the spreadsheet. If a sieve retained a small number of particles (less than or equal to 100), an approximate count of the particle number was noted in the remarks column of the spreadsheet. This procedure was implemented to ensure that the total volume of the sample was large enough to be representative of all particle sizes. For example, one or two large particles that together make up more than one-fourth of the sample weight indicate a sample with insufficient volume to accurately represent the particle-size distribution of the channel fill. During collection, if a sample contained large pebbles and cobbles, about 20 pounds of material were taken from the site to ensure that the sample was large enough to be representative of the site. Sieve analyses are presented in appendix 2 (at back of report).

The channel-fill material is composed primarily of particles ranging in size from medium sand to coarse pebble (appendix 2). The d_{50} of these samples ranges from 0.15 to 35.5 mm. The dominant material size is characteristic of a gravel-bed river.

Fine-Grained Particle-Size Analysis

A laser diffraction particle-size analyzer (Coulter Counter) was used to measure the silt and clay size fraction (<0.0625 mm) of one sample, a very fine-grained layer encountered at the base of trench T-5. Particle-size characteristics using the Coulter Counter were a mean grain size of 0.033 mm, a d_{50} of 0.0013 mm, a d_{10} of 0.0001 mm, and a d_{90} of 0.108 mm. The grain-size distribution indicates that this sample is classified as clay. Clay, identified on the basis of visual examination, also was encountered in several other trenches (L-1-D, L-1-E, T-1-B, T-1-D, L-2-C, and T-5-A; see "Description of Trench Excavations") near the contact of the channel-fill with the underlying bedrock. Visual examination of the samples and the underlying bedrock indicated that the clay was of allothogenic origin (transported) and was not a basalt-weathering product (authigenic).

Description of Trench Excavations

Site 1 Trenches

Site 1 is about 2.2 mi downstream of the INEEL diversion dam and includes a section of the river that is about 2,200 ft long. This S-curved section of the river is controlled by a bedrock constriction (site 1 constriction in figs. 2 and 5*A*) which generates considerable backwater for flows greater than about 100 m^3/s. Twelve trenches inside the main channel and four trenches on an alluvial terrace, formed by an abandoned river meander north of the main channel, were excavated and thirty-eight samples were collected. For descriptive purposes, trenches have been organized into four groups at site 1.

Working from the upstream side (left to right, fig. 5*A*), the two groups for the trenches inside the channel (T-1-E and T-1-F) and along the meander scar (MT-1-C, ML-1-A, MT-1-B, and MT-1-A) are designated groups 1 and 2, respectively. Group 3 (T-1-D, T-1-B, and T-1-C) and group 4 (L-1-F, L-1-D, L-1-C, L-1-A, L-1-E, T-1-A, and L-1-B) another 500 ft downstream, is near the site 1 basalt constriction. Sieve analyses for each trench are presented in appendix 2.

Group 1 (Trenches T-1-E and T-1-F)

Trenches T-1-E and T-1-F were excavated into the left alluvial bank and part way into the main channel. Materials excavated from these two trenches consisted of poorly sorted sands and pebbles, interspersed with silts that gave the material a very dirty appearance. Stratification in T-1-F consisted of discontinuous lenses of fine sand and silt interspersed in a matrix of poorly sorted sands and pebbles (note: no samples were collected from T-1-F). T-1-F is near a basalt exposure and bedrock was encountered at a depth of 12 ft in the main channel. T-1-E also was excavated to a depth of 12 ft, but bedrock was not encountered. Stratification at T-1-E was similar to that at T-1-F and consisted of poorly sorted sands and pebbles overlain by moderately sorted pebbles and granules in a coarse sand matrix. Very fine-grained, well-sorted silt (loess?) and sand deposits overlie the channel fill deposits along the banks of the channel at both trench sites.

Group 2 (Trenches MT-1-C, ML-1-A, MT-1-B, and MT-1-A)

Four trenches were excavated on a meander-scarred terrace north of the main channel. Several feet of very fine-grained, well-sorted silt (loess?) and sand overlie the alluvial fill at this location. Trenches MT-1-C and MT-1-B exposed a 2- to 5-ft thick cover of silt and fine sand underlain by poorly stratified, and poorly sorted sands, pebbles, and cobbles. Trench ML-1-A, in an inset channel, consisted of a 4-ft thick stratified sequence of poorly sorted sands and pebbles near the base of the trench, fining upward into alternating sequences of medium- to well-sorted coarse sands to well-sorted fine sand and silt. Trench MT-1-B, near the center of the meander-scarred terrace was unique. Material from this trench consisted of many well-stratified layers composed of well-sorted sand and pebble layers near the bottom, grading upward into layers of fine sand and silt interspersed with layers of well-sorted sand and pebbles, overlain by a 2.5-ft thick layer of silt (loess?) and fine sand. The material from this trench appeared exceptionally “clean” compared to that in the other trenches that were excavated on this meander scar. Trenches within this group were excavated to depths of 10 to 12 ft and bedrock was not encountered.

Group 3 (Trenches T-1-B, T-1-D, and T-1-C)

Trenches T-1-B and T-1-D were constructed separately (offset by 10 ft) and later joined to construct a composite lithologic cross section of the streambed fill (fig. 7*A*; note: lithologic descriptions based on field observations). Trench T-1-C, 100 ft downstream of T-1-B and T-1-D, consists of two overlapping trenches that span the entire active channel (fig. 7*B*; note: lithologic descriptions based on field observations). Clay, likely of allothogenic origin, was found along the top of the basalt bedrock in T-1-B and T-1-D (not shown in fig. 7*A*). Depths to bedrock in these trenches ranged from 3.5 (T-1-C) to 8 ft (T-1-B) below the streambed. Trench cross sections indicated a poorly stratified basal section composed of poorly sorted sands, pebbles, cobbles, and small boulders. Both the size and quantity of the cobble- and boulder-size material increased with depth, with the highest concentrations occurring near the bedrock contact. Discontinuous, well-sorted, fine- to medium-grained sand lenses were found just above the basal fill in both sets of trenches. These were overlain by poorly stratified sequences of moderately-sorted sands, pebbles and cobbles below the channel surface.

Thick deposits of loess (?), underlain by well-sorted sands and silty sands, form the banks above the active channel. A well-preserved animal bone and a large wood fragment (2-ft long and 1 to 2 in. in diameter; mountain mahogany?) were found in trench T-1-D at a depth of about 2.5 ft below the active channel (fig. 7*A*). Many more poorly preserved wood fragments were found interspersed in allothogenic clay deposits near the bedrock contact.

Group 4 (L-1-F, L-1-D, L-1-C, L-1-A, L-1-E, T-1-A, and L-1-B)

Seven trenches were excavated immediately upstream, downstream, and within the site 1 constriction (fig. 5*A*). Trench L-1-F was excavated in a gravel (pebble and cobble) bar upstream of a basalt subcrop that spans the entire width of the channel. The material from this trench consisted of well-sorted pebbles, cobbles, and small boulders overlain by a thin cover of sands, pebbles, and cobbles. The trench was excavated to a depth of 6 ft and bedrock was not encountered (note: no samples were collected from trench L-1-F). Trench L-1-D, 75 ft upstream of the site 1 constriction, was excavated to bedrock at a depth of 4 ft. Material from this trench consisted of a poorly sorted mixture of coarse sands, pebbles, cobbles, and small boulders overlain by well-sorted, stratified layers of fine sands and coarse sands mixed with pebbles. Clay, in contact with bedrock, was present at the base of the trench. Trench L-1-C, about 35 ft upstream of the site 1 constriction, was excavated to bedrock at a depth

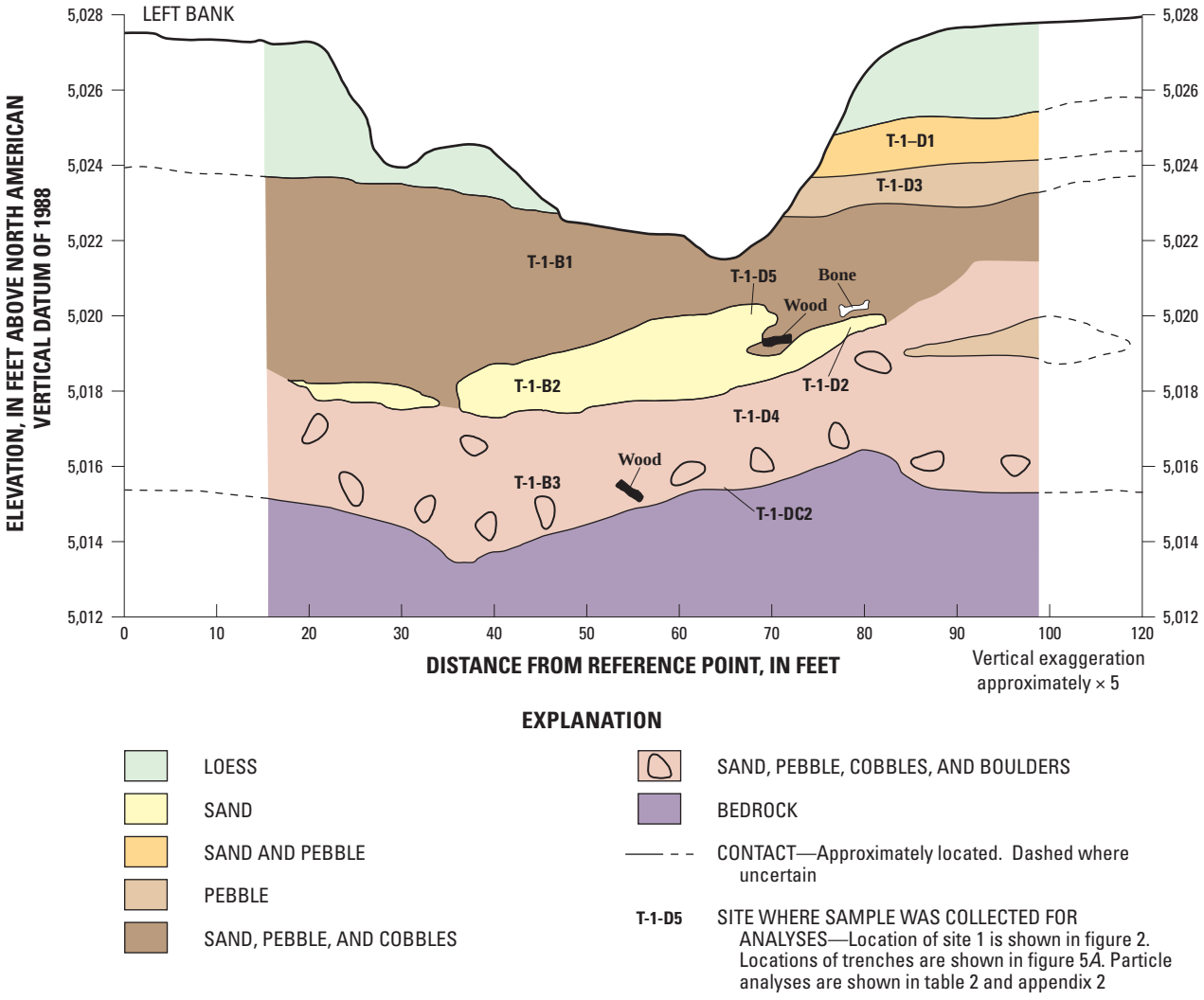

A. **Trenches T-1-B and T-1-D**

Figure 7. Lithology of trenches T-1-B, T-1-D, and T-1-C across the Big Lost River at site 1, Idaho National Engineering and Environmental Laboratory, Idaho.

of 3 ft. Material in this trench exhibited no stratification, and consisted of poorly sorted sands and pebbles. Trench L-1-A, within the site 1 constriction, was excavated to bedrock at a depth of 5.5 ft. No stratification was observed and material from this trench consisted of poorly sorted sands, pebbles, cobbles, and small boulders.

Three trenches, L-1-E, T-1-A, and T-1-B, 25, 80 and 100 ft downstream of the site 1 constriction, respectively, were excavated to bedrock ranging in depth from 3 to 4.5 ft. Bedding structure was absent in these trenches, and material from these trenches consisted of poorly sorted coarse sands, pebbles, and cobbles overlain by a 1-ft thick layer of well-sorted fine to coarse sand.

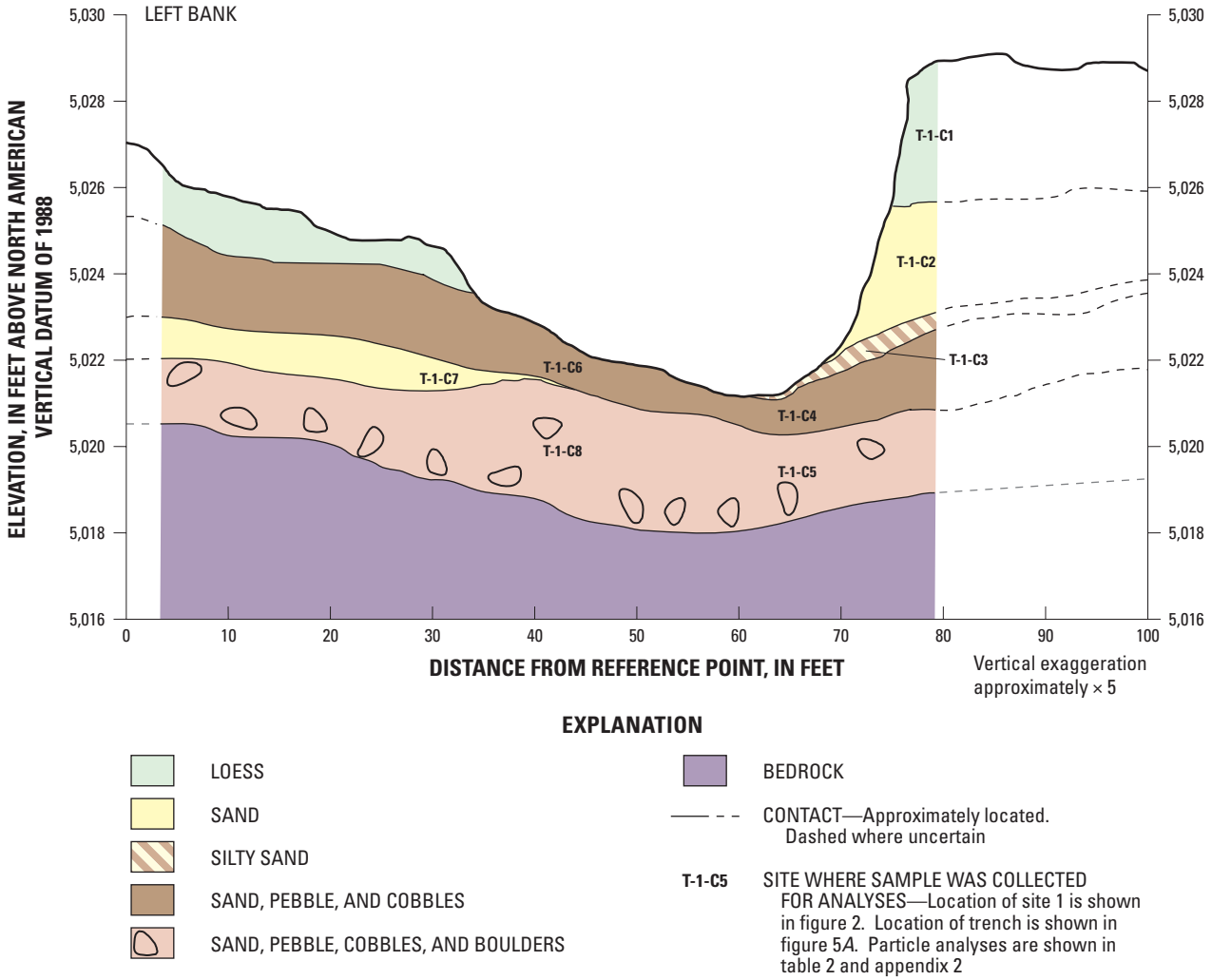

B. Trench T-1-C

Figure 7.—Continued.

Site 2 Trenches

The site 2 constriction is about 200 ft long and is at an old bridge site about 3.6 mi downstream of the INEEL diversion dam (figs. 2 and 5*B*). At this location, 4 trenches were excavated, 1 upstream and 3 downstream of the abandoned bridge site. Sixteen sediment samples were collected from multiple stratified layers in these trenches. The three downstream trenches all exhibited similar sediment stratification that differed appreciably from stratification that was observed in the upstream trench.

Working from the upstream side (left to right), the trench excavation site upstream of the basalt constriction is designated group 1. The three downstream trenches are designated group 2. Sieve analyses for each trench are shown in appendix 2.

Group 1 (T-2-B)

Trench T-2-B is 15 ft upstream of the old bridge abutments within the site 2 constriction. This trench was excavated to bedrock at a depth of 4.5 ft. Excavated material consisted of well-sorted fine to coarse sand with well-developed horizontal and cross-bedding stratification to a depth of 2.5 ft. A poorly sorted mixture of coarse sands and pebbles with no obvious bedding structure underlies these sands.

Group 2 (L-2-A, T-2-A, and L-2-C)

Three trenches, excavated downstream of the bridge constriction, range in depth from 2.5 to 7.7 ft. Trench L-2-A was excavated to bedrock at a depth of 5 ft. Material from

this trench consisted of alternating layers of well-sorted fine to medium sand interspersed with layers of coarse sand and granules, in turn overlying a basal layer of fine to coarse sand with pebble lenses near the bedrock contact. Trench T-2-A was excavated to bedrock at a depth of 7.5 ft. Material in this trench consisted of alternating fining-upward layers of poorly sorted sands, granules, and pebbles down to a depth of 4.5 ft, underlain by medium to coarse sands containing lenses of very-fine sand and silt. Trench L-2-C was excavated to bedrock at a depth of 2.5 ft. Material from this trench consisted of well-sorted medium sands and pebbles to a depth of 1 ft, overlying a 1-ft thick section of poorly sorted sands, pebbles, and small boulders, in turn overlying a well-sorted layer of clayey silt and sand. A fragment of a dummy artillery-shell casing was found at a depth of 1 ft in the L-2-C trench.

Site 3 Trenches

This trench site is at a basalt constriction about 3.4 mi downstream of the INEEL diversion dam (figs. 2 and 5*B*). At this site two trenches were excavated to depths of about 4 ft, and 16 alluvial horizons were sampled and analyzed. Trench T-3-A was excavated perpendicular to the channel and trench L-3-A was excavated parallel to the channel. Alluvial horizons indicated similar sedimentary features in both trenches. Just above bedrock, the basal deposits consisted of a poorly sorted mixture of sands and pebbles. A well-sorted, fine- to medium-grained sand layer was interbedded between poorly sorted sands and pebbles. This well-sorted, fine- to medium-grained sand lens increased in thickness toward the channel terrace and almost pinched out toward the channel thawleg. The channel surface deposits consisted of poorly sorted sands and pebbles with some cobbles present.

Site 4 Trenches

Trench T-4-A, about 2.0 mi downstream of the INEEL diversion dam, is in a channel-controlled reach of the river (fig. 4). This trench was excavated to a depth of 7.9 ft; bedrock was not encountered. The channel at this site is 43 ft wide and exhibits a well-developed, armored surface layer. One large-volume bulk sample was collected. Material in this trench consisted of a poorly sorted mixture of sands, pebbles, cobbles, and small boulders with no discernible stratification. Site 4 was selected to provide information needed to formulate the upstream sediment-boundary condition for the HEC-6 sediment-transport model.

Site 5 Trenches

Trench T-5-A, about 2.8 mi downstream of the INEEL diversion dam is in a channel-controlled section of the river (fig. 4). This trench was excavated to bedrock at a depth of 6.5 ft. Two representative samples were collected. From the channel surface to a depth of 5 ft, the alluvial deposits consisted of a poorly sorted mixture of sands, pebbles, cobbles, and small boulders. No armored surface layer was present in the channel at this location. Streambed material at the surface consisted of sand and small pebbles. Material in contact with bedrock consisted of a 1.5-ft thick layer of dense allothogenic clay. This trench site was selected to obtain streambed sediment information in a channel-controlled section of the river between sites 1 and 2.

Channel Surveys

The HEC-RAS and HEC-6 computer models, which were used to simulate water-surface and streambed elevations, require accurate representation of the channel and floodplain cross-section geometry. Channel and floodplain geometries were defined by a series of cross sections measured at variably spaced distances along lines oriented perpendicular to the direction of flow. Cross sections were surveyed in a local coordinate system using conventional surveying techniques and transformed from the local coordinate system to a common, geographically referenced coordinate system using global positioning system (GPS) data and a geographic information system (GIS) interface.

In September 2000, USGS personnel surveyed the Big Lost River from the Pioneer weir and canal diversion structures (fig. 2) to a point about 2 mi upstream. Seventy-six cross sections were surveyed (fig. 8). At each cross section, a tag line was stretched across the channel and held in place by wooden stakes to insure that the orientation of the measured section remained perpendicular to the direction of flow. Cross-section locations were placed closer together in areas near constrictions and large river bends. Sections within constrictions were spaced less than 50 ft apart, and sections in straight reaches were spaced several hundred feet apart. Each section also was located to best represent the hydraulic characteristics of that part of the river. The most downstream cross section, at the Pioneer weir and canal diversion structures, was assigned cross-section number 1 and numbering increased in an upstream direction for each section (note: figure 8 does not include cross sections 30 through 39 because of errors that were discovered in the field surveys for these cross sections. These missing cross sections were replaced with TIN-generated cross sections using a 1-ft contour map of the study area described in the section "TIN-Generated Cross Sections").

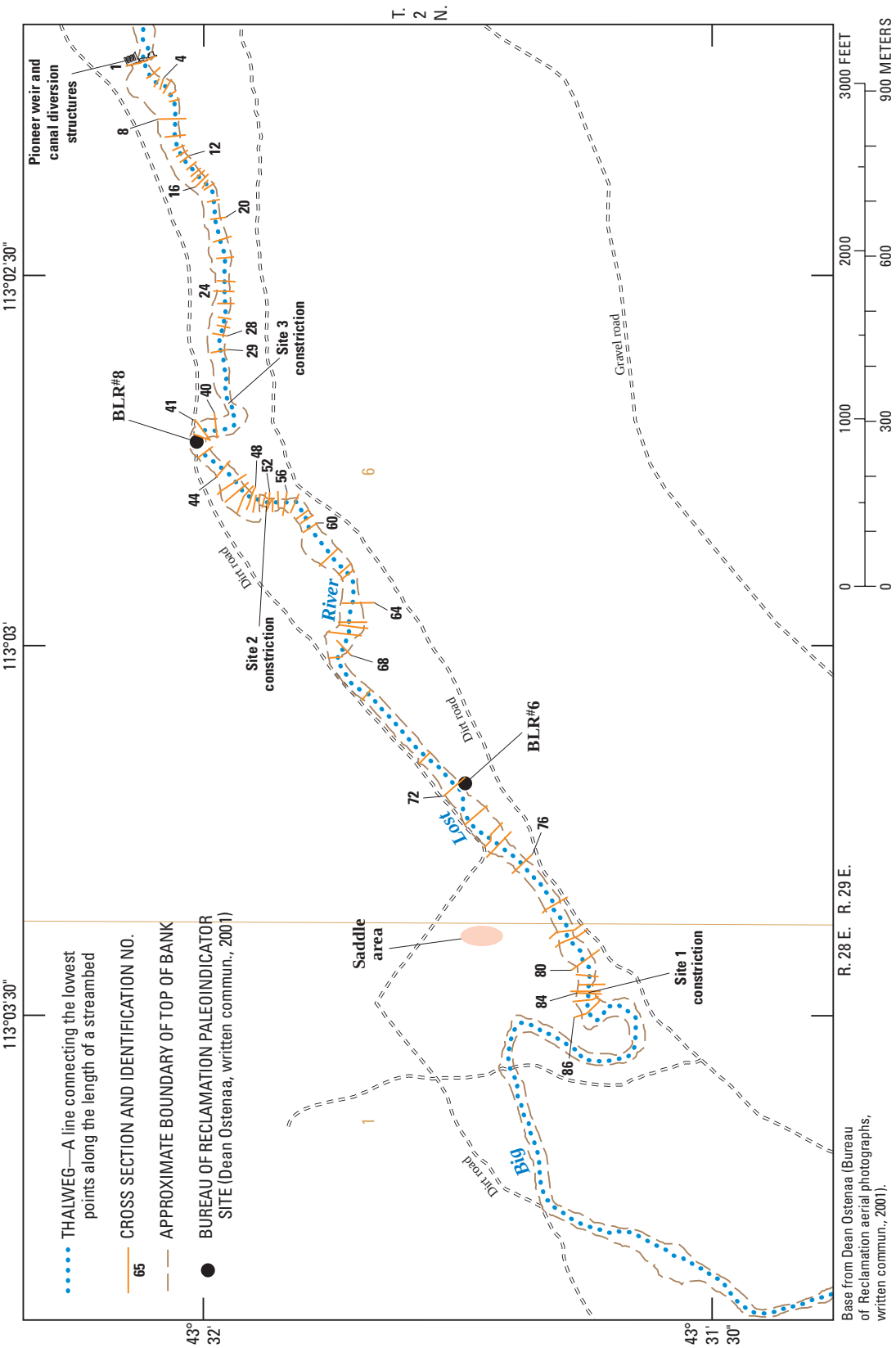

Figure 8. Location of field-surveyed cross sections on the Big Lost River upstream of the Pioneer diversion structures, Idaho National Engineering and Environmental Laboratory, Idaho.

Horizontal Referencing

All cross-section data were referenced to a common datum. Horizontal control was based on the North American Datum of 1983 (NAD 83), State Plane Coordinates, Idaho East Zone, in feet. Horizontal referencing of the cross sections and control points was accomplished using a differential GPS and a GIS interface. A GPS receiver (base station) was positioned at N892 (fig. 2), a well-documented survey-reference marker on the INEEL. A second roving GPS receiver was used to obtain coordinates at 20 additional control points between the INEEL diversion dam and the Pioneer diversion structures (fig. 2). For differential GPS, the GPS coordinates for the base station (N892) were compared with the known coordinates for the base station, and the differences inserted into the calculations for the roving GPS receiver. Both receivers must use the same satellites, and a minimum of four satellites. The differential GPS procedure assumes that error sources are the same for all GPS receivers in the survey area that are using the same GPS satellites at any given instant. These errors are measured at the base station and inserted into calculations for the roving receiver. Three other reference points (fig. 2 and table 3) near the study area were included in the differential GPS survey to verify accuracy. The horizontal accuracy for this survey was determined to be better than ±0.1 ft. A number of the control points used in this survey were established by the Bureau of Reclamation (D.A. Ostenaa, Bureau of Reclamation, written commun., 2000) for use in the development of a 1-ft contour digital-terrain map (DTM) of the study area. The location and identification number of each reference mark and control point used during the survey are shown in figures 2 and 4. The latitude and longitude (horizontal position) and a description of each of the control and reference points used in this study are presented in table 3.

Vertical Referencing

Vertical control was based on the North American Vertical Datum of 1988 (NAVD 88), in feet. Vertical referencing of cross-section data and control points was accomplished using the differential GPS and GIS interface previously described. The vertical accuracy for this survey was determined to be better than ±0.05 ft on the basis of a comparison of the differential GPS survey results to known elevations at the three reference points (fig. 2 and table 3) that were used to verify survey accuracy.

TIN-Generated Cross Sections

To simulate floods in the study area, field-surveyed cross sections were extended out into the floodplain using a procedure approved by the Federal Emergency Management Agency (1998). Cross sections were extended using the Triangulated Irregular Network (TIN) interpolating procedure and data obtained from the 1-ft contour DTM of the study area that was prepared by the Bureau of Reclamation (D.A. Ostenaa, Bureau of Reclamation, written commun., 2000). TIN-generated cross sections are constructed from interpolation of a network of triangulated DTM derived points (nodes) that define latitude, longitude, and elevation. Thus any point (*x*, *y*, and *z*) can be interpolated within the boundaries defined by the TIN control points.

To properly simulate flow through the site 1 constriction, additional cross sections were needed upstream of cross section 86 so that boundary conditions in the models would not affect flow computations at the site 1 constriction. An additional 22 cross sections, numbered 87 through 108, were generated using the TIN procedure (figs. 9*A*, 9*B*, 9*C*).

Seven cross sections, numbered 30 through 36, were generated using the TIN procedure because of problems with the data that prevented transformation of the field-surveyed cross sections at these locations to NAD 83 (horizontal) and NAVD 88 (vertical) coordinates.

Three in-fill cross sections (60.5, 70.5, and 76.5) were generated using the TIN procedure. These cross sections were needed in the model simulations to minimize excessive conveyance changes between surveyed cross sections and to maintain computational stability.

Five TIN-generated cross sections, numbered S1 through S5 (fig. 9*B*), were constructed for a small channel to represent water flowing around a small knob north of the channel near the site 1 constriction. These cross sections were used for flow simulations of 50 m^3/s.

A comparison of data from the field surveys and those generated from the TIN procedure indicated that the TIN-generated cross sections were within an accuracy of ±0.5 ft as recommended by the Federal Emergency Management Agency (1998). The average difference at most sections was less than 0.5 ft, except in areas where terrain relief was extreme. Because of extreme terrain relief, TIN-generated cross sections in and around the constrictions at sites 1 and 2 differed significantly from the field-surveyed cross sections. Consequently, TIN-generated cross sections were not used in these areas; instead, seven linearly interpolated cross sections, between sections 49 and 54 (49.5, 50.5, 51.25, 51.5, 51.75, 52.5, and 53.5) were used to model flows greater than 70 m^3/s through the site 2 constriction. Two adjacent field-surveyed cross sections were used to produce each interpolated cross section. These linearly interpolated sections were needed to maintain gradually-varied flow through the site 2 constriction for flows that transitioned from subcritical to supercritical.

The type of material composing the streambed, banks and floodplain was noted at each surveyed point. If there was more than one type of material at a point, all were noted with the dominant material listed first and the other materials listed in decreasing order. The occurrence of bedrock was especially important to note because model simulations assumed that scour depths would be limited by the presence of bedrock.

Table 3. Location and description of elevation control and reference points used to establish horizontal and vertical control for the thalweg and cross-section surveys on the Big Lost River upstream of the Pioneer diversion structures, Idaho National Engineering and Environmental Laboratory, Idaho.

[Locations of reference points and control points are shown in figures 2 and 4. **Latitude and longitude** are based on the North American Datum of 1983 and are shown in degrees (°), minutes (′), and seconds (″). **Reference mark elevations** are based on the North American Vertical Datum of 1988. **Abbreviations**: ft, ft; COE, U.S. Army Corps of Engineers; USGS, U.S. Geological Survey; Reclamation, Bureau of Reclamation]

Reference or control point and identification	Latitude	Longitude	Elevation (ft)	Description
		Reference Points		
BIGLOST[1, 2]	43°32′50.89476″	113°01′14.78261″	5,021.950	COE, Bronze disk
N892[2]	43°30′56.03889″	113°04′52.79188″	5,058.018	Brass disk near well NA-89-2
		Control Points		
0S12	43°32′02.25472″	113°02′13.87089″	5,021.562	Aluminum cap on rebar on Pioneer diversion structure
GAGE[2]	43°30′56.86456″	113°04′55.03646″	5,053.861	Brass disk near gaging station 13132520
HUB2	43°31′56.02522″	113°02′46.54081″	5,026.880	USGS, wooden stake
HUB3	43°31′41.96139″	113°03′15.27893″	5,030.466	USGS, wooden stake
HUB4	43°31′38.85863″	113°03′43.37538″	5,031.512	USGS, rebar
HUB5	43°31′29.32913″	113°03′57.21326″	5,037.493	USGS, rebar
HUB6	43°31′34.93367″	113°04′13.17101″	5,041.906	USGS, rebar
HUB7	43°31′32.47292″	113°04′28.92617″	5,043.596	USGS, rebar
HUB8	43°31′12.50069″	113°04′49.56396″	5,047.861	USGS, rebar
HUB9	43°30′50.83204″	113°05′03.43743″	5,070.190	USGS, rebar on INEEL diversion dam
PKR1	43°31′57.49975″	113°02′32.57683″	5,025.561	PK nail in basalt rocks
PT01	43°31′49.64287″	113°03′01.12794″	5,027.379	Reclamation, rebar
PT02	43°31′22.06486″	113°04′43.87643″	5,049.590	Reclamation, rebar
PT03	43°31′20.13931″	113°04′44.34819″	5,047.031	Reclamation, rebar
PT04	43°31′33.15356″	113°03′34.20555″	5,031.870	Reclamation, rebar
PT05	43°31′34.23366″	113°03′29.47427″	5,030.000	Reclamation, rebar
PT06	43°31′57.28505″	113°02′41.77107″	5,022.274	Reclamation, rebar
PT07	43°32′00.40034″	113°02′42.22723″	5,018.763	Reclamation, rebar
WEL3	43°31′42.89729″	113°03′33.95965″	5,028.665	USGS, rebar
WELL[2]	43°31′42.85368″	113°03′34.08158″	5,029.938	Top of well casing at well

[1]Elevation reference point not shown in figures 2 and 4.

[2]Used for survey verification.

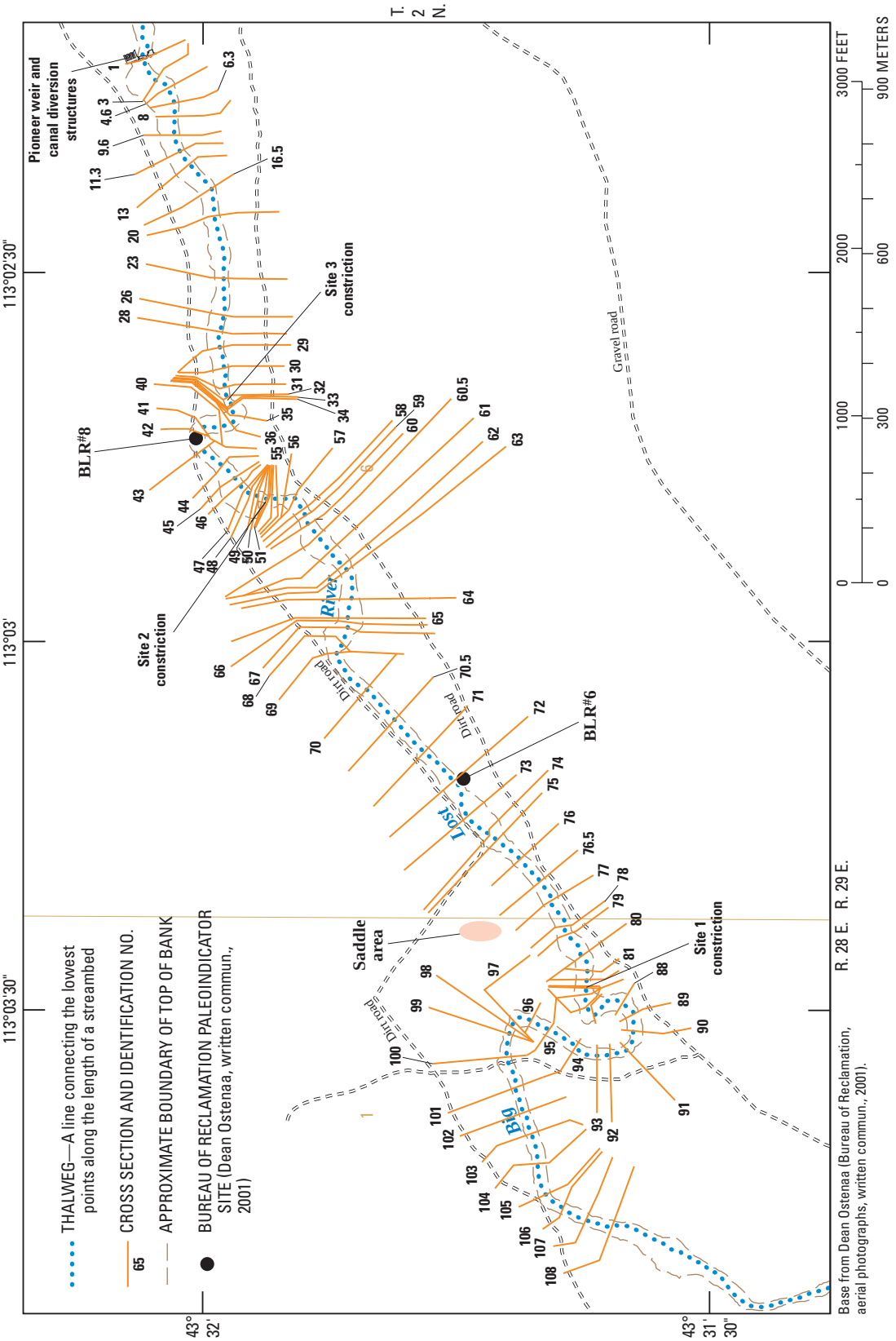

A. Cross sections used for flow simulations of 10 cubic meters per second

Figure 9. Location of field-surveyed, TIN-extended, and TIN-generated cross sections used for flow simulations of 10, 50, and 70 cubic meters per second and greater on the Big Lost River upstream of the Pioneer diversions structures, Idaho National Engineering and Environmental Laboratory, Idaho

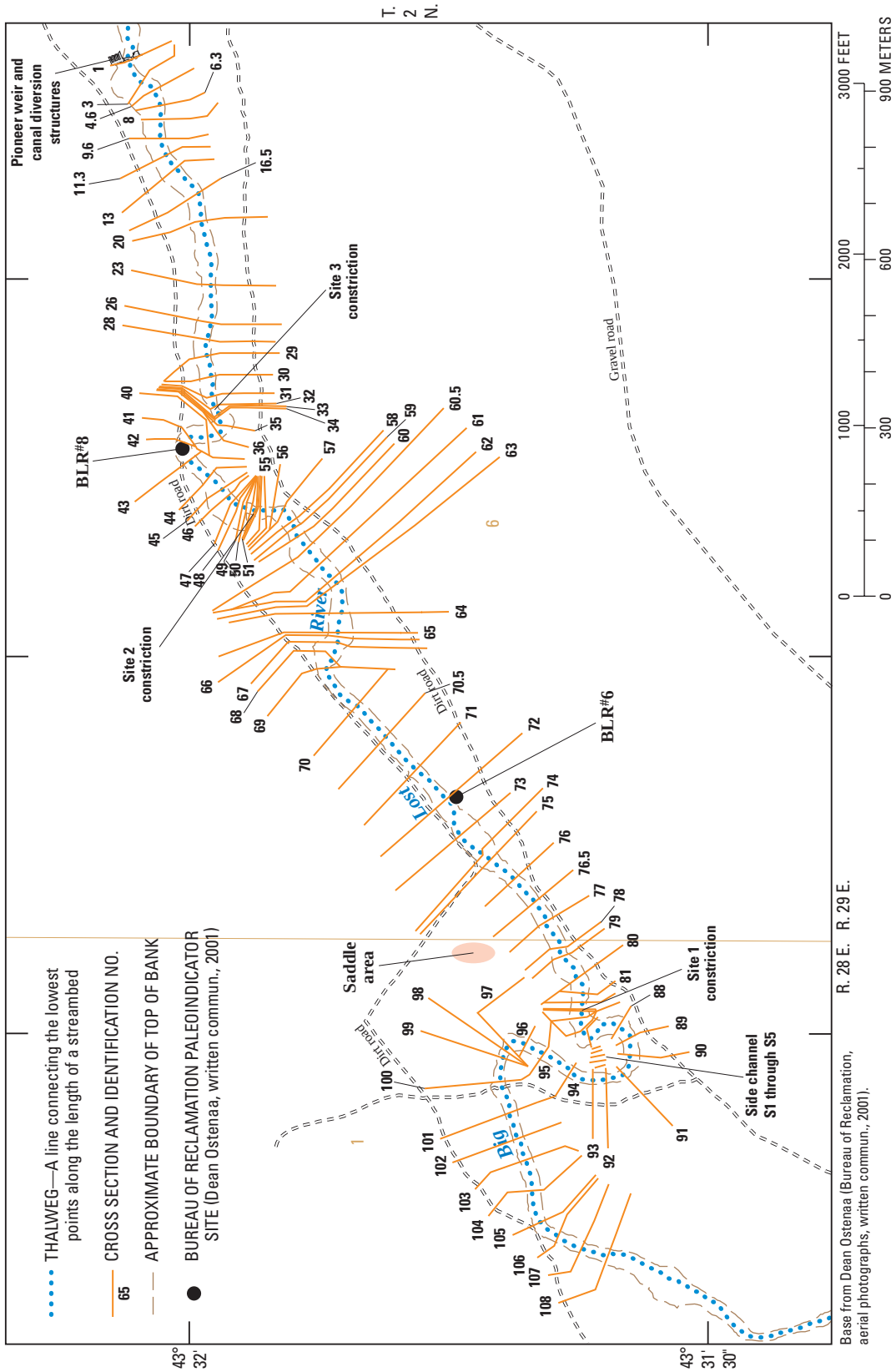

***B.* Cross sections used for flow simulations of 50 cubic meters per second**

Figure 9.—Continued.

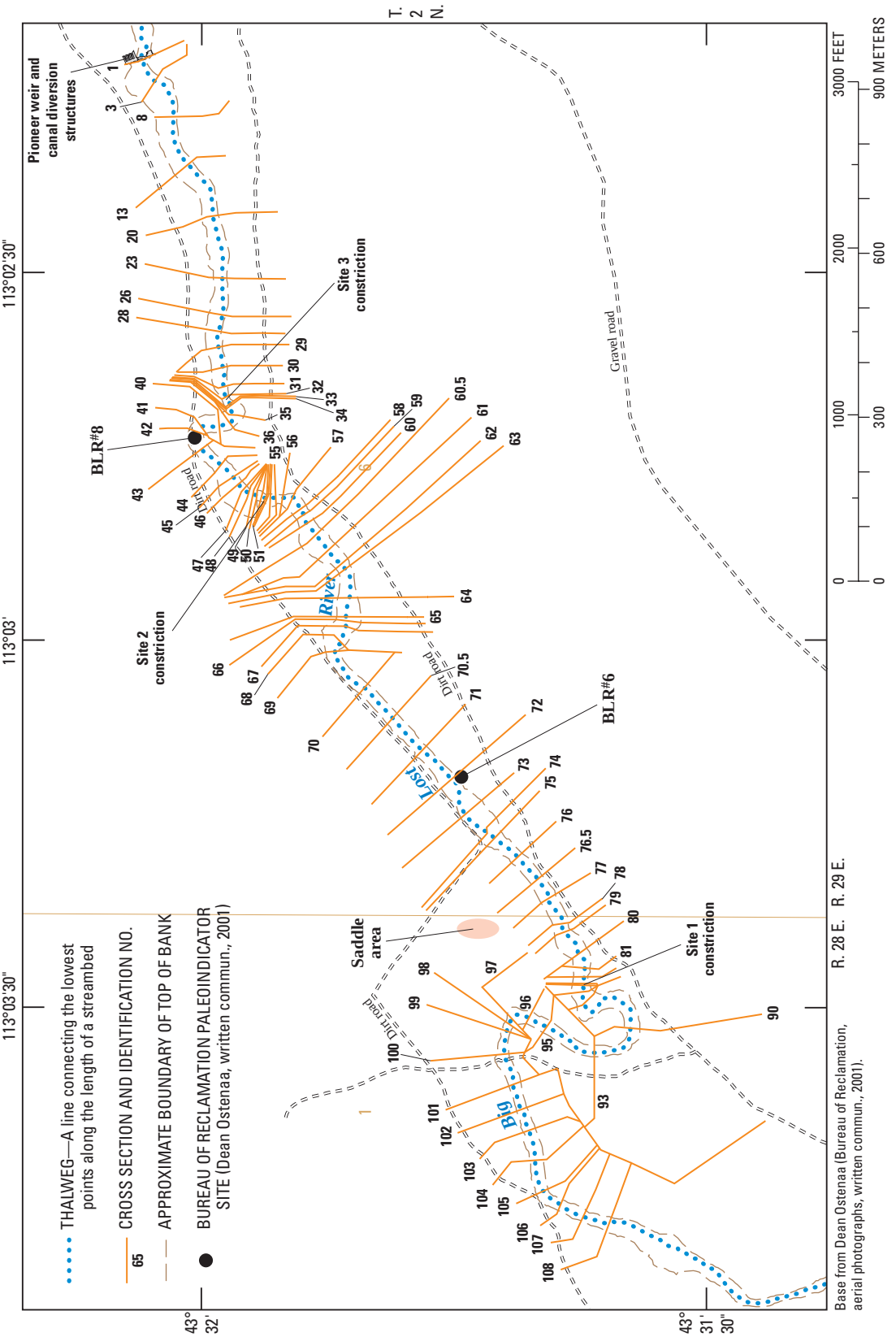

C. **Cross sections used for flow simulations of 70 cubic meters per second and greater**

Figure 9.—Continued.

Hydraulics of the Study Reach

In the study reach, the Big Lost River is incised into Holocene and upper Pleistocene alluvium and middle to upper Pleistocene basalt lava flows (fig. 3) (Kuntz and others, 1994). Shallow subcropping basalt beneath the alluvial fill strongly influences the present-day course of the river and channel slope. At three locations in the study area bedrock forms constrictions in the channel that locally control the course of the river and the slope of the channel. Bedrock also is exposed in the streambed at cross sections 1, 6, 7, 41, 59, 62, and 65-67 (fig. 8). These bedrock controls locally restrict the depth of scour and thus control streambed slope. The distinction between a constriction-controlled section and channel-controlled section is based on HEC-RAS simulations of backwater and the effect that backwater accumulation has on frictional resistance to flow and hence on scour.

In the study reach, the general slope of the streambed is about 0.0023 between cross sections 1 and 108. The slope of the streambed between the sites 1 and 2 constrictions is 0.0019. The slope of the streambed in this section of the river is lower than elsewhere in the study area and reflects the effects of backwater accumulation upstream of the site 2 constriction. Locally, the streambed slope varies considerably, especially in the immediate vicinity of the constrictions at sites 1, 2, and 3 and in sections of the river where basalt is exposed in the streambed.

Constriction-Controlled Sections

Constriction-controlled sections, for the purposes of this study, occur within the boundaries that define sites 1, 2, and 3 (fig. 4). These boundaries are defined by the extent of backwater accumulation upstream of bedrock constrictions. Convergence of streamflow inside constrictions and upstream velocity reduction cause upstream water-surface elevations to be higher and channel slopes to be lower than would be the case in the absence of flow convergence.

At three locations in the study area, bedrock walls narrow and confine the river. The hydraulic effect of constrictions, or a local reduction in channel width, depends on flow magnitude and channel size. For natural rivers and streams, resistance or friction from the channel sides and bottom controls the flow. Constrictions cause flows to converge. If the approaching flow to the constrictions is subcritical, the constriction causes a backwater effect that may extend for a long distance upstream. Model simulations, described in the section "Numerical Modeling," indicate that flow approaching all the constrictions is subcritical. Constriction-controlled reaches are susceptible to backwater, resulting in water-surface elevations that are higher than those that would occur in the absence of the constriction.

The constriction at site 2 is quite narrow, about 17 ft wide, with nearly vertical bedrock walls greater than 20 ft high. The constrictions at sites 1 and 3 are much wider. At site 1 the constriction is about 27 ft wide, and at site 3 it is about 46 ft wide. Another constriction occurs just downstream of the gaging station below the INEEL diversion dam (13132520) (fig. 2). This constriction is upstream of the study area and was not included in the surface-water flow and sediment-transport simulations described in this report. It is, however, included in the TRIM2D simulations described in the report by Ostenaa and others (1999).

The channel bed within the confines of the constrictions consists of a 4- to 6-ft thick accumulation of easily erodible alluvium. At the site 2 constriction, the bed material is composed of loose, unconsolidated sands and silts. Depth to bedrock inside this constriction ranges from 4.5 to 5.5 ft. During a flood, all bed materials at this site probably are removed and the underlying bedrock is exposed. As the flood recedes and velocities decrease, residual bed load and finer suspended sediments are deposited inside the constriction. Water often pools inside this constriction when flows in the river recede. Pooling of water is indicated by the accumulation of very-fine sand and silt materials inside this constriction.

The channel fill material in the constrictions at sites 1 and 3 consists of fine- to medium-grained sand near the surface that becomes coarser with depth. Because these constrictions are wider than the constriction at site 2, flow velocities through these constrictions are less than those through the constriction at site 2. The greater width of these constrictions limits flow velocities and, as demonstrated in the HEC-6 model, decreases the depth of scour. Only very large floods have the potential to scour the channel down to bedrock at these constrictions. Trenching inside the three constrictions indicated that depths to bedrock are as much as 6, 5.5, and almost 4 ft at the site 1, 2, and 3 constrictions, respectively.

Channel-Controlled Sections

Unlike the constriction-controlled sections, channel-controlled sections are not strongly influenced by backwater effects. In channel-controlled sections, frictional resistance forces dominate, the streambed slope is steeper, and flow velocities are higher. Flow in these sections is more uniform than in the constriction-controlled sections. Cross-section geometry and the armored surface layer within the channel-controlled sections also tend to be more uniform than in the constriction-controlled reaches. Most armored surface-layer sampling sites in the channel-controlled sections of the river are near the center of the active channel. These locations generally are representative of conditions across the entire bed because armoring appears to be uniform from bank to bank in the channel-controlled sections of the river.

For discussion purposes, it is convenient to divide the study area into upper, middle, and lower reaches (fig. 9). The upper reach extends from cross section 108, at the upstream end of the model reach, to the site 1 constriction; the middle reach extends from the site 1 constriction to the site 2 constriction; and the lower reach extends from the site 2 constriction to cross section 1, at the downstream end of the model reach. Each of these subdivisions includes both channel- and constriction-controlled sections of the river as previously described.

Numerical Modeling

The primary objective of numerical modeling was to simulate the effects of the constrictions at sites 1, 2, and 3 on flood elevations. Numerical models can be used to estimate water-surface elevations, flow depths, flow velocities, stream power, scour, deposition, and sediment transport for flows of varying magnitude. In the two previous modeling studies, one conducted by the USGS (Kjelstrom and Berenbrock, 1996) using WSPRO, and the other conducted by the Bureau of Reclamation (Ostenaa and others, 1999) using TRIM2D, the channel bed was assumed to remain stable during all flows, and sediment transport processes were not simulated. For the present study, HEC-RAS (U.S. Army Corps of Engineers, 1997a, 1997b, and 1997c) version 3.0.1 was used to construct a surface-water flow model, and HEC-6 (U.S. Army Corps of Engineers, 1993) version 4.1.0 was used to construct a surface-water flow and sediment-transport model. The modeled reach of the river in this study extends from a point about 2.3 mi downstream of the INEEL diversion dam to the Pioneer diversion structures, a distance of 9,850 ft. The reach that was modeled in the Bureau of Reclamation study using TRIM2D (Ostenaa and others, 1999) extends from the INEEL diversion dam to the Pioneer diversion structures, a distance of 22,050 ft.

HEC-RAS Model Implementation

HEC-RAS is a computer program that simulates 1-D, gradually varied, steady flow in open channels with fixed boundaries. In areas where flow velocity is changing rapidly, the gradually varied flow assumption requires the use of closely spaced cross sections. The HEC-RAS model uses the standard step method (Chow, 1959, p. 265) to determine changes in water-surface elevations from one cross section to the next by balancing total energy head at the sections. This 1-D model assumes that energy is uniform in a cross section. This assumption is not valid at locations where flow is not parallel to the main channel or where vertical velocities are significant. The model also assumes that flow is unobstructed with the channel and floodplain free of debris.

The field-surveyed and TIN-generated cross sections and the roughness coefficients (*n* values) derived from the earlier WSPRO model (Kjelstrom and Berenbrock, 1996) were used to define channel and floodplain hydraulic characteristics for the initial HEC-RAS simulations. Roughness coefficients in the WSPRO model were determined by calibrating the model against field-measured flows and stages at three cross sections downstream of the INEEL diversion dam gaging station (13132520) (fig. 2). These stage-discharge measurements were made in the spring and summer of 1995 (L.C. Kjelstrom, U.S. Geological Survey, oral commun., 2003).

Three separate HEC-RAS models were developed to accommodate the different hydraulic conditions that occur upstream of the site 1 constriction for the peak flows that were simulated. In the first model a flow of 10 m^3/s (353 ft^3/s), representing a 2-year (or 50-percent probability) flood, was simulated, and in the second model a flow of 50 m^3/s (1,765 ft^3/s) was simulated. The 10 m^3/s model included the field-surveyed and TIN-generated cross sections shown in figure 9*A*. Five side-channel cross sections, numbered S1 through S5, were added to the second HEC-RAS model to represent water that flows around a small knob north of the channel at cross section 90 (fig. 9*B*). The third model simulated flows equal to and greater than 70 m^3/s. The third model differs from the first by the exclusion of cross sections 87, 88, 89, 91, 92, and 94 and the elongation of cross sections 86, 90, and 93 (fig. 9*C*); and differs from the second by the exclusion of cross sections numbered S1 through S5. The removal of cross sections and the elongation of cross sections were necessary because the meander bend upstream of the site 1 constriction was completely flooded for flows greater than about 70 m^3/s. Figures 9*A*, 9*B*, and 9*C* show the cross sections that were used for flow simulations of 10, 50, and 70 m^3/s and greater, respectively.

Critical depth occurs at free outfalls. A free outfall occurs at cross section 1, where the streambed drops nearly 15 ft vertically (Berenbrock and Kjelstrom, 1998; and 1-ft contours from the Bureau of Reclamation's aerial-photography mapping, D.A. Ostenaa, Bureau of Reclamation, written commun., 2001) below the Pioneer diversion structures. For critical flow, the Froude (*Fr*) number is set equal to 1. To determine the starting elevation, equations 1 and 2 are expressed in terms of velocity and set equal to each other. The resulting equation is solved iteratively by adjusting average flow depth (*D*) and width of the water surface (*W*) to compute the average depth of flow for each simulated flow discharge (*Q)* with $Fr = 1$. For rectangular cross sections, *W* is held constant and *D* is equal to the depth of flow (Chow, 1959, p. 81).

Starting water-surface elevations for the HEC-RAS and HEC-6 models at cross section 1 were determined by computing critical depth from the Froude number:

$$Fr = V/(gD)^{1/2}, \quad (1)$$

and the flow equation:

$$Q = VA = VDW, \quad (2)$$

where:

Fr is Froude number [$L0$],
V is mean velocity [L/T],
g is acceleration of gravity [L/T^2], (9.81 m/s^2 in SI units, 32.16 ft/s^2 in English units),
D is average flow depth [L]
Q is flow discharge [L^3/T]
A is cross section area [L^2], and
W is width of the water surface [L].

The units for these terms are length [L], time [T], and dimensionless [$L0$].

At the upstream end of the model reach, cross section 108, the starting water-surface elevation was determined from the flow equation (2) and a slope-conveyance computation of normal depth using Manning's equation for open-channel flow:

$$V = (1/n)R^{2/3}S^{1/2}, \quad (3)$$

where:

V is velocity [L/T],
n is Manning's roughness coefficient [$L0$], (note: in equation (3) use $1/n$ for SI units, and $1.486/n$ for English units),
R is hydraulic radius [L],
S is slope of the energy grade line [$L0$],
A is cross-section area [L^2], and
Q is flow discharge [L^3/T].

The units for these terms are length [L], time [T], and dimensionless [$L0$].

In channel-controlled sections, where the stage-discharge relation is determined primarily by the channel shape and local channel-bed friction, the channel slope can be used to approximate the energy grade line (S). Equation (3) is solved for each simulated Q using this assumption.

The upper boundary condition is required only if flow in the modeled reach is supercritical. If flow in the entire reach is subcritical, then the upper boundary condition is not required and was not used during the simulation. It was noted during simulations that flow through the site 2 constriction transitioned from subcritical to supercritical when modeled flow was equal to and greater than 100 m^3/s. For the modeled reach, flows equal to and greater than 100 m^3/s at the site 2 constriction were supercritical, and flows equal to and less than 70 m^3/s were subcritical. It was not the purpose of this study to determine the minimum flow necessary to initiate supercritical flow. Transitioning from one flow regime to the other was done automatically by HEC-RAS with the inclusion of the specified upstream boundary condition for supercritical flow. As noted previously, to maintain computational stability, seven interpolated cross sections were used to model flows greater than 70 m^3/s through the site 2 constriction.

Manning's *n* Determination

Manning's *n*, also known as the roughness coefficient, represents the flow resistance in a channel. Factors that affect flow resistance include: (1) size, gradation, and angularity of materials composing the streambed; (2) channel shape; (3) type of bed forms (for example dunes, antidunes, and ripples); (4) presence of bars; (5) riparian vegetation; (6) man-made and natural structures (for example bridges, causeways, and constricted openings); (7) presence of suspended sediment and movement of bed load; and (8) degree of meandering. In channel-controlled sections, resistance decreases as flow increases; resistance also decreases as the size of the bed material decreases. In the straight channel-controlled sections of the model reach, the size, gradation, and angularity of the materials composing the streambed probably are more important than the other factors for determining flow resistance. In constriction-controlled sections, the size of the constriction is the major control on flow resistance. Flow-resistance equations and the roughness coefficients established from the previous 1-D WSPRO model (Berenbrock and Kjelstrom, 1998) were used to determine *n* values at selected cross sections where resistance forces are dominated by the character of the streambed materials. The WSPRO-derived *n* values were modified on the basis of flow-resistance equations for gravel-bed channels because no stage-discharge or *n*-verification measurements have been made in the study area. Cross sections 20, 70.5, and 76 (fig. 9) were selected as representative sections for initial estimates of Manning's *n* because these sections are in virtually straight reaches of the river, and the materials composing the channel bed in these reaches of the river are the primary source of flow resistance.

The flow-resistance equations developed by Limerinos (1970), Bray (1979), Hey (1979), and Mussetter (1989) have been used extensively for gravel-bed rivers. The Mussetter (1989) equations were not used in this study, however, because preliminary scoping calculations estimated Froude numbers in the supercritical range ($Fr > 1$), which is not realistic for the flows being considered in these channel-controlled sections. The calculated *n* values, derived by using the aforementioned flow-resistance equations, ranged from 0.019 to 0.037, with an average of 0.025 for the relatively straight channel reaches represented by cross sections 20, 70.5, and 76. To account for

the irregular land surface, vegetation, and other obstructions an *n* value of 0.040 was assigned to the floodplain portion of these sections.

For channel reaches with modest curvature or changes in cross-section shape from one section to another, the *n* values were increased from the straight-channel-section values by about 30 percent (Chow, 1959); and for channel sections where there is substantial variation in cross-section shape or severe curvature, the values were increased by 50 percent (Chow, 1959) of the straight-section values. With these adjustments, *n* values for modest curvature of the channel were 0.033 and 0.052 for the channel and floodplain, respectively; and *n* values for severe curvature of the channel were 0.038 and 0.060 for the channel and floodplain, respectively.

Elevations of high-water marks at cross sections in and adjacent to the constrictions at sites 1 and 2 also were surveyed at the time of the cross-section field surveys. These marks consisted of white, sub-horizontal water stains on basalt outcrops that form the banks of these constrictions (cover photograph shows the character of the high-water marks for the site 2 constriction) and were interpreted to represent the high water marks for floods with short return periods, in this case assumed to be the 2-year flood[2]. The quality of the high-water marks at the site 3 constriction, the widest of the three constrictions, were poor and were not used to represent the elevation of the 2-year flood. Simulations of the 2-year flood and elevations of the high-water marks (assumed to represent the 2-year flood) were used to evaluate the initial estimates of the *n* value chosen to represent frictional resistance in the main channel of the river.

Daily mean discharges for the Big Lost River below the INEEL diversion dam (13132520) gaging station, about 1.5 mi upstream of site 1 (fig. 2), are shown in figure 10. This gaging station has been in operation since 1984. Peak flows measured at this gaging station are all less than 13.2 m^3/s (466 ft^3/s) and only two events exceeded 13 m^3/s (459 ft^3/s) (fig. 10). A zero flow was recorded 77 percent of the time at this station. The diversion dam just upstream of this gaging station affects flows and peak flows at this gaging station and in the study area. Flow downstream of the diversion dam can be entirely shut off and rerouted into a diversion channel that discharges into a series of off-channel depressions or spreading areas southwest of the study area. Because flow is regulated at the diversion dam, peak-flow data for the gaging station Big Lost River near Arco (13132500) were used to estimate the 2-year flood in the study area. A three-parameter log-Pearson Type III flood-frequency analysis of these data, as outlined in "Guidelines for Determining Flood Flow Frequency" (Bulletin #17B by the Interagency Advisory Committee on Water Data, 1982), showed that the 2-year flood is about 10 m^3/s (353 ft^3/s) (fig. 11) with lower and upper 95-percent confidence limits of 7.1 and 13.9 m^3/s, respectively. The period of record used for this computation was 1947 through 1961, and 1965 through 2000 (n=51; six of these peak values were zero for the period of record).

Water-surface elevations simulated by the HEC-RAS model, with cross sections configured to simulate a flow of 10 m^3/s (fig. 9*A*), were compared to elevations of the surveyed high-water marks. If differences occurred, then *n* values pertaining only to the channel portion of the cross section were modified because the mean annual flood (10 m^3/s) can be contained wholly within the active channel. For calibration purposes, the *n* value is the only parameter that can be adjusted in the HEC-RAS model.

Simulated water-surface elevations for the 2-year flood plot between the measured high-water marks (figs. 12*A* and 12*B*). The average difference between the high-water marks and model simulation results was 0.38 ft at site 1 (5 measured marks) and 0.12 ft at site 2 (7 measured marks), and the maximum differences were 1.2 ft at the site 1 constriction and 0.8 ft at the site 2 constriction. The closely spaced distribution of high-water marks, both above and below the simulated water-surface elevation line, suggests that the initial estimates of the *n* values for low flows in the main channel of the river were appropriate[3].

HEC-RAS Simulation Results

Water-surface elevations for peak flows of 50, 70, 100, 150, 187, and 200 m^3/s were simulated with HEC-RAS. Flows of 70, 100, 150, and 187 m^3/s also were simulated in the TRIM2D model (Ostenaa and others, 1999). For presentation clarity, only the results for simulations of 50, 100, 150, and 200 m^3/s (fig. 13*A*) are presented in this section. Results for the intermediate flows of 70, 100, and 150 m^3/s are presented in the section "Comparisons of HEC-RAS, HEC-6, and TRIM2D Simulation Results."

At the sites 1 and 2 constrictions, where the channel slope abruptly steepens, large changes in water-surface elevation occur for all simulated flows greater than 50 m^3/s (fig. 13*A*). As peak flow increases, differences between water-surface elevations upstream and downstream of the constrictions also increase. For a flow of 200 m^3/s, these differences are about 2.0 ft through the site 1 constriction (between cross sections 85 and 83) and 5.0 ft through the site 2 constriction (between cross sections 53.5 and 51.25). For a flow of 50 m^3/s, these differences are about 1.0 ft for both the site 1 and 2 constrictions. Because the channel is much wider and the slope much gentler, changes in water-surface elevation through the site 3 constriction were minimal for all simulated flows.

[2]The 2-year flood is approximately equal to the mean annual flood which is defined as a flood with a return period of 2.33 years (Chow, 1964, p. 8-25). The computed mean annual flood is 12.8 m^3/s (n=51), with lower and upper 95-percent confidence limits of 9.1 m^3/s and 18.0 m^3/s, respectively.

[3]The HEC-RAS simulated water-surface elevation for a flow of 10 m^3/s was confirmed at the site 2 constriction in July 2006. The water-surface line for a measured flow of about 10 m^3/s (9.97 m^3/s) at cross section 53.5 was marked on May 31, 2006; and the elevation of this mark was measured on July 11, 2006. The surveyed elevation was 5,014.02 ft—in very close agreement with the HEC-RAS simulated elevation of 5,014.03 ft (fig. 12*B* and photograph on inside of report cover).

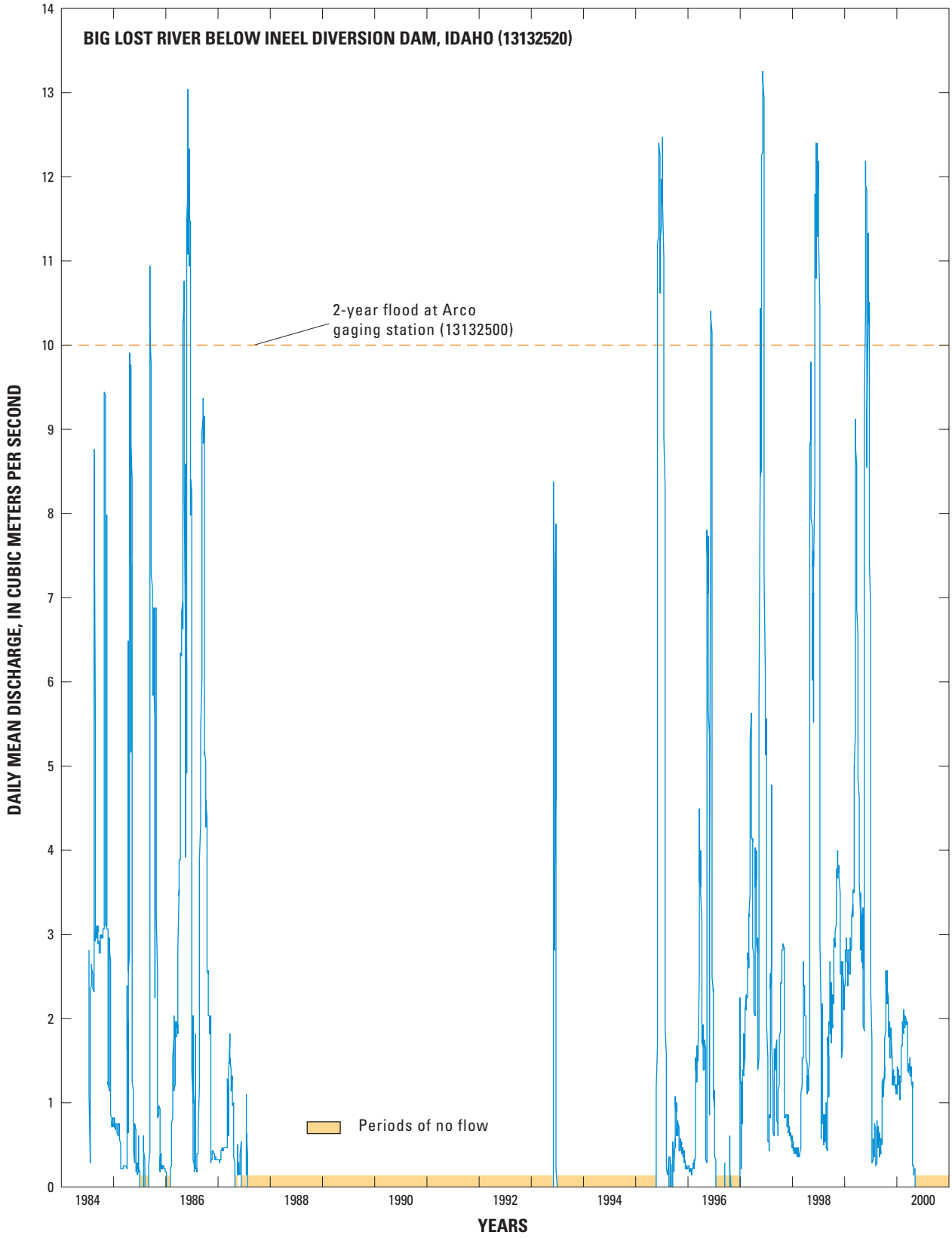

Figure 10. Daily mean discharge for the Big Lost River below the Idaho National Engineering and Environmental Laboratory diversion dam (13132520), Idaho, 1984–2000.

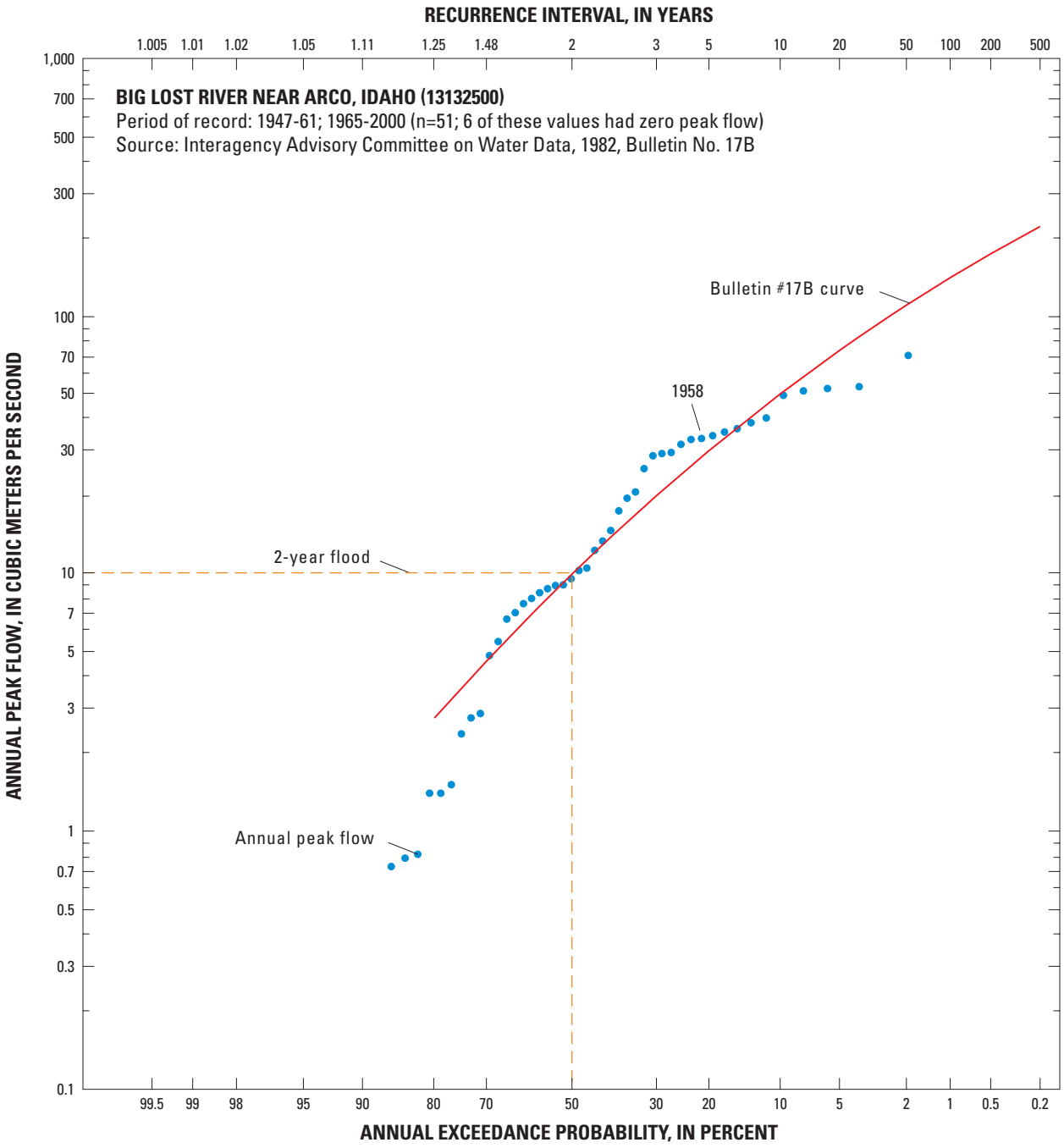

Figure 11. Flood-frequency curve for the Big Lost River near Arco (13132500), Idaho, 1947–61 and 1965–2000.

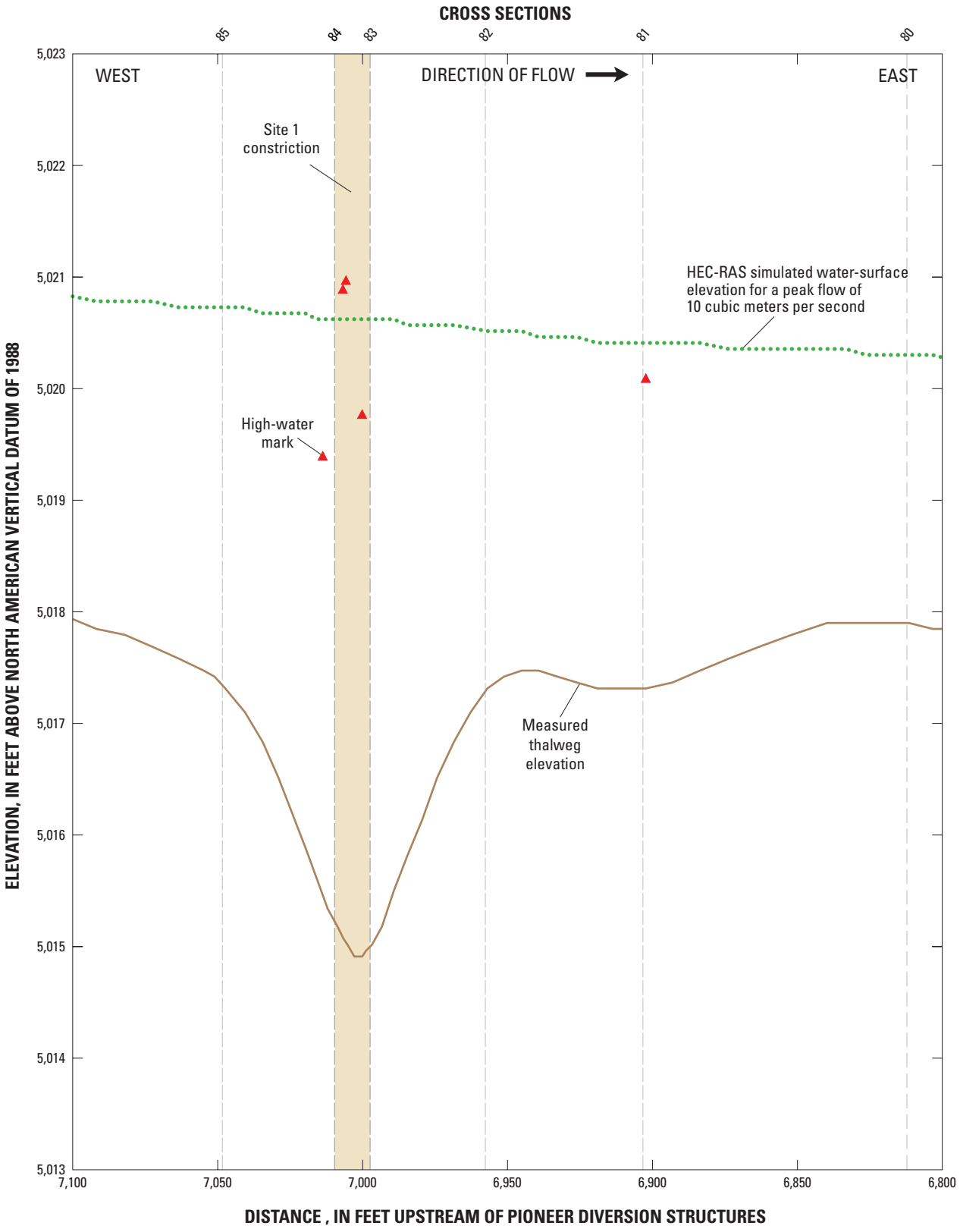

A. Site 1 constriction

Figure 12. High-water marks, measured thalweg elevation, and HEC-RAS simulated water-surface elevation for a peak flow of 10 cubic meters per second at the sites 1 and 2 constrictions on the Big Lost River upstream of the Pioneer diversion structures, Idaho National Engineering and Environmental Laboratory, Idaho.

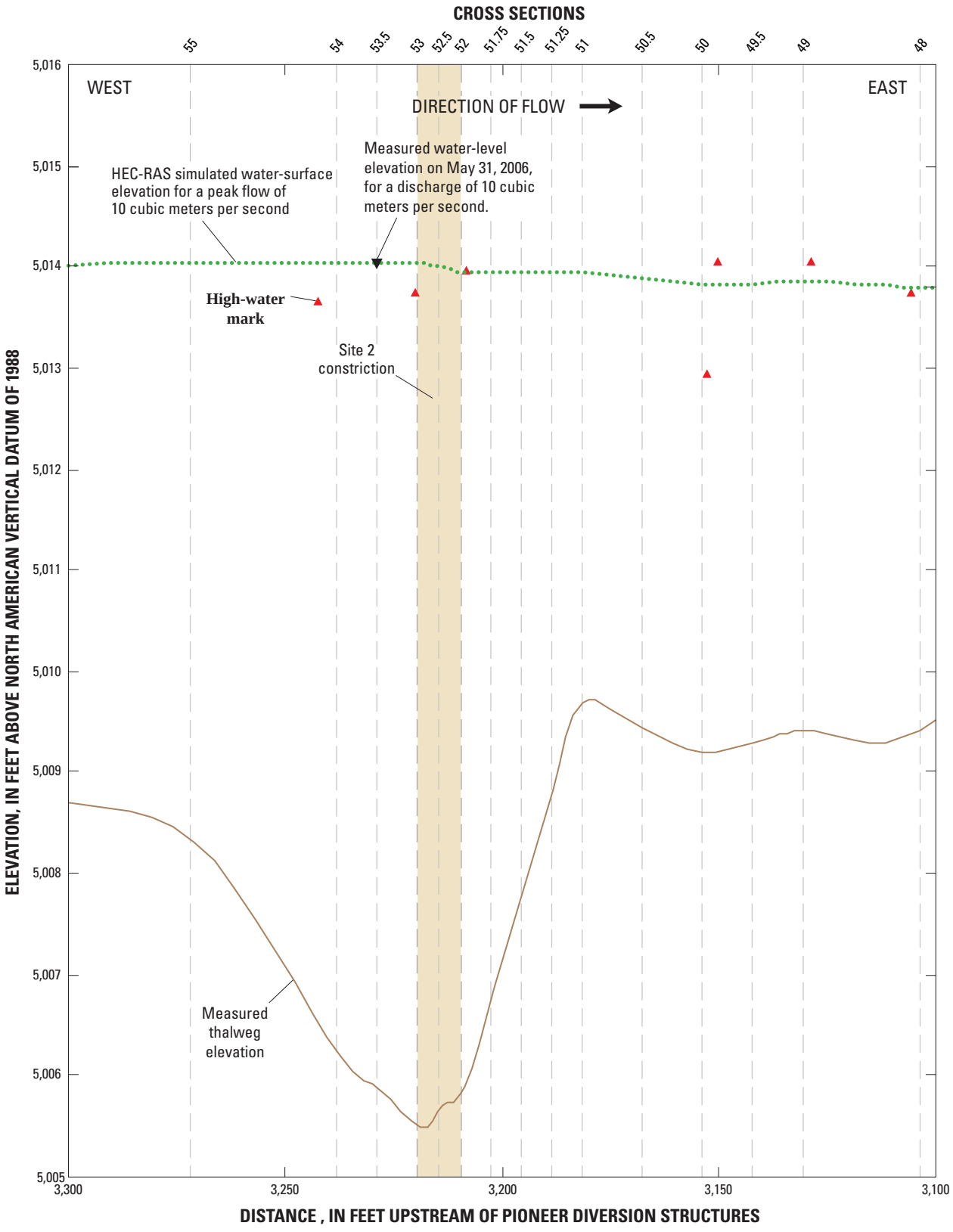

B. Site 2 constriction

Figure 12.—Continued.

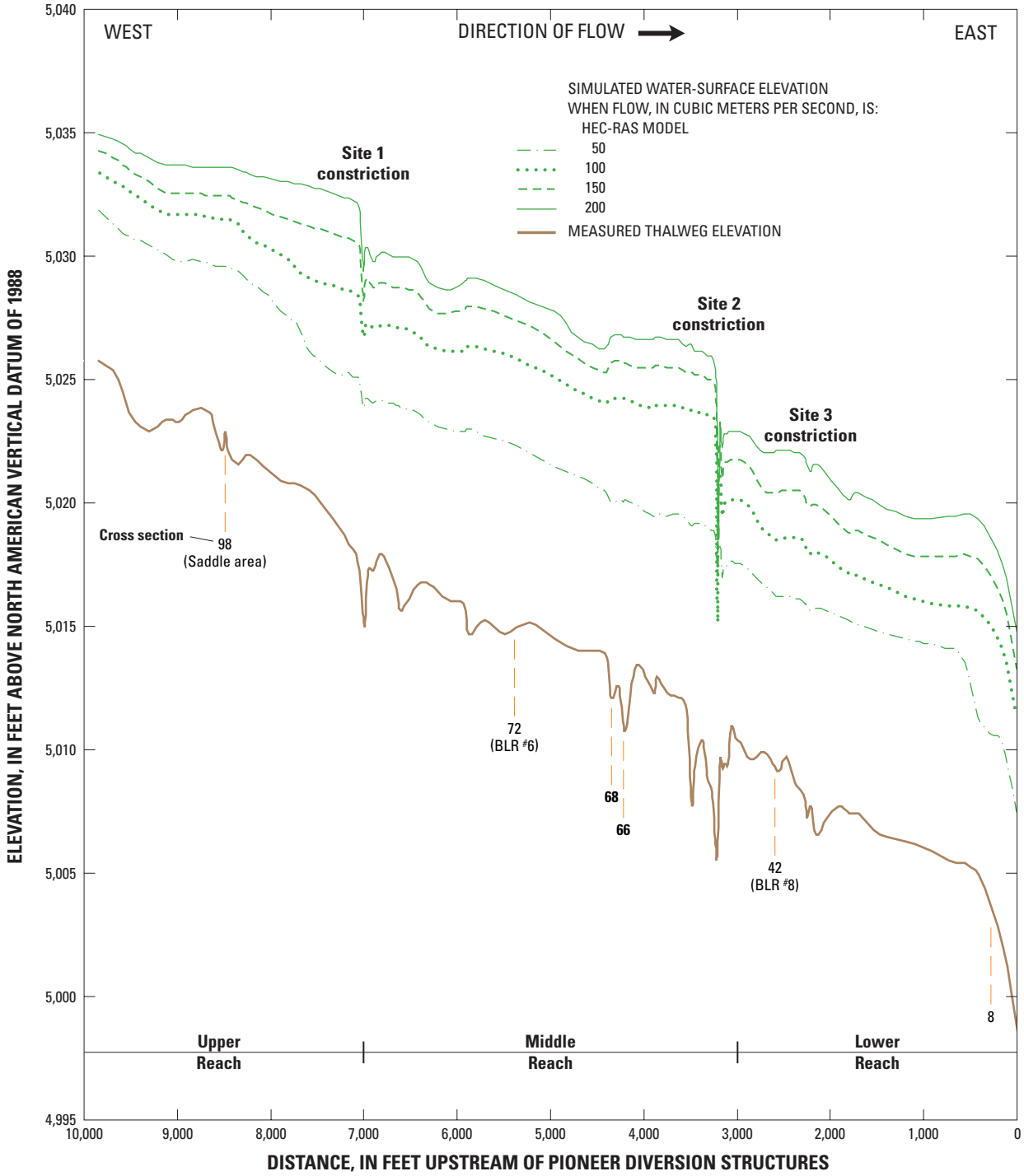

A. Big Lost River

Figure 13. Measured thalweg elevation and HEC-RAS simulated water-surface elevations for selected flows of 50, 100, 150, and 200 cubic meters per second on the Big Lost River and sites 1 and 2 constrictions upstream of the Pioneer diversion structures, Idaho National Engineering and Environmental Laboratory, Idaho.

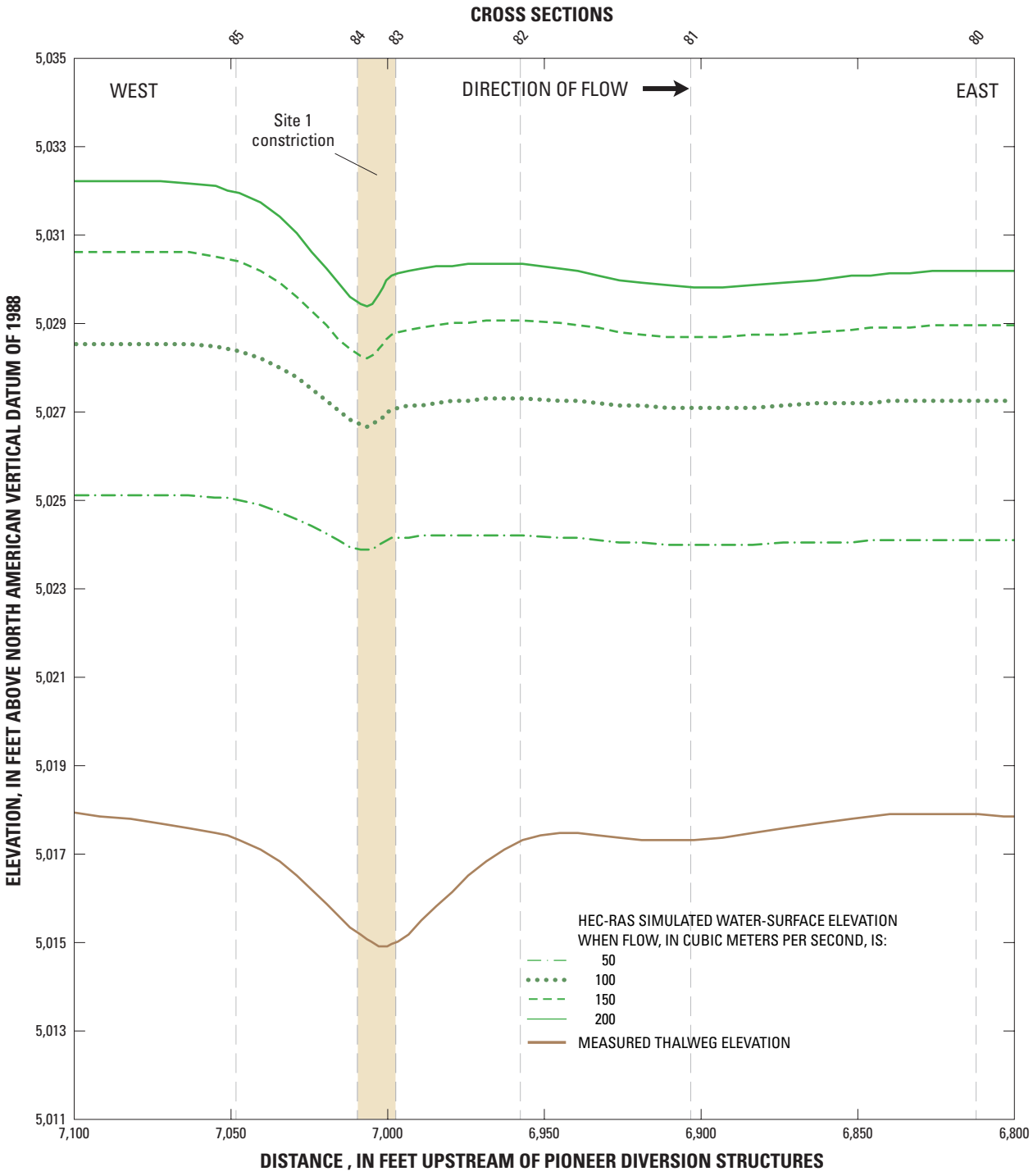

B. Site 1 contriction on Big Lost River

Figure 13.—Continued.

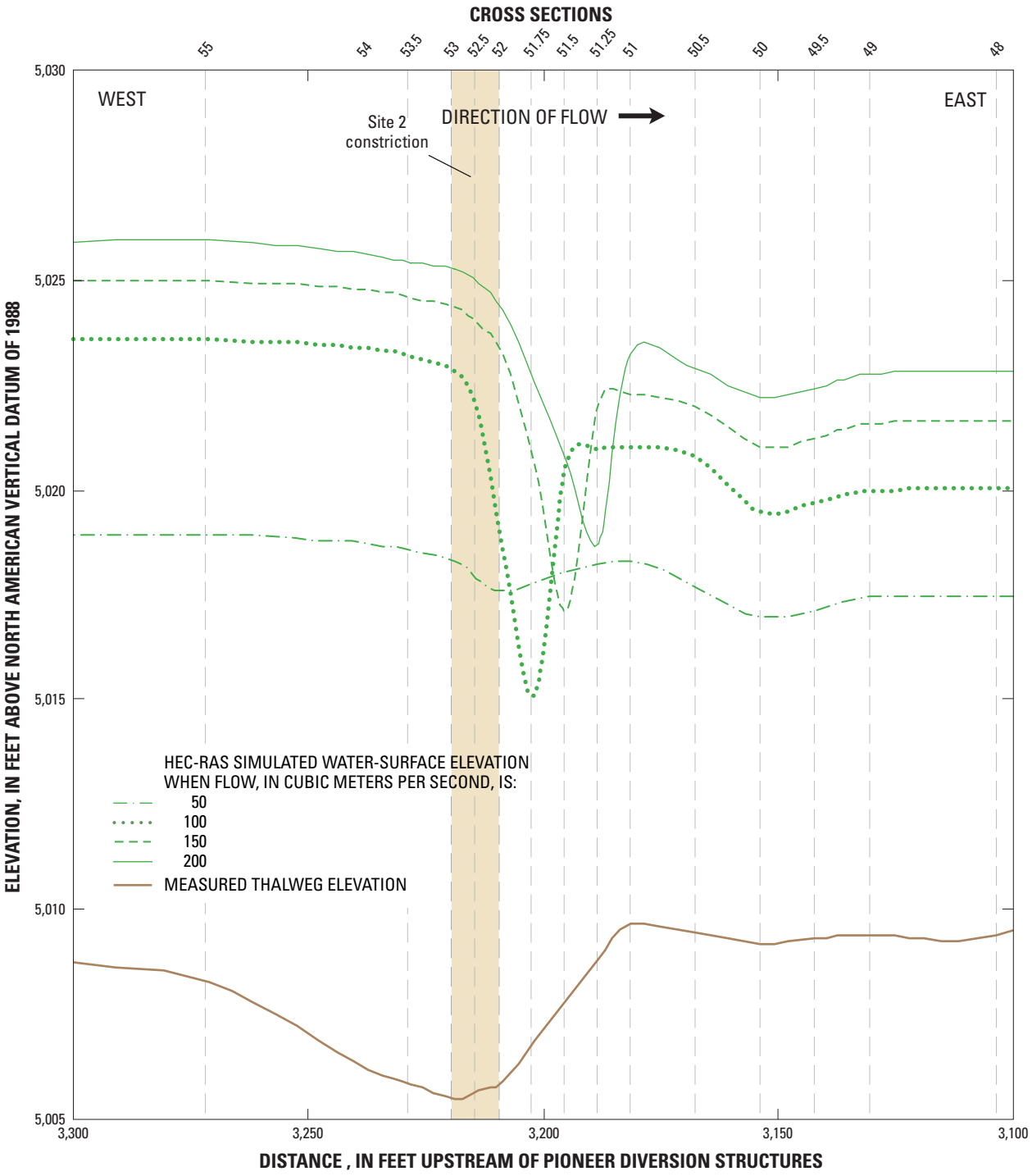

C. Site 2 constriction on Big Lost River

Figure 13.—Continued.

The development of extensive backwater upstream of the constrictions at sites 1 and 2 also is shown in figure 13*A*. Backwater effects are indicated in areas where the water-surface slope becomes significantly less than the channel slope. Simulation results indicate that backwater extends more than 2,000 ft upstream of the site 1 constriction for a peak flow of 200 m^3/s, and that backwater decreases as discharge decreases (fig. 13*A*). For a peak flow of 100 m^3/s, backwater at the site 1 constriction affects about 500 ft of the river upstream of the constriction. Backwater affects about 1,000 ft of the river upstream of the site 2 constriction for a peak flow of 100 m^3/s, but does not extend upstream of cross section 68 for the higher flow simulations. This is due to a local control at cross sections 69 and 70 (figs. 9*C* and 13*A*), where the cross-section flow area is much less than the adjacent sections (cross sections 68 and 71), and to supercritical flow through the site 2 constriction for flows equal to and greater than 100 m^3/s thereby limiting the upstream extent of backwater accumulation at higher flows.

Backwater also occurs upstream of cross section 8 (figs. 9*C* and 13*A*) and extends about 1,000 ft to almost cross section 23 for flows greater than 100 m^3/s. Backwater at this location occurs upstream of a minor constriction that was not emphasized in this study. The constriction at cross section 8 is a considerable distance downstream of BLR#6 and BLR#8, two locations in the Bureau of Reclamation's study where TRIM2D model simulations of water-surface elevations (Ostenaa and others, 1999) were used to establish the magnitude of peak flows with a 300-to 500-year return period.

The water-surface elevations upstream of several local controls within the modeled reach are affected by these controls at low flow. As discharge increases, however, many of these smaller controls become submerged and their influence on backwater accumulation gradually is reduced or drowned out, leaving a small depression on the water surface. For example, the control at cross section 66 probably becomes drowned out at flows equal to and greater than 50 m^3/s, thus limiting the accumulation of additional backwater at higher flows.

HEC-RAS model simulations indicate that the constrictions at sites 1 and 2 are the two major controls that have a significant effect on the accumulation of backwater in the study reach. These controls begin to have major effect when flows exceed 50 m^3/s at the site 2 constriction, and when flows exceed 100 m^3/s at the site 1 constriction.

The water-surface profile through the constrictions also is influenced by flow magnitude and channel size. As flow passes through these constrictions, flow depths decrease and velocities increase until there is no more decrease in flow depth. The observed effect depends on whether flow depth is greater than or less than critical depth. If flow depth is greater than critical depth, then flow depth or the water surface gradually will decrease as flow accelerates through the constriction. This occurs at the site 1 constriction for all modeled flows (fig. 13*B*). Flow through the site 1 constriction remains subcritical and the constriction does not act as a choke (see glossary at end of report). The streambed elevation also increases slightly downstream of the constriction (between cross sections 80 and 81). The elevated streambed downstream of the constriction likely is due to deceleration after flow exits the constriction and to the deposition of suspended sediment and bed load during flood recession.

If flow depth in the constriction is less than the critical depth, then flow is supercritical and a hydraulic jump forms downstream to bring the flow back to subcritical. This occurs at the site 2 constriction for peak flows of 100 m^3/s and greater (fig. 13*C*) and, in the case of supercritical flow, the constriction is considered to have choked flow. The maximum difference in flow depth through the constriction is greater for a peak flow of 100 m^3/s than at 200 m^3/s because the increased flow drowns out the effect of the constriction. Flows less than 70 m^3/s are subcritical and the water-surface elevation remains relatively steady through the constriction. At the site 2 constriction, the elevation of the streambed is significantly higher downstream of the constriction than upstream. This elevation difference likely is the result of the deposition of sediment and bed load caused by a hydraulic jump that is accompanied by a sudden reduction in flow velocity.

HEC-RAS Sensitivity Analysis

The sensitivity of the HEC-RAS model to variations in Manning's *n* and to variations in streambed elevation was evaluated. The procedure involves holding all input parameters constant except the one being analyzed and then varying that value. Changes in model-simulated water-surface elevations were used to determine the sensitivity of the model to changes in Manning's *n* and to changes in streambed elevation. For all sensitivity simulations, the boundary conditions at the upstream and downstream cross sections were not changed. All sensitivity analyses were conducted for a peak flow of 100 m^3/s—the flow that is of primary interest to this study. Water-surface elevation changes, however, at these high peak flows probably are more dependent on the magnitude of the flow than on the channel roughness indicated by Manning's *n*.

Manning's *n*

To determine the sensitivity of the model to variations in Manning's *n*, a series of simulations for a peak flow of 100 m^3/s were made in which the *n* value was varied by a factor of 0.5 and by a factor of 1.5 times the initial calibrated values.

Variations in the results of the simulations in response to changes in *n* values (figs. 14*A*, 14*B*, and 14*C*) indicate that the model is sensitive to the *n* values chosen to represent frictional resistance. Varying *n* values by 0.5 times (decreasing) and by 1.5 times (increasing) the calibrated values resulted in water-surface elevation changes from near 0 to about 2.0 ft (fig. 14*A*). Larger changes, from 4 to 5 ft, occur through the sites 1 and 2 constrictions (figs. 14*B* and 14*C*); however, these changes probably are more a reflection of flow regime

changes than changes in frictional resistance. The average difference was -0.8 and +1.0 ft for the 0.5 and 1.5 times simulations, respectively. The average difference in simulated water-surface elevations for all cross sections (1 through 108) and the cross sections at the paleoindicator sites [cross section 42 (BLR#8), cross section 72 (BLR#6), and cross section 98 (near the saddle area)] are shown in table 4. The differences are large and indicate that the model is sensitive to changes in *n* values for flows as large as 100 m^3/s. Stage is most sensitive to changes in Manning's *n* in channel-controlled sections of the river, and least sensitive in backwatered reaches where the dominant effect is the hydraulic control of the bedrock constrictions (for example immediately upstream of the site 2 constriction sections).

Ostenaa and others (1999, p. 31 and 32) indicated that water-surface elevations changed by 0.23 ft [7 centimeters (cm)] at cross section 42, and by 0.33 ft (10 cm) at cross section 98 when the *n* values (*n*=0.038) were adjusted by factors of 0.8 (*n*=0.03) and 1.6 (*n*=0.06) for a flow of 100 m^3/s. These results are presented in terms of the total change in water-surface elevation over a range of *n* values from *n*=0.03 to 0.06. For comparison purposes the HEC-RAS sensitivity changes range from 1.0 ft (30 cm at cross section 98) to 2.7 ft (82 cm at cross section 42) over a range of *n* values from *n*=0.012 to 0.038. 1-D models generally exhibit much greater sensitivity to variations in Manning's roughness coefficient than do 2-D models because roughness coefficients in 1-D models are used to account for both channel bed roughness and larger-scale resistance features such as channel curvature, bars, and bank irregularities. In 2-D models, roughness parameters generally are used to represent frictional resistance effects that result primarily from channel bottom roughness.

Table 4. Sensitivity of simulated water-surface elevations to changes in Manning's *n* (roughness coefficient) for a peak flow of 100 cubic meters per second on the Big Lost River upstream of the Pioneer diversion structures, Idaho National Engineering and Environmental Laboratory, Idaho.

[Location of cross sections is shown in figure 9*C*. Positive value indicates an increase in the water-surface elevation as compared with the calibrated model; negative value indicates a decrease in the water-surface elevation as compared with the calibrated model. –, no data]

Cross section	Difference in water-surface elevation, in feet, when Manning's *n* is changed by		
	HEC-RAS		TRIM2D
	1.5 times	0.5 times	1.6 to 0.8 times
42 (BLR#8)	1.4	–1.3	[1]0.2
72 (BLR#6)	1.1	–.9	–
98 (near Saddle area)	.6	–.4	.3
Average difference (cross sections 1 through 108; n=89)	1.0	–.8	–

[1]Value represents total difference between water-surface elevations for *n*=0.06 and *n*=0.03.

Cross-Section Geometry

Sensitivity simulations also were conducted to evaluate the effects of streambed scour on water-surface elevations during flooding. In these simulations, the streambed elevation between the toes of the confining banks was artificially lowered by 1, 2, and 4 ft except in areas where bedrock is exposed or was encountered at depths that were shallower than those selected for simulating the effects of streambed scour. All cross sections were lowered to the specified depths except as noted. For example, cross sections 1, 41, 59, 62, 65, 66, and 67 were not lowered because bedrock is present at the surface. Cross section 58 was lowered 1.4 ft to bedrock.

As anticipated, artificial lowering of the streambed in these model simulations resulted in water-surface elevations that were equal to or lower than those in the fixed-streambed simulations (fig. 15*A*). The presence of shallow bedrock at cross section 50 (fig. 15*B*) indicates that the streambed cannot be lowered more than 1.1 ft, and thus may act as a local control at lower flows. For the 100 m^3/s simulation, deeper flow depth drowns out the effect of this local control on water-surface elevations that would occur for smaller flow simulations. The average differences between the original simulation and the simulations in which the bed was lowered by 1, 2, and 4 ft were -0.4, -0.8, and -1.1 ft, respectively (table 5). The largest changes occur upstream of the site 1 constriction. Water-surface elevation differences increased as the streambed was lowered and varied from -1.0, -1.5, and -1.2 ft for the 4 ft lowering, and from -0.4, -0.5, and -0.2 ft for the 1 ft lowering at cross sections 42 (BLR#8), 72 (BLR#6), and 98 (near the saddle area), respectively.

Table 5. Sensitivity of simulated water-surface elevations to lowering of the streambed elevation by 1, 2, and 4 feet for a peak flow of 100 cubic meters per second on the Big Lost River upstream of the Pioneer diversion structures, Idaho National Engineering and Environmental Laboratory, Idaho.

[Location of cross sections is shown in figure 9*C*. Positive value indicates an increase in the water-surface elevation as compared with the calibrated model; negative value indicates a decrease in the water-surface elevation as compared with the calibrated model]

Cross section	Difference in water-surface elevation, in feet, when the streambed is lowered by		
	1 ft	2 feet	4 feet
42 (BLR#8)	-0.4	-0.6	-1.0
72 (BLR#6)	-.5	-1.0	-1.5
98 (near saddle area)	-.2	-.4	-1.2
Average difference (cross sections 1 through 108; n=89)	-.4	-.8	-1.1

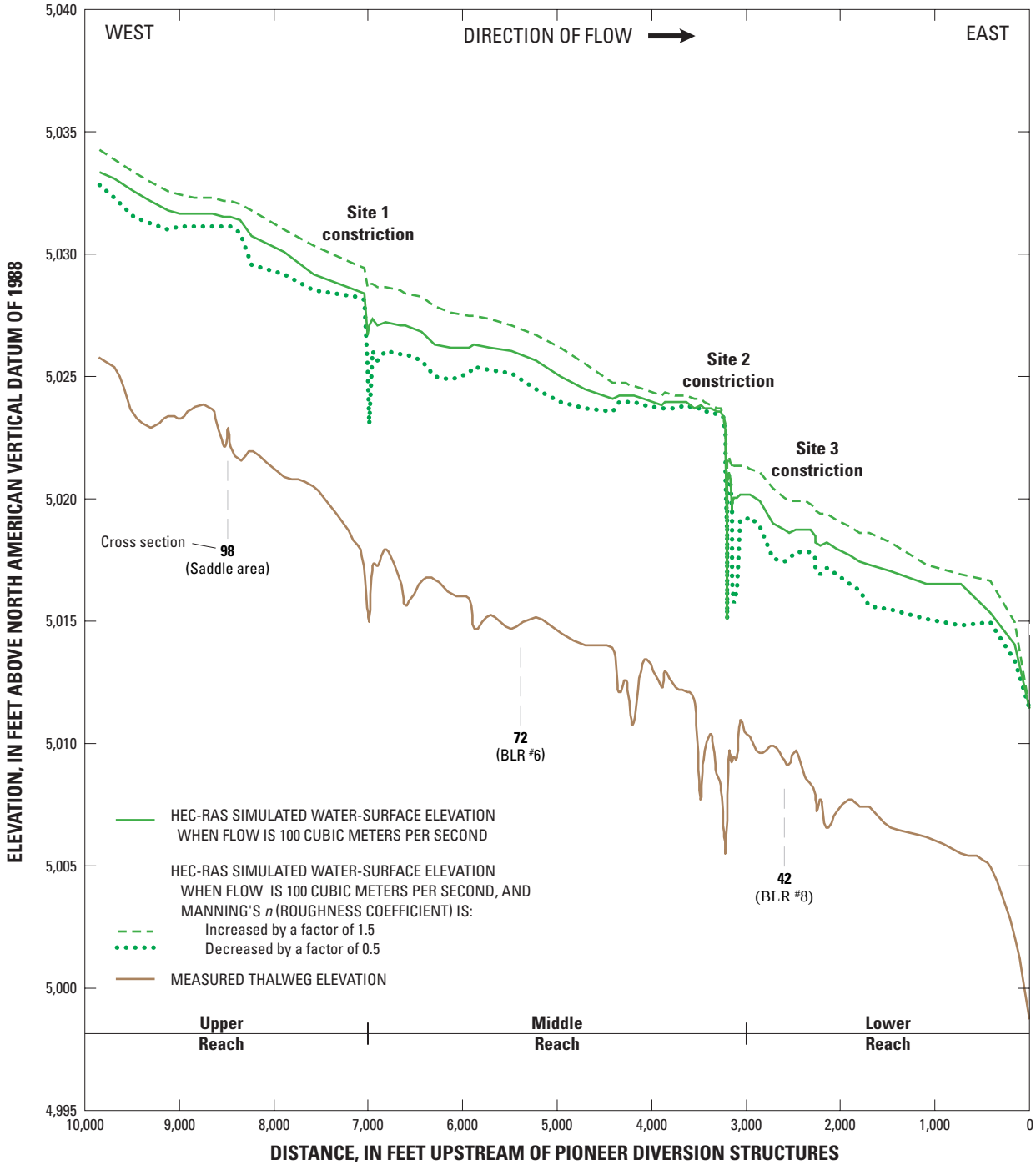

A. Big Lost River

Figure 14. Effects of changes in Manning's *n* (roughness coefficient) on HEC-RAS simulated water-surface elevations for a peak flow of 100 cubic meters per second on the Big Lost River and sites 1 and 2 constrictions upstream of the Pioneer diversion structures, Idaho National Engineering and Environmental Laboratory, Idaho.

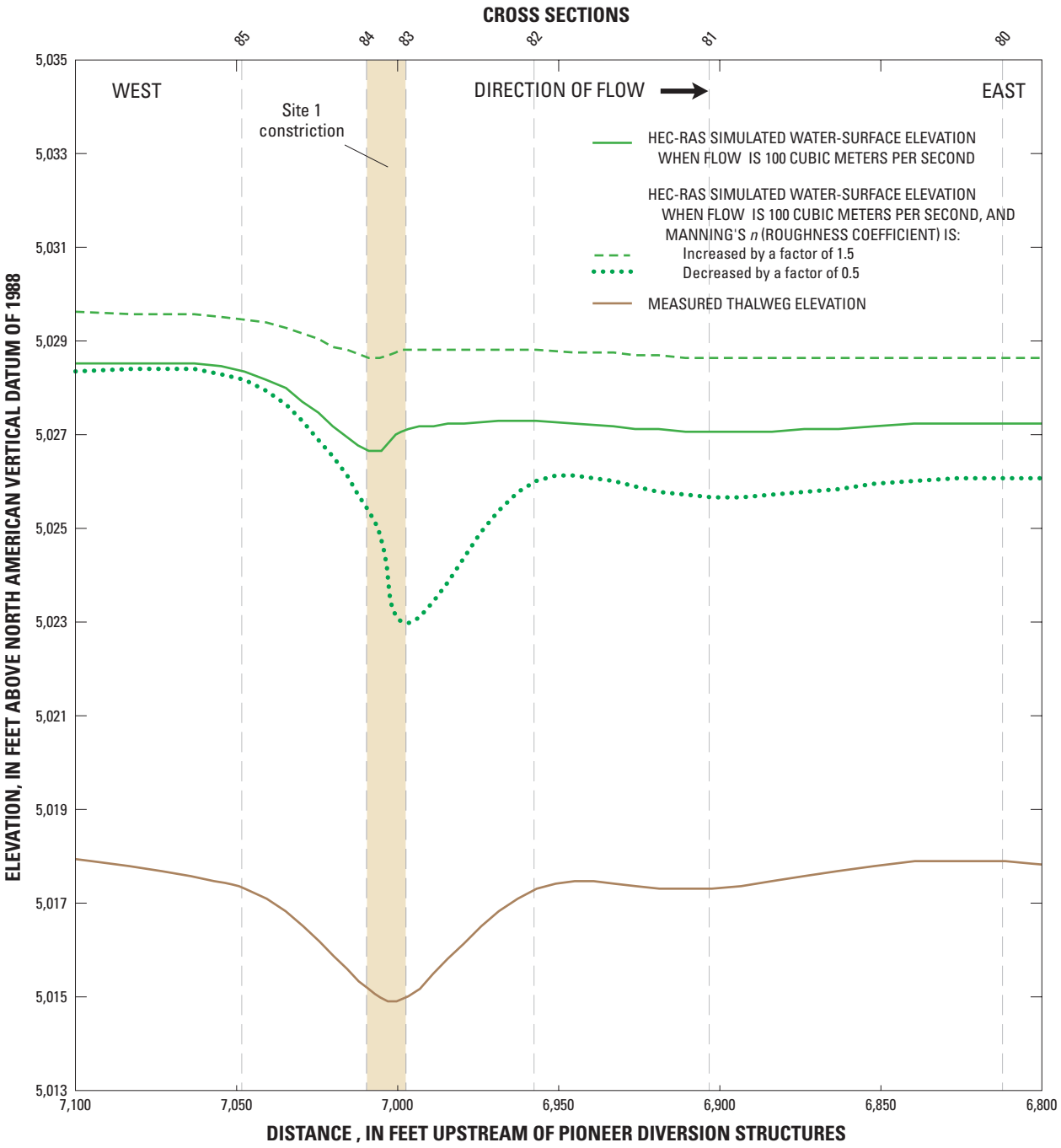

B. Site 1 constriction on the Big Lost River

Figure 14.—Continued.

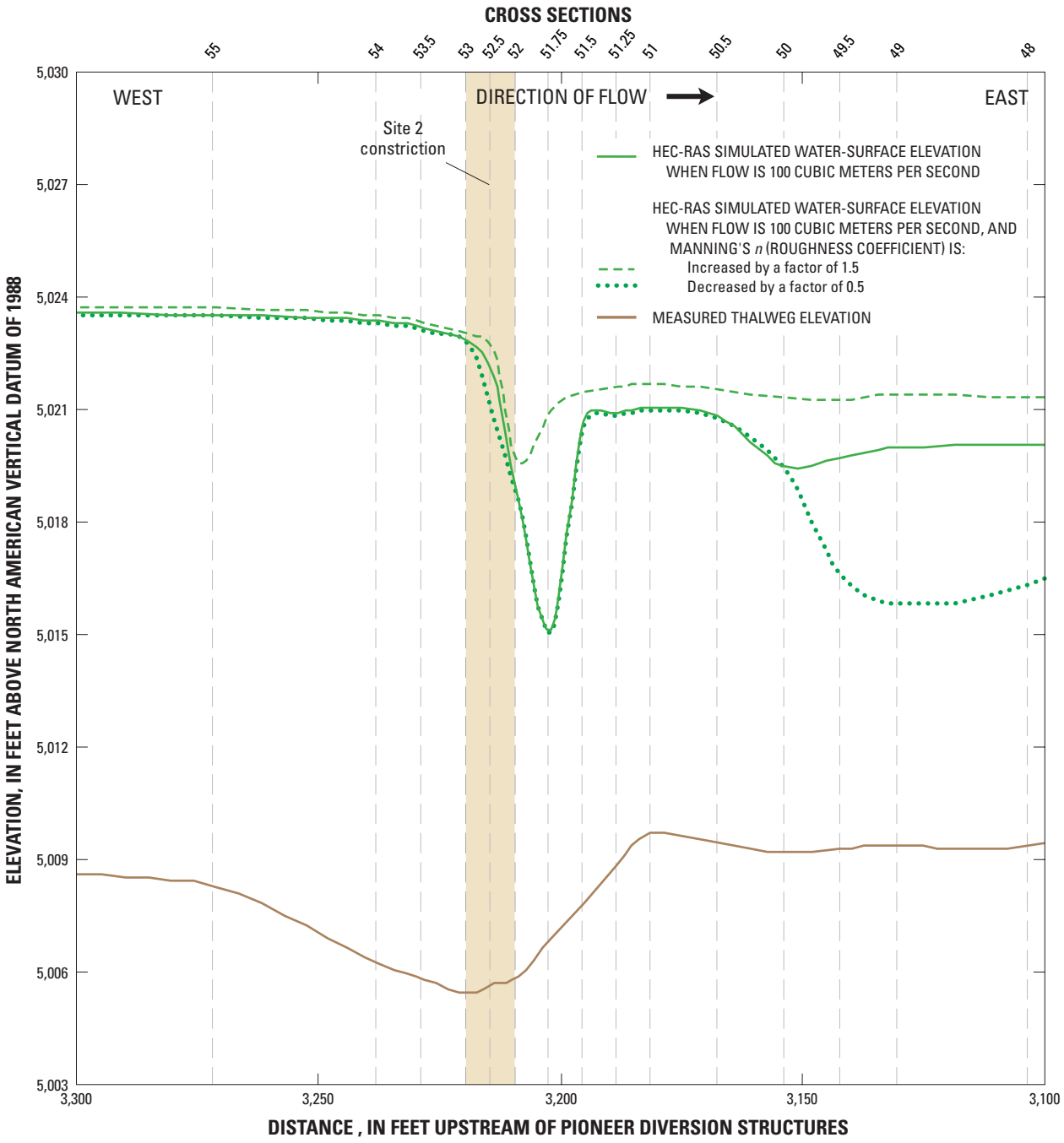

C. Site 2 constriction on Big Lost River

Figure 14.—Continued.

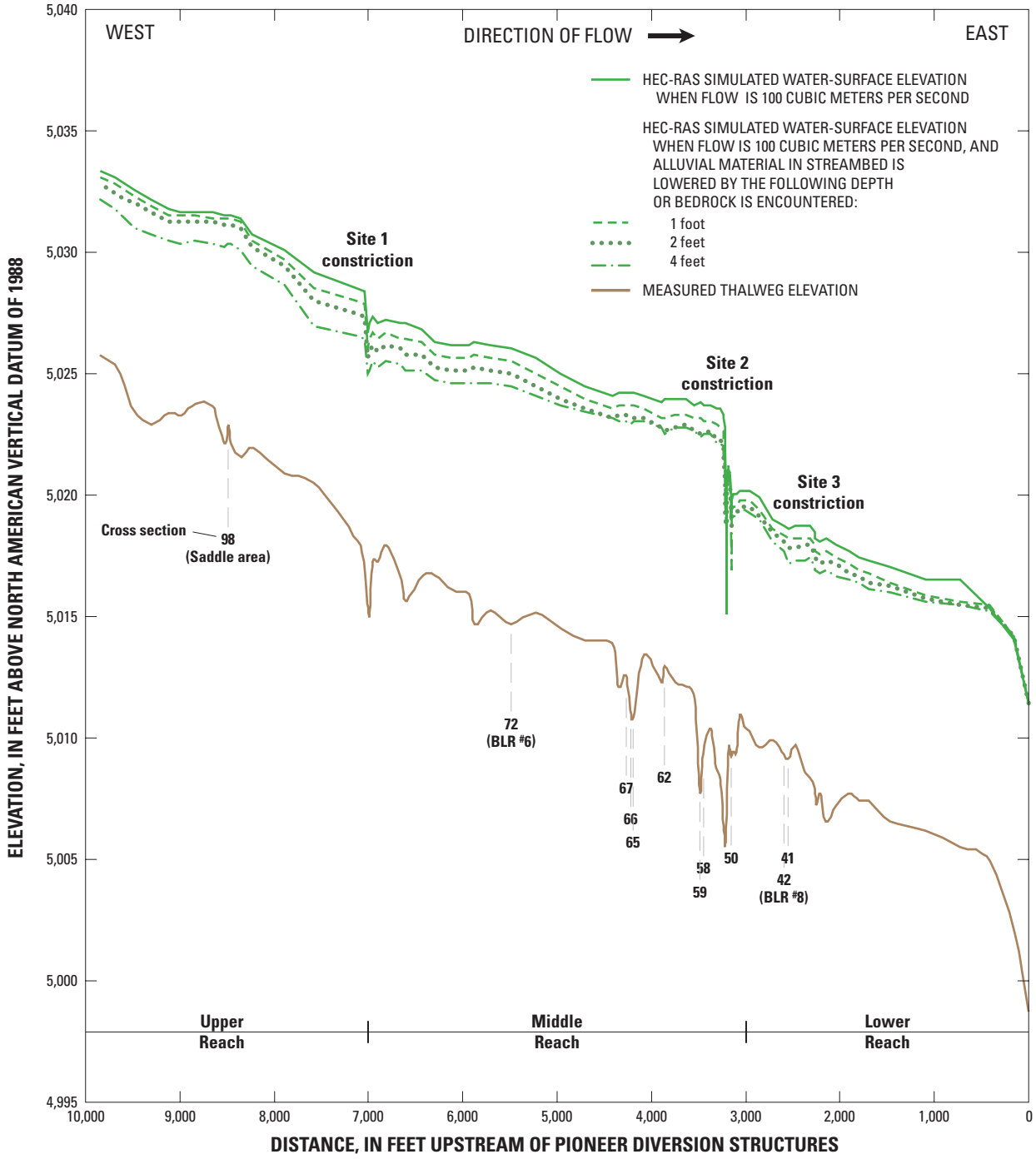

A. Big Lost River

Figure 15. Effects of lowering streambed elevation on HEC-RAS simulated water-surface elevations for a peak flow of 100 cubic meters per second on the Big Lost River and site 2 constriction upstream of the Pioneer diversion structures, Idaho National Engineering and Environmental Laboratory, Idaho.

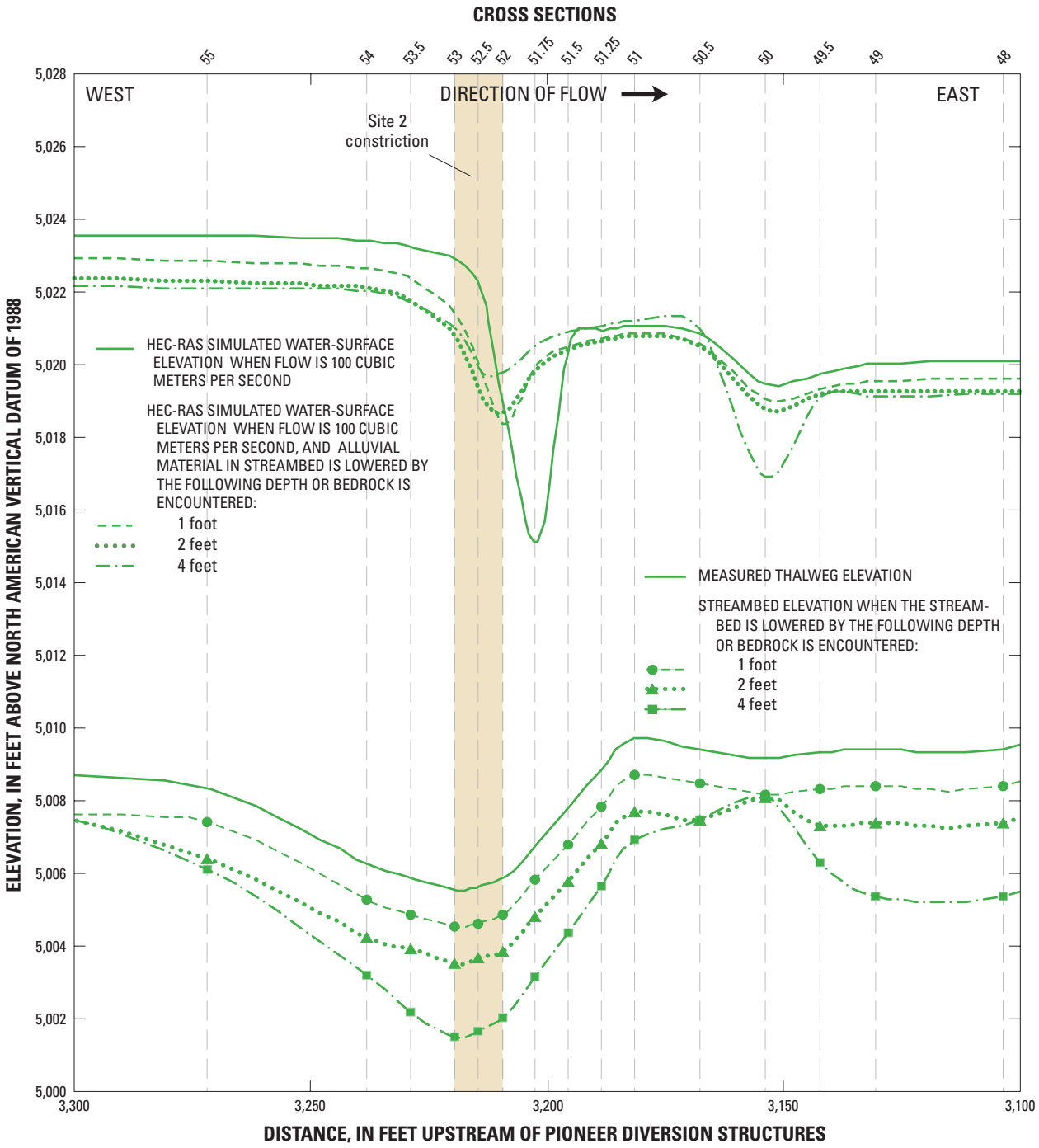

B. Site 2 constriction on the Big Lost River

Figure 15.—Continued.

HEC-6 Model Implementation

HEC-6 is a computer program that analyzes 1-D, gradually varied, steady flow in open channels with movable boundaries due to scour and deposition. HEC-6 allows for simultaneous erosion and deposition to occur depending on the competency of the stream to transport suspended sediment and bed load. HEC-6 does not, however, enable the simulation of bank erosion or lateral migration of the channel. This model can simulate the transport of sediment from upstream sources, transport of bed and suspended loads, and the effects of an armored surface layer on flow. The model can simulate transport of sediment sizes up to 2,048 mm and has 11 pre-defined sediment transport equations. The model first calculates the water-surface elevation at each cross section using the standard step method (Chow, 1959, p. 265). Potential sediment transport rates are computed at each section and are combined with the flow to determine the volume of suspended sediment within each reach. If this volume exceeds the transport capacity of the reach, deposition occurs in the reach. If the volume is less than the transport capacity of the reach, scouring occurs. After each time step, the model updates the channel geometry in each section of the reach to account for the effects of scour and deposition. Finally, the flow value from the next time step is read and a new water-surface elevation is calculated using the updated channel geometries. This procedure is repeated until all time steps specified by the user have been completed. The number of time steps is based on trial-and-error simulations to determine when changes in streambed elevation are minimal between one time step and the next. Sediment calculations are performed by grain-size class, which allows the model to simulate hydraulic sorting and to control the rate of erosion and redeposition of sediment during the simulation period.

Channel geometry characteristics (cross-section data, *n* values, reach lengths) used for the 70 m^3/s and greater HEC-RAS model (fig. 9*C*) were used to develop a HEC-6 model of the study reach. In addition, the HEC-6 model required information for each cross section on the elevation of bedrock beneath the streambed, movable bed limits, particle-size distribution for the armored surface layer and underlying channel fill, bed and sediment loads of the incoming flows, and the selection of an appropriate transport equation. HEC-6 specifies that no scour will occur below the specified model bottom and outside the lateral limits of the movable bed. For this study, bedrock was defined as the model bottom. The model bottom was determined from measurements of bedrock elevation during trenching and from field-surveyed cross sections where bedrock occurs at or near the surface of the channel. At cross sections where no trenches were constructed or where no bedrock was present at the surface, the elevation was estimated by linearly interpolating between cross sections or trenches with known bedrock elevations. Movable bed limits were defined as the toes of the channel banks. For most cross sections this was easy to determine because of the flatness of the streambed profile and the well-defined boundaries of the channel banks. For bed material distributions, particle-size analyses obtained from trench samples and sampling of the armored surface layer (appendixes 1 and 2) were input into the model at the appropriate sections. For sections without particle-size data, the model linearly interpolated the bed material distribution from adjacent sections where these data were available.

Because no measurements were available on sediment inflow to the model at the upstream end of the model reach (cross section 108), several transport-capacity equations were used to estimate the incoming sediment load at this section. Many transport equations have been used for gravel-bed rivers. The Meyer-Peter and Müller equation (1948) and the mountain-river modification of the Schoklitsch (1962) equation were used in this study because river conditions in the study area, defined by thalweg slope, channel width, flow depths, and flow velocities were well suited to these equations. Results from the solution of these equations were averaged for each particle-size fraction and used in the model to represent the incoming sediment load at cross section 108. The incoming sediment load was calculated for each peak flow that was simulated.

The HEC-6 model requires that the user select a sediment-discharge equation. Eleven transport functions are available in the HEC-6 model. These equations were developed under different flow, hydraulic, and sediment conditions. Some of these equations are used for sand-bed streams, gravel-bed streams, or both; small streams, large streams, or both; and some are used to simulate bed load, suspended load, or both (total load). Stream-discharge equations based on the stream-power concept are more accurate than those based on other concepts (Gomez and Church, 1989; Nakato, 1990; Yang and Huang, 2001) such as the regression-equation approach of Rottner (1959), the probabilistic approach of Einstein (1950), and the shear-stress approach of Kalinske (1947) and Meyer-Peter and Müller (1948). For the Big Lost River study reach, an equation was needed that can compute total load for particles ranging in size from very-fine sands to cobbles. Although the Ackers and White (1973) equation was developed from particles ranging in size from 0.04 to 4 mm, White and Day (1982) and Yang and Huang (2001) successfully applied the Ackers and White (1973) equation to particles as large as 11 and 32 mm, respectively. Muskatirovic (2005) also demonstrated that the Ackers and White (1973) equation performed the best to measured data. Her analysis included several dozen rivers and creeks in the Salmon River basin, Idaho with d_{50}'s ranging from 10 mm to greater than 100 mm and with channel slopes ranging from mild to very steep. In a paper about accuracies of transport equations, Yang and Huang (2001) indicated that the Ackers and White (1973) equation was quite accurate for a wide range of stream power. Therefore, the Ackers and White (1973) equation was selected as the transport equation for the HEC-6 simulations.

At the site 2 constriction, HEC-RAS model simulations indicated that flows of 100 and 150 m^3/s are supercritical. These simulations also showed that subcritical flow was reestablished after one or two cross sections, about 10 to 20 ft downstream of the location where flow became critical (fig. 13*C*). The HEC-6 model does not have the capability to transition from subcritical to supercritical flow and back again. If supercritical conditions had persisted for an appreciable distance, then separate models would be needed to simulate each flow condition. Because subcritical flow was reestablished within a relatively short distance downstream of the site 2 constriction, only one model was developed to represent scour at this location.

All flows were held constant during each simulation, and each simulation was run until water-surface elevations and streambed elevations remained nearly constant from one time step to the next. A time step of 0.001 day (86.4 seconds) was used to simulate peak flows equal to and greater than 70 m^3/s. It took about 2,000 time-step iterations or about 2 days of model simulation time, equivalent to 5 to 10 minutes of computer runtime, for the computations to stabilize using a time step of 0.001 day.

HEC-6 Simulation Results

Water-surface elevations and changes in streambed elevations for peak flows of 70, 100, 150, 187, and 200 m^3/s were simulated with the HEC-6 model. For presentation clarity, only results for simulations of 70, 100, and 150 m^3/s are shown in figure 16*A*. These results also are used later in this report for comparisons with HEC-RAS and TRIM2D simulation results.

The constrictions at sites 1 and 2 produce noticeable backwater effects at upstream distances comparable to those of the HEC-RAS simulations for a peak flow of 150 m^3/s. At lower peak flows HEC-6 backwater effects are less pronounced than those for the HEC-RAS simulations (compare figs. 13*A* and 16*A*). For a peak flow of 150 m^3/s, backwater effects also can be seen in the simulated water surface upstream of the site 3 constriction (fig. 16*A*). Within the site 2 constriction water-surface elevations decline sharply, from 2 to 4 ft between cross sections 49 to 55 for peak flows of 100 and 150 m^3/s, respectively (fig. 16*B*), and about 1 ft for a peak flow of 70 m^3/s.

Profiles for the movable streambed in HEC-6 also are shown in figure 16*A* for peak flows of 70, 100, and 150 m^3/s. The measured streambed profile is markedly different from the streambed profile that develops during the passage of a flood (fig. 16*A*). Both streambed erosion and sediment deposition occur within each of the three reaches. Immediately upstream of the sites 2 and 3 constrictions and near the center section of the middle reach several feet of sediment accumulation is simulated by the HEC-6 model for all three peak flows.

The average differences in streambed elevations between the measured thalweg and the HEC-6 thalweg for all three peak flows are given in table 6. Average differences for the entire model reach range from 0.5 to 0.7 ft for the 70, 100, and 150 m^3/s flow simulations and indicate that streambed erosion dominates in the upper and middle reaches of the river and that substantial sediment deposition occurs in the lower reach for all simulated flows shown in figure 16*A*.

At the site 2 constriction, the streambed was eroded to bedrock (fig. 16*B*) for flows greater than and equal to 70 m^3/s. At the sites 1 and 3 constrictions, flows did not scour the streambed completely to bedrock. For a peak flow of 150 m^3/s, the residual thickness of the channel fill inside the sites 1 and 3 constrictions averaged about 1.0 and 1.5 ft, respectively.

At the BLR#8 (cross section 42) paleoindicator site, the HEC-6 simulated streambed elevation was 0.4 ft higher than the measured streambed elevation for peak flows of 70 and 100 m^3/s, and 1.1 ft lower for a peak flow of 150 m^3/s. At BLR#6 (cross section 72) the HEC-6 simulated streambed was 1.0, 2.6, and 0.2 ft lower than the measured streambed for peak flows of 70, 100, and 150 m^3/s, respectively (table 6 and fig. 16*A*). Near the saddle area (cross section 98), the HEC-6 simulated streambed elevation was slightly higher, from 0.1 to 0.2 ft, than the measured streambed for the three simulated peak flows.

Quantitative comparisons of the HEC-RAS and HEC-6 thalweg profiles, for a peak flow of 100 m^3/s, are represented by the slope of a linear-regression fit to the thalwegs along the upper, middle, and lower reaches of the river as shown in figure 17. Linear-regression fits to the resulting HEC-6 thalweg profiles indicate a slightly steeper slope along the upper reach, a flatter slope along the middle reach, and almost no change in slope along the lower reach of the river. Streambed elevation changes occur in all three reaches. The most notable of these changes is the nearly 3 ft decrease in elevation at the upstream end of the middle reach, and the 1 ft increase in elevation along the entire length of the lower reach.

Figures 16 and 17 indicate considerable disturbance to the measured thalweg profile resulting from a combination of sediment deposition and streambed erosion. The resulting HEC-6 thalweg profiles represent equilibrium profiles for sustained, steady flow at the simulated peak discharge. During the receding limb of a flood and during long periods of low to moderate flow between major flood events, much of the temporary disturbance to the channel bed resulting from a large flood is destroyed. The last major flood event (event with the highest peak flow) in the study area occurred in 1958 prior to construction of the INEEL diversion dam. The peak flow for the 1958 event was 33.7 m^3/s (1,190 ft^3/s) (fig. 11), considerably less than the simulated peak flows shown in figure 16*A*. Since enlargement of the diversion dam in 1984, peak flows in the study area have been limited to a maximum of about 13.2 m^3/s (466 ft^3/s) (fig. 10).

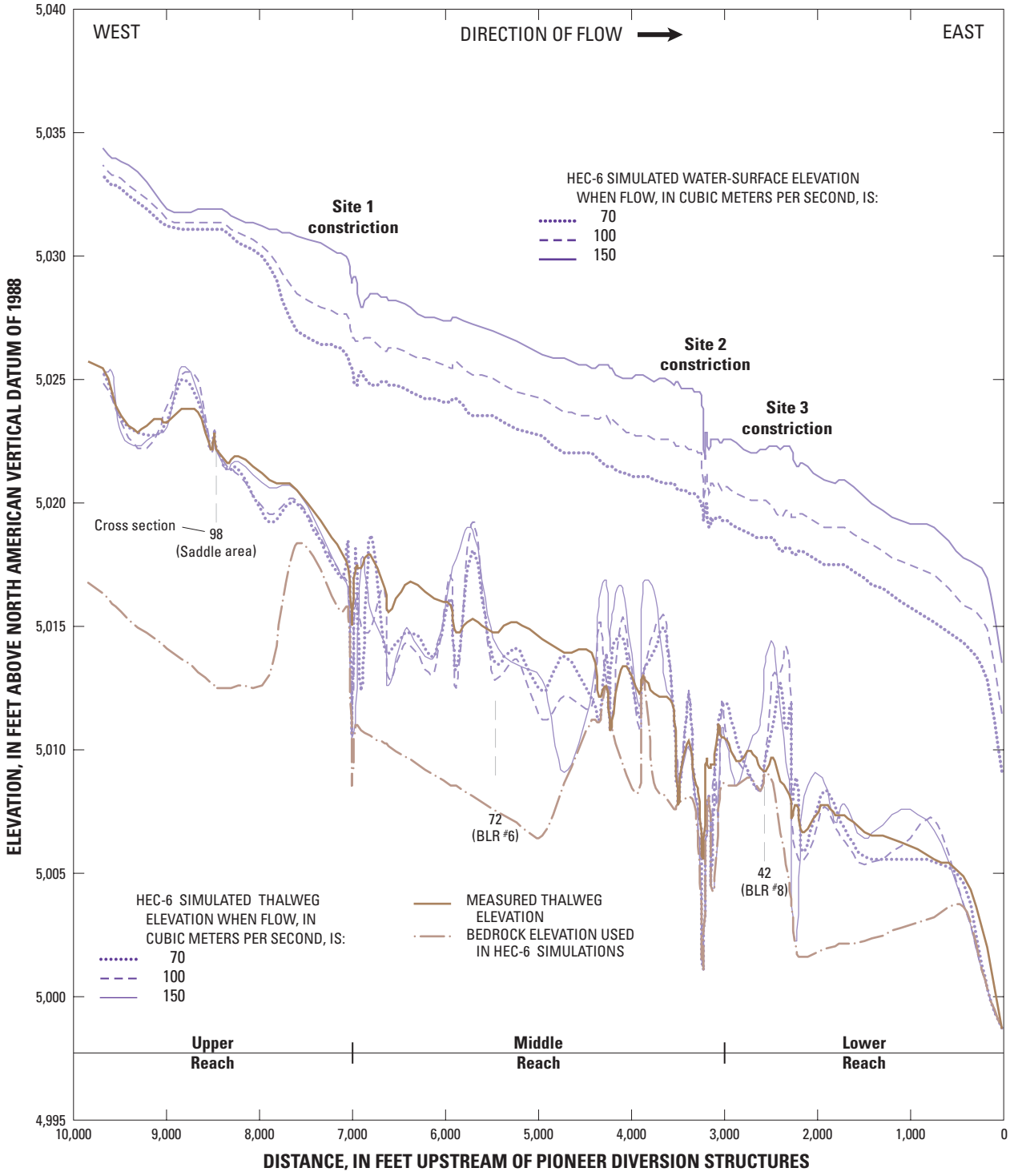

A. Big Lost River

Figure 16. HEC-6 simulated water-surface and thalweg elevations for peak flows of 70, 100, and 150 cubic meters per second on the Big Lost River and at the site 2 constriction upstream of the Pioneer diversion structures, Idaho National Engineering and Environmental Laboratory, Idaho.

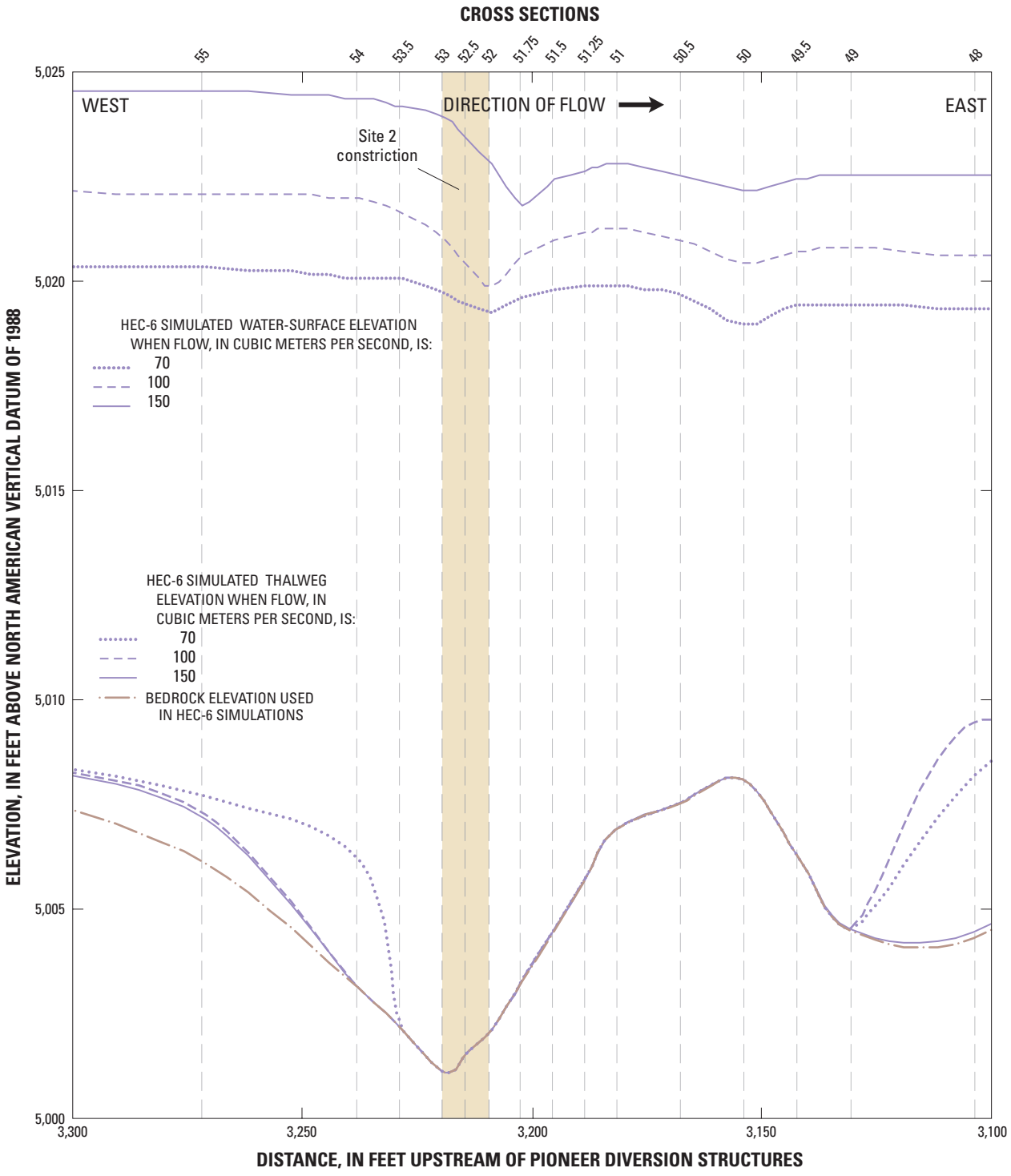

B. Site 2 constriction on the Big Lost River

Figure 16.—Continued.

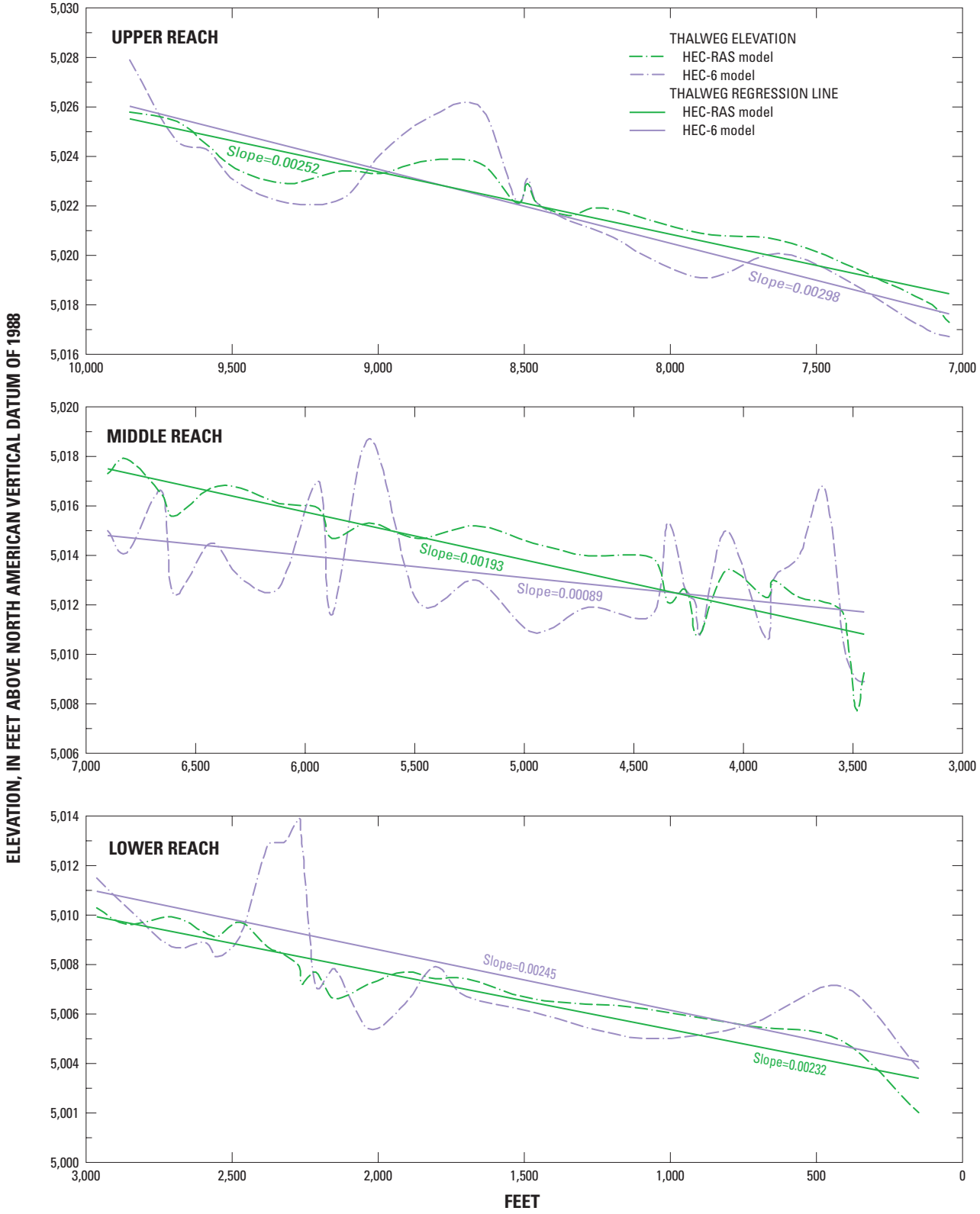

Figure 17. Linear-regression fits to the HEC-RAS and HEC-6 thalweg elevations for a peak flow of 100 cubic meters per second for the upper, middle, and lower reaches of the Big Lost River upstream of the Pioneer diversion structures, Idaho National Engineering and Environmental Laboratory, Idaho.

Table 6. Differences in HEC-RAS and HEC-6 simulated water-surface and thalweg elevations for peak flows of 70, 100, and 150 cubic meters per second on the Big Lost River upstream of the Pioneer diversion structures, Idaho National Engineering and Environmental Laboratory, Idaho.

[Location of cross sections is shown in figure 9*C*. m^3/s, cubic meter per second]

Cross section	Differences in water-surface elevations, $HEC\text{-}RAS_{elev}$ minus $HEC\text{-}6_{elev}$ in feet, for a peak flow of			Differences in thalweg elevations, $HEC\text{-}RAS_{elev}$ minus $HEC\text{-}6_{elev}$ in feet, for a peak flow of		
	70 m^3/s	100 m^3/s	150 m^3/s	70 m^3/s	100 m^3/s	150 m^3/s
20	-2.2	-2.4	-2.4	0.5	1.2	-0.3
42 (BLR#8)	-1.6	-1.4	-1.6	.4	.4	-1.1
56	.6	1.5	.5	.3	.4	.3
72 (BLR#6)	.5	1.0	.6	1.0	2.6	.2
76	-.0	.5	.2	2.3	3.4	2.3
98 (near saddle area)	-.2	.2	.5	-.1	-.2	-.1
	Average difference			Average difference		
Entire reach (all, n = 89)	-0.4	-0.1	-0.4	0.5	0.7	0.5
Upper reach (85 to 108)	-.4	.0	.3	.1	.1	.1
Middle reach (58 to 81)	.4	1.0	.4	.4	.7	-.4
Lower reach (3 to 45)	-1.5	-1.5	-1.8	-1.0	-.9	-.9

Comparisons of HEC-6 and HEC-RAS Water-Surface Elevations

Simulated HEC-6 and HEC-RAS water-surface elevations for peak flows of 70, 100, and 150 m^3/s are shown in figure 18. The average difference in water-surface elevations simulated by the two models along the entire model reach is less than 0.5 ft for the three flows (table 6). The most notable difference in the water-surface elevation profiles simulated by these two models occurs between the combined upper and middle reaches of the river and the lower reach of the river. Along the upper and middle reaches of the river HEC-6 water-surface elevations generally are lower than those of HEC-RAS, and along the lower reach of the river HEC-6 water-surface elevations everywhere are higher than those of HEC-RAS. Higher HEC-6 water-surface elevations reflect the effects of sediment deposition in the lower reach of the river, and lower HEC-6 water-surface elevations reflect the effects of erosion in the upper and middle reaches of the river. These differences are consistent with changes in streambed elevation as reflected in the HEC-6 thalweg profiles shown in figure 16*A*.

Differences in water-surface elevations at the paleoindicator sites also are shown in table 6. Differences in water-surface elevations at the paleoindicator sites indicate that flows lower than those simulated by the HEC-RAS model will overtop the BLR#8 (cross section 42) site because of sediment deposition, and that flows higher than those simulated by the HEC-RAS model will overtop the saddle area (near cross section 98) and BLR#6 (cross section 72) because of streambed erosion.

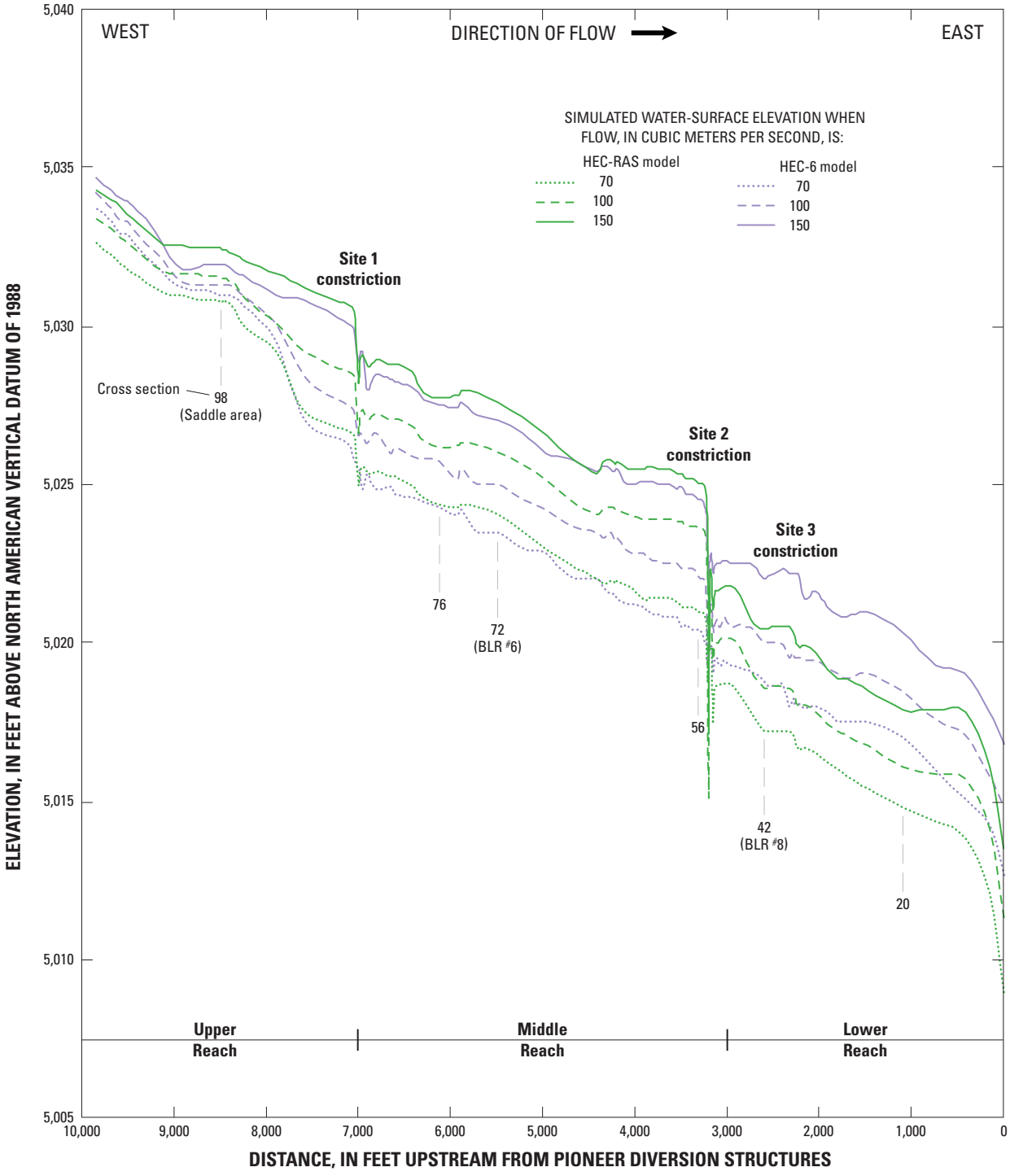

Figure 18. HEC-RAS and HEC-6 simulated water-surface elevations for peak flows of 70, 100, and 150 cubic meters per second on the Big Lost River upstream of the Pioneer diversion structures, Idaho National Engineering and Environmental Laboratory, Idaho.

Comparisons of Channel and Floodplain Geometries Used in HEC-RAS and HEC-6 Models with Those Used in TRIM2D Model

Channel and floodplain geometries are defined by thalweg slope, cross-section flow area, and changes that occur in these features along the course of the river. The field survey that was conducted to define channel and floodplain geometries for the HEC-RAS and HEC-6 models revealed topographic errors and inconsistencies in the 2-ft contour base map that was used in the TRIM2D model. These included a datum shift of 3.484 ft between the NGVD 29 datum and the NAVD 88 datum (the established INEEL datum standard), and elevation errors amounting to about 5.0 ft of relief between the upstream and downstream ends of the study area. Although the TRIM2D model did not simulate the effects of streambed erosion on water-surface elevations, differences between the channel and floodplain geometries used in the TRIM2D model and those used in the HEC-RAS/HEC-6 models probably are the primary reasons for the large differences in simulated water-surface elevations, flow depths, flow velocities, and stream power between the TRIM2D and HEC-RAS/HEC-6 models that are described in the section "Comparisons of HEC-RAS, HEC-6, and TRIM2D Simulation Results."

Channel and floodplain geometries used in the TRIM2D model were constructed from a 2-ft contour map of the study area prepared by Aerial Mapping, Inc. (Wayne Eskridge, Aerial Mapping, Inc., written commun., 1996). The 2-ft contour interval implies a topographic resolution of ±1 ft. Inside the main channel, spacing between contours on the 2-ft contour map averaged 932 ft. The maximum distance between adjacent contours was 2,184 ft, and the minimum distance was 50 ft. Twelve contour lines were used to map the 24 ft of relief between the upstream and downstream ends of the model reach shown on the 2-ft contour map. Channel and floodplain geometries used in the TRIM2D model were represented by elevations assigned to a rectangular array of grid nodes located at 1-m spacings that were subsequently subsampled to generate a computational grid consisting of 2×2 m cells. The TRIM2D computational grid consisted of about 4.2 million cells; of these, about 2.5 million were active (Ostenaa and others, 1999, p. 31). Because of the sparse contour spacing, interpolation over long distances was required to construct the elevation control grid used in the TRIM2D model.

The channel and floodplain geometries used in the HEC-RAS and HEC-6 models were constructed from (1) a field survey of the channel thalweg that incorporated more than 430 leveling stations spaced at distances averaging 23 ft; (2) 76 field-surveyed cross sections oriented perpendicular to the direction of flow and spaced at intervals ranging from 50 to several hundred feet depending on complexity and uniformity of the channel section; and (3) TIN-generated, TIN-extended, and linearly interpolated cross sections. The accuracy of the field-surveyed data was better than ±0.1 ft. Field-surveyed cross sections were extended and 31 additional cross sections were added using the TIN interpolating procedure, described in the section "TIN-Generated Cross Sections," and elevation data from a 1-ft contour map of the study area that was prepared in 2000 by the Bureau of Reclamation (D.A. Ostenaa, Bureau of Reclamation, written commun., 2001). The elevation datum for this map (figs. 5*A* and 5*B*) is 1.955 ft lower than the NAVD 88 datum, and an elevation correction of +1.955 ft is needed to convert elevations on this map so that these conform to the NAVD 88 datum. The elevation accuracy of the channel cross sections that were constructed using the TIN interpolating procedure was ±0.5 ft.

Thalwegs

Profiles of the field-surveyed and TIN-generated thalweg used in the HEC-RAS model (and for initial conditions in the HEC-6 model), and the 2×2 m grid-generated thalweg used in the TRIM2D model are shown in figure 19. Elevations of the TRIM2D thalweg have been adjusted by +3.484 ft to account for the elevation difference between the NGVD 29 datum and NAVD 88 datum. The profiles indicate major differences in the elevation, slope, and topographic character of the thalwegs used in the HEC-RAS and TRIM2D models.

The elevation of the TRIM2D thalweg is higher than the HEC-RAS thalweg throughout the model reach. Elevation differences increase in a downstream direction. At the downstream end of the model reach, cross section 1, the elevation of the TRIM2D thalweg is about 7 ft higher than the HEC-RAS thalweg (fig. 19). The average elevation difference, based on a one-to-one comparison of the field-surveyed and TIN-generated data with those extracted from the computational grid used in the TRIM2D model, was 2.5 ft (table 7). At the paleoindicator sites, BLR#8 (cross section 42), BLR#6 (cross section 72), and the saddle area (near cross section 98), the TRIM2D streambed was 2.2, 2.8, and 0.6 ft higher, respectively, than the HEC-RAS streambed. Elevation differences between the upstream (cross section 108) and downstream (cross section 1) ends of the model reach indicate that the overall slope of the TRIM2D thalweg (0.0019) is 15 percent less than the slope of the HEC-RAS thalweg (0.0023). The higher TRIM2D streambed elevations (adjusted for the +3.484 ft elevation difference between the NGVD 29 and NAVD 88 datums) and flatter thalweg slope imply that TRIM2D-simulated water-surface elevations should be higher than those of the HEC-RAS and HEC-6 models.

The topographic character of the TRIM2D and HEC-RAS thalwegs also differ noticeably (fig. 19). The TRIM2D thalweg is characterized by numerous high- and low-amplitude undulations, resulting in a pattern of positive- and negative-relief features that obscures the more uniform character of the profile. In contrast, the field-surveyed thalweg is punctuated by narrow, widely-spaced, and deeply-incised negative-relief features that, for the most part, have only a very local influence on the thalweg slope.

Table 7. Differences in HEC-RAS and TRIM2D thalweg elevations and slopes along the upper, middle, and lower reaches of the Big Lost River upstream of the Pioneer diversion structures, Idaho National Engineering and Environmental Laboratory, Idaho.

[Location of sampling sites is shown in figure 9C. **Abbreviations**: ft, ft; ft/ft, ft per ft]

Cross section	Difference in thalweg elevation ($TRIM2D_{elev}$ minus $HEC\text{-}RAS_{elev}$) (ft)
42 (BLR#8)	2.2
72 (BLR#6)	2.8
98 (near saddle area)	.6

	Average difference (ft)	Thalweg slope (ft/ft)	
		HEC-RAS	TRIM2D
Entire reach (all, n = 89)	2.5	0.0023	0.0019
Upper reach (85 to 108)	1.3	.0025	.0022
Middle reach (58 to 81)	2.0	.0019	.0015
Lower reach (3 to 45)	3.1	.0023	.0013

A quantitative comparison of elevation and topographic differences between the TRIM2D and HEC-RAS thalwegs is represented by the slope of a linear-regression fit to the thalwegs along the upper, middle, and lower reaches of the river. The upper-reach regression extends from the upstream model boundary (cross section 108) to a point immediately upstream (cross section 85) of the site 1 constriction, the middle-reach regression from a point immediately downstream (cross section 81) of the site 1 constriction to a point about 500 ft upstream (cross section 58) of the site 2 constriction, and the lower-reach regression from a point immediately downstream (cross section 45) of the site 2 constriction to a point about 250 ft (cross section 3) upstream of the downstream boundary (fig. 19). The regression fits do not include (1) the scoured depressions within the site 1 and site 2 constrictions, and (2) the free outfall section of the lower reach near the downstream boundary. These were excluded from the slope computations to avoid biasing that would result from inclusion of these topographically prominent, but locally-isolated negative-relief features that appear in the field-surveyed thalweg profile.

The regression fits along the upper, middle, and lower reaches of the river are shown in figure 20. The slope of the TRIM2D thalweg is 13 percent less than the HEC-RAS thalweg along the upper reach, 23 percent less along the middle reach, and 44 percent less along the lower reach.

The undulating pattern of positive- and negative-relief features along the TRIM2D thalweg is conspicuous near cross section 72 (BLR#6), cross section 42 (BLR#8), and cross section 20 (fig. 19). The undulating pattern of the thalweg slope in these areas tends to obscure the overall smoothness of the thalweg because the 2-ft contour map (Eskridge, Aerial Mapping Inc., 1996) did not have sufficient resolution to support construction of a computational grid for the 2-D model. This may, to some extent, account for (1) the very large difference in water-surface elevations between the HEC-RAS and TRIM2D simulations for a flow of 70 m^3/s, (2) an anomalous bulge in the water surface near cross section 72 (BLR#6), and (3) higher water-surface elevations than simulated by HEC-RAS and HEC-6 as described in the section "Comparisons of HEC-RAS, HEC-6, and TRIM2D Simulation Results."

Channel Cross Sections

Comparisons of selected cross sections used in the HEC-RAS model (and for the initial conditions in the HEC-6 model) with those used in the TRIM2D model are shown in figure 21. The locations of these six cross sections are shown in figure 9. Elevations of the TRIM2D floodplain and main channel are higher than those of HEC-RAS at cross sections 20, 42, and 56 (fig. 21). Elevations of the TRIM2D floodplain are lower and the elevations of the main channel are higher than HEC-RAS at cross sections 72 and 76 (fig. 21). Floodplain and channel elevation differences are small near the upstream boundary (cross section 108) and are large near the downstream boundary of the model reach (cross section 1). The transition between predominantly higher floodplain elevations and lower floodplain elevations between the TRIM2D and HEC-RAS models appears to occur in the middle reach of the river between cross sections 56 and 72.

Graphical comparisons of the cross sections used in the HEC-RAS (and for initial conditions in the HEC-6 model) with those used in the TRIM2D model are represented by the stage-area and depth-area curves shown in figure 22. The depth-area curves indicate larger cross-section areas per unit of depth for the TRIM2D cross sections than for the HEC-RAS cross sections. At low stages, the TRIM2D and HEC-RAS stage-area curves, corrected for elevation datum differences, are similar; at high stages, however, these curves deviate considerably. The stage-area curves, corrected for elevation datum differences, indicate similar TRIM2D and HEC-RAS stage-area relations at cross sections 42, 72, 76, and 98 for flows that remain within the confines of the main channel and are less than about 10 ft deep, and higher stage-area relations for flow that occurs outside the main channel. Lower TRIM2D stage-area relations are indicated for flow that occurs both within and outside the confines of the main channel at cross sections 20 and 56.

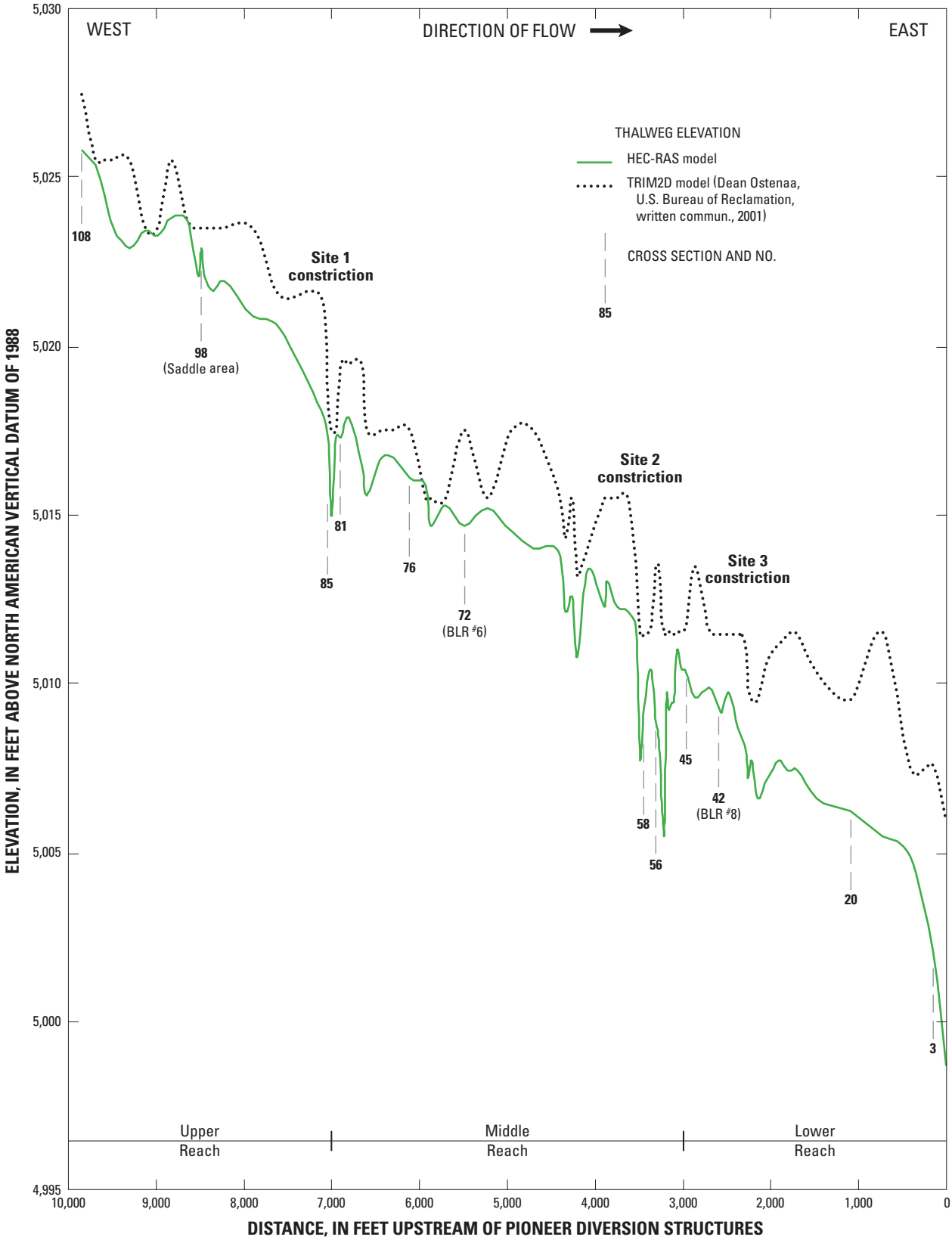

Figure 19. Thalweg elevations used in the HEC-RAS and TRIM2D models of the Big Lost River upstream of the Pioneer diversion structures, Idaho National Engineering and Environmental Laboratory, Idaho.

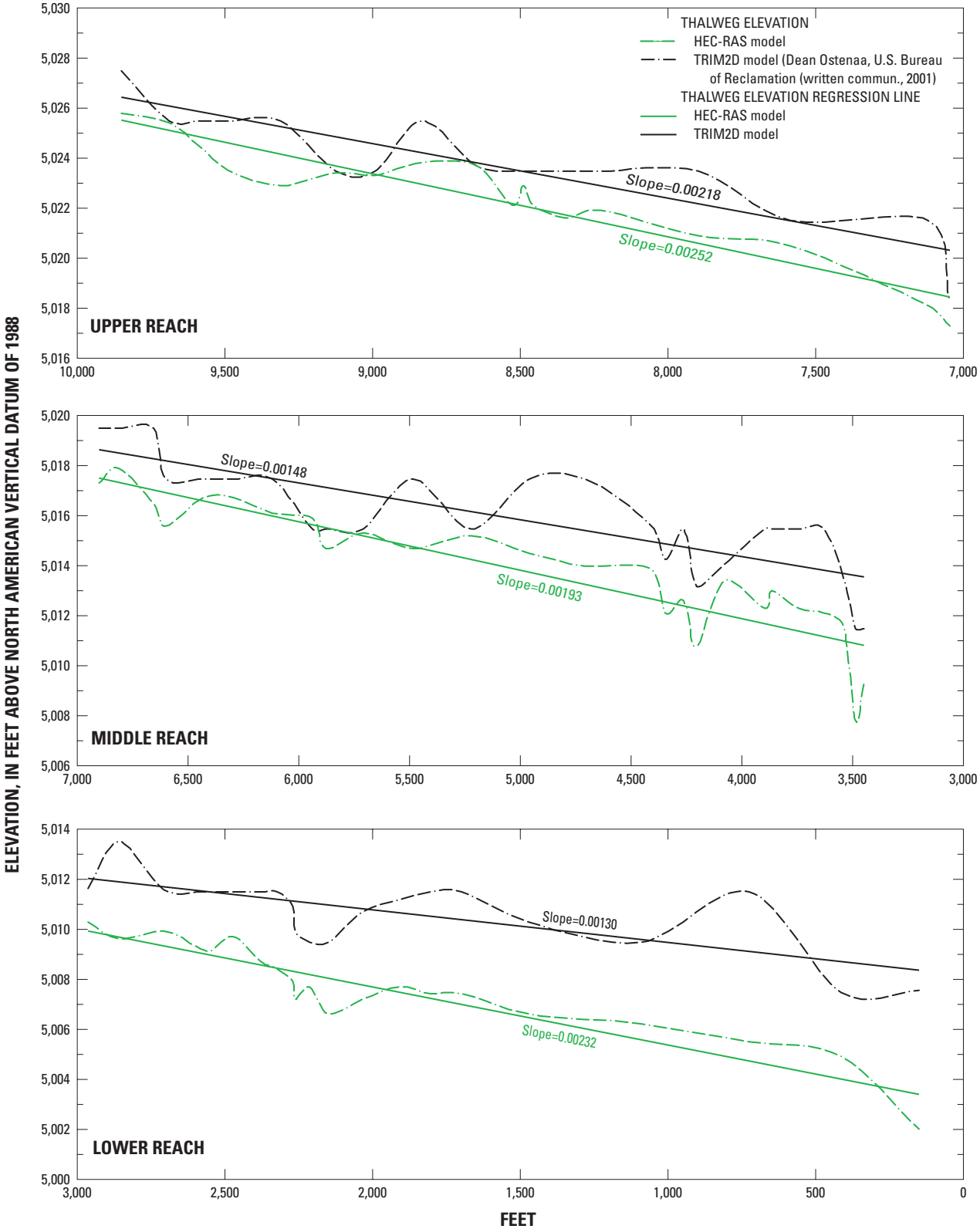

Figure 20. Linear-regression fits to the HEC-RAS and TRIM2D thalweg elevations for the upper, middle, and lower reaches of the Big Lost River upstream of the Pioneer diversion structures, Idaho National Engineering and Environmental Laboratory, Idaho.

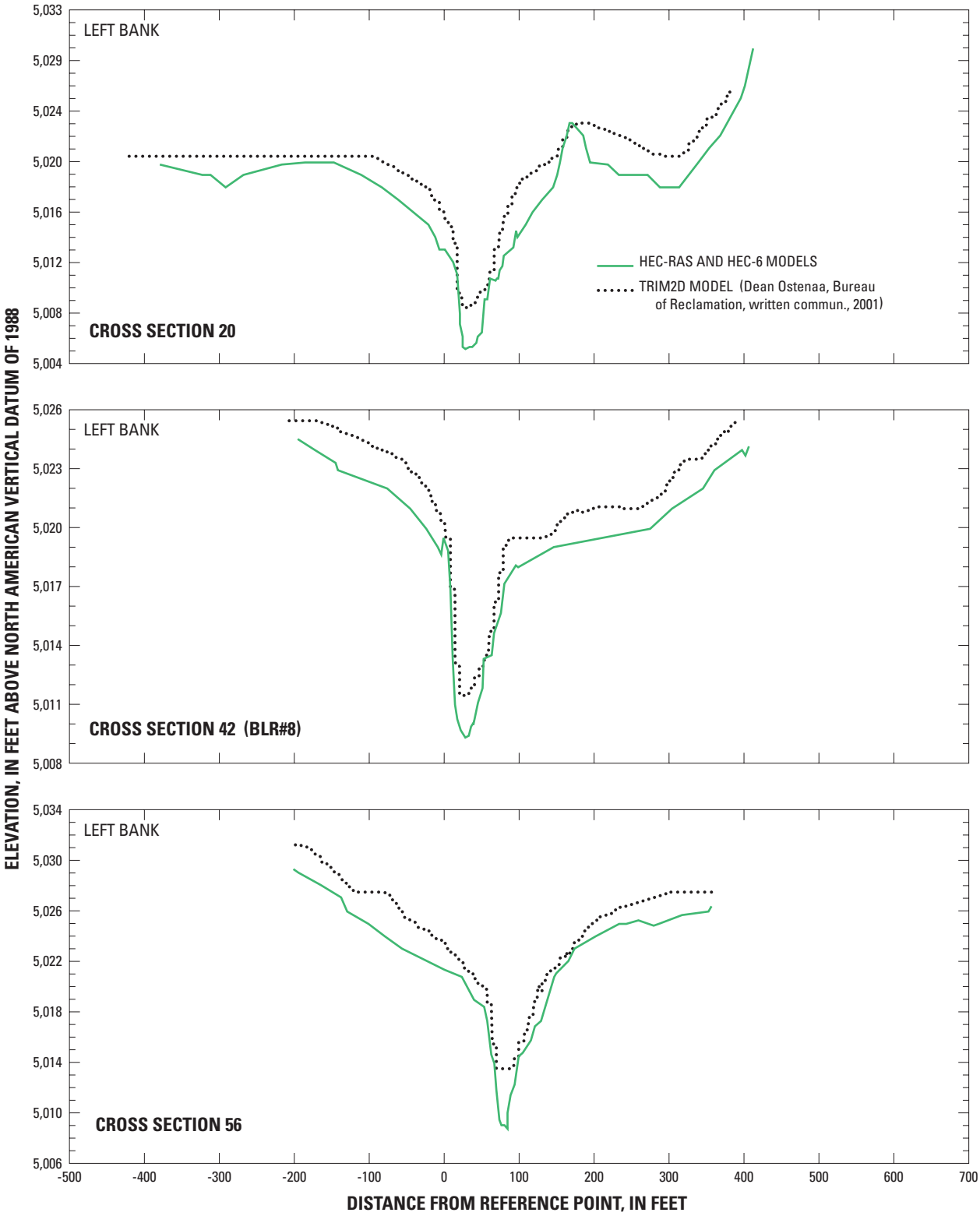

Figure 21. Selected channel cross sections used in the HEC-RAS, HEC-6, and TRIM2D models of the Big Lost River upstream of the Pioneer diversion structures, Idaho National Engineering and Environmental Laboratory, Idaho.

Locations of cross sections shown in figure 9.

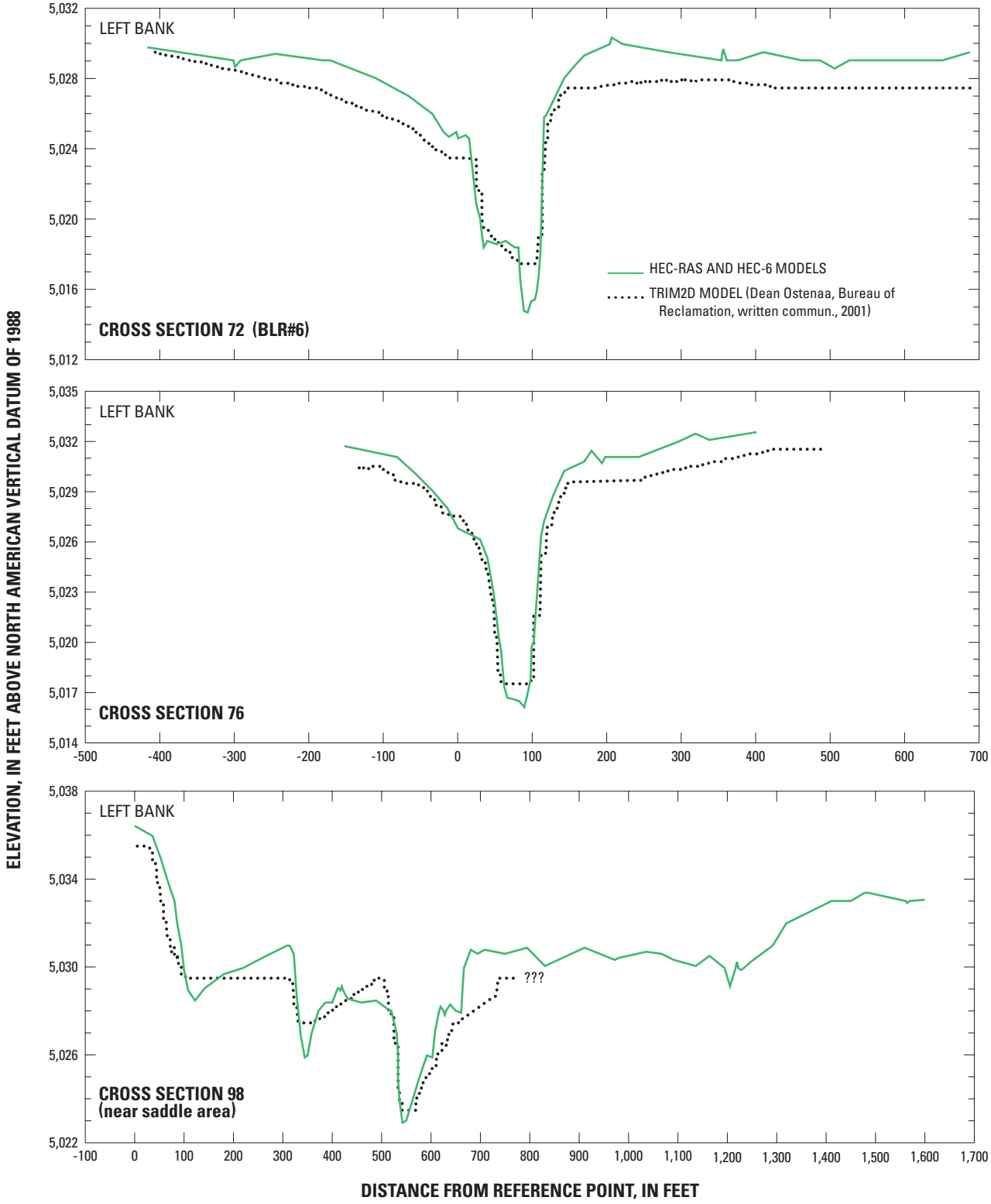

Figure 21.—Continued.

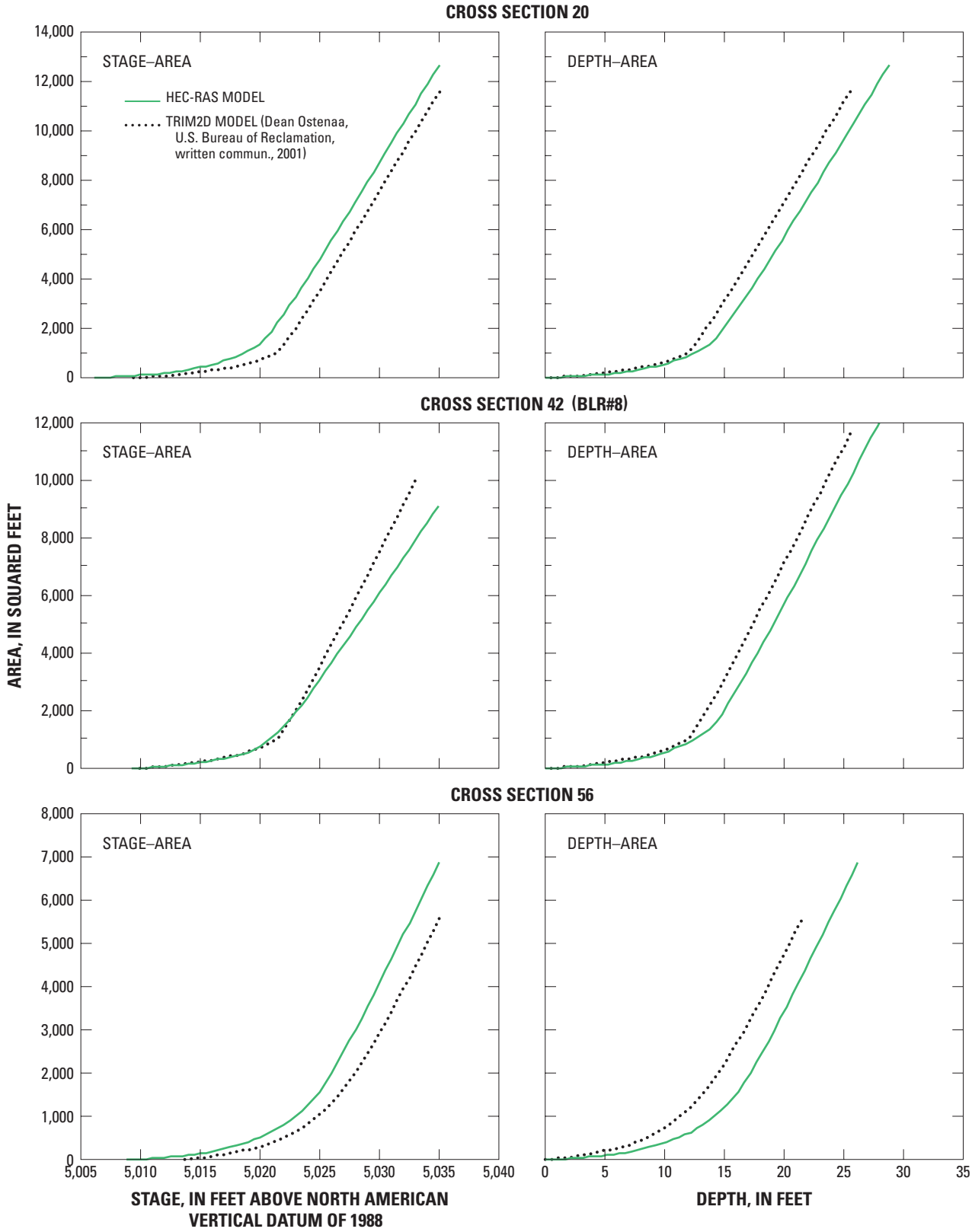

Figure 22. Stage- and depth-area curves for selected channel cross sections used in the HEC-RAS and TRIM2D models of the Big Lost River upstream of the Pioneer diversion structures, Idaho National Engineering and Environmental Laboratory, Idaho. (Locations of cross sections shown in figure 9.)

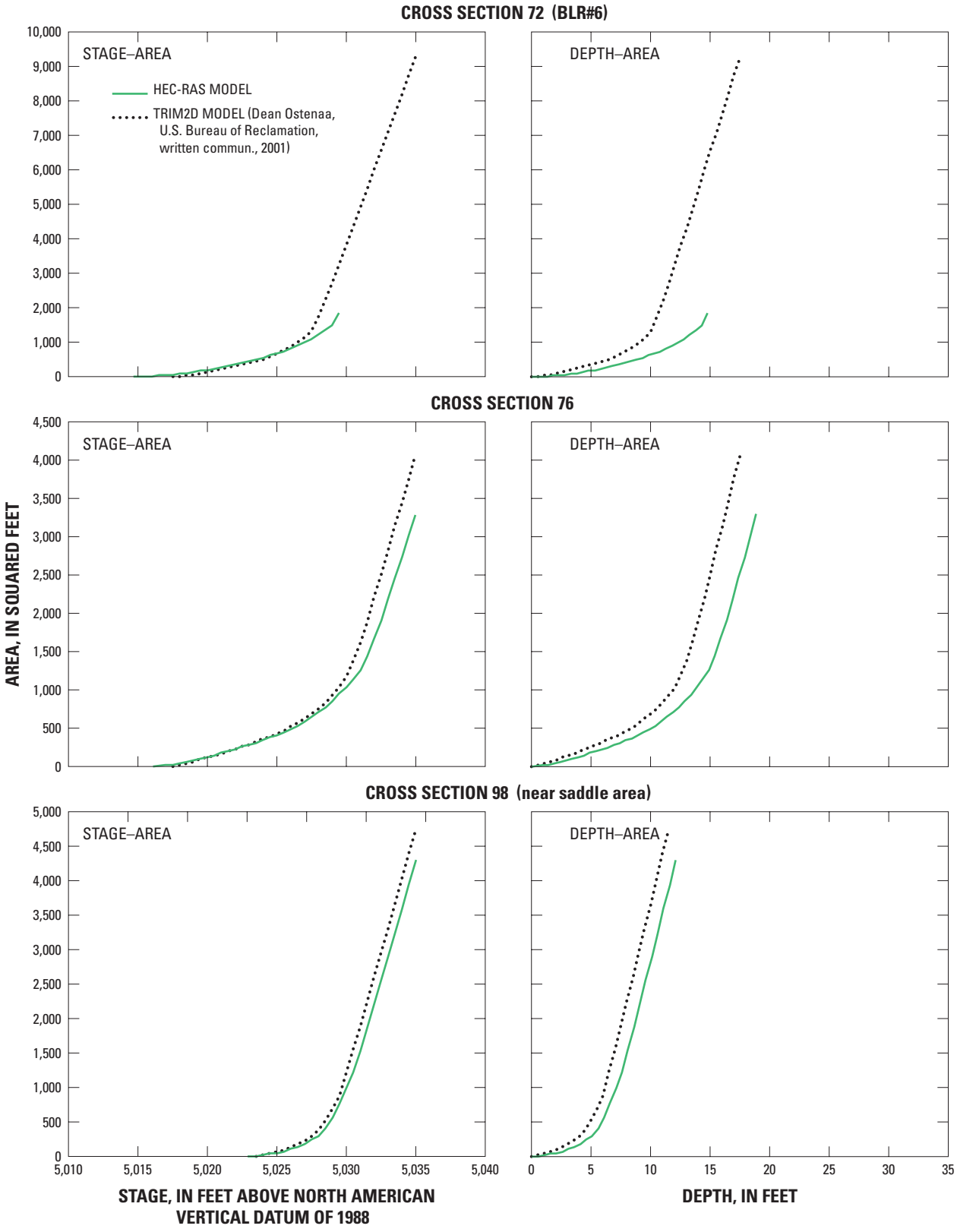

Figure 22.—Continued.

The depth-area curves indicate that flow depths should be shallower in the TRIM2D simulations than in the HEC-RAS simulations. The stage-area curves indicate that water-surface elevations should be higher in the TRIM2D simulations than in the HEC-RAS simulations for the same flow. However, as noted previously, lower thalweg slopes imply that TRIM2D flow depths, in the absence of extensive overbank flow, should be deeper than HEC-RAS flow depths to compensate for the effects of lower velocity that should result from the lower thalweg slopes in the upper, middle, and lower reaches of the river (fig. 20). Comparisons of simulated water-surface elevations, flow depths, and flow velocities presented in the section "Comparisons of HEC-RAS, HEC-6, and TRIM2D Simulation Results" indicate that in simulations made with TRIM2D (1) water-surface elevations are higher, (2) flow depths are shallower, and (3) flow velocities generally are higher in the upper and middle reaches of the river, and lower in the lower reach of the river than those simulated with HEC-RAS. Under steady-flow conditions these results do not appear to be internally consistent with the thalweg-slope, stage-area, and depth-area relations presented in figures 19, 20, and 22.

Comparisons of HEC-RAS, HEC-6, and TRIM2D Simulation Results

Comparisons of model simulation results in the previous sections were restricted to 1-D simulations involving a fixed-bed model (HEC-RAS) and a movable-bed model (HEC-6), and to comparisons of HEC-RAS sensitivity simulations involving the effects of changes in Manning's *n* (roughness coefficient), and changes in streambed elevation. Comparisons were presented to emphasize the effects of roughness coefficients, bedrock constrictions, and streambed erosion and sediment deposition on water-surface elevations.

HEC-RAS model simulation results indicated that flows greater than or equal to 100 m^3/s will accelerate through the site 2 constriction and will transition from subcritical to supercritical. HEC-6 model simulation results indicated that supercritical flow velocities are sufficient to scour the 4.5- to 5.5-ft thick section of fine-grained channel fill inside this constriction. A combination of flow acceleration and scouring tends to limit the extent of backwater accumulation upstream of the site 2 constriction that would result if flow through the constriction remained subcritical.

HEC-6 model simulation results indicated that streambed erosion will reduce water-surface elevations an average of 0.4, 1.0, and 0.4 ft in the middle reach of the river for peak flows of 70, 100, and 150 m^3/s, respectively; and that sediment deposition will increase water-surface elevations an average of 1.5, 1.5, and 1.8 ft in the lower reach of the river for peak flows of 70, 100, and 150 m^3/s, respectively (fig. 16*A*, table 6). In the upper reach, sediment deposition will increase water-surface elevations an average of 0.4 ft for a peak flow of 70 m^3/s, and streambed erosion will reduce water-surface elevations an average of 0.3 ft for a peak flow of 150 m^3/s (fig. 16*A*, table 6). On average, no changes in the elevation of the streambed will result for a peak flow of 100 m^3/s.

Differences in elevation datums, floodplain and channel geometries, and topographic relief complicate comparisons of HEC-RAS and HEC-6 model simulations to those of TRIM2D. For comparison purposes, elevation datum shifts are generally straightforward to apply; however, corrections for differences in channel and floodplain geometries and topographic relief are virtually impossible to apply. As noted previously:

1. The NVGD 29 elevation datum used in the TRIM2D model is 3.484 ft lower than the NAVD 88 elevation datum used in the HEC-RAS and HEC-6 models;

2. The slope of the TRIM2D thalweg along the entire model reach is 15 percent lower than the thalweg slope used in the HEC-RAS model resulting in a 5-ft difference in the topographic relief of these two models between the upstream and downstream ends of the model reach (fig. 19);

3. Thalweg slopes used in the TRIM2D model are 13, 23, and 44 percent lower than those used in the HEC-RAS model along the upper, middle, and lower reaches, respectively (fig. 20);

4. Topographic variability of the TRIM2D thalweg is greater than the HEC-RAS thalweg along the upper, middle, and lower reaches (figs. 19 and 20);

5. Cross-section areas at many locations in the TRIM2D model are larger than those in the HEC-RAS model for the same flow depth—the slope of the depth-area curves are steeper (fig. 22); and

6. Cross-section areas in the TRIM2D model generally are smaller than those in the HEC-RAS model for the same stage or water-surface elevation over the upper one-half of the model reach (stage-area curves are steeper) and larger over the lower one-half of the model reach (stage-area curves are flatter) (fig. 22).

Other topographic differences occur throughout the model reach, particularly in the overbank areas; however, these are difficult to characterize on the basis of trend or offset. The most significant difference of interest to this study is the elevation of the lowest point in the saddle area upstream of the site 1 constriction. The most recent aerial-photography mapping (fig. 5) indicates that the elevation of the lowest

point on this topographic feature is between 5,034.0 and 5,035.0 ft (1-ft contour survey, Bureau of Reclamation, 1999; D.A. Ostenaa, Bureau of Reclamation, written commun., 2001)[4]. The elevation of the lowest point in the saddle area derived from the 1-ft contour map indicates that the saddle-area elevation is between 5,031.5 and 5,033.5 ft (5,028.0 to 5,030.0 ft using the 2-ft contour survey by Eskridge, Aerial Mapping Inc, 1996; NVGD 29)[5]. Field-surveyed data indicate that the lowest point of the saddle area is at an elevation of 5,033.7 ft (NAVD 88; appendix 3, at back of report). The field-surveyed elevation (5,033.7; NAVD 88 datum) is 0.8 ft lower than the interpolated elevation (5,034.5 ft) based on the 1-ft contour map, and 1.2 ft higher than the interpolated elevation (5,032.5 ft) based on the 2-ft contour map. The 1.2 ft elevation difference indicates that peak flows higher than those predicted by the TRIM2D model are needed to produce overtopping and erosion of the saddle area.

Comparisons of HEC-RAS and HEC-6 water-surface elevations to those of TRIM2D, corrected for the 3.484 ft datum shift, are presented in this section. These comparisons provide a means of evaluating the overall reliability of TRIM2D simulations of peak flows needed to overtop and erode surfaces that were used to establish minimum return periods for hypothetical flood events with return periods of 300 to 500 years, and 10,000 years. Because simulated TRIM2D water-surface elevations formed the basis for assigning flood magnitudes to these return periods, comparisons of water-surface elevations take into account the simulation results for both the fixed-bed (HEC-RAS) and movable-bed (HEC-6) models, even though TRIM2D is a fixed-bed model.

Comparisons of simulated flow depths, flow velocities, and stream power offer an alternative way to assess model results and to evaluate the effects that differences in floodplain and channel geometries and topographic relief have on these results. To some extent these comparisons are less dependent on elevation, and are therefore useful for determining if flow simulations are internally consistent. These comparisons are limited to the fixed-bed HEC-RAS and TRIM2D simulations and assume that:

1. Flow into and out of the model reach and at each cross section within the model reach is steady—inflow equals outflow everywhere within the model reach (appendix 4, at back of report)[6];
2. Deeper flow depths and/or larger cross-section flow areas are needed to maintain steady flow at lower velocities;
3. Flow velocities in channels with flatter thalweg slopes should be lower than flow velocities in channels with steeper thalweg slopes;
4. Stream power is a linear function of and is directly proportional to flow depth and velocity; and
5. The highest flow velocities and stream power will occur within the main channel along, or in close proximity to the alignment of the thalweg. This will normally be the case if flow is contained within the main channel and overbank and side-channel flow are limited. High stream powers, offset from the thalweg alignment, also are possible in areas where flow is forced to accelerate around a bend.

Comparisons of HEC-RAS and TRIM2D Water-Surface Elevations

Simulated HEC-RAS and TRIM2D water-surface elevations for peak flows of 70, 100, and 150 m^3/s are shown in figure 23*A*. The TRIM2D water-surface elevations have been adjusted by +3.484 ft to account for elevation differences between the TRIM2D datum (NGVD 29) and the HEC-RAS datum (NAVD 88). Simulated TRIM2D water-surface elevations generally are higher than corresponding HEC-RAS water-surface elevations throughout the model reach (fig. 23*A*). To some extent, the higher TRIM2D water-surface elevations can be attributed to:

1. Topographic relief between the upstream (cross section 108) and downstream (cross section 1) ends of the model reach that is 5 ft less in the TRIM2D model than in the HEC-RAS model;
2. Elevation of the TRIM2D thalweg (corrected for the +3.484 ft datum shift) that is on average 2.5 ft higher than the HEC-RAS thalweg (table 7); and
3. Thalweg slopes that are 13, 23, and 44 percent less in the TRIM2D model than in the HEC-RAS model along the upper, middle, and lower reaches of the river, respectively.

[4]To conform to the NAVD 88 datum, a +1.955 ft elevation correction has been applied to the contours shown in figure 5.

[5]To conform to the NAVD 88 datum, a +3.484 ft elevation correction has been applied to the 2-ft contour map prepared by Eskridge, Aerial Mapping Inc. (1996).

[6]TRIM2D model simulations were initialized for a flow of 10 m^3/s and increased incrementally to 50, 70, 100, 150, 187, 263, and 400 m^3/s using results from the previous and smaller flow simulation as the initial conditions for the specified simulation (Ostenaa and others, 1999, p. 31). Appendix 4 includes an evaluation of the steady-flow assumption at three cross sections for the TRIM2D 100 m^3/s simulation.

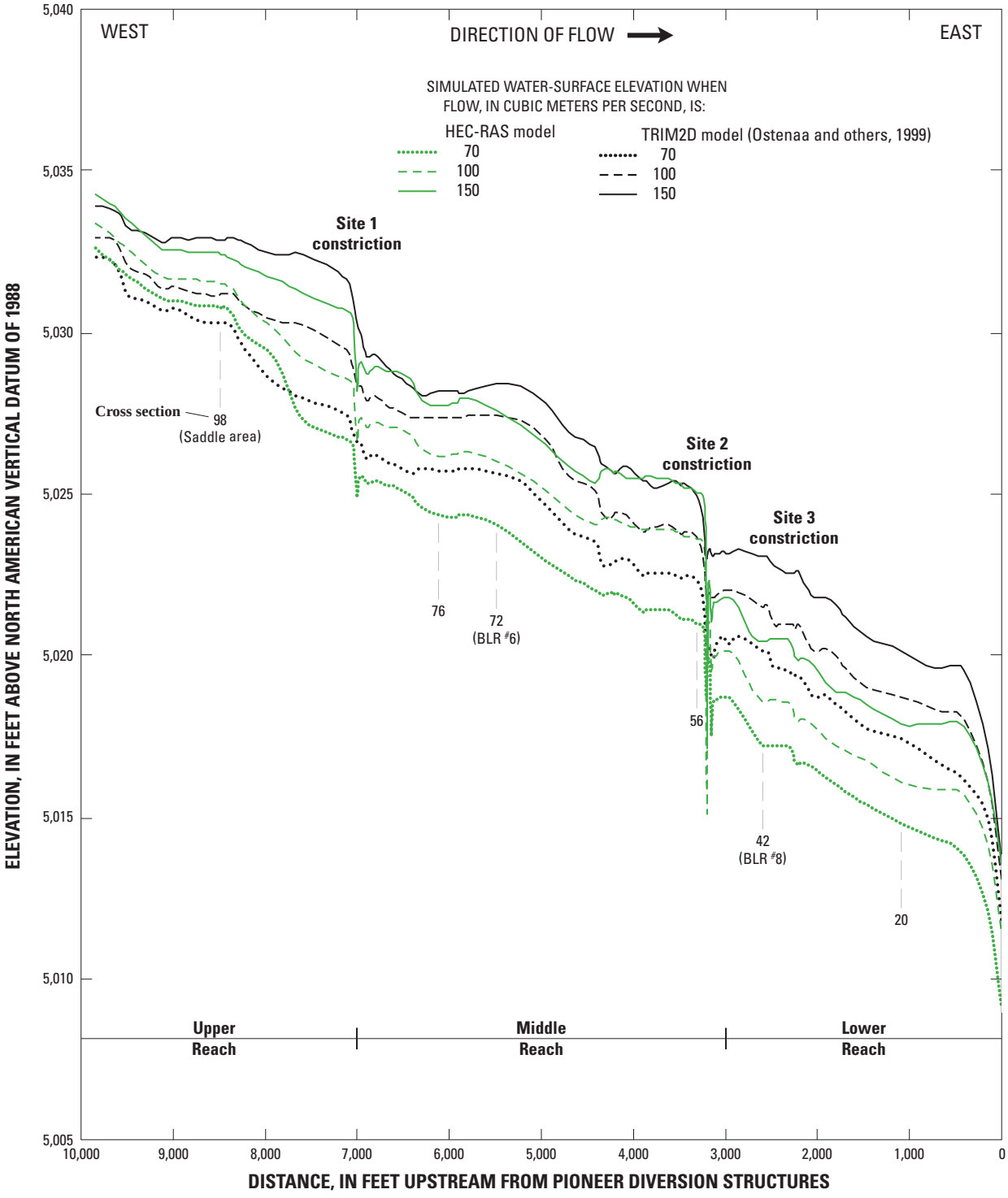

A. Big Lost River

Figure 23. HEC-RAS and TRIM2D simulated water-surface elevations for peak flows of 70, 100, and 150 cubic meters per second on the Big Lost River and sites 1 and 2 constrictions upstream of the Pioneer diversion structures, Idaho National Engineering and Environmental Laboratory, Idaho.

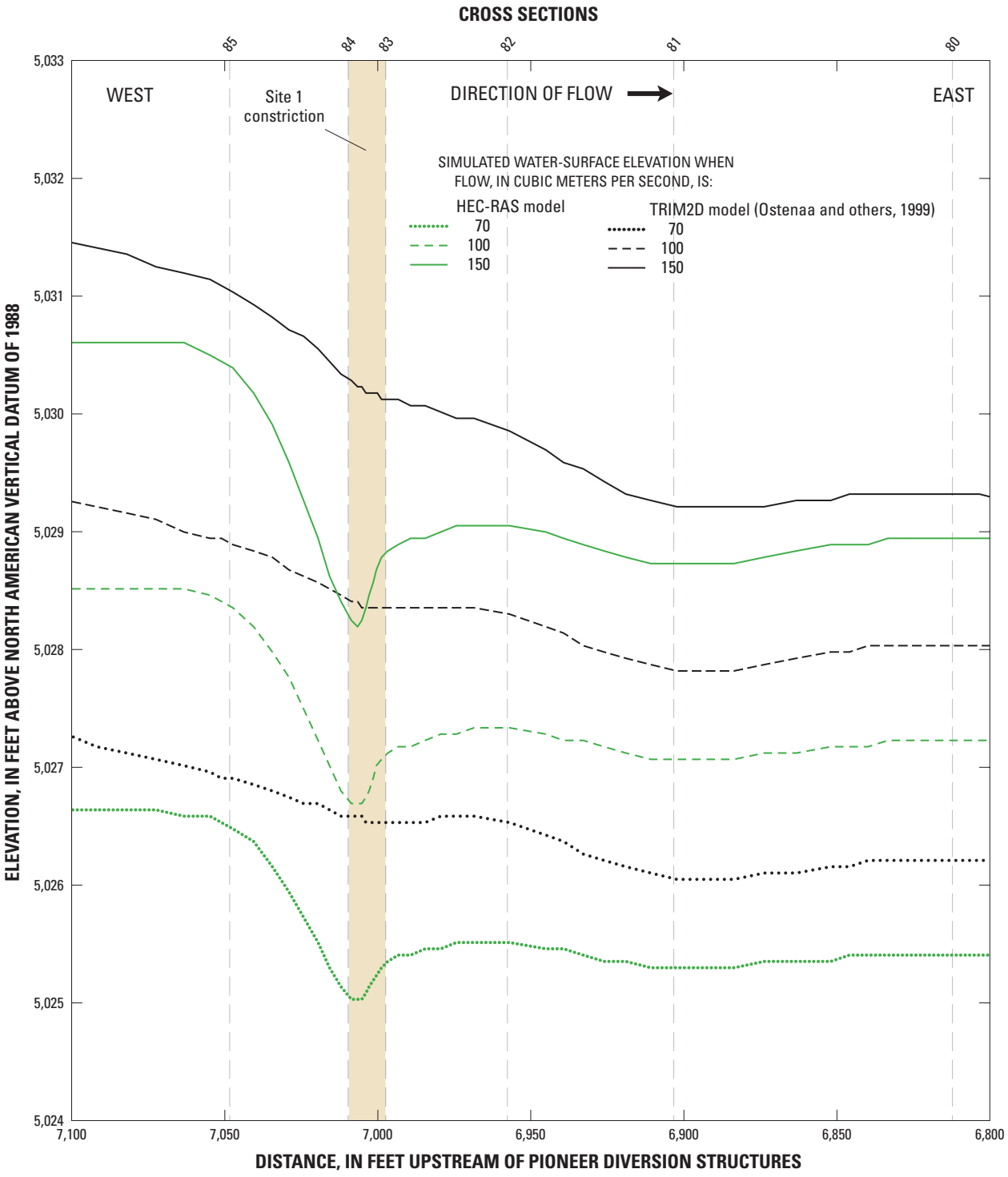

B. Site 1 constriction

Figure 23.—Continued.

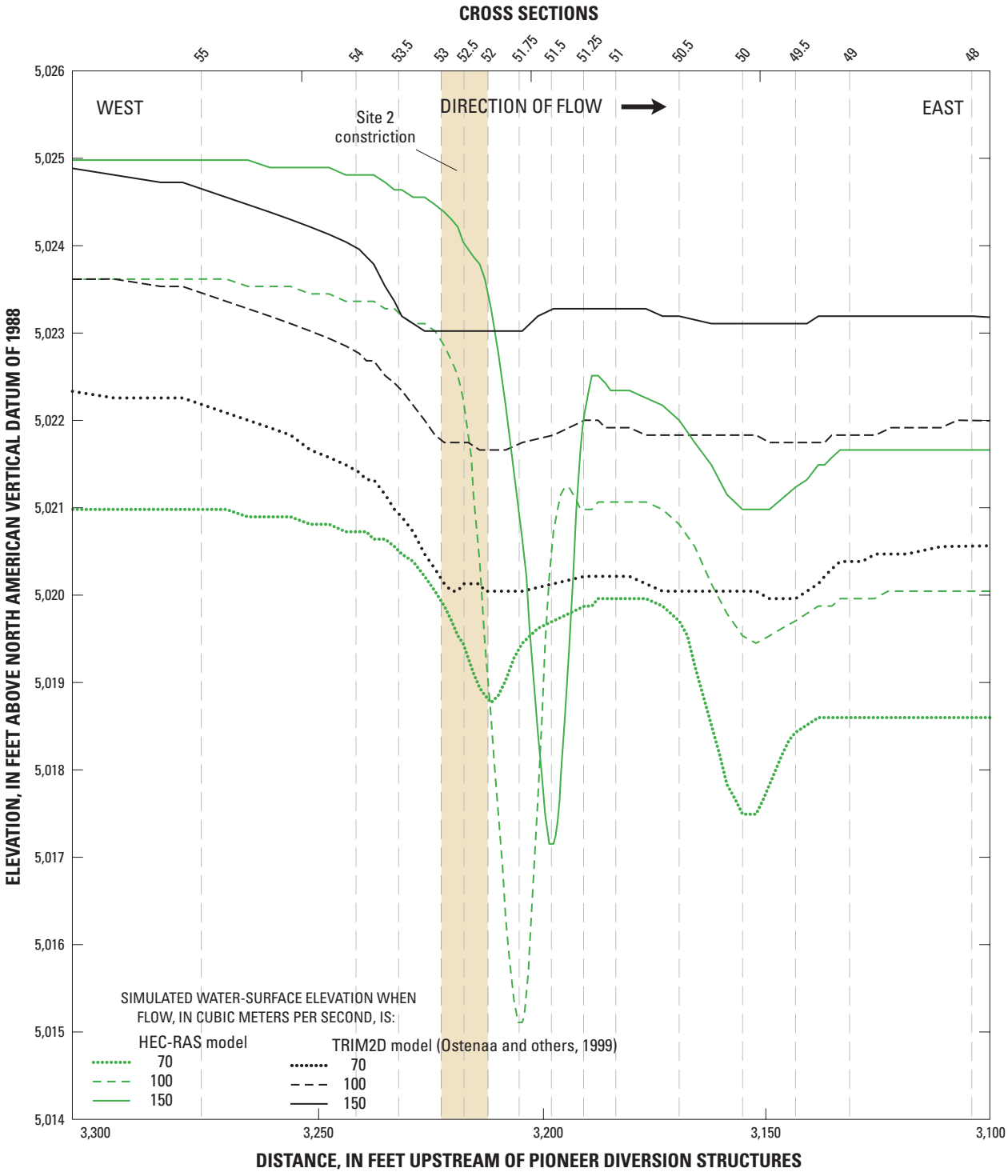

C. Site 2 constriction

Figure 23.—Continued.

A few minor exceptions in which HEC-RAS water-surface elevations are higher than those of TRIM2D occur immediately upstream and downstream of cross section 98 (near the saddle area) for peak flows of 70 and 100 m^3/s, downstream of the site 1 constriction for a peak flow of 150 m^3/s, and immediately upstream of the site 2 constriction for a peak flow of 150 m^3/s. The average elevation of the TRIM2D water surface for the entire model reach, computed on the basis of a one-to-one comparison of HEC-RAS water-surface elevations to those of TRIM2D at all cross sections, was 1.2, 1.1, and 0.9 ft higher than HEC-RAS water-surface elevations for peak flows of 70, 100, and 150 m^3/s, respectively (table 8). The largest average difference in water-surface elevations between the two models (1.2 ft) is associated with the lowest peak flow, 70 m^3/s, and probably reflects the combined effects of differences in the thalweg slopes and channel-bottom topographies (figs. 19 and 20) used in the HEC-RAS and TRIM2D models.

Constrictions

Maximum energy dissipation, represented by large changes in water-surface elevations over short distances, should occur within and immediately downstream of the sites 1 and 2 constrictions where flow is forced to converge and accelerate and where energy is lost to the formation of hydraulic jumps. At the downstream end of the site 1 constriction (cross section 81, fig. 23*B*), TRIM2D water surfaces are 0.5 to 1.0 ft higher than HEC-RAS water surfaces; and the TRIM2D water-surface depressions through this constriction are not as well defined as the HEC-RAS water-surface depressions (cross sections 81 to 85, fig. 23*B*). However, changes in water-surface elevation through the site 1 constriction are comparable for both models. Changes in HEC-RAS water-surface elevations of 1.2, 1.3, and 1.7 ft (cross sections 81 to 85) compare closely to changes in TRIM2D water-surface elevations of 1.0, 1.1, and 1.8 ft (cross sections 81 to 85) for peak flows of 70, 100, and 150 m^3/s, respectively.

At the site 2 constriction, the character of the TRIM2D and HEC-RAS water-surface profiles are very different. At the downstream end of the site 2 constriction (cross section 49, fig. 23*C*) TRIM2D water surfaces are 1.5 to 2.0 ft higher than HEC-RAS water surfaces; and elevation changes through the constriction are much smaller than HEC-RAS elevation changes (cross sections 49 to 55, fig. 23*C*). TRIM2D elevation changes of 1.4, 1.4, and 1.7 ft do not compare closely to HEC-RAS elevation changes of 3.4, 3.3, and 2.4 ft for flows of 70, 100, and 150 m^3/s, respectively. The smaller changes in TRIM2D water-surface elevations through the site 2 constriction contribute significantly to the much higher TRIM2D water-surface elevations downstream of the site 2 constriction, even though the water-surface elevations immediately upstream of this constriction are nearly identical

Table 8. Differences in HEC-RAS, HEC-6, and TRIM2D simulated water-surface elevations for peak flows of 70, 100, and 150 cubic meters per second on the Big Lost River upstream of the Pioneer diversion structures, Idaho National Engineering and Environmental Laboratory, Idaho.

[Location of cross sections is shown in figure 9*C*. ft, ft; m^3/s, cubic meter per second]

Cross section	Differences in water-surface elevations (ft)					
	Between HEC-RAS and TRIM2D models ($HEC\text{-}RAS_{elev}$ minus $TRIM2D_{elev}$) for a peak flow of			Between HEC-6 and TRIM2D models ($HEC\text{-}6_{elev}$ minus $TRIM2D_{elev}$) for a peak flow of		
	70 m^3/s	100 m^3/s	150 m^3/s	70 m^3/s	100 m^3/s	150 m^3/s
20	-2.6	-2.4	-2.2	-0.4	-0.2	0.2
42 (BLR#8)	-2.9	-2.9	-2.7	-1.3	-1.5	-1.1
56	-1.4	-.1	.1	-1.9	-1.6	-.4
72 (BLR#6)	-1.6	-1.4	-.8	-2.1	-2.4	-1.4
76	-1.4	-1.2	-.5	-1.4	-1.7	-.7
98 (near saddle area)	.5	.3	-.4	.7	.1	-1.0
	Average difference			Average difference		
Entire reach (n = 89)	-1.2	-1.1	-0.9	-0.8	-1.0	-0.5
Upper reach (85 to 108)	.2	.1	-.4	.6	.0	-.7
Middle reach (58 to 81)	-1.2	-.6	-.3	-1.6	-1.6	-.7
Lower reach (3 to 45)	-2.5	-2.5	-2.2	-1.0	-1.0	-.4

to those of HEC-RAS for the 100 and 150 m^3/s simulations (figs. 23*A* and 23*C*). The much larger changes in HEC-RAS water-surface elevations through the site 2 constriction reflect the effects of subcritical to supercritical flow acceleration [from 6.0 ft/s immediately upstream of the constriction (cross section 54) to a maximum of 22.3 ft/s inside the constriction (cross section 51.75) for a peak flow of 100 m^3/s]. This flow regime change was not simulated in the TRIM2D model.

Paleoindicator Sites

TRIM2D model simulations indicate that a flow of about 100 m^3/s will overtop and erode the 300- to 500-year old paleoindicator sites at BLR#6 and BLR#8. TRIM2D simulations also indicated that "…discharges only slightly larger than about 110 m^3/s will initiate extensive flow across the unmodified Pleistocene alluvial surfaces" (Ostenaa and others, 1999; referring to the saddle area) and that overtopping and severe erosion of the saddle area would occur at a flow of 150 m^3/s, thus establishing the basis for "… a paleohydrologic bound at a discharge of 150 m^3/s for the past 10 k.y." (10 thousand years).

TRIM2D water-surface elevations for peak flows of 70, 100, and 150 m^3/s were 2.9, 2.9, and 2.7 ft higher at BLR#8 (cross section 42) and 1.6, 1.4, and 0.8 ft higher at BLR#6 (cross section 72) than HEC-RAS water-surface elevations (table 8). The TRIM2D model simulation results predict that a flow of 100 m^3/s will overtop the inset terraces at BLR#6 (water-surface elevation = 5,027.5 ft) and BLR#8 (water-surface elevation = 5,021.5 ft) (fig. 24). This flow is significantly smaller than flows simulated by the HEC-RAS model that are discussed in the section on "Flow Equivalency."

At cross section 98 (near the saddle area), the TRIM2D water-surface elevation was 0.5 and 0.3 ft lower than HEC-RAS for peak flows of 70 and 100 m^3/s, respectively, and 0.4 ft higher for a peak flow of 150 m^3/s (table 8). However, a field survey of the saddle area (appendix 3) indicates that the saddle-area elevation (5,033.7 ft, NAVD 88) is about 1.2 ft higher than indicated on the 2-ft contour map (Eskridge, Aerial Mapping Inc., 1996), corrected for the 3.484 ft datum shift that was used in the TRIM2D model, and 0.8 ft lower than the 1-ft contour map (fig. 5; D.A. Ostenaa, Bureau of Reclamation, written commun., 2001), corrected for the 1.955 datum shift that was used in the HEC-RAS model. These elevation differences indicate that flows higher than simulated by the TRIM2D model are needed to overtop and erode the 10,000-year old Pleistocene saddle-area surface.

Flow Equivalency

Estimates of HEC-RAS peak flows needed to match TRIM2D water-surface elevations at six selected cross sections are presented in table 9. Equivalent flow estimates assume that simulated changes in water-surface elevation are linear from one flow simulation to the next (fig. 25). Thus, at cross section 42 (BLR#8), increases in HEC-RAS peak flows of 72 m^3/s (103 percent), 83 m^3/s (83 percent), and 79 m^3/s (53 percent); and at cross section 72 (BLR#6), increases in HEC-RAS peak flows of 24 m^3/s (34 percent), 45 m^3/s (45 percent), and 37 m^3/s (25 percent) are needed to match water-surface elevations in the TRIM2D model for peak flows of 70, 100, and 150 m^3/s, respectively.

Table 9. HEC-RAS peak flows needed to match TRIM2D water-surface elevations for peak flows of 70, 100, and 150 cubic meters per second on the Big Lost River upstream of the Pioneer diversion structures, Idaho National Engineering and Environmental Laboratory, Idaho.

[Location of cross sections is shown in figure 9*C*. m^3/s, cubic meter per second]

Cross section	TRIM2D peak flow of								
	70 m^3/s			100 m^3/s			150 m^3/s		
	Equivalent HEC-RAS peak flow	Difference		Equivalent HEC-RAS peak flow	Difference		Equivalent HEC-RAS peak flow	Difference	
		Flow	Percent		Flow	Percent		Flow	Percent
20	137	67	9	176	76	76	221	71	47
42 (BLR#8)	142	72	103	183	83	83	229	79	53
56	86	16	23	103	3	3	148	-2	-1
72 (BLR#6)	94	24	34	145	45	45	187	37	25
76	93	23	32	140	40	40	176	26	17
98 (near saddle area)	62	-8	-11	87	-13	-13	169	19	13

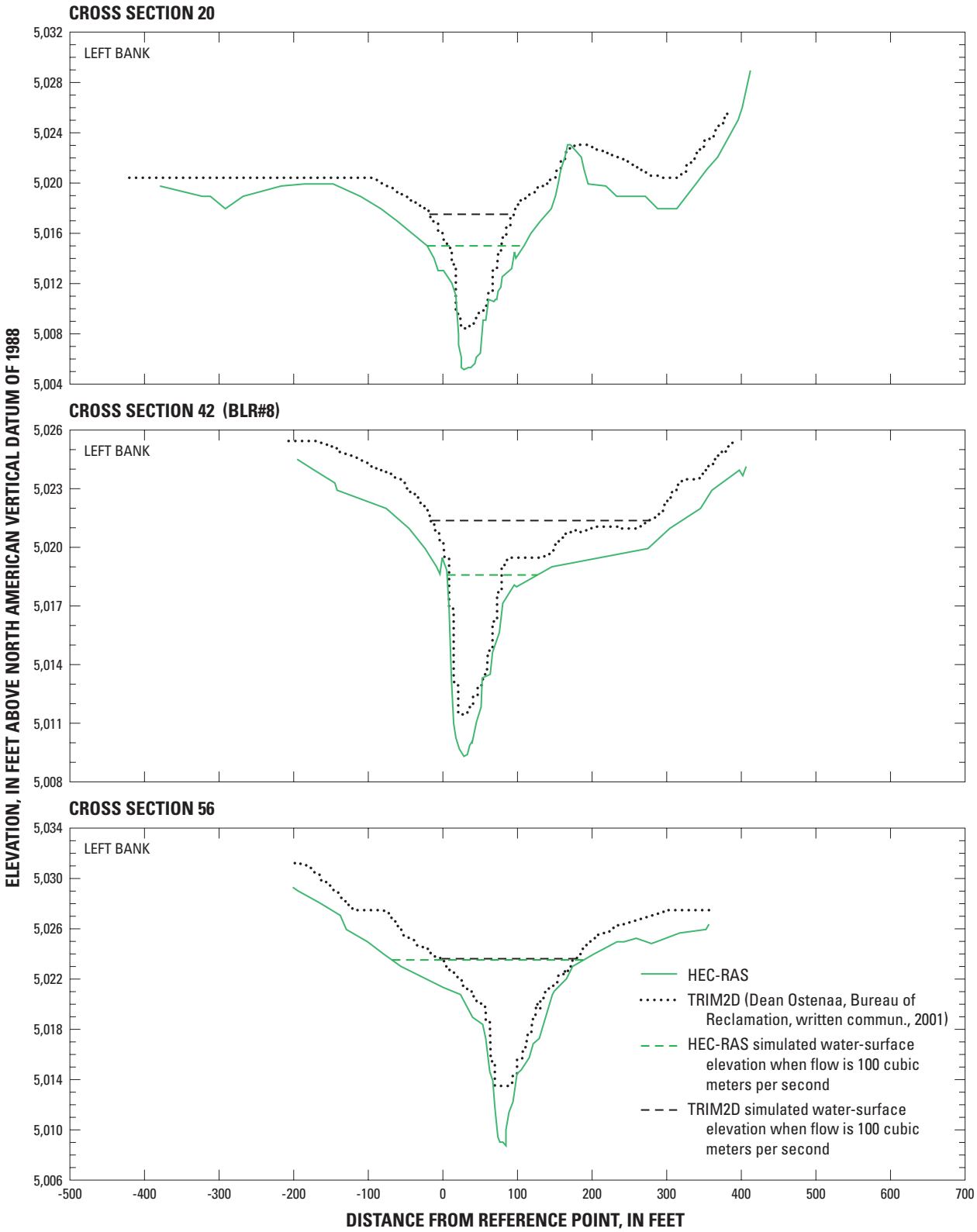

Figure 24. HEC-RAS and TRIM2D simulated water-surface elevations at selected cross sections for a peak flow of 100 cubic meters per second on the Big Lost River upstream of the Pioneer diversion structures, Idaho National Engineering and Environmental Laboratory, Idaho.
(Location of cross sections shown in figure 9*C*.)

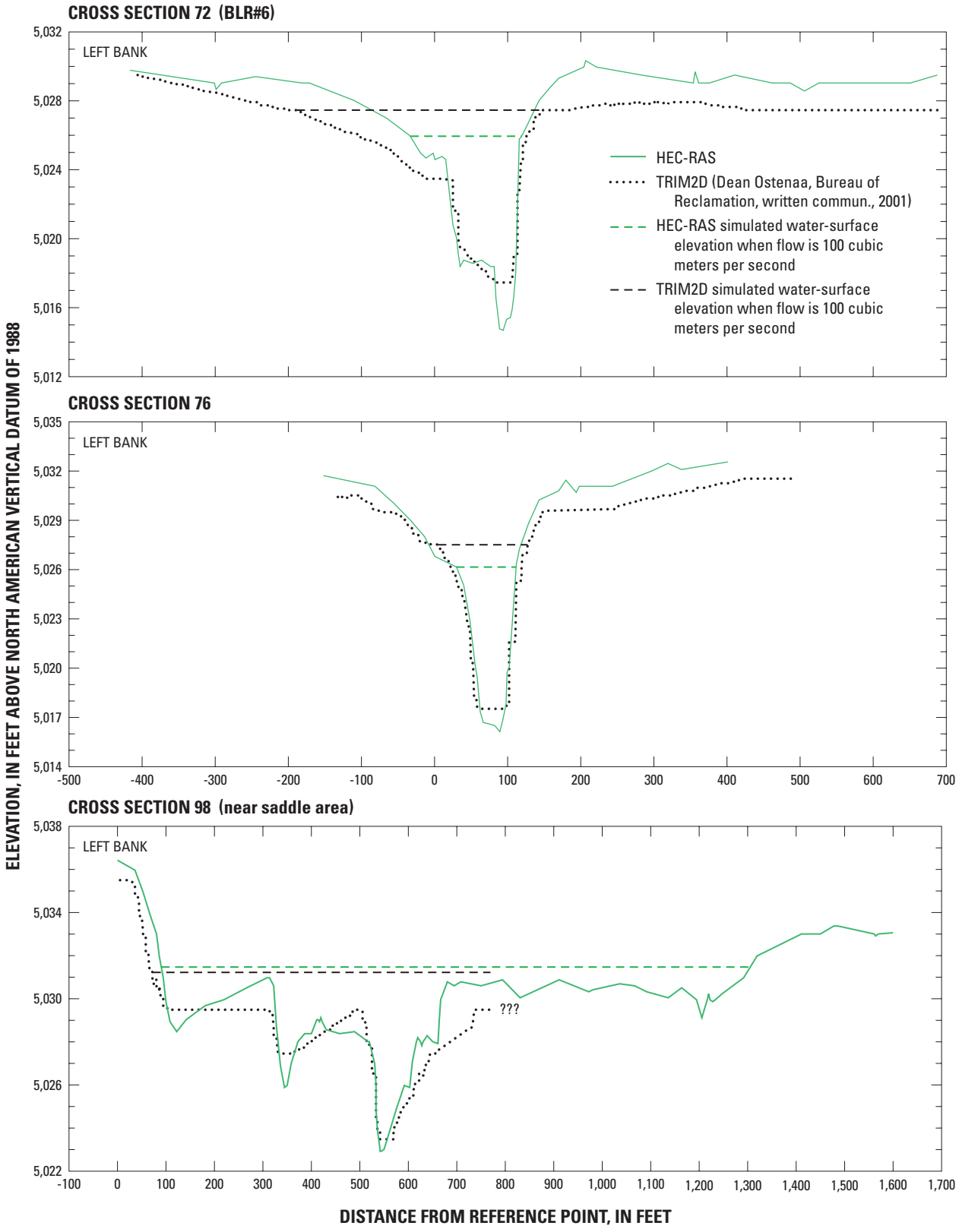

Figure 24.—Continued.

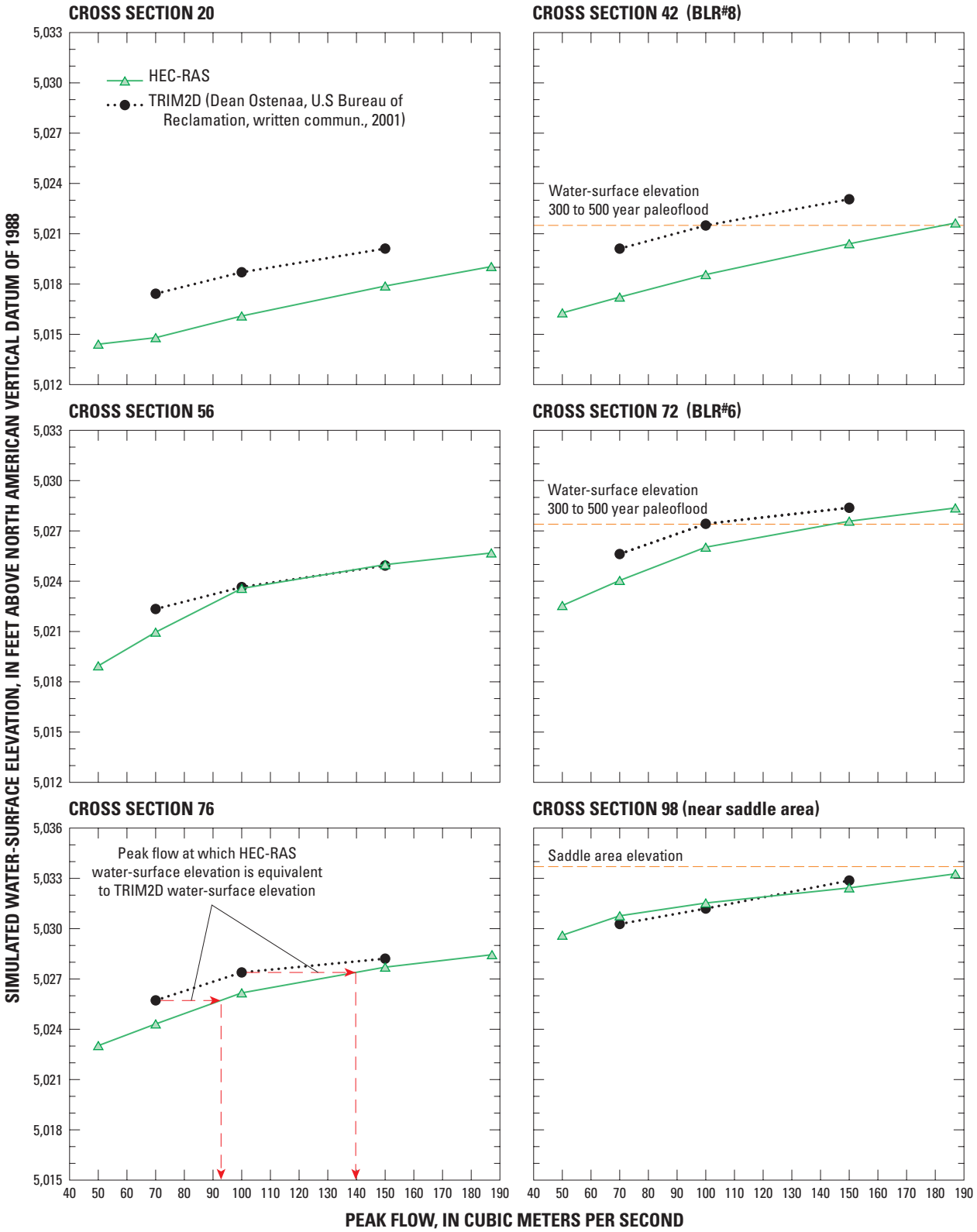

Figure 25. HEC-RAS and TRIM2D simulated water-surface elevations at selected cross sections for peak flows of 70, 100, and 150 cubic meters per second on the Big Lost River upstream of the Pioneer diversion structures, Idaho National Engineering and Environmental Laboratory, Idaho.
Locations of cross sections shown in figure 9.

At cross section 98 (near the saddle area), decreases in HEC-RAS peak flows of 8 m^3/s (11 percent) and 13 m^3/s (13 percent) are needed to match water-surface elevations in the TRIM2D model for peak flows of 70 and 100 m^3/s, respectively; and an increase in HEC-RAS peak flow of 19 m^3/s (13 percent) is needed to match TRIM2D water-surface elevations for a peak flow of 150 m^3/s.

Results of the HEC-RAS model simulations indicate that the TRIM2D model simulations underestimate the magnitude of peak flows representing return periods of 300 to 500 years and 10,000 years. The TRIM2D model probably predicted higher water-surface elevations than the HEC-RAS model because of higher thalweg elevations, lower thalweg slopes, greater topographic variability of the thalweg, limited energy dissipation through the site 2 constriction, and steeper depth-area curves and flatter stage-area curves used to represent the channel and floodplain geometries in the TRIM2D model. Although the stage-area curves for HEC-RAS and TRIM2D are similar near cross section 98, HEC-RAS results indicate that a flow greater than 190 m^3/s (about 210 m^3/s based on linear extrapolation of the HEC-RAS stage-area curve for cross section 98 shown in fig. 25) is needed to initiate flow across the saddle area because the elevation of the lowest point on the saddle area is 1.2 ft higher than indicated on the 2-ft contour map (corrected for the 3.484 ft datum) that was used in the TRIM2D model.

Comparisons of HEC-6 and TRIM2D Water-Surface Elevations

Along the upper and middle reaches of the river, average differences in water-surface elevation between HEC-6 and TRIM2D generally are larger than those between HEC-RAS and TRIM2D for all simulated flows (fig. 26 and table 8). Along the lower reach, differences in HEC-6 and TRIM2D water-surface elevations ($HEC\text{-}6_{elev}$ minus $TRIM2D_{elev}$) are less than those of HEC-RAS and TRIM2D ($HEC\text{-}RAS_{elev}$ minus $TRIM2D_{elev}$), which reflects the effects of sediment deposition in this reach of the river. Average differences in water-surface elevation between HEC-6 and TRIM2D were 0.6, 0.0, and -0.7 ft in the upper reach, -1.6, -1.6, and -0.7 ft in the middle reach, and -1.0, -1.0, and -0.4 ft in the lower reach for peak flows of 70, 100, and 150 m^3/s, respectively (table 8). Differences in water-surface elevations between HEC-6 and TRIM2D at the paleoindicator sites ranged from -1.4 ft (peak flow of 150 m^3/s) to -2.4 ft (peak flow of 100 m^3/s) at BLR#6 (cross section 72); from -1.1 ft (peak flow of 150 m^3/s) to -1.5 ft (100 m^3/s) at BLR#8 (cross section 42); and from -1.0 ft (peak flow of 150 m^3/s) to 0.7 ft (peak flow of 70 m^3/s) near the saddle area (cross section 98).

When the effects of streambed erosion and sediment deposition are included, HEC-6 model results indicate that flows greater than those simulated by HEC-RAS are needed to match TRIM2D water-surface elevations in the upper and middle reaches of the river, where streambed scour dominates, and that flows less than those simulated by HEC-RAS are needed to match TRIM2D water-surface elevations in the lower reach of the river, where sediment deposition dominates. HEC-6 model results indicate that the TRIM2D model underestimates the magnitude of peak flows needed to overtop and erode paleoindicator surfaces that were used to establish the return periods of hypothetical flood events with minimum return periods of 300 to 500 years and 10,000 years. These paleoindicator surfaces are in the upper and middle reaches of the river.

Comparisons of HEC-RAS and TRIM2D Flow Depths

Flow depths for the HEC-RAS and TRIM2D models for peak flows of 70, 100, and 150 m^3/s are shown in figures 27*A*, 27*B*, and 27*C*. Flow depths at each cross section were computed by subtracting water-surface elevation from the thalweg elevation used in the respective model simulations. In the case of HEC-RAS, this difference represents the maximum depth of flow at each cross section shown in figure 9*C*. In the case of TRIM2D, this difference represents an approximate maximum depth within 2×2 m grid cells aligned along the thalweg of the model reach. The size of the grid cell in the TRIM2D model is sufficiently small that the flow depth represented by the grid cell should reasonably approximate the maximum flow depth. To facilitate comparisons of flow depths, a locally-weighted least-squares regression routine (LOWESS[7]) was used to produce a smooth profile of simulated flow depths through the irregularly spaced cross sections shown in figure 9*C*.

The LOWESS-smoothed depth profiles shown in figures 27*A*, 27*B*, and 27*C* indicate that the TRIM2D flow-depth profiles bear little resemblance to the HEC-RAS flow-depth profiles. TRIM2D flow depths are shallower than HEC-RAS flow depths along the entire length of the model reach for all simulated flows. The LOWESS-smoothing routine clearly masks a few isolated exceptions to this observation as can be seen in the point-to-point graphs of flow depth that accompany the LOWESS-smoothed depth profiles in figures 27*A*, 27*B*, and 27*C*. At the upstream end of the model reach (near cross section 108), TRIM2D flow depths are 24, 21, and 11 percent shallower, and at the downstream end (near cross section 1), 31, 34, and 38 percent shallower than HEC-RAS flow depths for peak flows of 70, 100, and 150 m^3/s, respectively. To some extent shallower TRIM2D flow depths in the upper and middle reaches of the river can be explained by the depth-area geometry of the channel cross sections that were used in the TRIM2D model. This explanation, however, is difficult to apply in the lower reach of the river.

[7]The LOWESS smoothing routine was implemented using the S-Plus Curve Fitting Toolbox utility (Insightful Corporation, copyright 1998, 2002) with an automatic span setting of 0.5 to compute the flow-depth profiles shown in figure 27.

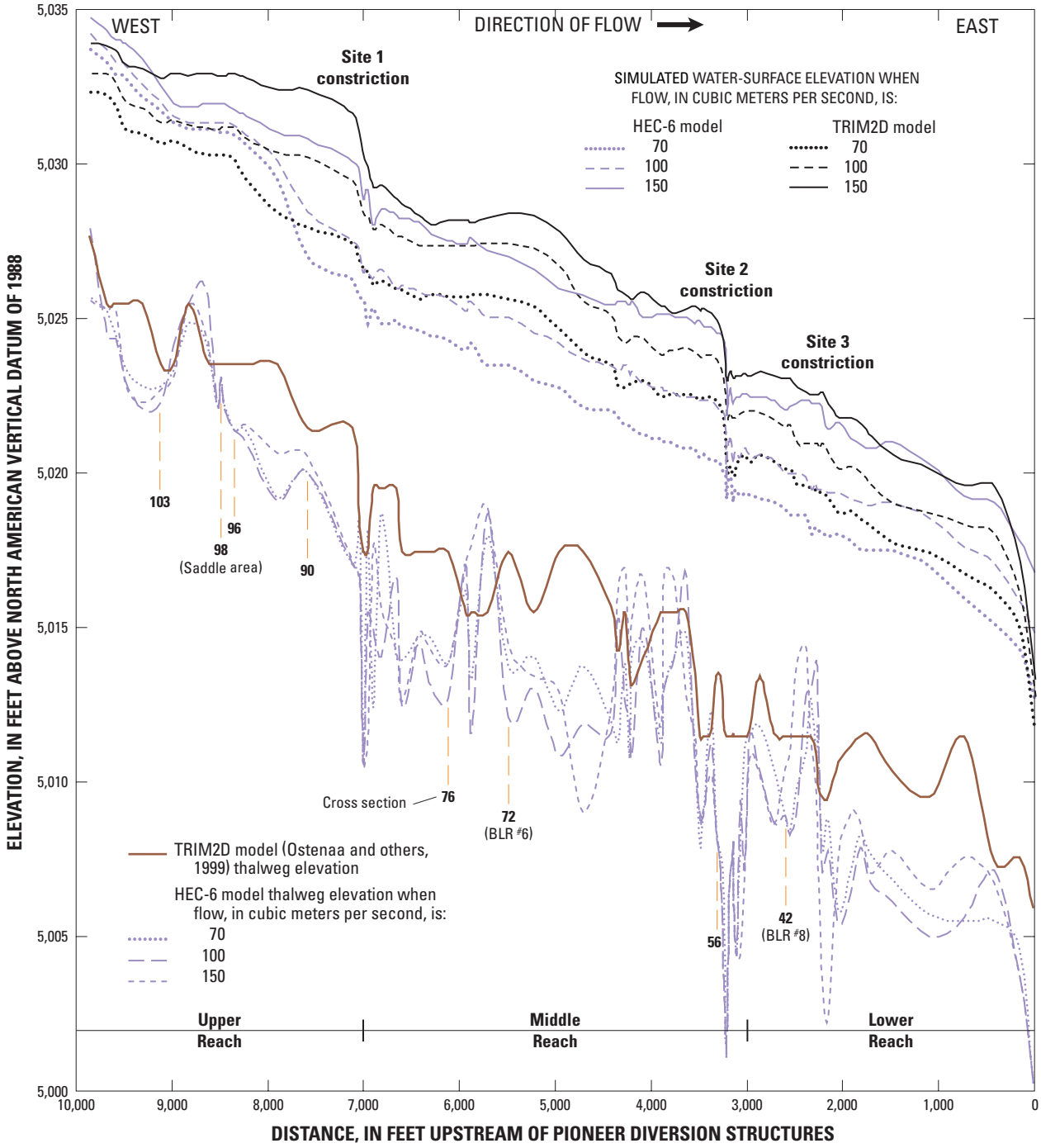

Figure 26. HEC-6 and TRIM2D simulated water-surface and thalweg elevations for peak flows of 70, 100, and 150 cubic meters per second on the Big Lost River upstream of the Pioneer diversion structures, Idaho National Engineering and Environmental Laboratory, Idaho.

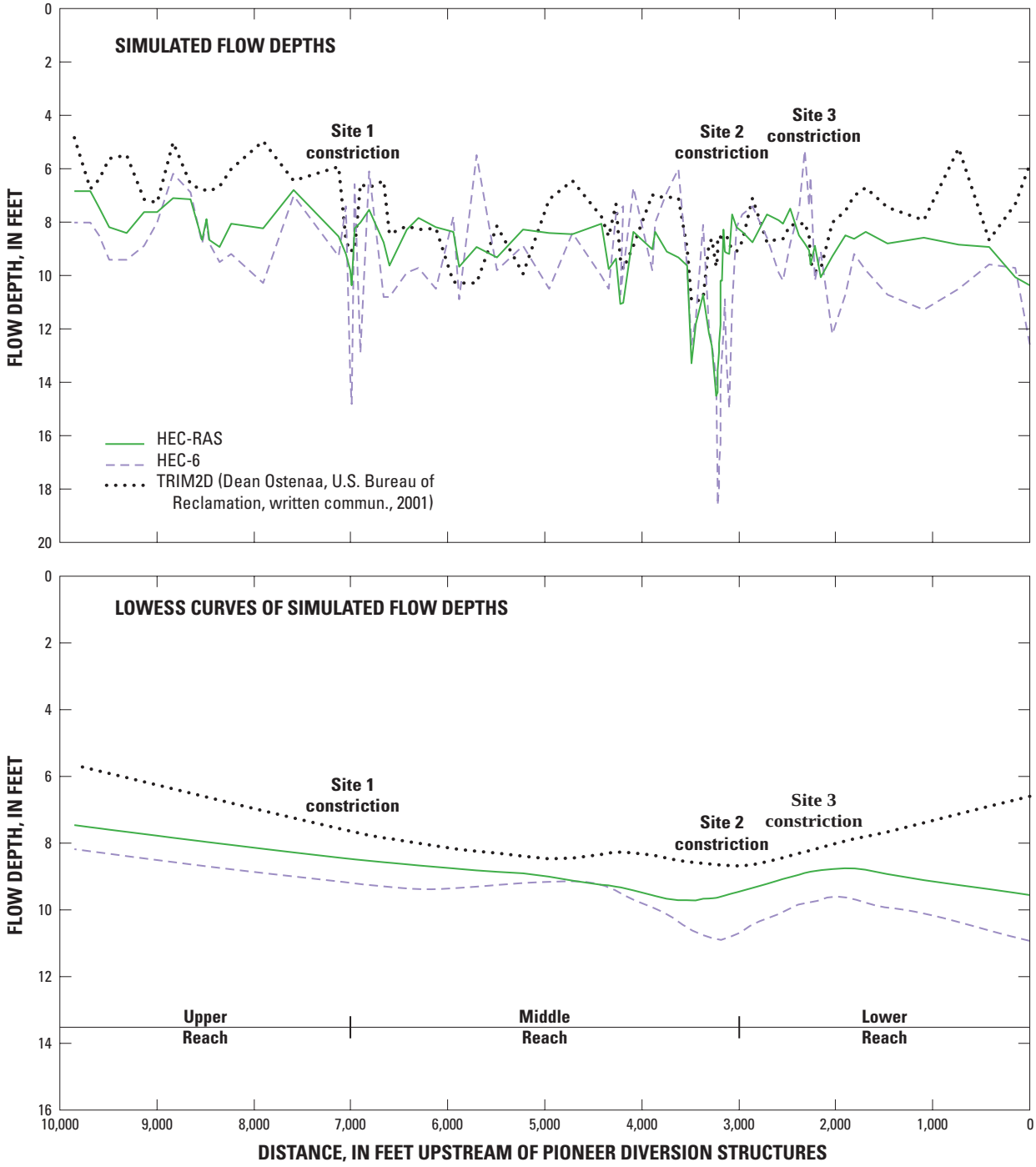

A. Peak Flow of 70 cubic meters per second

Figure 27. HEC-RAS, HEC-6, and TRIM2D simulated flow depths and LOWESS-smoothed flow depths for peak flows of 70, 100, and 150 cubic meters per second on the Big Lost River upstream of the Pioneer diversion structures, Idaho National Engineering and Environmental Laboratory, Idaho.

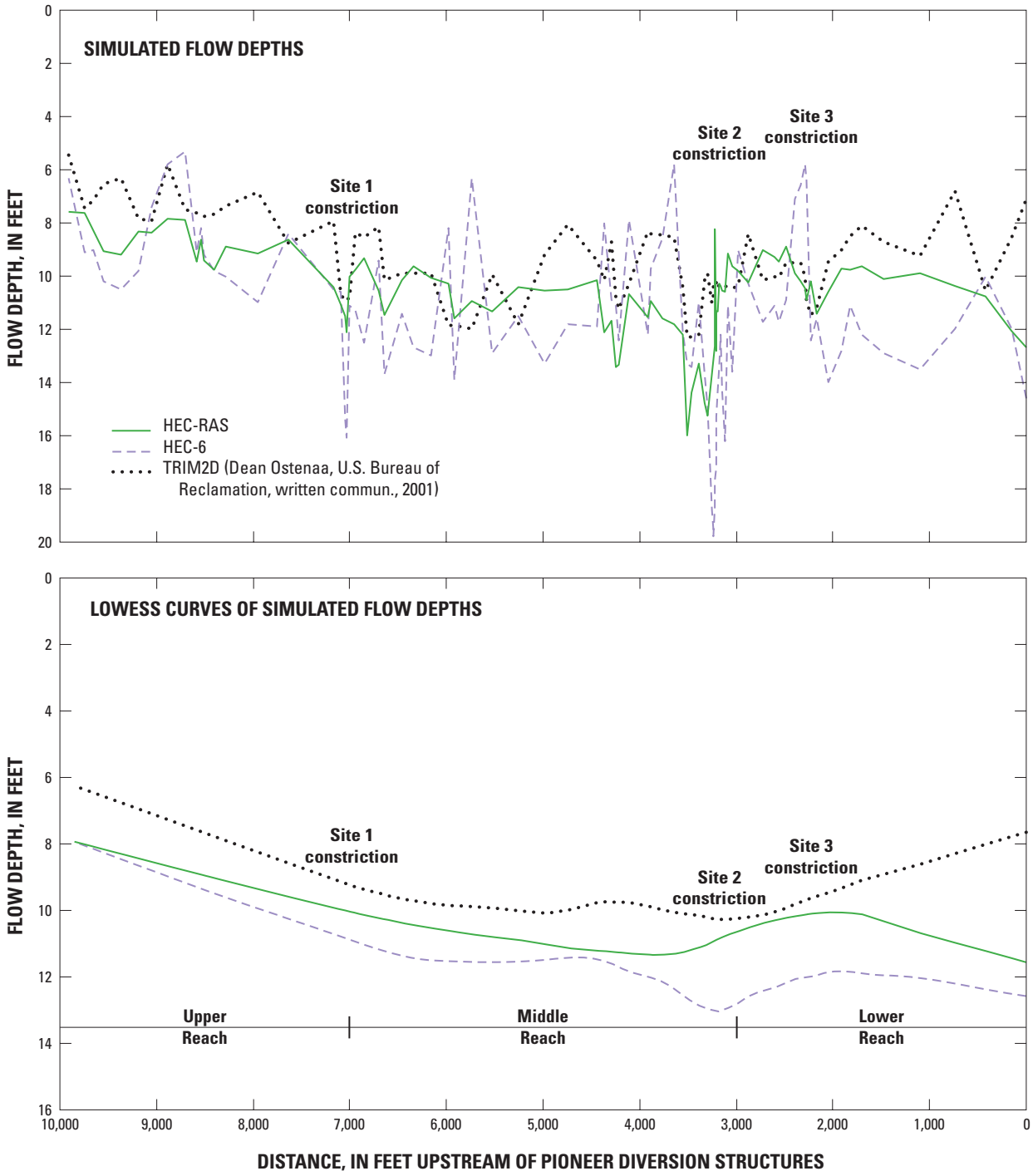

B. Peak flow of 100 cubic meters per second

Figure 27.—Continued.

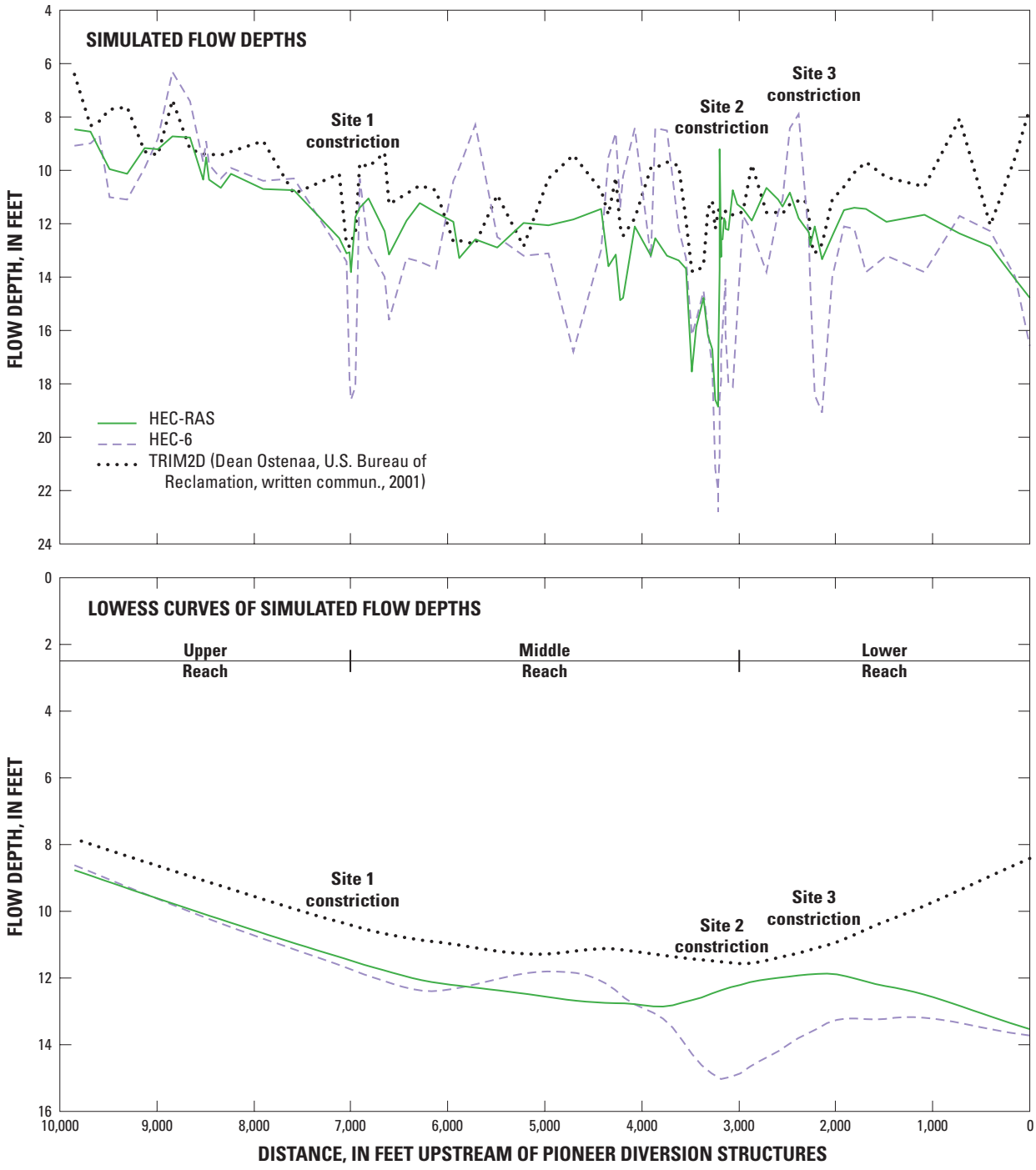

C. Peak flow of 150 cubic meters per second

Figure 27.—Continued.

The most conspicuous difference in the shape of the LOWESS-smoothed flow-depth profiles occurs downstream of the site 3 constriction where flow depths for the HEC-RAS model trend in an opposite direction to those of the TRIM2D model. To maintain steady flow, TRIM2D flow-depth profiles imply that cross-section flow areas per unit of flow depth and(or) flow velocities must be greater than those for the HEC-RAS model and that either or both of these must increase systematically in a downstream direction to compensate for the apparent systematic reduction in TRIM2D flow depths that occur downstream of the site 3 constriction (figs. 27*A*, 27*B*, and 27*C*). The depth-area curves for the field-surveyed and TIN-extended cross sections (for example cross sections 20 and 42, fig. 22) do not indicate an appreciable or systematic increase in cross-section flow area as a function of depth that would be sufficient to compensate for the TRIM2D flow-depth trend shown in figures 27*A*, 27*B*, and 27*C*.

In the lower reach of the river, TRIM2D model results for a peak flow of 100 m^3/s (appendix 4) indicate extensive overbank flow between cross section 1 and cross section 43 (fig. 9*C*). Overbank flow was not simulated in the HEC-RAS model in the lower reach of the river. Comparisons of HEC-RAS and TRIM2D thalweg elevations in this reach of the river indicate a substantial difference in relief between cross section 1 and cross section 42 (fig. 19). In the TRIM2D model, relief between these two locations was 5.6 ft, compared to 10.6 ft in the HEC-RAS model, suggesting that higher TRIM2D flow velocities are not likely to occur in this reach of the river to compensate for shallower flow depths. Extensive overbank flow in the TRIM2D model along this reach of the river, however, may be sufficient to compensate for shallower flow depths to satisfy the steady-flow assumption.

The effect of the site 2 constriction on flow depths is evident in the HEC-RAS, HEC-6, and TRIM2D flow-depth profiles (figs. 27*A*, 27*B*, and 27*C*). Comparisons of the flow-depth profiles for peak flows of 70, 100, 150 m^3/s indicate that this constriction does not appear to have as much influence on the overall shape of the TRIM2D depth profile as it does on the HEC-RAS and HEC-6 profiles from one flow simulation to another. Furthermore, TRIM2D flow depths (smoothed) increase as flow approaches and moves through the site 2 constriction, whereas HEC-RAS and HEC-6 flow depths decrease as flow approaches and moves through the site 2 constriction. Reduced HEC-RAS and HEC-6 flow depths, immediately upstream of the site 2 constriction, is consistent with flow acceleration and the transitioning of flow from subcritical to supercritical flow inside this constriction. Increasing flow depths, immediately upstream of the site 2 constriction in the TRIM2D model, suggest that flow is not accelerating sufficiently through the site 2 constriction to produce supercritical flow.

To maintain steady flow into and out of a model reach, shallower flow depths imply that average TRIM2D flow velocities must be higher than those for HEC-RAS, or that cross-section flow areas per unit of depth must be greater (or both). Depth-area curves (fig. 22) indicate that cross-section flow areas are greater in the TRIM2D model for the same flow depth over much of the upper and middle reaches of the river. The flatter thalweg slopes used in the TRIM2D model, however, imply that flow velocities should be lower than those of HEC-RAS. Higher average velocities (discussed in the section "Comparisons of HEC-RAS and TRIM2D Flow Velocities") are not consistent with this observation, and indicate that cross-section flow areas must be sufficiently different to compensate for lower flow velocities for the steady-flow assumption to be valid.

Comparisons of HEC-RAS and TRIM2D Flow Velocities

Flow-velocity profiles for the 100 m^3/s HEC-RAS and TRIM2D simulations are shown in figure 28 and flow velocities at selected cross sections for peak flows of 70, 100, and 150 m^3/s are presented in table 10. HEC-RAS velocities represent average velocities within a rectangular slice of each channel cross section shown in figure 9*C*. The width of the cross-section slice is defined by the left and right banks of the main channel. TRIM2D velocities represent maximum velocities within the main channel at each of the cross sections shown in figure 9*C*. In the upper reach of the river, overbank flow was simulated in both the TRIM2D and HEC-RAS models, and because of the wide and complex character of the cross sections in this reach of the river, comparisons of average velocities are difficult to make. In the lower reach of the river, velocity comparisons are less meaningful because extensive overbank flow was simulated in the TRIM2D model but was not simulated in the HEC-RAS model (appendix 4).

In the middle reach of the river, velocity comparisons between models are more meaningful because all of the flow in the HEC-RAS model and most of the flow in the TRIM2D model occurs inside the main channel. Flow-depth profiles presented previously indicate that flow depths are deepest for both the HEC-RAS and the TRIM2D model along the middle reach of the river (figs. 27*A*, 27*B*, and 27*C*). For a deep, narrow channel, vertically averaged velocity will vary more strongly across the channel because of increased frictional resistance along the banks of the channel. And because of this, maximum TRIM2D flow velocities should be higher than average HEC-RAS velocities along the middle reach of the river.

Table 10. HEC-RAS and TRIM2D simulated flow velocities at selected cross sections for peak flows of 70, 100, and 150 cubic meters per second on the Big Lost River upstream of the Pioneer diversion structures, Idaho National Engineering and Environmental Laboratory, Idaho.

[Location of cross sections is shown in figure 9*C*. ft/s, ft per second; m^3/s, cubic meter per second]

Cross section	Simulated velocity (ft/s) for selected peak flows in the					
	HEC-RAS model			TRIM2D model		
	70 m^3/s	100 m^3/s	150 m^3/s	70 m^3/s	100 m^3/s	150 m^3/s
20	6.0	7.2	7.9	1.8 [1](7.2)	2.5 (8.0)	6.7 (9.1)
42 (BLR#8)	6.7	7.4	7.6	3.1 (7.6)	2.5 (8.3)	1.6 (8.9)
56	5.2	5.0	6.1	6.0	6.8	7.9
72 (BLR#6)	4.4	4.6	5.5	3.8	4.3	5.9
76	6.8	7.1	8.4	5.5	6.7	8.3
98 (near saddle area)	2.5	2.6	2.7	2.4 (4.9)	2.1 (4.1)	0.3 (4.2)
84 (site 1 constriction)	10.1	10.8	12.3	8.3	9.0	10.8
52 (site 2 constriction)	12.0	17.5	12.7	9.2	10.0 (15.5)	11.1 (11.3)
33 (site 3 constriction)	5.9	6.7	7.5	4.5 (8.6)	5.4 (9.2)	3.6 (8.5)

[1](7.2) Value in parenthesis represents the maximum velocity in overbank areas.

Along the upstream section of the middle reach average HEC-RAS flow velocities are comparable to maximum TRIM2D flow velocities at and immediately downstream of the site 1 constriction for a peak flow of 100 m^3/s. At the site 1 constriction (cross section 84), for a peak flow of 100 m^3/s, TRIM2D and HEC-RAS flow velocities are 9.0 and 10.8 ft/s, respectively, and between cross sections 84 and 70.5, TRIM2D velocities are, on average, 11 percent higher than HEC-RAS velocities. Along the downstream section of the middle reach, TRIM2D flow velocities are much higher and do not compare closely to HEC-RAS velocities between cross sections 53 through 70. Along this section of the river, TRIM2D velocities are, on average, 70 percent higher than HEC-RAS velocities. Immediately upstream of the site 2 constriction, HEC-RAS and TRIM2D simulation results are comparable. Within the site 2 constriction, however, the maximum TRIM2D velocity (12.7 ft/s) is much lower than the maximum HEC-RAS velocity (22.3 ft/s). The lower TRIM2D velocity is below the threshold velocity required for critical flow, 18.6 ft/s, and consequently LOWESS-smoothed TRIM2D flow depths increase as flow moves through this constriction; this is in contrast to the HEC-RAS flow depths that decrease as flow moves through this constriction (figs. 27*A*, 27*B*, and 27*C*).

Under the assumption of steady flow, TRIM2D flow velocities that are higher than those of HEC-RAS along the downstream section of the middle reach of the river are consistent with the shallower TRIM2D flow depths in this reach of the river (figs. 27*A*, 27*B*, and 27*C*); however, velocities higher than HEC-RAS are not consistent with the lower thalweg slope that was used in the TRIM2D model (23 percent less than the HEC-RAS thalweg slope).

Downstream of the site 2 constriction, TRIM2D velocities are much higher than those of HEC-RAS. As noted previously, extensive overbank flow was simulated in the TRIM2D model along this reach of the river, and because of this velocity comparisons between TRIM2D and HEC-RAS are not meaningful. Under the assumption of steady flow, higher TRIM2D velocities accompanied by overbank flow may be sufficient to compensate for the systematic flow-depth reductions that were described previously. However, TRIM2D velocities higher than those of HEC-RAS in the lower reach of the river are not consistent with the much lower thalweg slope that was used in the TRIM2D model (44 percent less than the HEC-RAS thalweg slope).

Comparisons of HEC-RAS and TRIM2D Stream Power

Stream power is used as an indicator of the erosional forces acting on a channel and floodplain. Stream power was used by Ostenaa and others (1999) to identify areas where simulated erosional forces would be sufficient to remove evidence of older alluvial deposits and floodplain terrain features that were used to define non-exceedance bounds for paleofloods with return periods of 300 to 500 years and 10,000 years. In general, stream power is maximum where both flow depth and velocity are maximum, and, in most cases, both of these conditions will occur along or near the thalweg of the channel, assuming off-channel and overbank flow are limited and flow is not forced to accelerate around bends in the river. Stream power is defined as (Yang, 1996, p. 66):

$$\text{Stream Power} = \tau V = (\gamma DS)V, \quad (4)$$

where:

τ is shear stress acting over the wetted perimeter $[M/LT]$,
γ is specific weight of water $[M/L^3]$,
D is average depth of flow in the cross section $[L]$,
S is energy slope $[L0]$, and
V is average stream flow velocity $[L/T]$.

The units for these terms are mass $[M]$, length $[L]$, time $[T]$, and dimensionless $[L0]$.

Stream power is included in the computational output of both the HEC-RAS and TRIM2D models. Stream-power profiles for the 100 m³/s TRIM2D and HEC-RAS flow simulations are shown in figure 29. HEC-RAS stream power was computed on the basis of maximum flow depth (fig. 27*B*) and average flow velocity (fig. 28) at each cross section shown in figure 9*C*. TRIM2D stream power represents the highest stream power in the main channel at these cross sections; however, in many cases this occurs in areas where extensive overbank flow was simulated (appendix 4). Stream power should not be expected to compare closely in areas where simulated flow depths (fig. 27*B*) and flow velocities (fig. 28) differ significantly (primarily in the upper and lower reaches of the river). However, there are very few locations where TRIM2D and HEC-RAS stream power are comparable (fig. 29).

In general, stream power was much greater in the TRIM2D model than in the HEC-RAS model (table 11). The average TRIM2D stream power for all cross sections shown in figure 9C (fig. 29) is 1.5 times greater than HEC-RAS, this in spite of the fact that TRIM2D flow depths are shallower than HEC-RAS flow depths throughout the model reach (figs. 27*A*, 27*B*, and 27*C*) and the average maximum TRIM2D flow velocities are only 1.1 times higher than the average HEC-RAS flow velocities (fig. 28). For the HEC-RAS simulations, stream power ranged by almost three orders of magnitude, from a low of 3.6 W/m² to a high of 3,009 W/m². For the TRIM2D simulations, stream power ranged by almost two orders of magnitude, from a low of 8.1 W/m² to a high of 559 W/m² in the main channel (overbank flow excluded).

With the exception of the peak stream power inside the site 2 constriction, TRIM2D and HEC-RAS stream powers are comparable only in the immediate vicinity of the sites 1, 2, and 3 constrictions. The much lower TRIM2D stream power at the site 2 constriction results from the much lower velocity that was simulated at this location (supercritical flow was not simulated). The very high HEC-RAS stream power at the site 2 constriction reflects the high flow velocities through this constriction during supercritical flow.

A stream power value of 100 W/m² or more is capable of eroding and transporting pebble- and cobble-size particles as demonstrated in the HEC-6 simulations. HEC-6 simulations indicated that the lowest stream power would occur at or near the saddle area (section 98), and the highest value would occur inside the site 2 constriction. Because stream power inside the site 2 constriction was much greater than 100 W/m², HEC-6 results showed that sediment fill inside this constriction would be eroded to bedrock (figs. 16*A* and 16*B*). Stream powers for the HEC-RAS simulations at the site 3 constriction were much less than at the site 1 and 2 constrictions. HEC-6 simulations indicated that for a peak flow 100 m³/s stream power would not be sufficient to erode the channel fill inside these constrictions down to bedrock.

Table 11. HEC-RAS and TRIM2D simulated stream power at selected cross sections for peak flows of 70, 100, and 150 cubic meters per second on the Big Lost River upstream of the Pioneer diversion structures, Idaho National Engineering and Environmental Laboratory, Idaho.

[Location of cross sections is shown in figure 9*C*. W, watts; m², squared meter; W/m², watts per squared meter; m³/s, cubic meter per second]

Cross section	Simulated stream power (W/m²) for selected peak flows in the					
	HEC-RAS model			TRIM2D model		
	70 m³/s	100 m³/s	150 m³/s	70 m³/s	100 m³/s	150 m³/s
20	29	44	59	25 [1](114)	139 (145)	205 (204)
42 (BLR#8)	106	133	130	139 (149)	147 (227)	165 (269)
56	31	27	46	75	92	199 (237)
72 (BLR#6)	12	13	21	18	22	58
76	47	51	79	52	82	230
98 (near saddle area)	4	5	5	19 (41)	10 (27)	0.4 (24)
84 (site 1 constriction)	161	193	279	160	259	323
52 (site 2 constriction)	440	1,384	482	348	327 (1,841)	382 (2,537)
33 (site 3 constriction)	61	82	109	67 (271)	102 (289)	37 (210)

[1](114) Value in parenthesis represents the maximum stream power in overbank areas.

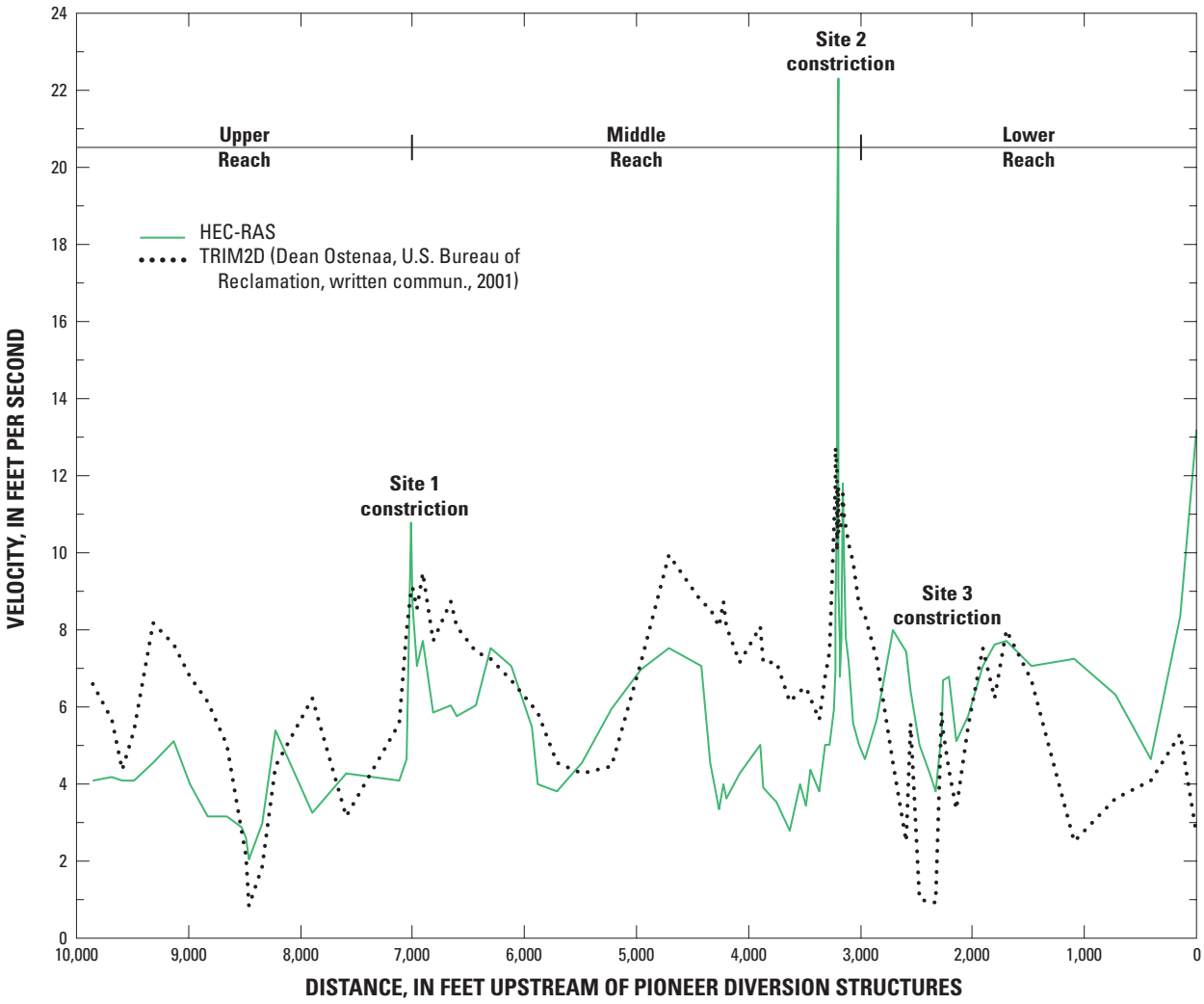

Figure 28. HEC-RAS and TRIM2D simulated flow velocities in the main channel for a peak flow of 100 cubic meters per second on the Big Lost River upstream of the Pioneer diversion structures, Idaho National Engineering and Environmental Laboratory.

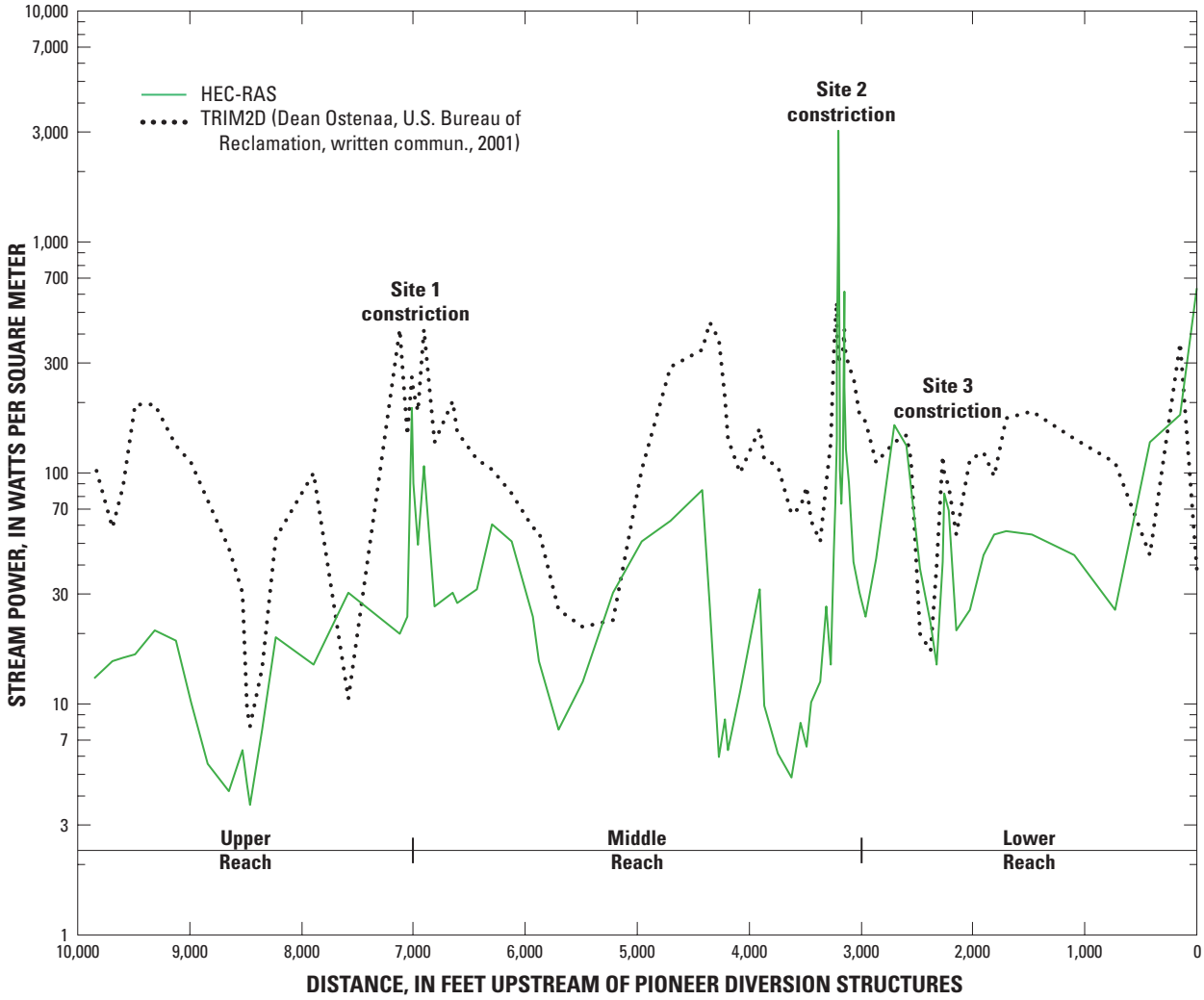

Figure 29. HEC-RAS and TRIM2D simulated stream power in the main channel for a peak flow of 100 cubic meters per second on the Big Lost River upstream of the Pioneer diversion structures, Idaho National Engineering and Environmental Laboratory, Idaho.

Summary and Conclusions

A 1.9-mile reach of the Big Lost River, between the Idaho National Engineering and Environmental Laboratory (INEEL) diversion dam and the Pioneer diversion structures, was investigated to evaluate the effects of streambed erosion and bedrock constrictions on model predictions of water-surface elevations. Two one-dimensional (1-D) models, a fixed-bed surface-water flow model (HEC-RAS) and a movable-bed surface-water flow and sediment-transport model (HEC-6), were used to evaluate these effects. The results of these models were compared to the results of a two-dimensional (2-D) fixed-bed model [Transient Inundation 2-Dimensional (TRIM2D)] that had previously been used to predict water-surface elevations for peak flows with sufficient stage and stream power to erode floodplain terrain features (Holocene inset terraces referred to as BLR#6 and BLR#8) dated at 300 to 500 years old, and an unmodified Pleistocene surface (referred to as the saddle area) dated at 10,000 years old.

Previously developed models of flooding in the Big Lost River, the U.S. Geological Survey (USGS) Water-Surface PROfile (WSPRO) model and the Bureau of Reclamation TRIM2D model, did not account for scouring of the streambed and did not simulate the effects of supercritical flow during flooding. Because of these limitations, TRIM2D predictions of flood stage may have underestimated the magnitude of flows required to overtop and erode floodplain terrain features that were used to estimate the minimum return period of floods with sufficient stage and stream power to erode the dated surfaces. TRIM2D model simulation results were used to extend the period of record at the streamflow-gaging station near Arco for flood-frequency analysis to estimate the magnitude of the 100-year flood, and the magnitude of floods with return periods as long as 10,000 years. The results of the study described in this report were also used to evaluate the results of the TRIM2D model simulations that were used to predict flood elevations at different assumed peak flows.

On the INEEL, the Big Lost River is an ephemeral stream that typically is incised less than 20 ft into Holocene and upper Pleistocene alluvium and middle to upper Pleistocene basalt lava flows. Alluvial fill overlies basalt bedrock over most of the streambed, but in several places bedrock is exposed. At three locations in the study reach (designated sites 1, 2, and 3) the river is constricted by basalt bedrock and the channel narrows considerably. At the site 2 constriction, the narrowest point along the river, the channel narrows from a width of 53 to 17 ft and is more than 20 ft deep. The site 1 and site 3 constrictions are less dramatic. The channel at these two constrictions narrows from a width of 45 to 27 ft at site 1, and from 53 to 46 ft at site 3.

Twenty-four trenches were excavated to determine the grain-size distribution of sediments composing the channel fill. The dominant material in the streambed is coarse sand, pebbles, and cobbles. The median diameter (d_{50}) of the channel-fill samples ranges from 0.17 to 35.5 mm. Except near the constrictions, the streambed is armored with a thin veneer of lightly-cemented pebbles and cobbles that protects the streambed from scour at low to moderate flows. The median diameter of particles composing the armored surface layer ranges from 6 to 47 mm, significantly larger than the underlying channel fill. The results of streambed and channel-fill sampling indicate that the river would be classified as a gravel-bed river.

Inside the three constrictions the channel fill consists predominantly of sands and silts with widely dispersed pebbles. Stratification of the sands and silts is common inside the constrictions and armoring is absent. The fill material inside the constrictions is very susceptible to erosion. Bedrock was encountered in these constrictions at depths of 4 to 6 ft. Grain-size distributions for the armored surface layer and underlying channel fill were used in the HEC-6 model to simulate flow and sediment transport and to evaluate the effects of streambed erosion and sediment deposition on water-surface elevations.

Channel and floodplain geometries used in this study were defined by 76 field-surveyed cross sections. Field-surveyed cross sections inside the constrictions were spaced less than 50 ft apart, and sections in straight reaches of the channel were spaced several hundred feet apart. Field-surveyed cross sections were extended out into the floodplain and additional cross sections were constructed using a 1-ft contour digital terrain map acquired from a 1999 aerial photography survey of the area by the Bureau of Reclamation. Several different cross-section assemblages, using a combination of field-surveyed, TIN (Triangulated Irregular Network) -generated, TIN-extended, and linearly-interpolated cross sections were used to simulate peak flows ranging from 10 to 200 cubic meters per second (m^3/s).

Water-surface elevations for peak flows of 10, 50, 70, 100, 150, 187, and 200 m^3/s were simulated with the HEC-RAS and HEC-6 models. The roughness coefficient, or *n* value used in the HEC-RAS model was calibrated against the 2-year flood (10 m^3/s) to evaluate the *n* values that were selected to characterize frictional resistance in the active channel. Representative *n* values were calculated using several flow-resistance equations developed for gravel-bed rivers. Comparisons of simulated to field-surveyed high-water marks, assumed to represent the water-surface elevation of a 2-year flood, indicated that the hydraulic characteristics of the channel bed were adequately represented by the initial choices for the *n* values—0.025 for straight reaches, 0.033 for moderately curved reaches, and 0.038 for severely curved reaches.

The HEC-RAS model results also indicated that simulated water-surface elevations for flows less than 100 m^3/s were most sensitive to the *n* values chosen to represent bed roughness in the channel-controlled sections of the river and least sensitive in constriction-controlled sections of the river, the effects of which were simulated by adjusting the *n* value

by factors of 0.5 and 1.5. The HEC-RAS model also was used to evaluate the sensitivity of channel erosion on water-surface elevations by artificially reducing streambed elevation by 1, 2, and 4 ft, except in areas where bedrock is exposed or was encountered at shallower depths. As anticipated lowering of the streambed in these model simulations resulted in water-surface elevations that were equal to or less than water-surface elevations using the measured streambed.

HEC-RAS model simulations indicated that the constrictions at sites 1 and 2 have the most influence on backwater accumulations in the study reach. These controls begin to have major impact when flows exceed 50 m^3/s at the site 2 constriction and 100 m^3/s at the site 1 constriction. Backwater affects about 500 ft of the river upstream of the site 1 constriction and 1,000 ft of the river upstream of the site 2 constriction for a peak flow of 100 m^3/s. The HEC-RAS simulations also indicated that flow through the site 2 constriction becomes supercritical at flows greater than and equal to 100 m^3/s. For peak flows less than and equal to 70 m^3/s, flow remained subcritical throughout the model reach.

Because HEC-RAS is a fixed-bed model, the HEC-6 model was used to study the effects of streambed erosion and sediment deposition on water-surface elevations. HEC-6 model simulations indicated that the streambed was scoured down to bedrock at the site 2 constriction for peak flows greater than and equal to 70 m^3/s. The resulting HEC-6 streambed elevation averaged about 0.5 to 0.7 ft lower than the HEC-RAS fixed-streambed elevation throughout the model reach for peak flows ranging from 70 to 150 m^3/s. HEC-6 water-surface elevation differences at the paleoindicator sites indicated that sediment deposition will produce overtopping of the BLR#6 site at flows smaller than those predicted by the HEC-RAS model simulations; and that streambed erosion will produce overtopping of BLR#8 and the saddle area at flows that are larger than those predicted by the HEC-RAS model simulations.

Simulation results from the 1-D HEC-RAS and HEC-6 models were compared to the results of the 2-D TRIM2D model that was used by the Bureau of Reclamation to evaluate flood flows in the study reach. In most cases the TRIM2D model simulated higher water-surface elevations, shallower flow depths, higher flow velocities, and higher stream powers than the HEC-RAS and HEC-6 models for the same peak flows. The HEC-RAS model required flow increases of 83 percent (from 100 to 183 m^3/s) and 45 percent (from 100 to 145 m^3/s) to match TRIM2D simulations of water-surface elevation at the BLR#6 and BLR#8 paleoindicator sites; and an increase of 13 percent (from 150 to 169 m^3/s) to match TRIM2D simulations of water-surface elevation at the saddle area. However, a field survey of the saddle area indicated that the elevation of the lowest point on the saddle area was 1.2 ft higher than indicated on the 2-ft contour map that was used in the development of the TRIM2D model. Because of this elevation discrepancy, HEC-RAS model simulations indicated that a peak flow of at least 210 m^3/s would be needed to initiate flow across the 10,000 year-old Pleistocene surface, and flows greater than 210 m^3/s (not modeled in this study) would be needed to erode this surface.

The increases in flow that needed to be simulated in the HEC-RAS and HEC-6 models to match TRIM2D water-surface elevations were attributed in part to the effects of supercritical flow through one constriction in the reach and to differences in the channel geometry input data that were used in the TRIM2D and HEC-RAS models and for initial conditions in the HEC-6 model. Field-surveys of the model reach indicated that:

1. The average TRIM2D thalweg elevation (corrected for a 3.484 ft datum shift between the NVGD 29 elevation datum used in the TRIM2D model and the NAVD 88 elevation datum used in the HEC-RAS and HEC-6 models) is 2.5 ft higher than the field-surveyed thalweg elevation;

2. The slope of the TRIM2D thalweg along the entire model reach is 15 percent lower than the thalweg slope used in the HEC-RAS model resulting in a 5 ft difference in the topographic relief of these two models between the upstream and downstream ends of the model reach;

3. The thalweg slopes used in the TRIM2D model are 13, 23, and 44 percent flatter than those used in the HEC-RAS model along the upper, middle, and lower reaches, respectively;

4. The topographic variability of the TRIM2D thalweg is greater than the HEC-RAS thalweg along the upper, middle, and lower reaches;

5. The cross-section flow areas at many locations in the TRIM2D model are larger than those in the HEC-RAS model for the same flow depth (the slope of the depth-area curves are steeper); and

6. The cross-section flow areas in the TRIM2D model generally are smaller than those in the HEC-RAS model for the same stage or water-surface elevation over the upper half of the model reach (stage-area curves are steeper) and larger over the lower half of the model reach (stage-area curves are flatter).

Differences in simulated water-surface elevations between the TRIM2D model and the HEC-RAS and HEC-6 model are attributed primarily to differences in topographic relief and to differences in the channel and floodplain geometries used in these models. Topographic differences were sufficiently large that it was not possible to isolate the effects of these from those attributable to the effects of supercritical flow, streambed scour, and sediment deposition.

Acknowledgments

The authors express their appreciation to Kenneth Beard, with Bechtel BWXT Idaho (BBWI), for providing the field-surveyed horizontal- and vertical-control data that were used in this study. Appreciation is extended to Jay T. Brown, with BBWI, and Sabrina A. Conti and Douglas C. Werner, with the USGS, for their assistance with surveying the cross sections that were used to model flow and sediment transport; to Larry Matson and Matthew J. Gilbert, with the USGS, for their untiring efforts with the extensive trench excavations that were undertaken under severe field conditions following a range fire in 2000; to Amy J. Wehnke, with the USGS, for her assistance with the particle-size analyses; to Brennon R. Orr, formerly with the USGS, for his assistance in obtaining the environmental permits to excavate trenches in the river channel and for coordinating the field logistics for this study; to Dr. James H. Milligan, Professor of Civil Engineering at the University of Idaho, for his assistance with formulating the flow resistance (Manning's *n*) and sediment loading equations used in the HEC-RAS and HEC-6 models; to Jon Hortness and Stephen Wiele, with the USGS, Dean A. Ostenaa, with the Bureau of Reclamation, and Robert J. Creed, with the DOE, for their reviews of this manuscript; and finally to Peter J. Dirkmaat, formerly with the DOE, for arranging the funding to conduct this study.

References Cited

Ackers, P., and White, W.R., 1973, Sediment transport: New approach and analysis: Journal of Hydraulics, American Society of Civil Engineers, v. 99, no. HY11, p. 2041-2060.

American Society of Civil Engineers, 1975, Sedimentation engineering, American Society of Civil Engineers, Hydraulics Division, Sedimentation Committee, Task Committee for the Preparation of the Manual on Sedimentation, Manuals and Reports on Engineering Practice, no. 54, 745 p.

American Society for Testing and Materials, 1985, Manual on test sieving methods, guidelines for establishing sieve analysis procedures: American Society for Testing and Materials, STP 447 B, 43 p.

Bennett, C.M., 1986, Capacity of the diversion channel below the flood-control dam on the Big Lost River at the Idaho National Engineering Laboratory, Idaho: U.S. Geological Survey Water-Resources Investigations Report 86-4204, 25 p.

Berenbrock, Charles, and Kjelstrom, L.C., 1998, Preliminary water-surface elevations and boundary of the 100-year peak flow in the Big Lost River at the Idaho National Engineering and Environmental Laboratory, Idaho: U.S. Geological Survey Water-Resources Investigations Report 98-4065, 13 p.

Berenbrock, Charles, and Doyle, J.D., 2003, Stage-discharge relations for selected culverts and bridges in the Big Lost River flood plain at the Idaho National Engineering and Environmental Laboratory, Idaho: U.S. Geological Survey Water-Resources Investigations Report 03-4066, 62 p.

Bray, D.I., 1979, Estimating average velocity in gravel-bed rivers: American Society of Civil Engineers, Journal of the Hydraulics Division, v. 105, no. 9, pp. 1103-1122.

Carrigan, P.H., 1972, Probability of exceeding capacity of flood-control system at the National Reactor Testing Station, Idaho: U.S. Geological Survey Open-File Report, 102 p.

Chow, V.T., 1959, Open-channel hydraulics: New York, McGraw-Hill, 680 p.

Chow, V.T., 1964, Handbook of applied hydrology—a compendium of water-resources technology: McGraw-Hill, New York, variously paged.

Crosthwaite, E.G., Thomas, C.A., and Dyer, K.L., 1970, Water Resources in the Big Lost River Basin, south-central Idaho: U.S. Geological Survey Open-File Report, 109 p., 4 pls.

Dawdy, D.R., 1979, Flood frequency estimates on alluvial fans: American Society of Civil Engineers, Journal of the Hydraulics Division, v. 105, no. 5, pp. 1407-1413.

Downs, W.A., Miller, W., Bledsoe, J., Nelson, E.J., Radaideh, M., and Smemoe, C., 1999, Probabilistic hydrologic modeling for the proposed High Level Waste Treatment Facility at the Idaho National Engineering and Environmental Laboratory, Part 2—Hydraulic Routing: Brigham Young University, Department of Civil and Environmental Engineering, 162 p.

Druffel, L., Stiltner, G.J., and Keefer, T.N., 1979, Probable hydrologic effects of a hypothetical failure of Mackay Dam on the Big Lost River Valley from Mackay, Idaho, to the Idaho National Engineering Laboratory: U.S. Geological Survey Water-Resources Investigation Report 79-99, 47 p.

Einstein, H.A., 1950, The bed-load function for sediment transportation in open channel flows: U.S. Department of Agriculture, Soil Conservation Service, Technical Bulletin 1026, Washington, D.C., p. 71.

Federal Emergency Management Agency, 1998, Guidelines and specifications for study contractors: U.S. Government Printing Office, Sept. 7, 202 p.

Folk, R.L., 1980, Petrology of sedimentary rocks: Hemphill Pub. Co., Austin, TX, 182 p.

Geslin, J.K., Link, P.K., and Fanning, C.M., 1999, High-precision provenance determination using detrital-zircon ages and petrography of Quaternary sands on the eastern Snake River Plain, Idaho, Geology, v. 27, no. 4, p. 295-298.

Gomez, B., and Church, M., 1989, An assessment of bed load sediment transport formulae for gravel bed rivers: Water Resources Research, v. 25, no. 6, p. 1161-1186.

Hey, R.D., 1979, Flow resistance in gravel-bed rivers: Journal of Hydraulics, American Society of Civil Engineers, v. 105, no. HY 4, p. 365-379.

Hortness, J.E., and Rousseau, J.P., 2002, Estimating the magnitude of the 100-year peak flow in the Big Lost River at the Idaho National Engineering and Environmental Laboratory, Idaho: U.S. Geological Survey Water-Resources Investigations Report 02-4299, 36 p.

Interagency Advisory Committee on Water Data, 1982, Guidelines for determining flood flow frequency, Bulletin #17B of the Hydrology Subcommittee: Reston, Va., U.S. Geological Survey, Office of Water Data Coordination, 183 p.

Kalinske, A.A., 1947, Movement of sediment as bed load in rivers: American Geophysical Union Transactions, v. 28, p. 615-620.

Kjelstrom, L.C., and Berenbrock, Charles, 1996, Estimated 100-year peak flows and flow volumes in the Big Lost River and Birch Creek at the Idaho National Engineering Laboratory, Idaho: U.S. Geological Survey Water-Resources Investigations Report 96-4163, 23 p.

Koslow, K.N., and Van Haaften, D.H., 1986, Flood routing analysis for a failure of Mackay Dam: Idaho Falls, Idaho, EG&G Idaho, Inc., EFF-EP-7184, 33 p.

Kuntz, M.A., Skipp, B., Lanphere, M.A., Scott, W.E., Pierce, K.L., Dalrymple, G.B., Champion, D.E., Embree, G.F., Page, W.R., Morgan, L.A., Smith, R.P., Hackett, W.R., and Rodgers, D.W, 1994, Geologic map of the Idaho National Engineering Laboratory and adjoining area, eastern Idaho: U.S. Geological Survey Miscellaneous Investigations Series Map I-2330, scale 1:100,000.

Lamke, R.D., 1969, Stage-discharge relations on Big Lost River within National Reactor Testing Station, Idaho: U.S. Geological Survey Open-File Report, IDO-22050, 29 p.

Limerinos, J.T., 1970, Determination of the Manning Coefficient from measured bed roughness in natural channels: U.S. Geological Survey Water-Supply Paper 1898-B, 47 p.

Meyer-Peter, E., and Müller, R., 1948, Formula for bed load transport: Proceedings, 2nd Meeting, v. 6, Int. Assn. Hydr. Res., Stockholm, p. 39-64.

Muskatirovic, Jasna, 2005, Prediction of sediment transport in gravel-bed rivers at the watershed scale for the purpose of assigning river restoration activities: Boise, University of Idaho, Ph.D. Dissertation, 460 p.

Mussetter, R.A., 1989, Dynamics of mountain streams: Ft. Collins, Colorado State University, Dept. of Civil Engineering, Ph.D. dissertation, 389 p.

Nakato, Tatsuaki, 1990, Test of selected sediment-transport formulas: Journal of Hydraulic Engineering, American Society of Civil Engineers, v. 116, no. 3, p. 362-379.

Nobel, C., 1980, A two-dimensional analysis of flooding of the Big Lost River below Box Canyon Outlet: Idaho Falls, Idaho, EG&G Idaho, Inc., EFF–EI–80–2, 26 p.

O'Dell, I., Lehmann, A.K., Campbell, A.M., Beattie, S.E., Brennan, T.S., 2002, Water Resources Data, Idaho, Water Year 2001, Part 1: U. S. Geological Survey Water-Data Report ID-01-1, 373 p.

Ostenaa, D.A., Levish, D.R., Klinger, R.E., 1999, Phase 2, Paleohydrologic and geomorphic studies for the assessment of flood risk for the Idaho National Engineering and Environmental Laboratory, Idaho: U.S. Bureau of Reclamation, Geophysics, Paleohydrology, and Seismotectonics Group, Technical Service Center, Report 9907, 300 p.

Rathburn, S.L., 1989, Pleistocene glacial outburst flooding along the Big Lost River, east-central Idaho: Tucson, Ariz., University of Arizona, M.S. thesis, 41 p.

Rottner, J., 1959, A formula for bed-load transportation: La Houille Blanche, v. 14, no. 3, p. 285-307.

Schoklitsch, A., 1962, Handbuch des Wasserbaues: Springer-Verlag, Vienna, 3rd ed.

Stearns, H.T., Crandall, L., and Steward, W.G., 1938, Geology and ground-water resources of the Snake River Plain in southeastern Idaho: U.S. Geological Survey Water-Supply Paper 774, 268 p.

U.S. Army Corps of Engineers, 1967, Postflood report, flood of June-July 1967, Big Lost River, Idaho: Walla Walla, Wash., U.S. Army Corps of Engineers, 15 p.

U.S. Army Corps of Engineers, 1991, Feasibility report, Big Lost River Basin, Idaho: Walla Walla, Wash., U. S. Army Corps of Engineers, variously paged.

U.S. Army Corps of Engineers 1993, HEC-6, Scour and deposition in rivers and reservoirs, user's manual: version 4.1.0: U.S. Army Corps of Engineers Hydrologic Engineering Center, August 1993, CPD-6, 287 p.

U.S. Army Corps of Engineers, 1997a, HEC-RAS, River analysis system, applications guide, version 3.0.1: U.S. Army Corps of Engineers Hydrologic Engineering Center, April 1997, 280 p.

U.S. Army Corps of Engineers, 1997b, HEC-RAS, River analysis system, hydraulic reference manual, version 3.0.1: U.S. Army Corps of Engineers Hydrologic Engineering Center, April 1997, 240 p.

U.S. Army Corps of Engineers, 1997c, HEC-RAS, River analysis system, user's manual, version 3.0.1: U.S. Army Corps of Engineers Hydrologic Engineering Center, April 1997, 243 p.

Walters, R.A., and Casulli, V., 1998, A robust finite-element model for hydrostatic surface water flows: Comm. in Num. Meth. Engr., v. 14, p. 931-940.

White, W.R., and Day, T.J., 1982, Transport of graded gravel bed material, *in* Hey, R.D., Bathurst, J.C., and Thorne, C.R., eds., Gravel-Bed Rivers: Fluvial Processes, Engineering, and Management: New York, John Wiley and Sons, p. 181-223.

Williams, R.P., and Krupin, P.J., 1984, Erosion, channel change, and sediment transport in the Big Lost River, Idaho: U.S. Geological Survey Water-Resources Investigations Report 84-4147, 87 p.

Wolman, M.G., 1954, A method of sampling coarse river-bed material: Transactions of the American Geophysical Union, v. 25, no. 6, p. 951-957.

Wright, A.E., 1903, Report on irrigation in the valley of Lost River, Idaho: U.S. Department of Agriculture Circular No. 58, 43 p.

Yang, C.T., 1996, Sediment Transport: theory and practice: McGraw-Hill Companies, Inc., New York, 396 p.

Yang, C.T., and Huang, C., 2001, Applicability of sediment transport formulas: International Journal of Sediment Research, v. 16, no. 3, p. 335-353.

This page intentionally left blank.

Glossary

Armor layer: A coarser surficial layer of sediments on the streambed. This layer ranges from one particle thickness to several. This layer can be quite resistant to scour—usually only high flows mobilize this layer and it may reform as flows decrease.

Backwater: Water backed up or retarded in its course as compared with its normal or natural condition of flow. Backwater is an increase in upstream flow depth. A sudden constriction in a channel can cause this effect.

Bank, left and right: Reference terms used to specify the banks on the left and right when facing downstream.

Bedform: Alluvial-channel bottom feature that depends on bed-material size, flow depth, and flow velocity. Bedforms include ripples, dunes, antidunes, and plane bed.

Conveyance: A measure of the carrying capacity of a channel section and is directly proportional to channel discharge. Conveyance is that part of Manning's equation that excludes the square root of the energy gradient or friction slope.

Choked flows: The constriction width is reduced to a point where critical flow conditions are reached or exceeded.

Critical flow: If the flow is critical, the Froude number is equal to one, and the inertial forces balance the gravitational forces. This balance takes place at the depth at which flow is at its minimum energy.

Ephemeral: A stream or reach of a stream that flows briefly in direct response to precipitation, and whose channel is at all times above the water table.

Floodplain: Land adjoining (or near) the channel of a watercourse which has been, or may be, covered by floodwaters. A flood plain functions as a temporary channel or reservoir for overbank flows. The lowland that borders a river, usually dry but subject to flooding.

Flow regime: A range of flows producing similar bed forms, resistance to flow, and mode of sediment transport.

Froude number: A dimensionless number used as an index to characterize the type of flow (subcritical, critical, and supercritical) in an open channel. The Froude number is the ratio of the inertial forces to the gravitational forces, and is computed as $Fr = V/(gD)^{1/2}$, where Fr is the Froude number; V is mean velocity of flow, in feet per second; g is acceleration of gravity, in feet per second squared; and D is hydraulic depth, in feet.

Grain size, coarse and fine: Coarse-grained bed material generally refers to those particles (pebble, cobble, and boulder) whose size can be individually measured with a graduated ruler or caliper; fine grained material (sand, silt, and clay) is measured by passage through a sieve, by rate of sedimentation, or by the Beckman Coulter Particle-Size Counter for very fine materials (< 0.0625 mm). See also particle size.

High-water marks: Evidence of the stage reached by flow. High-water marks generally consist of debris, scour marks, or staining of rocks found along the channel boundaries.

Hydraulic radius: Cross-section flow area divided by wetted perimeter.

Manning's roughness coefficient (*n* values): A measure of the frictional resistance exerted by a channel on the flow. The *n* value also can reflect other energy losses such as those resulting from the transport of material and debris, unsteady flow, extreme turbulence, that are difficult or impossible to isolate and quantify.

Particle-size: The size of material on the bed of a stream, referenced to a specific diameter (either maximum, intermediate, or minimum) of the measured particle.

Peak flow: The largest value of the runoff flow, which occurs during a flood, as observed at a particular point in the drainage basin.

Scour: Erosion due to flowing water, usually considered as being localized as opposed to general bed degradation.

Slope, water-surface: The slope of the water surface, computed as the change in elevation per unit change in the channel's length.

Stream power: A measure of energy transfer of the flow. Stream power is computed as $(\gamma DS)V$, where γ is the specific weight of water, D, water depth, in feet; S is the energy slope, dimensionless; and V is the mean velocity, in feet per second. Stream power also is defined as the energy dissipated per unit area of the streambed per unit time.

Subcritical flow: If the flow is subcritical, the Froude number is less than one and the inertial forces are less than the gravitational forces. The flow depth in subcritical flow is greater than the flow depth in critical flow.

Supercritical flow: If the flow is supercritical, the Froude number is greater than one and the inertial forces are greater than the gravitational forces. The flow depth in supercritical flow is less than the flow depth in critical flow.

Thalweg: A line connecting the lowest points along the length of a streambed. It can be quite sinuous and wander within the channel.

Transport capacity: The ability of a stream to transport a given volume or weight of sediment material of a specific size per time for a given flow condition. The units of transport capacity are usually given in tons per day of sediment transported past a given cross section for a given flow. Transport capacity for each sediment grain size is the transport potential for that size material multiplied by the actual fraction of each size class present in the bed and bank material.

Transport potential: Transport potential is the rate at which a stream could transport sediment of a given grain size for given hydraulic condition if the bed and banks were composed entirely of material of that size.

Water-surface profile: Longitudinal plots of the water-surface elevation as a function of distance downstream through a channel reach.

Wetted perimeter: Length of the line along which the water is in contact with the channel bottom in the cross-sectional area of the flow.

Appendix 1

Results of Armored-Surface-Layer Sampling at Various Locations on the Big Lost River Upstream of the Pioneer Diversion Structures, Idaho National Engineering and Environmental Laboratory

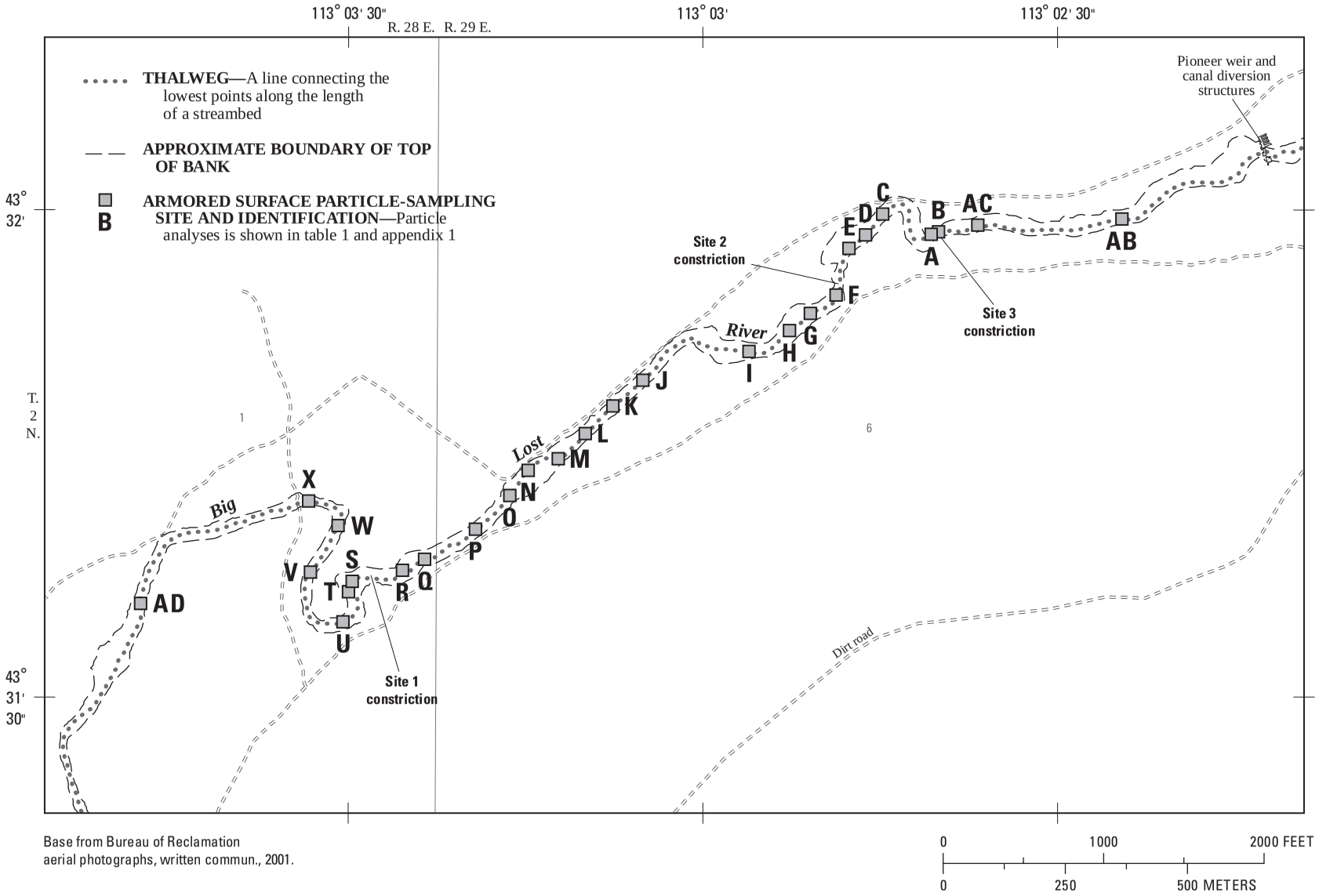

Figure 1–1. Location of armored-surface layer particle-sampling sites and constrictions on the Big Lost River upstream from Pioneer diversion structures, Idaho National Engineering and Environmental Laboratory, Idaho.

PARTICLE COUNTS

Site: A
Date: August 22, 2000
Measurement by: Brennon Orr
Remarks: Big Lost River below the INEEL Diversion Dam
10' x 10' plot
Sampled gravel bar--near the left bank

DATA: Particle size (mm)				
20	21	4	12	23
10	14	18	18	10
37	31	23	17	7
16	28	5	9	14
20	14	21	4	8
30	26	10	11	17
28	16	30	26	24
26	29	34	27	8
25	19	27	12	15
22	6	14	11	14
24	37	6	19	10
11	17	20	30	5
18	22	7	7	10
24	12	8	4	10
10	14	27	17	20
5	32	35	6	8
15	27	21	11	19
25	18	13	18	43
12	11	3	13	4
32	11	13	12	18

Particle Characteristics			
d_{90} =	30.0	mm
$d_{84.1}$ =	27.3	mm
d_{65} =	20.3	mm
d_{50} =	16.7	mm
d_{35} =	12.5	mm
$d_{15.9}$ =	8.42	mm
d_g =	15.2	mm
σ_g =	1.80	mm
G =	0.95	

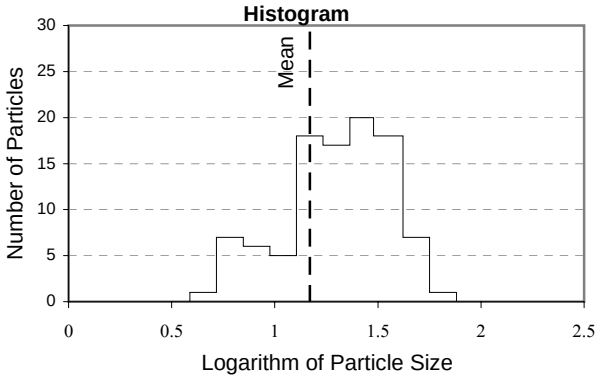

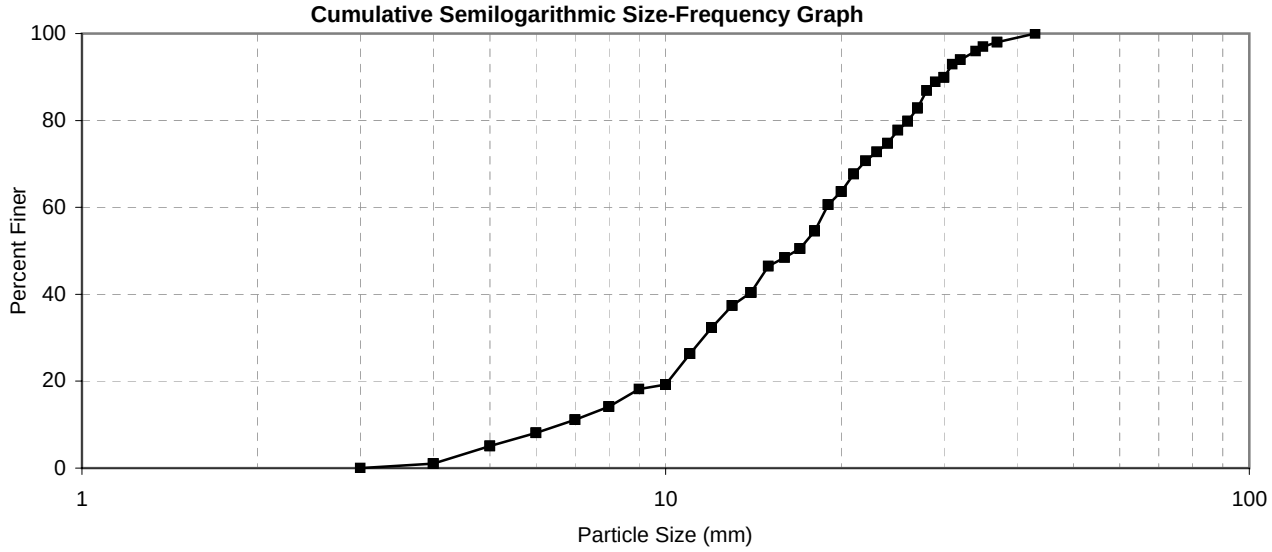

PARTICLE COUNTS

Site: B
Date: August 22, 2000
Measurement by: Jay T. Brown
Remarks: Big Lost River below the INEEL Diversion Dam
10' x 10' plot in center of channel
Near Trench Site #3

DATA: Particle size (mm)				
14	2	13	10	7
20	22	15	7	21
13	19	20	15	21
14	23	14	7	4
23	13	20	22	12
4	8	12	19	14
23	7	3	16	11
17	19	5	23	22
25	14	21	17	13
7	19	5	24	4
7	8	18	17	10
30	16	3	18	11
5	6	3	24	20
16	25	7	6	9
5	10	30	9	8
7	17	31	13	7
18	12	15	19	20
16	20	14	12	9
9	9	13	7	8
26	14	20	15	7

Particle Characteristics			
d_{90} =	23.3	mm
$d_{84.1}$ =	21.4	mm
d_{65} =	17.3	mm
d_{50} =	14.2	mm
d_{35} =	10.5	mm
$d_{15.9}$ =	7.24	mm
d_g =	12.4	mm
σ_g =	1.72	mm
G =	0.93	

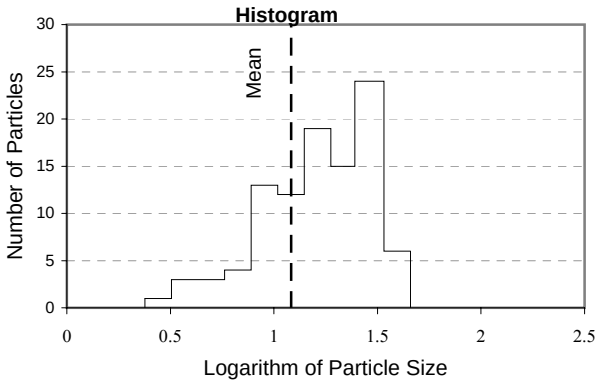

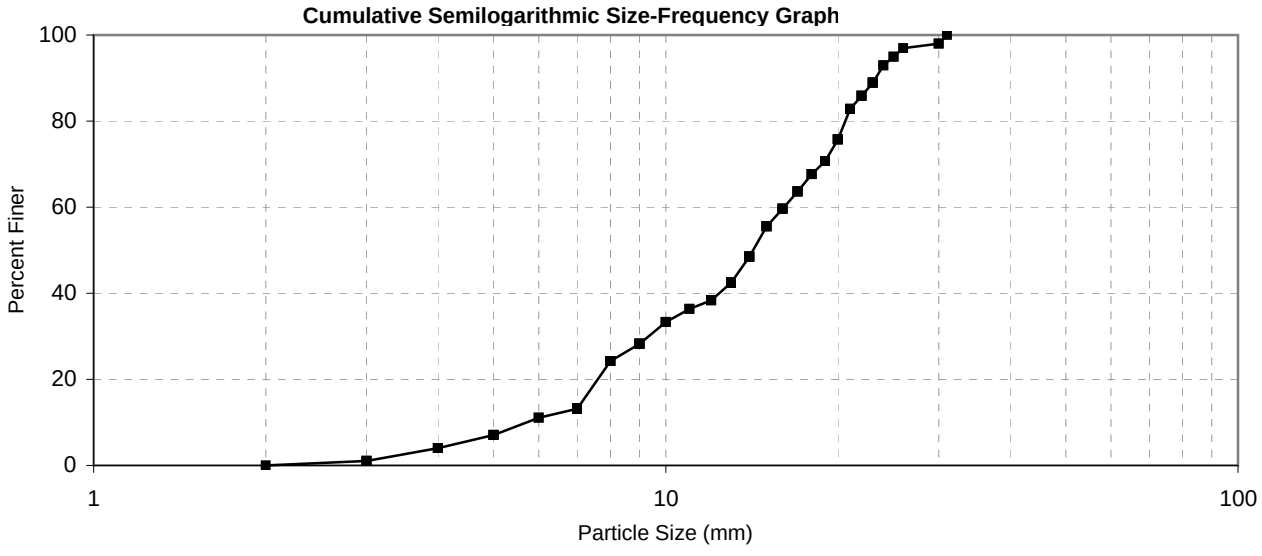

PARTICLE COUNTS

Site: C
Date: August 22, 2000
Measurement by: Brian Twining
Remarks: Big Lost River below the INEEL Diversion Dam
10' x 10' plot in center of channel
Poorly to moderately cemented particles
50% limestone and 50% basalt/tuff

DATA: Particle size (mm)				
23	14	17	13	4
14	14	10	8	8
15	17	15	43	21
21	6	11	33	9
17	9	22	22	29
13	7	27	19	14
37	5	13	16	8
25	21	10	30	88
5	14	10	17	36
7	15	7	25	10
39	5	7	18	22
10	9	28	3	23
7	19	3	8	3
22	10	26	13	20
8	9	10	17	22
10	18	21	12	14
10	11	11	59	5
9	15	23	4	22
12	8	8	7	13
7	5	29	3	44

Particle Characteristics			
d_{90}	=	29.0	mm
$d_{84.1}$	=	24.5	mm
d_{65}	=	17.7	mm
d_{50}	=	13.9	mm
d_{35}	=	10.4	mm
$d_{15.9}$	=	7.52	mm
d_g	=	13.6	mm
σ_g	=	1.80	mm
G	=	0.95	

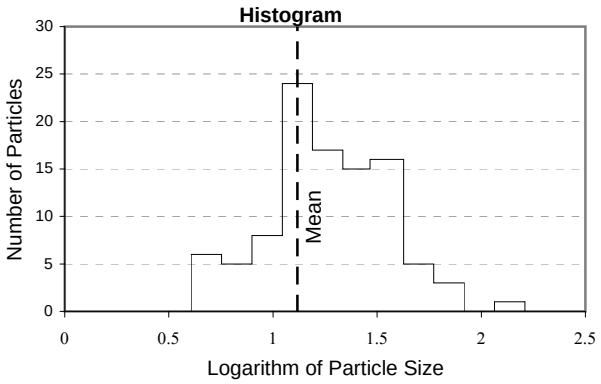

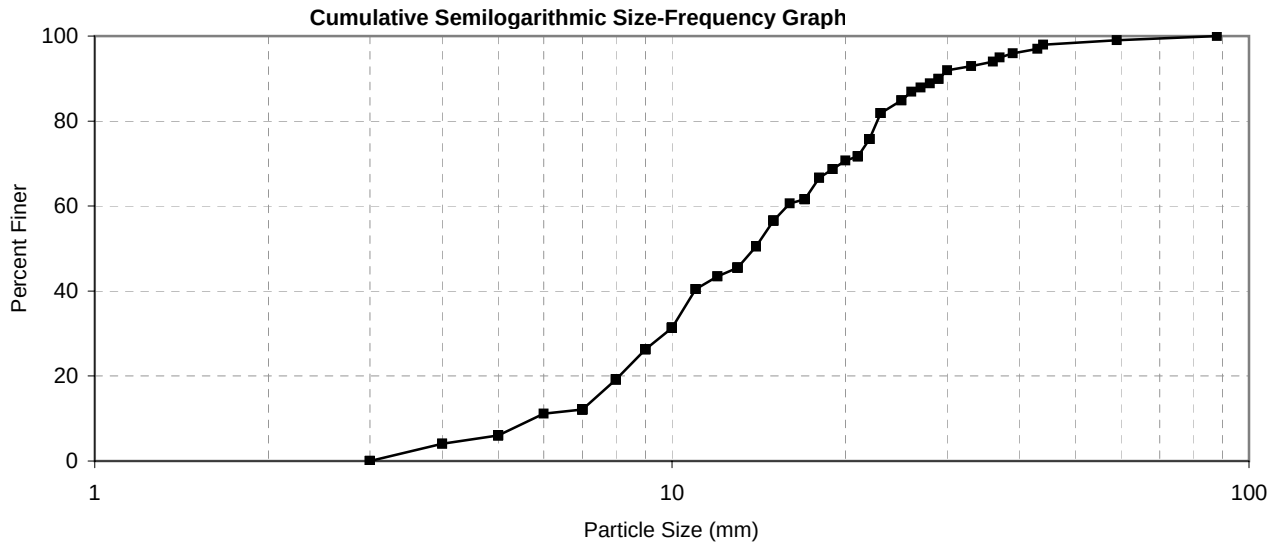

PARTICLE COUNTS

Site: D
Date: August 22, 2000
Measurement by: Brian Twining
Remarks: Big Lost River below the INEEL Diversion Dam
10' x 10' plot in center of channel
Mostly sub- to well-rounded rocks in a cemented matrix

DATA: Particle size (mm)				
20	10	27	26	28
9	3	23	13	37
22	26	12	51	29
19	5	23	26	28
14	20	25	11	11
4	19	12	43	3
6	44	34	20	8
11	38	8	7	12
24	3	19	11	31
8	16	38	22	48
20	2	44	48	14
21	4	32	31	28
7	31	29	8	24
30	14	10	19	9
20	8	18	26	23
5	13	9	38	19
9	7	24	19	44
32	18	28	11	38
35	24	8	6	29
6	44	30	8	43

Particle Characteristics			
d_{90} =	40.5	mm
$d_{84.1}$ =	33.2	mm
d_{65} =	25.3	mm
d_{50} =	20.1	mm
d_{35} =	12.9	mm
$d_{15.9}$ =	8.24	mm
d_g =	16.5	mm
σ_g =	2.01	mm
G =	1.00	

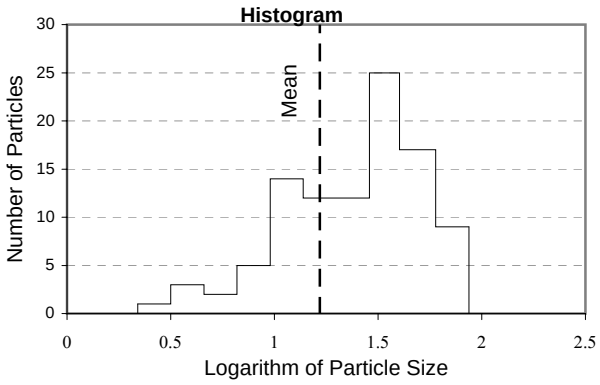

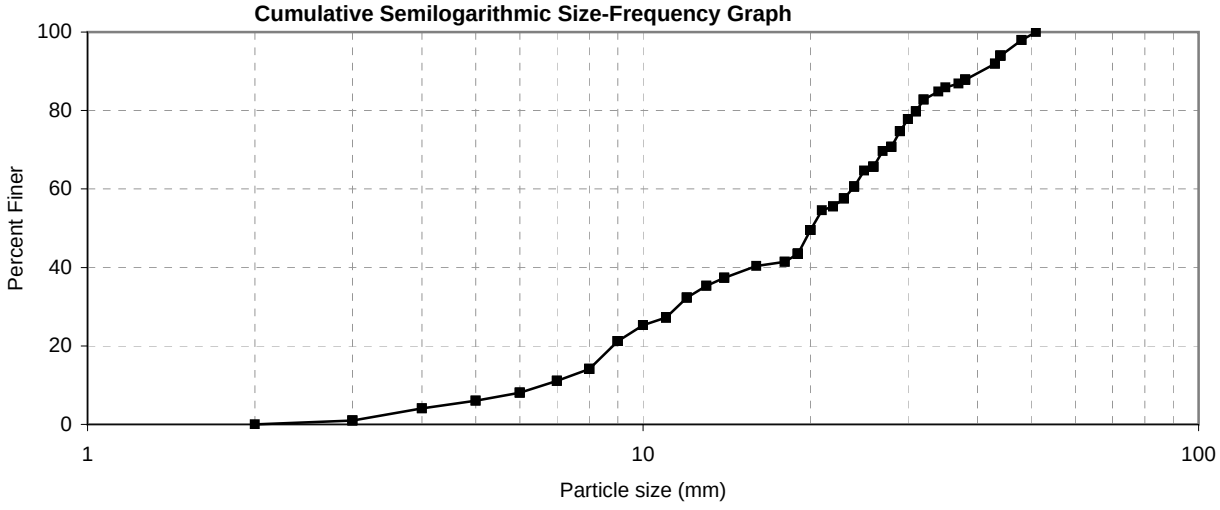

PARTICLE COUNTS

Site: E
Date: August 22, 2000
Measurement by: Brennon Orr
Remarks: Big Lost River below the INEEL Diversion Dam
10' x 10' plot in center of channel
50% limestone, 47% basalt, 2% granite, 1% quartz

DATA: Particle size (mm)				
46	43	17	27	40
13	31	8	15	15
13	27	24	8	22
17	13	10	19	17
27	27	8	8	8
18	23	20	28	14
17	29	52	21	36
27	25	24	16	52
38	7	15	34	53
11	19	17	18	7
40	21	11	29	17
5	21	13	45	8
33	30	26	20	23
18	12	38	105	30
21	40	22	57	34
45	52	13	10	18
16	57	22	8	32
16	9	13	38	30
35	47	19	45	18
42	25	24	26	16

Particle Characteristics			
d_{90}	=	45.4	mm
$d_{84.1}$	=	40.2	mm
d_{65}	=	27.5	mm
d_{50}	=	21.9	mm
d_{35}	=	17.8	mm
$d_{15.9}$	=	12.7	mm
d_g	=	22.6	mm
σ_g	=	1.78	mm
G	=	0.90	

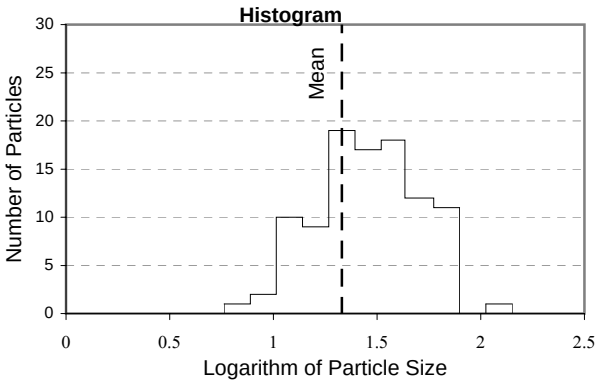

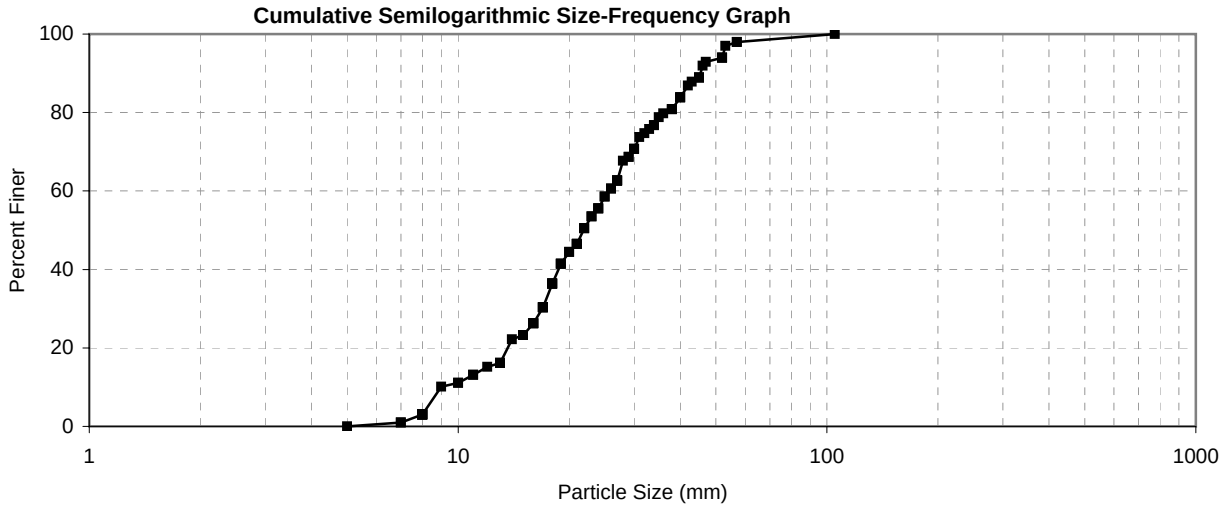

PARTICLE COUNTS

Site: F
Date: August 22, 2000
Measurement by: Brennon Orr
Remarks: Big Lost River below the INEEL Diversion Dam
10' x 10' plot in center of channel
40% Limestone, 40% ??, 20% basalt

DATA: Particle size (mm)				
8	3	34	28	21
17	10	18	28	28
10	15	21	12	14
25	4	9	8	24
7	14	12	52	75
20	30	37	32	46
51	30	29	30	28
20	48	38	18	7
25	42	36	17	46
21	23	22	27	37
24	27	32	25	42
18	14	42	30	24
32	57	32	26	29
50	44	42	15	10
13	11	11	45	18
30	37	28	40	25
8	48	7	17	29
22	30	10	17	34
23	7	32	14	27
4	20	36	14	30

Particle Characteristics			
d_{90} =	44.1	mm
$d_{84.1}$ =	38.5	mm
d_{65} =	30.1	mm
d_{50} =	25.4	mm
d_{35} =	19.8	mm
$d_{15.9}$ =	11.4	mm
d_g =	20.9	mm
σ_g =	1.84	mm
G =	1.00	

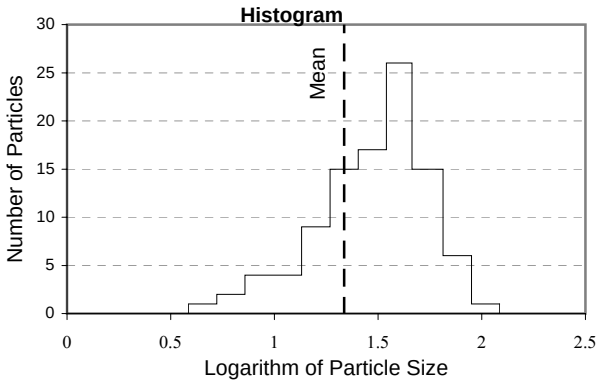

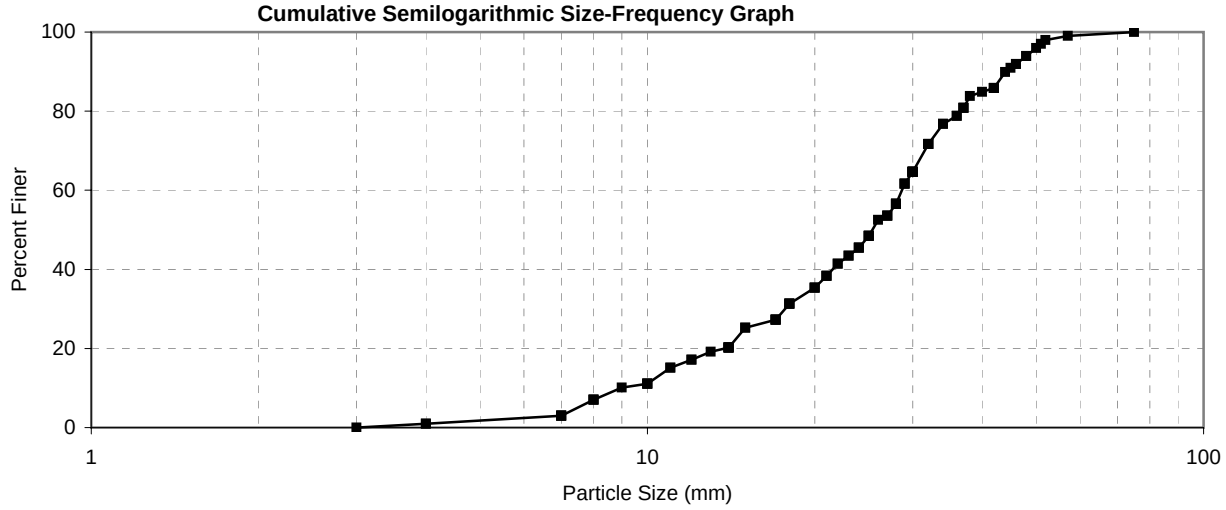

PARTICLE COUNTS

Site: G
Date: August 22, 2000
Measurement by: Brian Twining
Remarks: Big Lost River below the INEEL Diversion Dam
10' x 10' plot in center of channel
Well cemented, large cobbles, well and sub-rounded sediment

DATA: Particle size (mm)				
40	27	30	31	21
29	9	22	55	9
11	64	32	52	6
54	61	56	48	46
38	48	33	42	27
16	16	48	3	34
9	47	33	31	61
18	30	8	22	58
31	48	13	37	11
23	42	42	69	33
24	8	32	16	58
12	11	16	21	33
40	34	59	32	43
52	39	38	14	53
14	41	52	23	12
59	11	31	51	45
17	28	23	47	8
6	86	57	42	53
33	48	12	33	27
7	23	8	46	6

Particle Characteristics			
d_{90}	=	56.1	mm
$d_{84.1}$	=	52.4	mm
d_{65}	=	40.7	mm
d_{50}	=	32.5	mm
d_{35}	=	23.7	mm
$d_{15.9}$	=	11.9	mm
d_g	=	25.0	mm
σ_g	=	2.10	mm
G	=	1.00	

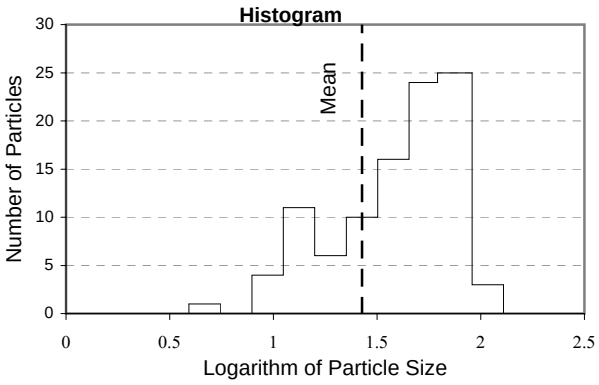

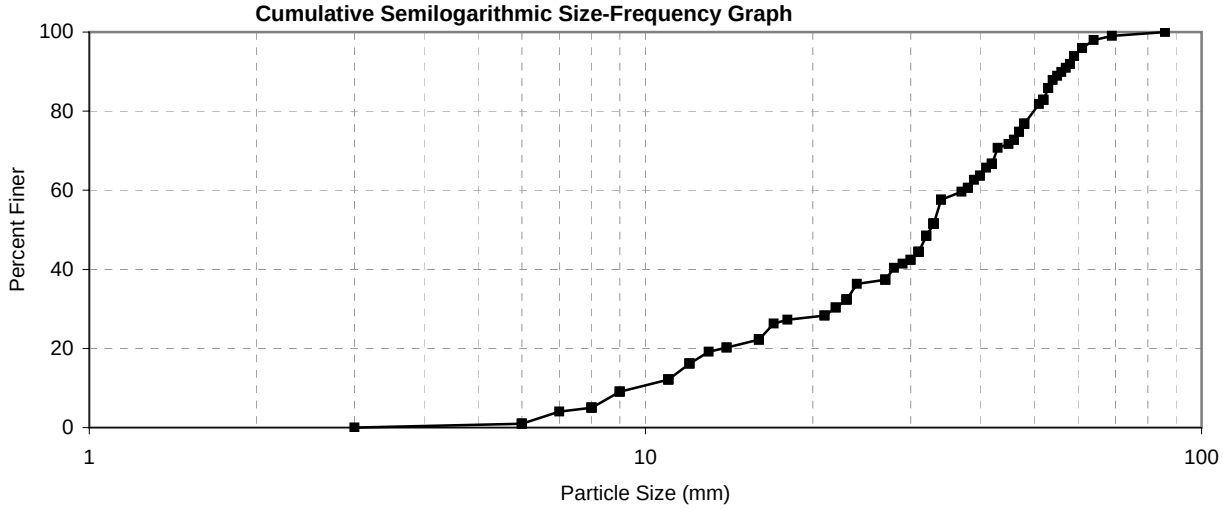

PARTICLE COUNTS

Site: H
Date: August 22, 2000
Measurement by: Jay T. Brown
Remarks: Big Lost River below the INEEL Diversion Dam
10' x 10' plot in center of channel
Particles are somewhat cemented

DATA: Particle size (mm)				
22	42	37	39	16
195	45	71	47	84
96	40	46	102	37
44	16	17	41	143
17	53	58	59	38
70	26	63	157	31
90	67	11	48	38
18	53	49	29	72
65	7	52	110	39
64	67	67	69	92
59	12	81	79	16
67	12	57	42	75
9	14	81	11	20
77	91	42	28	79
40	14	37	76	34
65	16	3	99	7
70	149	47	20	52
34	19	42	47	81
18	57	8	56	61
99	42	61	42	15

Particle Characteristics			
d_{90} =	91.1	mm
$d_{84.1}$ =	80.3	mm
d_{65} =	61.3	mm
d_{50} =	47.2	mm
d_{35} =	38.8	mm
$d_{15.9}$ =	16.9	mm
d_g =	36.8	mm
σ_g =	2.18	mm
G =	1.10	

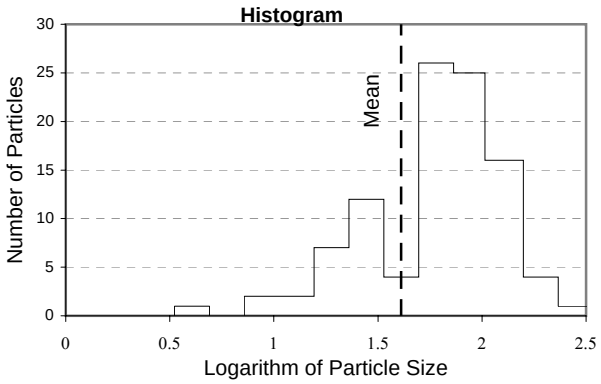

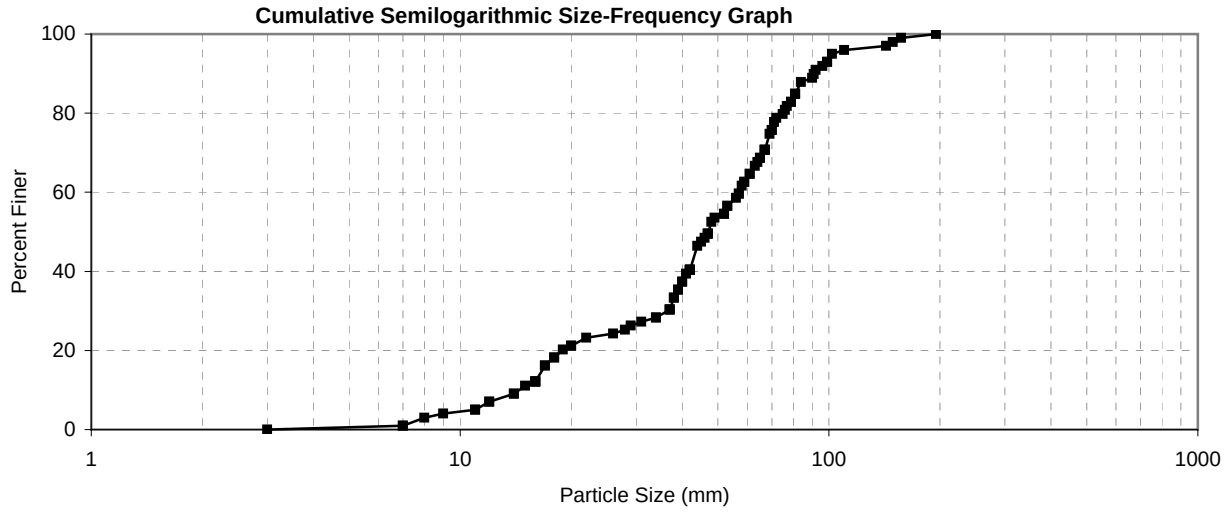

PARTICLE COUNTS

Site: I
Date: August 22, 2000
Measurement by: Jay T. Brown
Remarks: Big Lost River below the INEEL Diversion Dam
10' x 10' plot in center of channel

DATA: Particle size (mm)				
30	32	33	20	14
43	19	16	12	16
3	14	15	3	18
14	27	55	119	17
37	5	18	12	8
27	8	11	14	52
40	42	15	71	29
8	46	62	24	5
35	50	29	48	12
6	6	17	6	48
7	109	20	8	9
45	28	27	22	59
35	26	12	6	54
3	8	7	21	17
15	5	26	29	16
20	67	20	68	51
16	22	13	14	24
8	48	14	8	5
53	12	17	69	9
21	22	11	33	33

Particle Characteristics			
d_{90} =	53.1	mm
$d_{84.1}$ =	48.2	mm
d_{65} =	27.4	mm
d_{50} =	19.5	mm
d_{35} =	14.8	mm
$d_{15.9}$ =	8.38	mm
d_g =	20.1	mm
σ_g =	2.40	mm
G =	1.10	

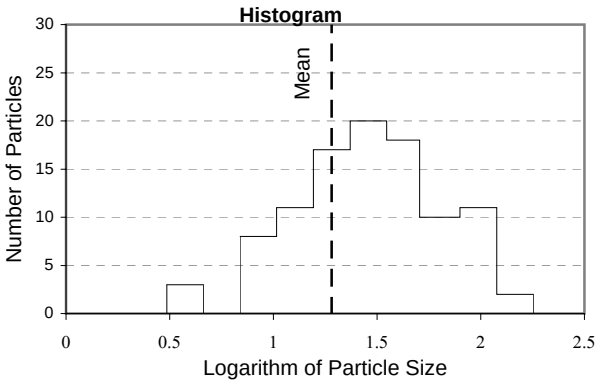

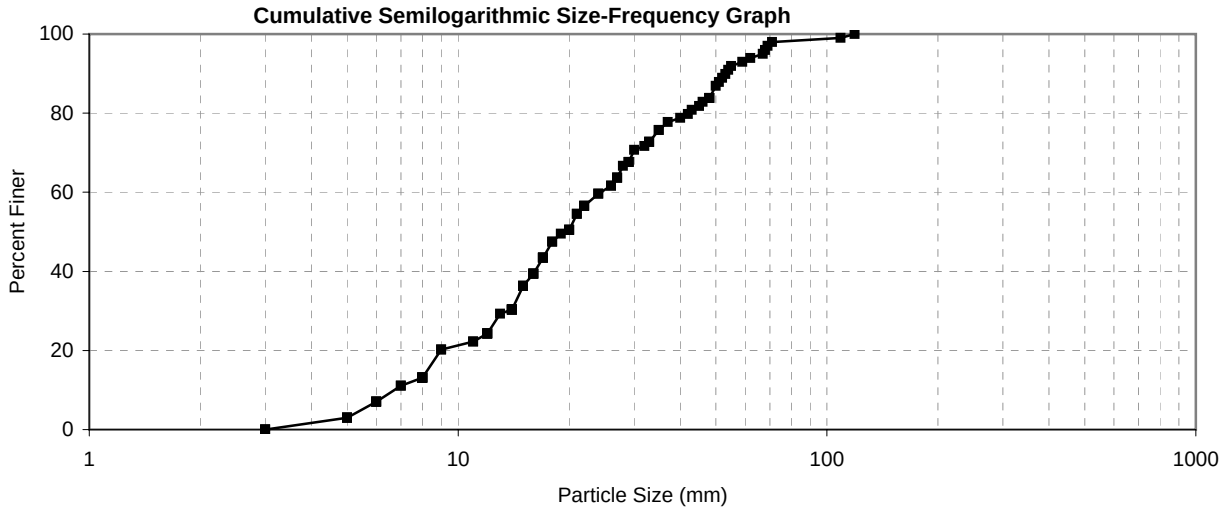

PARTICLE COUNTS

Site: J
Date: August 22, 2000
Measurement by: Brennon Orr
Remarks: Big Lost River below the INEEL Diversion Dam
10' x 10' plot in center of channel

DATA: Particle size (mm)				
16	7	4	8	7
2	7	6	11	4
3	3	6	5	4
5	5	8	6	9
3	2	4	9	13
7	4	5	5	7
8	7	8	10	7
42	4	7	5	6
7	4	4	8	7
6	3	3	4	7
3	3	3	7	8
6	3	4	7	4
5	7	2	5	5
6	14	4	11	5
2	6	6	15	6
1	7	7	6	5
3	4	23	11	4
5	5	12	9	11
7	9	4	9	9
4	2	3	7	5

Particle Characteristics			
d_{90}	=	11.0	mm
$d_{84.1}$	=	9.20	mm
d_{65}	=	7.34	mm
d_{50}	=	6.21	mm
d_{35}	=	5.11	mm
$d_{15.9}$	=	3.87	mm
d_g	=	5.97	mm
σ_g	=	1.54	mm
G	=	0.88	

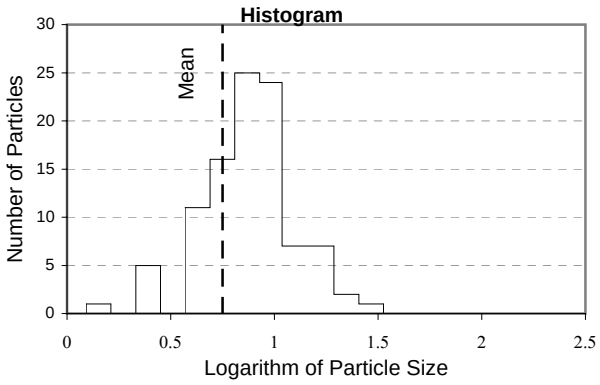

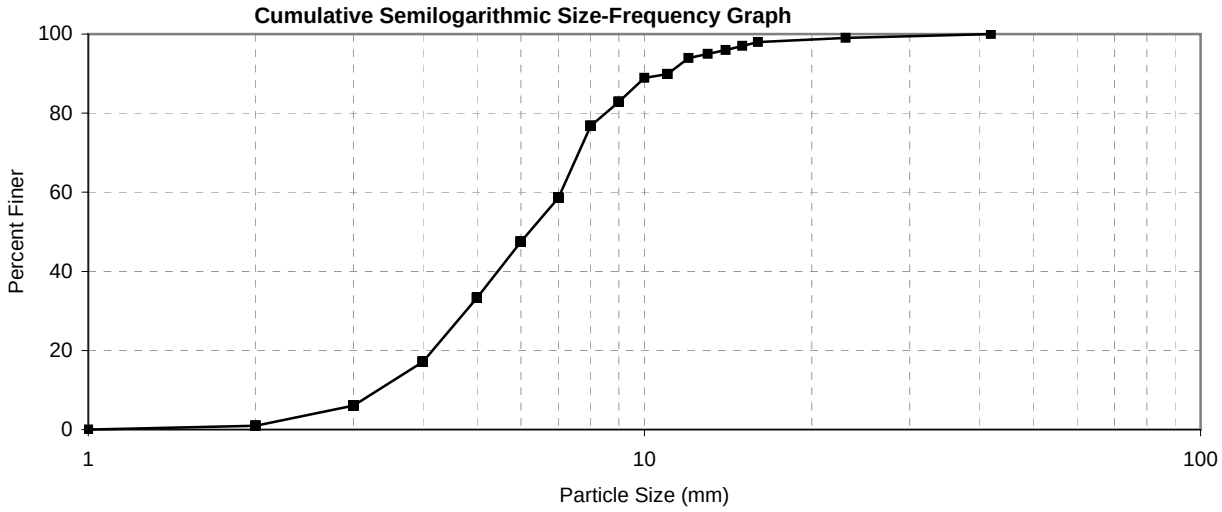

PARTICLE COUNTS

Site: K
Date: August 22, 2000
Measurement by: Jay T. Brown
Remarks: Big Lost River below the INEEL Diversion Dam
10' x 10' plot in center of channel

DATA: Particle size (mm)				
47	9	7	8	32
13	1	7	4	4
3	9	23	7	10
6	7	19	9	14
79	7	17	9	7
4	40	23	4	17
9	5	4	5	10
30	3	2	12	6
4	1	11	6	8
12	8	2	5	11
10	22	8	6	3
4	10	10	15	27
2	12	26	12	6
11	32	4	23	22
10	14	9	6	50
33	4	11	11	11
7	9	46	10	3
10	8	42	7	58
7	9	6	9	17
13	4	16	50	73

Particle Characteristics			
d_{90} =	32.5	mm
$d_{84.1}$ =	24.2	mm
d_{65} =	11.7	mm
d_{50} =	9.71	mm
d_{35} =	7.61	mm
$d_{15.9}$ =	4.65	mm
d_g =	10.6	mm
σ_g =	2.28	mm
G =	1.07	

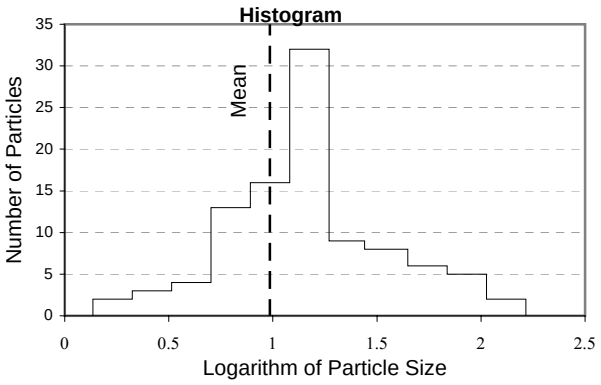

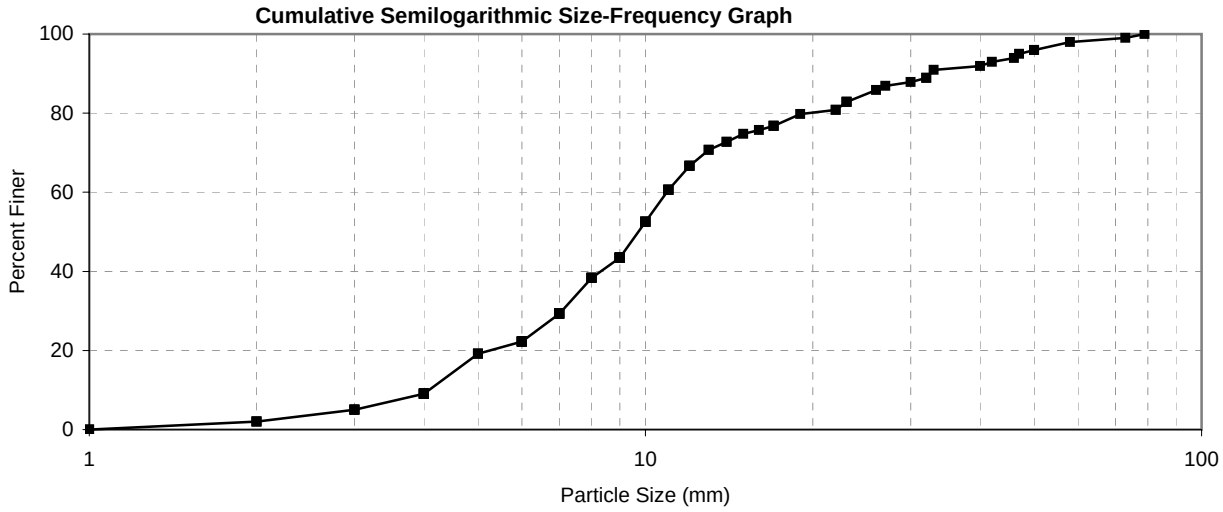

PARTICLE COUNTS

Site: L
Date: August 22, 2000
Measurement by: Brennon Orr
Remarks: Big Lost River below the INEEL Diversion Dam
10' x 10' plot in center of channel
Moderately cemented

DATA: Particle size (mm)				
20	42	35	35	80
20	65	40	56	17
32	9	36	34	44
22	35	25	37	25
27	25	50	34	7
26	20	42	26	30
22	9	24	31	22
30	40	14	45	22
35	44	29	29	44
24	12	25	19	64
55	15	40	47	62
45	40	62	32	19
29	33	36	45	5
22	36	30	55	7
16	24	38	28	42
39	27	32	34	16
33	24	23	25	30
35	34	27	52	12
30	14	32	39	30
28	30	44	30	29

Particle Characteristics			
d_{90} =	47.3	mm
$d_{84.1}$ =	44.3	mm
d_{65} =	35.3	mm
d_{50} =	30.7	mm
d_{35} =	26.8	mm
$d_{15.9}$ =	20.5	mm
d_g =	30.1	mm
σ_g =	1.47	mm
G =	0.90	

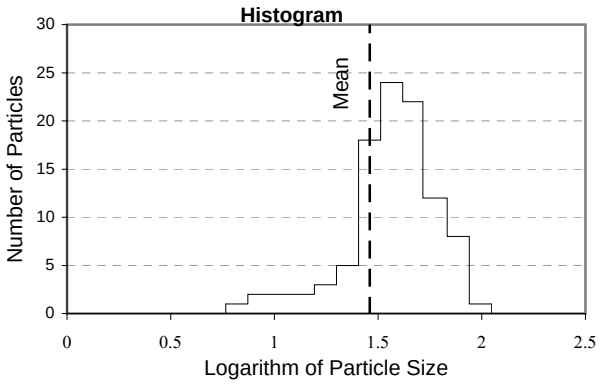

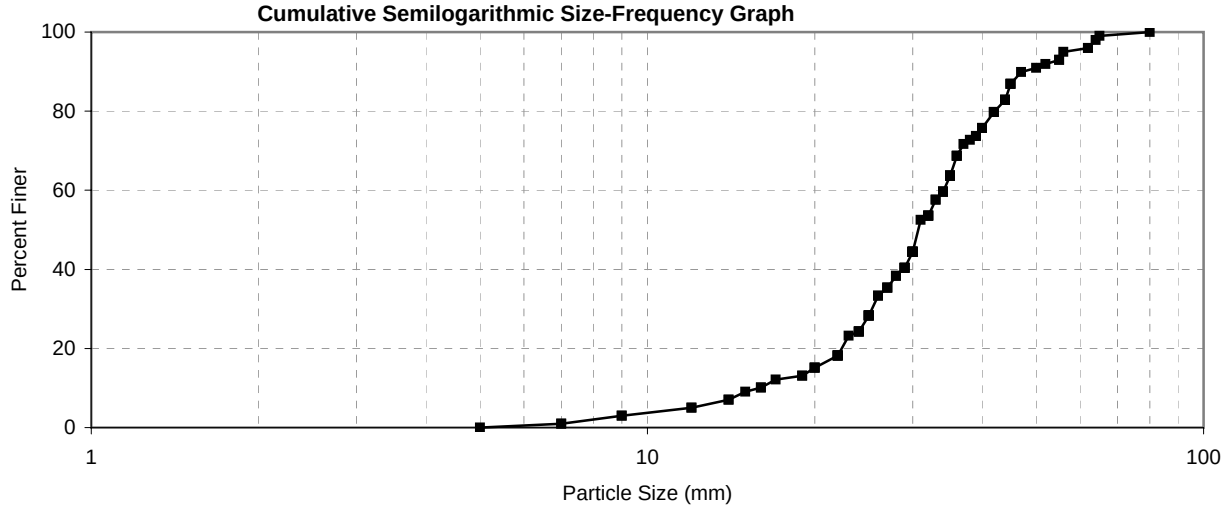

PARTICLE COUNTS

Site: M
Date: August 22, 2000
Measurement by: Brennon Orr
Remarks: Big Lost River below the INEEL Diversion Dam
10' x 10' plot in center of channel

DATA: Particle size (mm)				
46	58	18	15	22
11	25	12	41	27
36	36	13	37	45
33	19	63	44	35
13	31	27	32	36
38	12	65	50	36
95	44	14	52	24
60	56	25	30	28
16	32	30	21	18
8	27	34	40	40
16	38	26	32	30
52	42	40	29	20
75	42	28	22	30
72	68	32	21	22
14	50	40	28	42
55	32	32	26	38
16	17	26	32	28
32	45	30	18	26
35	25	20	25	20
18	16	24	46	22

Particle Characteristics			
d_{90}	=	53.6	mm
$d_{84.1}$	=	45.6	mm
d_{65}	=	36.1	mm
d_{50}	=	30.7	mm
d_{35}	=	26.2	mm
$d_{15.9}$	=	18.4	mm
d_g	=	29.0	mm
σ_g	=	1.57	mm
G	=	0.90	

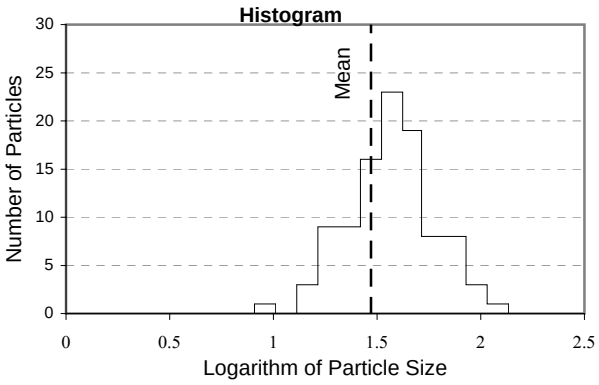

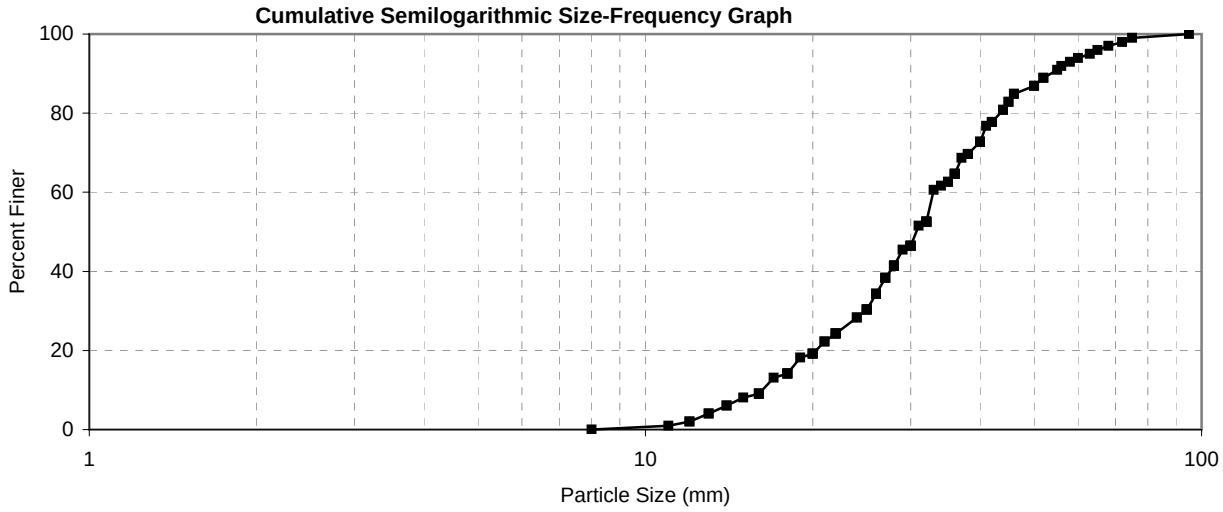

PARTICLE COUNTS

Site: N
Date: August 22, 2000
Measurement by: Jay T. Brown
Remarks: Big Lost River below the INEEL Diversion Dam
10' x 10' plot in center of channel

DATA: Particle size (mm)				
12	47	6	24	22
44	43	9	39	23
16	57	14	11	68
8	10	6	74	16
240	17	14	40	8
9	52	30	18	11
27	35	31	55	67
15	44	11	10	47
90	13	12	46	9
52	24	74	31	14
32	4	15	45	11
9	66	68	48	83
5	51	66	36	9
7	69	17	10	12
5	5	57	53	17
31	47	19	43	30
16	40	7	116	46
9	51	30	12	41
43	15	140	25	43
13	25	15	79	14

Particle Characteristics			
d_{90}	=	68.0	mm
$d_{84.1}$	=	55.5	mm
d_{65}	=	41.7	mm
d_{50}	=	25.5	mm
d_{35}	=	15.4	mm
$d_{15.9}$	=	9.95	mm
d_g	=	23.5	mm
σ_g	=	2.36	mm
G	=	1.10	

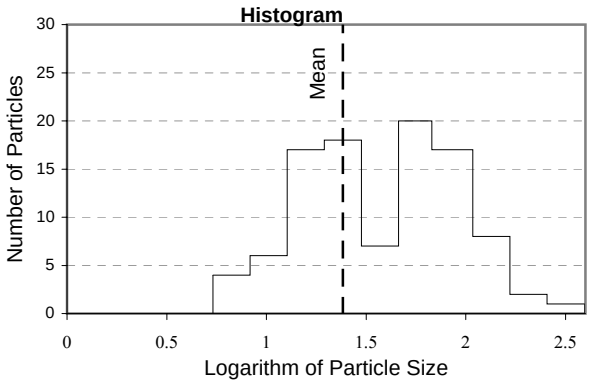

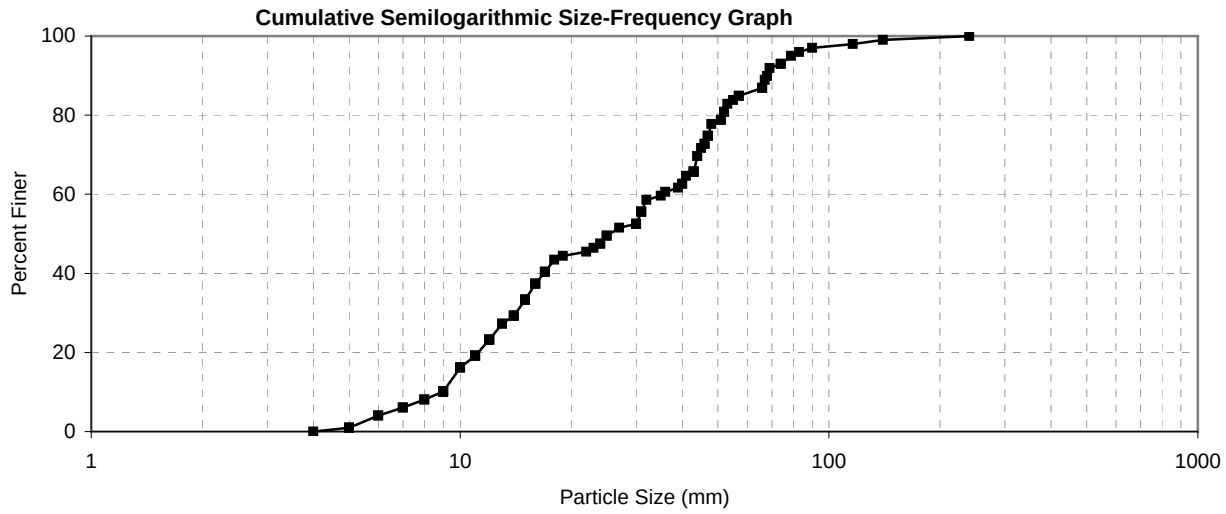

PARTICLE COUNTS

Site: O
Date: August 22, 2000
Measurement by: Jay T. Brown
Remarks: Big Lost River below the INEEL Diversion Dam
10' x 10' plot in center of channel

DATA: Particle size (mm)				
59	30	12	29	31
54	10	17	4	27
28	29	19	37	6
35	24	24	67	83
27	17	73	19	18
17	5	22	9	5
48	16	55	5	58
52	19	43	19	12
10	28	9	21	56
18	4	74	63	47
8	25	15	14	76
17	3	8	69	5
16	19	9	8	3
5	24	13	17	16
57	61	20	15	50
7	8	21	21	23
49	12	7	19	10
34	21	26	22	9
12	86	15	48	75
2	42	54	11	8

Particle Characteristics			
d_{90}	=	59.2	mm
$d_{84.1}$	=	54.1	mm
d_{65}	=	27.2	mm
d_{50}	=	19.7	mm
d_{35}	=	15.9	mm
$d_{15.9}$	=	8.53	mm
d_g	=	21.5	mm
σ_g	=	2.52	mm
G	=	1.10	

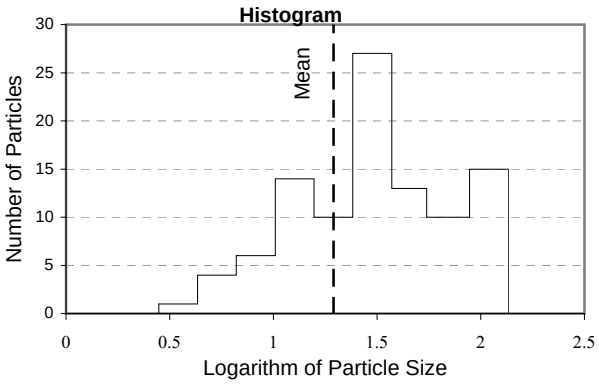

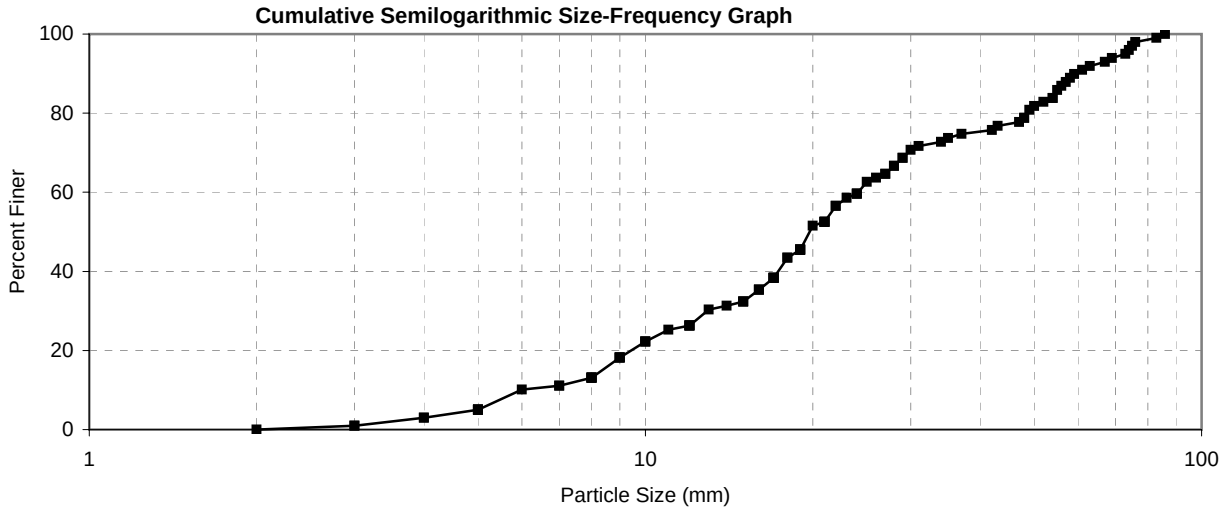

PARTICLE COUNTS

Site: P
Date: August 23, 2000
Measurement by: Jay T. Brown
Remarks: Big Lost River below the INEEL Diversion Dam
10' x 10' plot in center of channel

DATA: Particle size (mm)				
63	5	90	38	47
12	64	38	15	19
5	6	12	7	23
20	4	4	9	11
17	7	5	79	46
7	6	5	25	15
10	43	67	11	5
14	63	4	56	7
11	8	32	17	9
75	29	20	19	14
5	6	70	41	7
44	8	29	39	22
50	12	42	47	4
5	11	64	64	23
48	36	3	34	2
15	4	41	67	4
46	6	26	43	25
23	40	12	9	19
4	16	11	61	17
34	8	40	8	23

Particle Characteristics			
d_{90} =	63.0	mm
$d_{84.1}$ =	47.1	mm
d_{65} =	29.5	mm
d_{50} =	18.0	mm
d_{35} =	11.3	mm
$d_{15.9}$ =	5.96	mm
d_g =	16.8	mm
σ_g =	2.81	mm
G =	1.20	

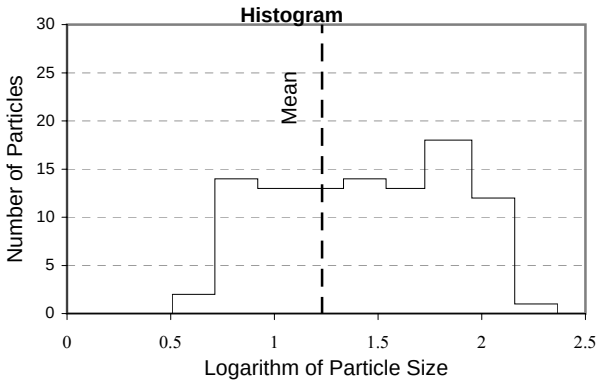

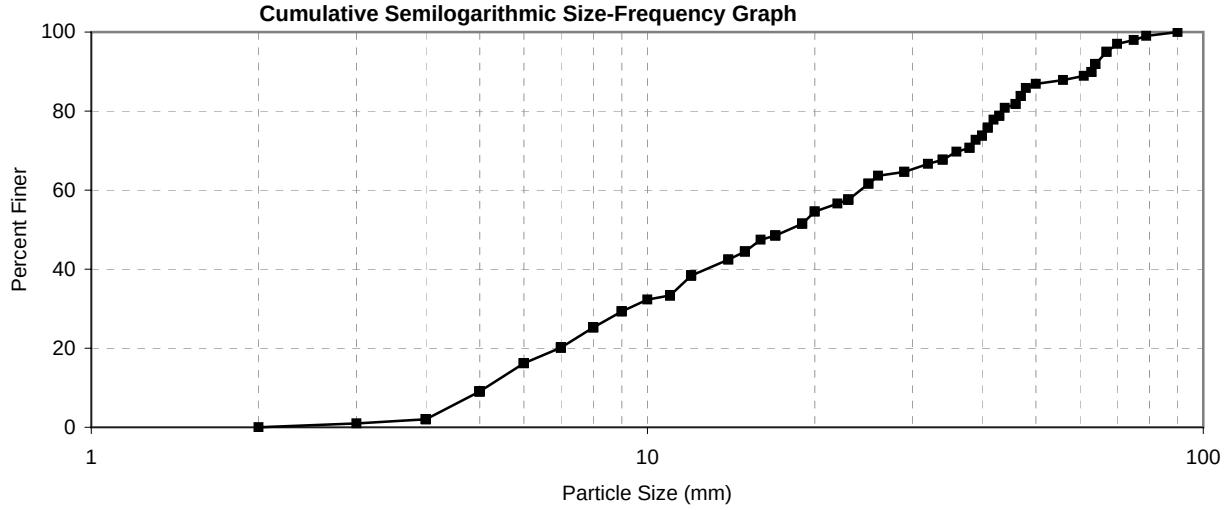

PARTICLE COUNTS

Site: Q
Date: August 23, 2000
Measurement by: Charles Berenbrock
Remarks: Big Lost River below the INEEL Diversion Dam
10' x 10' plot in center of channel

DATA: Particle size (mm)				
21	29	37	63	25
32	39	32	50	67
29	15	55	26	11
10	55	38	53	10
31	40	25	21	40
8	75	40	4	12
51	12	35	35	7
44	15	70	16	35
40	22	15	20	19
4	41	65	17	27
29	37	15	38	123
29	55	70	26	6
63	6	12	21	34
13	50	45	5	8
34	26	34	18	15
75	12	7	69	40
7	31	73	50	17
48	22	11	11	60
13	10	77	10	36
30	40	22	58	14

Particle Characteristics			
d_{90} =	64.1	mm
$d_{84.1}$ =	55.3	mm
d_{65} =	37.7	mm
d_{50} =	29.6	mm
d_{35} =	20.6	mm
$d_{15.9}$ =	11.6	mm
d_g =	25.3	mm
σ_g =	2.18	mm
G =	1.10	

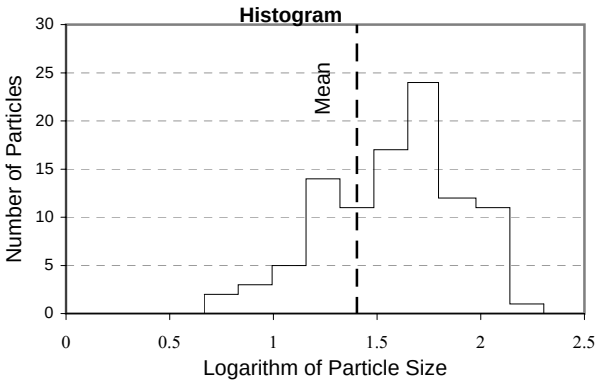

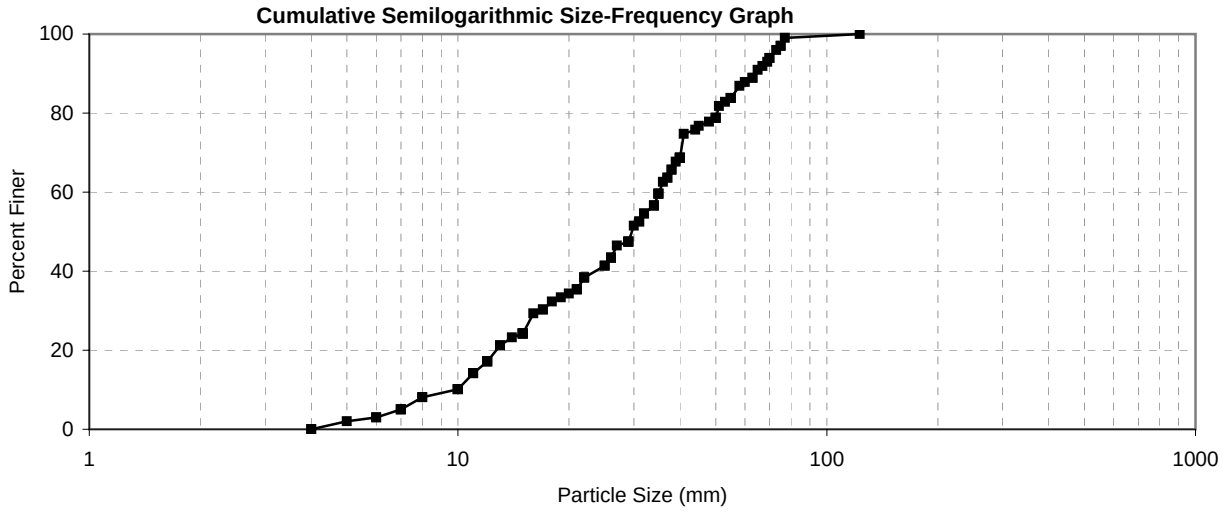

PARTICLE COUNTS

Site: R
Date: August 23, 2000
Measurement by: Charles Berenbrock
Remarks: Big Lost River below the INEEL Diversion Dam
10' x 10' plot in center of channel

DATA: Particle size (mm)				
49	32	9	21	34
10	23	15	11	19
20	25	34	79	25
8	31	20	54	40
35	40	46	27	50
34	9	26	40	67
65	18	15	47	79
15	11	28	8	62
40	47	60	5	23
8	18	35	29	19
25	11	16	20	30
4	4	47	23	39
30	30	23	27	16
25	44	47	21	23
12	9	62	40	36
21	14	8	16	23
50	45	50	37	17
22	4	28	33	32
13	21	59	17	44
17	51	37	58	12

Particle Characteristics			
d_{90} =	51.3	mm
$d_{84.1}$ =	48.1	mm
d_{65} =	34.4	mm
d_{50} =	25.9	mm
d_{35} =	20.9	mm
$d_{15.9}$ =	12.4	mm
d_g =	24.4	mm
σ_g =	1.97	mm
G =	1.00	

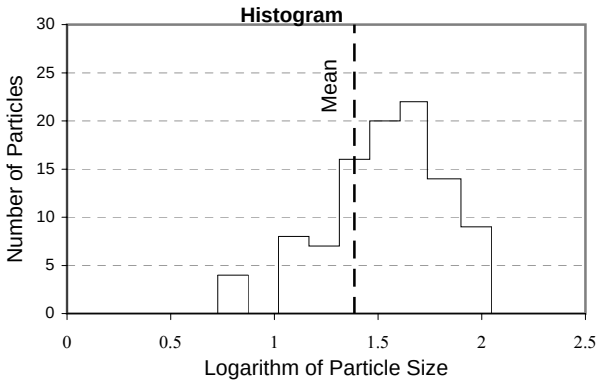

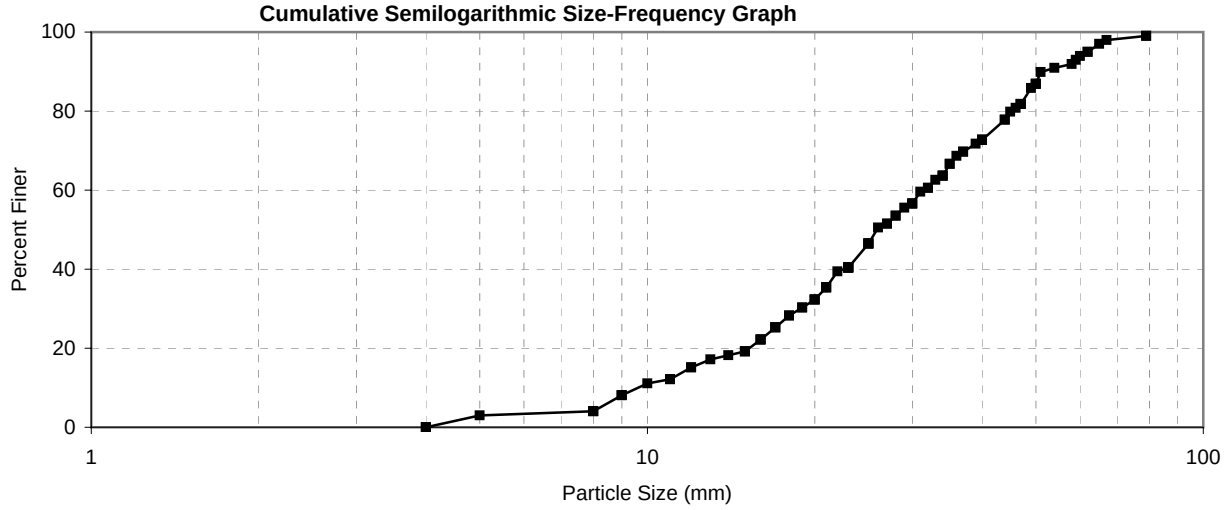

PARTICLE COUNTS

Site: S
Date: August 23, 2000
Measurement by: Brian Twining
Remarks: Big Lost River below the INEEL Diversion Dam
10' x 10' plot in center of channel
Well cemented pebbles and cobbles. Consist mostly of limestone (60%-70%) with 8%-15% basalt, 10%-15% breccia, 10% quartz, and 10% other

DATA: Particle size (mm)				
8	20	4	8	7
13	50	38	36	43
4	5	13	21	18
17	26	11	11	48
8	7	10	21	12
56	3	13	56	18
21	61	8	24	23
21	14	12	20	16
51	48	11	14	18
6	47	9	38	22
3	21	10	13	26
11	6	21	11	20
22	13	8	9	24
32	22	59	15	21
18	31	39	24	30
41	14	34	22	2
38	5	13	20	14
6	8	11	12	50
48	51	33	10	11
13	36	17	13	46

Particle Characteristics			
d_{90}	=	48.1	mm
$d_{84.1}$	=	38.8	mm
d_{65}	=	22.1	mm
d_{50}	=	18.2	mm
d_{35}	=	13.2	mm
$d_{15.9}$	=	8.61	mm
d_g	=	18.3	mm
σ_g	=	2.12	mm
G	=	1.00	

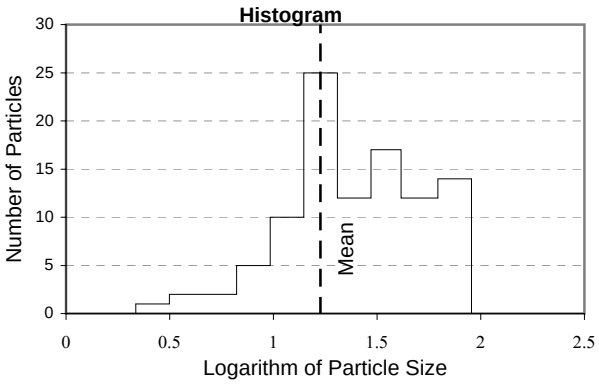

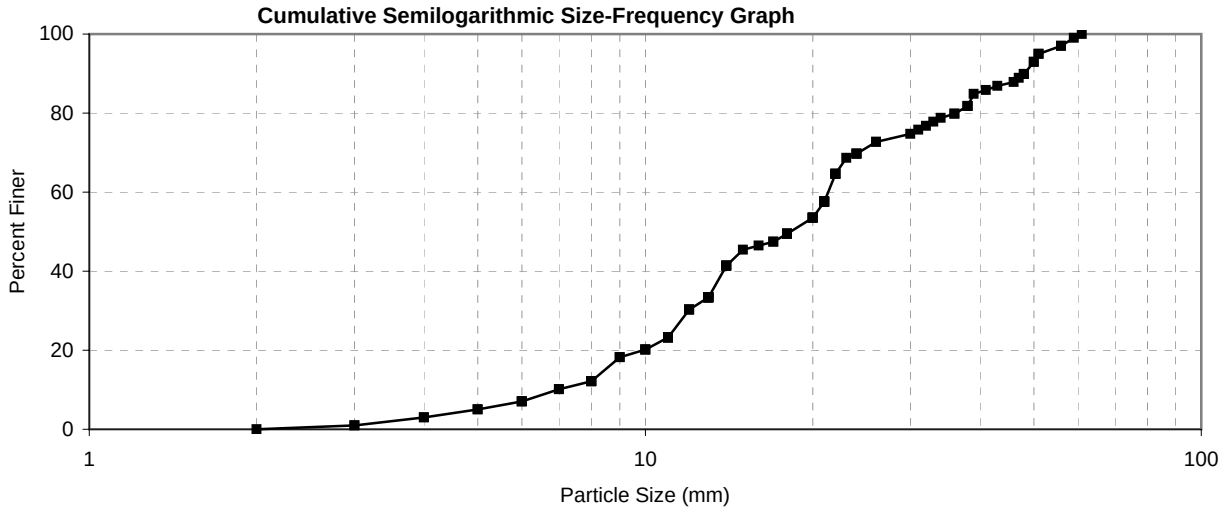

PARTICLE COUNTS

Site: T
Date: August 23, 2000
Measurement by: Brian Twining
Remarks: Big Lost River below the INEEL Diversion Dam; 10'x10' plot. Sampled a narrow chute of gravel between bedrock. Not representative of channel. Losely consolidated pebbles and cobbles. Mostly limestone (50%-65%), quartzite (10%-20%), basalt (10%-15%), breccia (10%), and other (10%)

DATA: Particle size (mm)				
26	41	12	43	13
29	6	51	51	54
30	31	14	9	23
14	7	48	41	14
18	8	23	38	21
56	23	21	53	32
18	19	4	72	53
12	17	12	22	40
57	16	54	20	36
36	61	16	41	8
31	22	40	40	74
6	50	23	11	41
9	37	26	46	39
18	22	64	32	23
29	14	33	33	56
41	43	19	27	43
28	22	9	49	81
31	23	47	38	18
26	20	29	22	21
28	31	58	40	72

Particle Characteristics			
d_{90} =	55.1	mm
$d_{84.1}$ =	50.3	mm
d_{65} =	38.2	mm
d_{50} =	29.2	mm
d_{35} =	22.5	mm
$d_{15.9}$ =	14.8	mm
d_g =	27.3	mm
σ_g =	1.84	mm
G =	1.00	

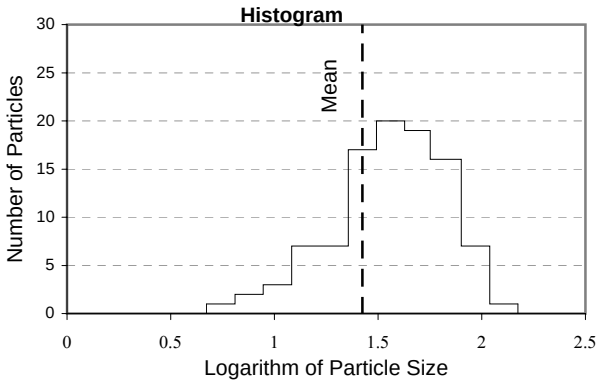

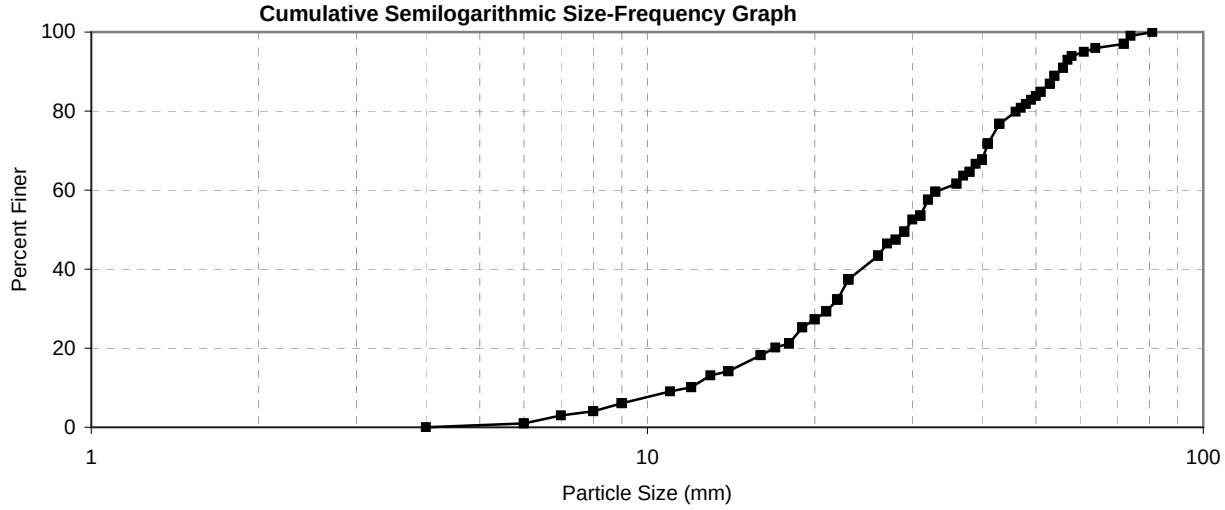

PARTICLE COUNTS

Site: U
Date: August 23, 2000
Measurement by: Jay T. Brown
Remarks: Big Lost River below the INEEL Diversion Dam
10' x 10' plot
Sampled gravel bar

DATA: Particle size (mm)				
31	81	8	77	21
42	51	96	44	16
47	9	4	33	34
47	81	51	43	42
42	64	67	62	98
16	49	61	35	51
54	53	17	53	61
53	114	35	21	10
27	37	64	29	34
58	50	89	85	41
39	52	43	25	21
55	13	52	46	65
60	22	26	32	53
11	55	66	37	9
77	53	69	10	66
52	44	30	45	52
14	18	74	34	61
63	38	8	4	38
51	7	28	16	12
75	57	66	39	68

Particle Characteristics			
d_{90}	=	74.1	mm
$d_{84.1}$	=	66.1	mm
d_{65}	=	53.1	mm
d_{50}	=	44.7	mm
d_{35}	=	35.6	mm
$d_{15.9}$	=	16.9	mm
d_g	=	33.4	mm
σ_g	=	1.98	mm
G	=	1.00	

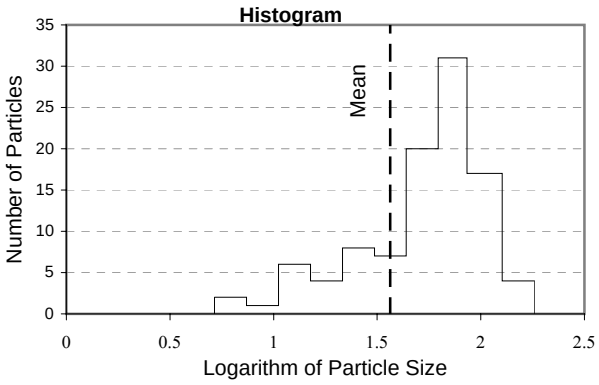

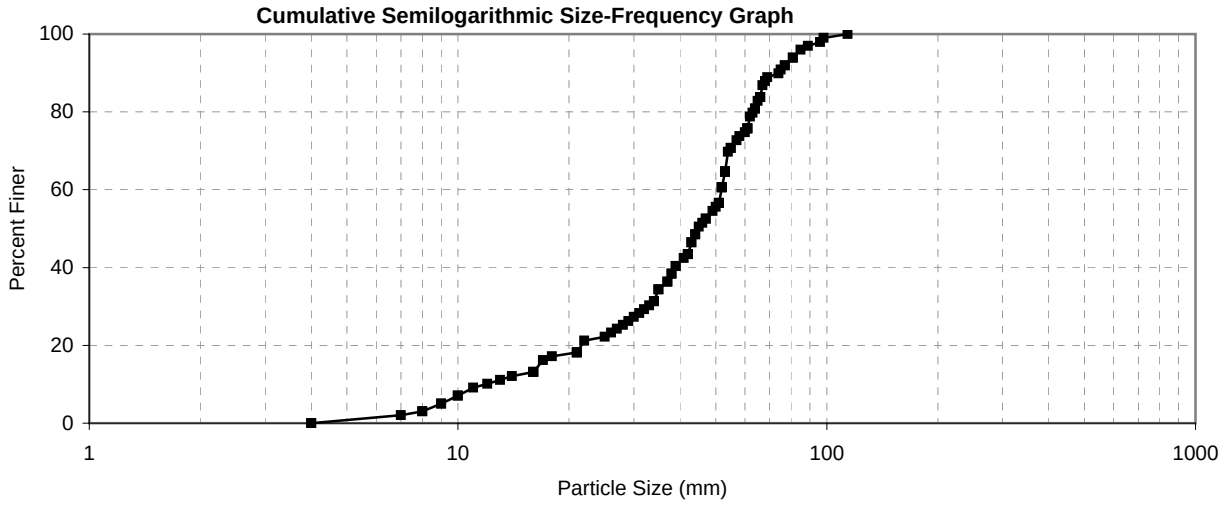

PARTICLE COUNTS

Site: V
Date: August 24, 2000
Measurement by: Jay T. Brown
Remarks: Big Lost River below the INEEL Diversion Dam
10' x 10' plot in center of channel

DATA: Particle size (mm)				
77	22	22	44	16
32	13	9	46	5
8	9	46	26	32
19	26	42	60	36
27	29	9	11	6
35	17	31	14	30
12	36	36	40	7
9	15	57	40	25
37	13	33	42	37
25	30	19	8	26
20	11	24	17	47
24	24	27	5	10
57	37	17	29	34
36	14	38	15	22
17	2	15	32	27
11	35	16	25	25
40	4	19	7	9
23	38	40	54	21
22	57	16	34	22
16	17	13	33	20

Particle Characteristics			
d_{90} =	43.1	mm
$d_{84.1}$ =	39.2	mm
d_{65} =	30.7	mm
d_{50} =	24.5	mm
d_{35} =	18.4	mm
$d_{15.9}$ =	11.2	mm
d_g =	21.0	mm
σ_g =	1.87	mm
G =	1.00	

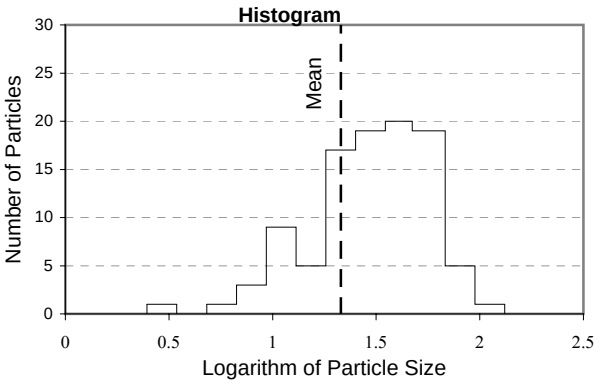

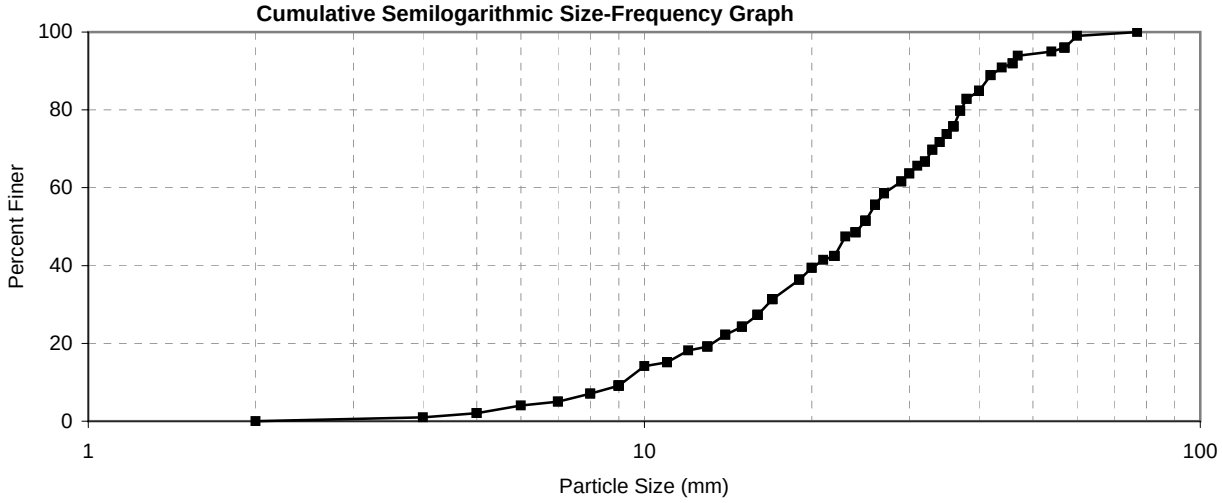

PARTICLE COUNTS

Site: W
Date: August 24, 2000
Measurement by: Charles Berenbrock
Remarks: Big Lost River below the INEEL Diversion Dam
10' x 10' plot in center of channel

DATA: Particle size (mm)				
65	48	38	65	17
62	40	26	37	6
65	42	12	9	43
21	10	12	55	33
7	27	44	17	43
44	35	9	77	68
48	50	16	7	18
20	55	45	3	49
70	55	27	4	4
80	34	18	69	40
18	16	56	50	3
5	86	49	21	51
38	47	60	45	29
50	7	40	12	95
42	53	45	55	56
33	17	23	9	55
45	36	21	67	43
9	18	25	80	2
65	9	45	20	73
20	73	8	9	66

Particle Characteristics			
d_{90}	=	67.1	mm
$d_{84.1}$	=	62.8	mm
d_{65}	=	46.7	mm
d_{50}	=	39.5	mm
d_{35}	=	22.1	mm
$d_{15.9}$	=	9.78	mm
d_g	=	24.8	mm
σ_g	=	2.53	mm
G	=	1.20	

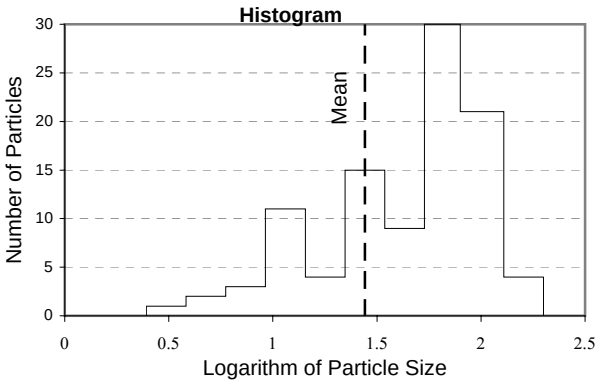

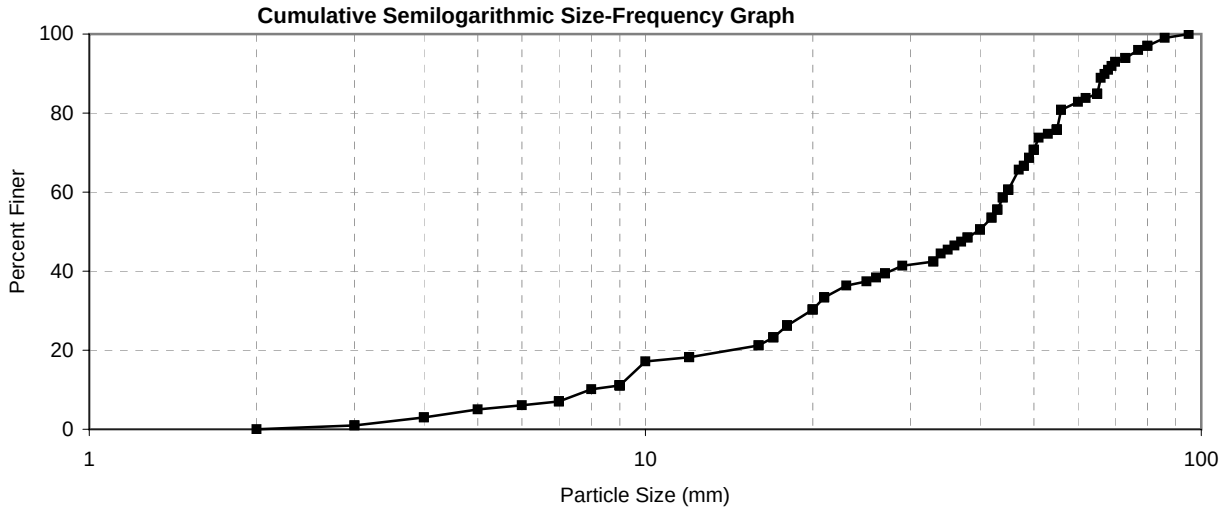

PARTICLE COUNTS

Site: X
Date: August 24, 2000
Measurement by: Jay T. Brown
Remarks: Big Lost River below the INEEL Diversion Dam
10' x 10' plot in center of channel

DATA: Particle size (mm)				
14	37	88	56	46
13	35	50	61	32
108	24	15	20	12
56	74	19	57	54
11	17	14	42	19
55	39	12	47	53
43	25	11	34	23
72	17	22	70	37
64	76	52	71	79
44	37	16	15	33
62	34	5	52	47
27	46	26	20	39
63	60	27	30	34
80	48	62	37	9
18	53	4	64	26
24	19	36	29	44
57	38	47	23	14
30	62	13	17	27
25	26	75	62	43
27	21	42	41	24

Particle Characteristics			
d_{90}	=	67.2	mm
$d_{84.1}$	=	62.1	mm
d_{65}	=	46.2	mm
d_{50}	=	36.5	mm
d_{35}	=	26.5	mm
$d_{15.9}$	=	17.2	mm
d_g	=	32.7	mm
σ_g	=	1.90	mm
G	=	1.00	

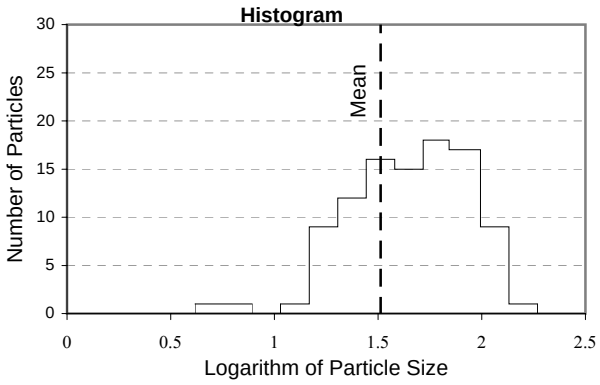

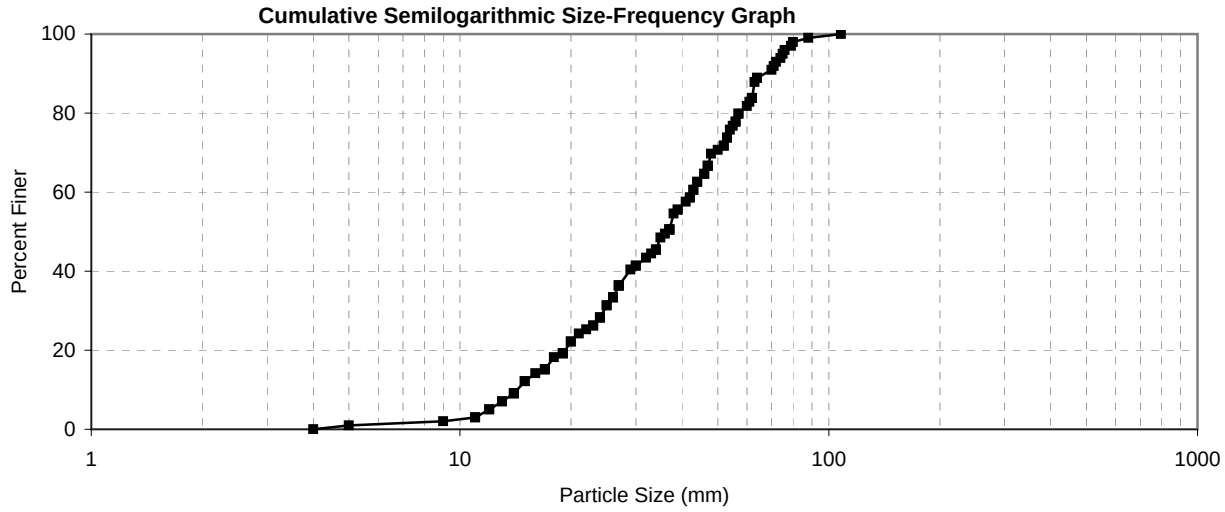

PARTICLE COUNTS

Site: Y
Date: September 21, 2000
Measurement by: Jay T. Brown
Remarks: Big Lost River below the INEEL Diversion Dam
10' x 10' plot in center of channel

DATA: Particle size (mm)				
5	7	6	5	7
7	9	10	7	11
5	2	11	8	8
8	7	13	12	8
6	17	8	9	7
9	9	7	10	4
9	5	17	11	9
3	7	9	6	6
7	9	12	12	8
10	14	11	8	6
11	8	9	10	7
7	9	13	9	10
4	16	8	7	11
7	8	9	8	8
11	6	7	7	12
6	14	7	9	16
6	6	10	5	9
12	19	12	9	10
8	9	4	9	12
6	4	6	9	9

Particle Characteristics			
d_{90}	=	12.7	mm
$d_{84.1}$	=	11.9	mm
d_{65}	=	9.69	mm
d_{50}	=	8.88	mm
d_{35}	=	7.78	mm
$d_{15.9}$	=	6.41	mm
d_g	=	8.73	mm
σ_g	=	1.36	mm
G	=	0.83	

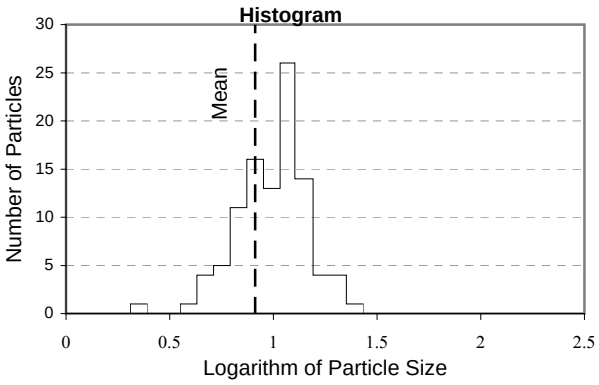

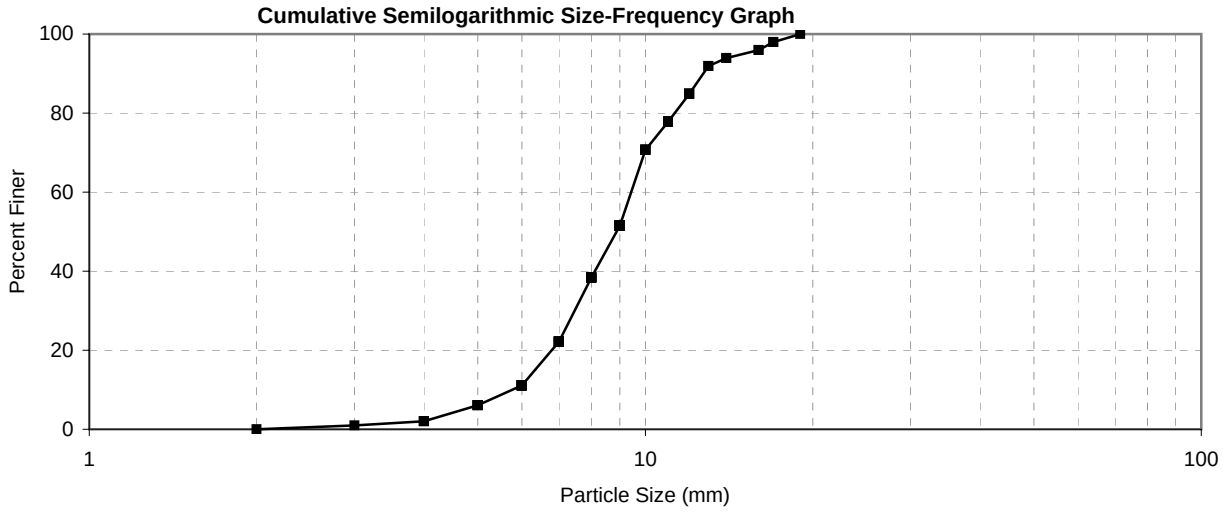

PARTICLE COUNTS

Site: Z
Date: September 21, 2000
Measurement by: Jay T. Brown
Remarks: Big Lost River below the INEEL Diversion Dam
10' x 10' plot in center of channel

DATA: Particle size (mm)				
44	47	42	24	62
27	14	19	15	14
30	58	9	82	60
41	10	90	78	55
45	58	86	43	47
77	37	74	19	15
67	35	62	27	54
38	19	60	14	67
36	12	7	19	36
49	36	59	55	35
44	14	52	9	50
82	54	16	10	48
12	9	17	48	87
57	23	12	14	43
92	83	20	67	45
40	52	31	6	75
51	11	47	53	37
29	56	58	45	94
50	37	26	44	6
48	17	28	16	110

Particle Characteristics			
d_{90}	=	77.1	mm
$d_{84.1}$	=	65.1	mm
d_{65}	=	50.2	mm
d_{50}	=	43.2	mm
d_{35}	=	29.6	mm
$d_{15.9}$	=	14.7	mm
d_g	=	30.9	mm
σ_g	=	2.10	mm
G	=	1.10	

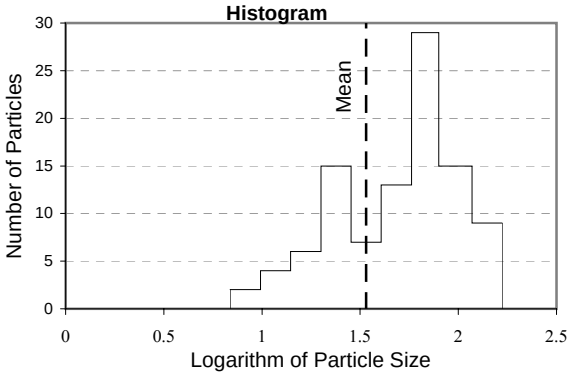

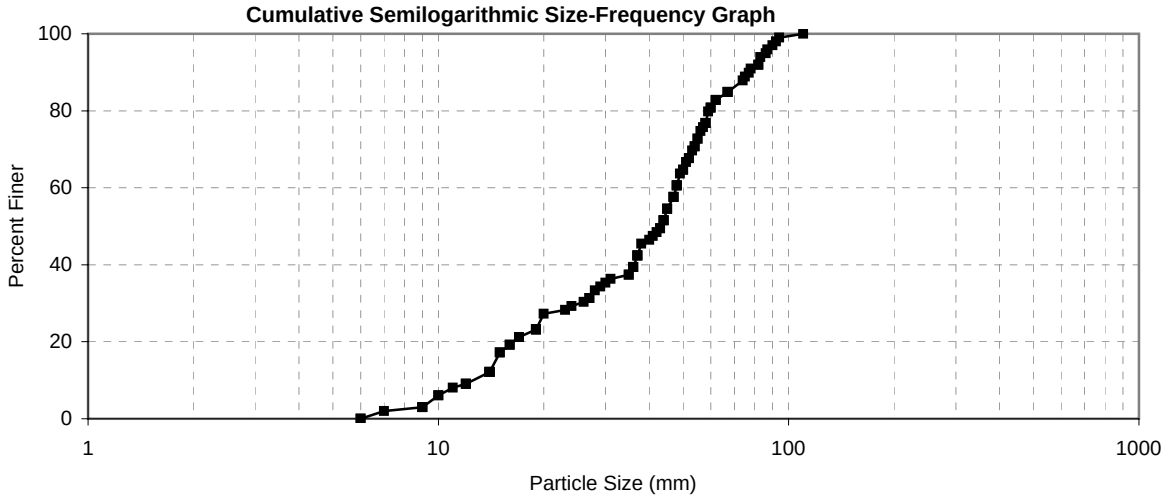

PARTICLE COUNTS

Site: AA
Date: September 21, 2000
Measurement by: Jay T. Brown
Remarks: Big Lost River below the INEEL Diversion Dam
10' x 10' plot in center of channel

DATA: Particle size (mm)				
42	27	29	16	11
50	53	56	53	83
26	58	87	67	19
87	65	51	60	10
68	55	25	27	15
41	70	62	77	83
74	82	46	72	122
57	35	55	80	105
48	81	76	34	79
57	79	66	37	87
85	13	60	25	35
40	29	9	13	15
45	24	47	73	52
34	32	14	14	108
48	27	48	12	27
42	27	32	172	50
14	60	47	26	30
15	80	60	8	76
17	62	67	47	12
22	64	51	8	48

Particle Characteristics			
d_{90} =	82.1	mm
$d_{84.1}$ =	77.5	mm
d_{65} =	58.7	mm
d_{50} =	48.7	mm
d_{35} =	34.3	mm
$d_{15.9}$ =	16.7	mm
d_g =	36.0	mm
σ_g =	2.15	mm
G =	1.10	

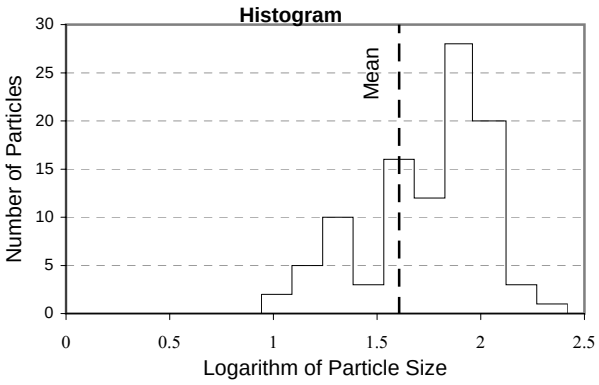

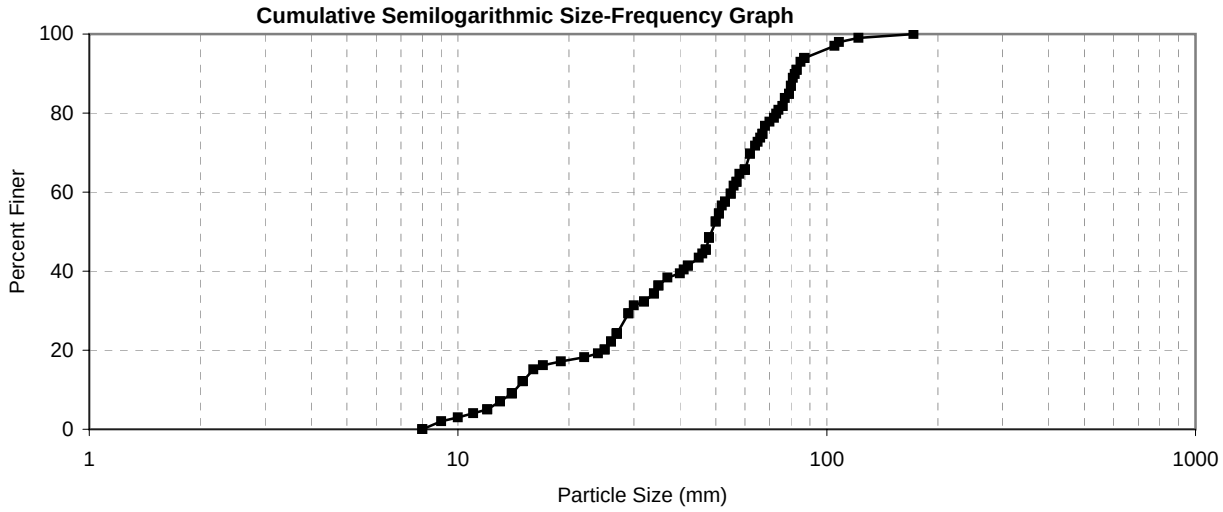

PARTICLE COUNTS

Site: AB
Date: September 22, 2000
Measurement by: Jay T. Brown
Remarks: Big Lost River below the INEEL Diversion Dam
10' x 10' plot in center of channel

DATA: Particle size (mm)				
12	17	17	10	22
14	16	20	16	11
17	11	7	29	19
25	8	17	9	14
3	37	22	16	21
34	22	25	16	25
35	34	12	10	15
22	17	22	19	30
2	19	10	24	16
23	10	9	21	27
8	9	10	17	8
10	31	8	9	36
16	15	32	25	20
14	29	35	23	7
25	19	3	18	22
29	24	26	14	14
13	8	21	13	42
21	9	13	21	23
13	23	15	17	11
10	18	22	34	34

Particle Characteristics			
d_{90} =	31.1	mm
$d_{84.1}$ =	26.3	mm
d_{65} =	21.9	mm
d_{50} =	17.6	mm
d_{35} =	14.7	mm
$d_{15.9}$ =	10.1	mm
d_g =	16.3	mm
σ_g =	1.61	mm
G =	0.90	

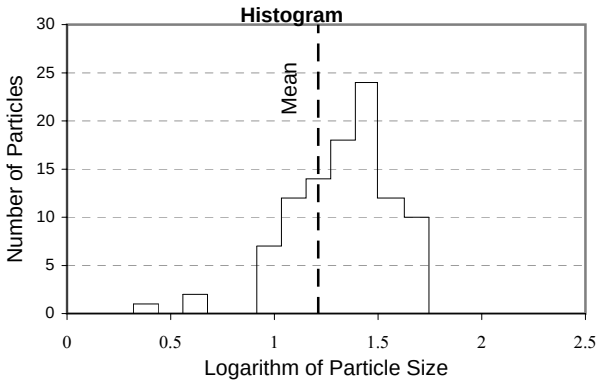

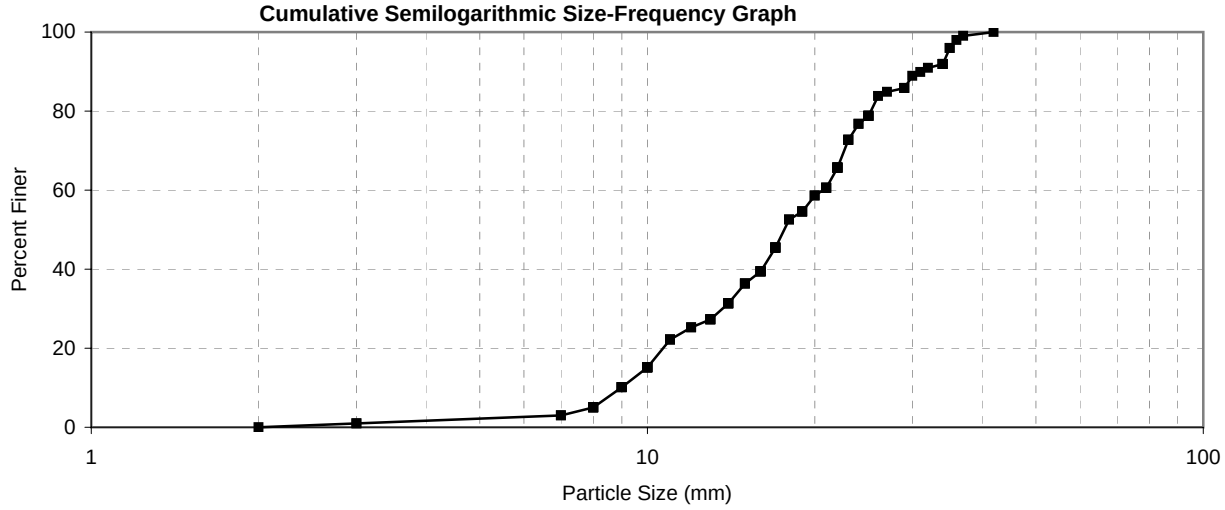

PARTICLE COUNTS

Site: AC
Date: September 22, 2000
Measurement by: Jay T. Brown
Remarks: Big Lost River below the INEEL Diversion Dam
10' x 10' plot in center of channel

DATA: Particle size (mm)				
13	30	11	25	11
35	38	10	6	25
85	37	13	24	16
24	5	17	10	4
34	6	12	17	16
14	50	20	21	31
45	27	29	29	16
37	29	13	12	18
22	42	25	26	20
16	9	29	19	10
14	16	12	15	8
10	16	23	22	32
31	18	27	10	5
23	12	9	24	11
14	32	21	41	47
42	16	23	14	24
23	42	14	23	16
38	22	12	25	37
7	41	21	29	8
17	36	16	8	19

Particle Characteristics			
d_{90}	=	38.1	mm
$d_{84.1}$	=	34.3	mm
d_{65}	=	24.6	mm
d_{50}	=	20.2	mm
d_{35}	=	16.2	mm
$d_{15.9}$	=	10.9	mm
d_g	=	19.3	mm
σ_g	=	1.77	mm
G	=	0.94	

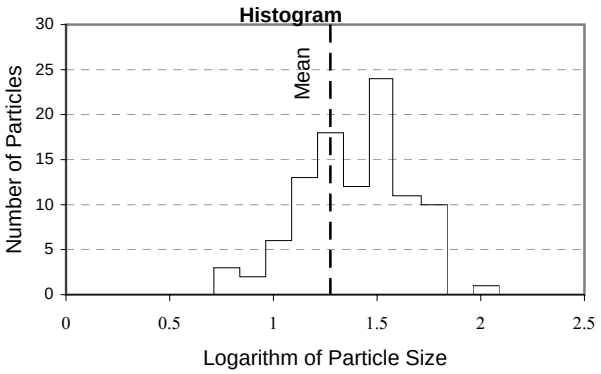

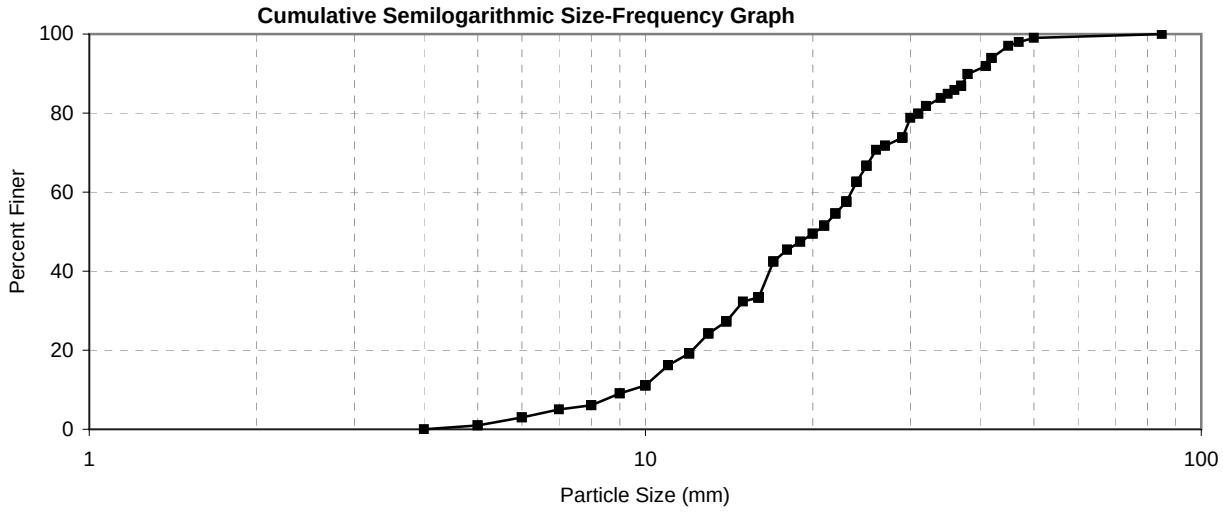

PARTICLE COUNTS

Site: AD
Date: June 21, 2001
Measurement by: Charles Berenbrock
Remarks: Big Lost River below the INEEL Diversion Dam
4' x 25' plot -- across entire channel

DATA: Particle size (mm)				
22	4	20	60	12
44	68	40	59	72
7	48	34	4	21
22	5	18	24	32
7	20	51	9	28
3	7	11	56	17
24	27	24	1	26
60	10	23	26	10
3	40	3	5	23
20	24	26	75	18
46	56	17	9	68
36	5	35	18	61
24	6	50	78	28
22	20	15	4	8
7	21	39	23	46
59	3	12	18	20
3	27	64	4	41
1	39	26	16	52
6	5	2	8	3
24	12	35	65	14

Particle Characteristics			
d_{90} =	59.5	mm
$d_{84.1}$ =	50.3	mm
d_{65} =	26.8	mm
d_{50} =	22.2	mm
d_{35} =	15.6	mm
$d_{15.9}$ =	5.67	mm
d_g =	16.9	mm
σ_g =	2.98	mm
G =	1.2	

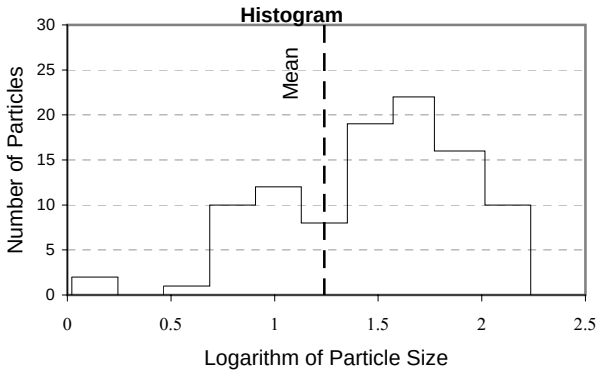

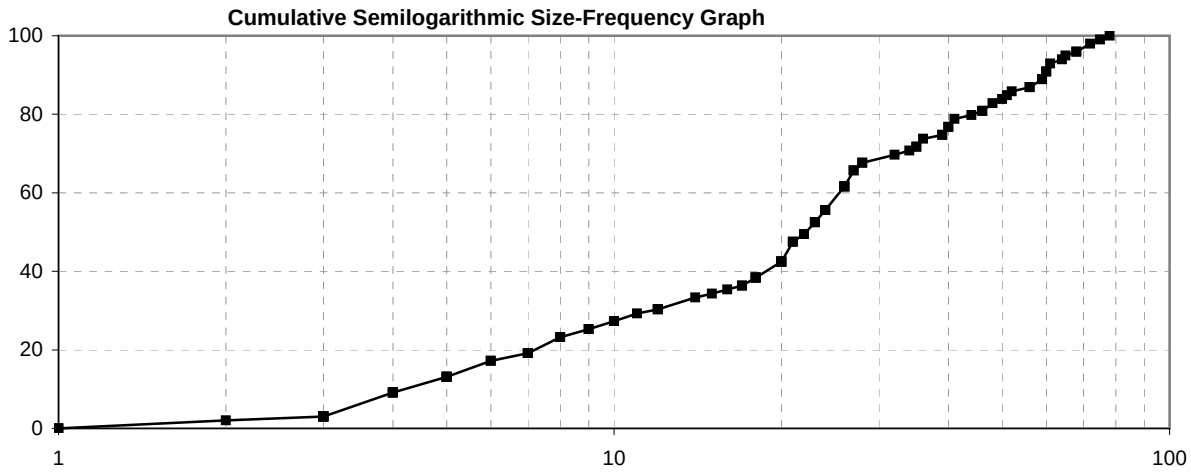

Appendix 2

Sieve Analyses of Trench Samples from Sites 1, 2, 3, 4, and 5 on the Big Lost River Upstream of the Pioneer Diversion Structures, Idaho National Engineering and Environmental Laboratory

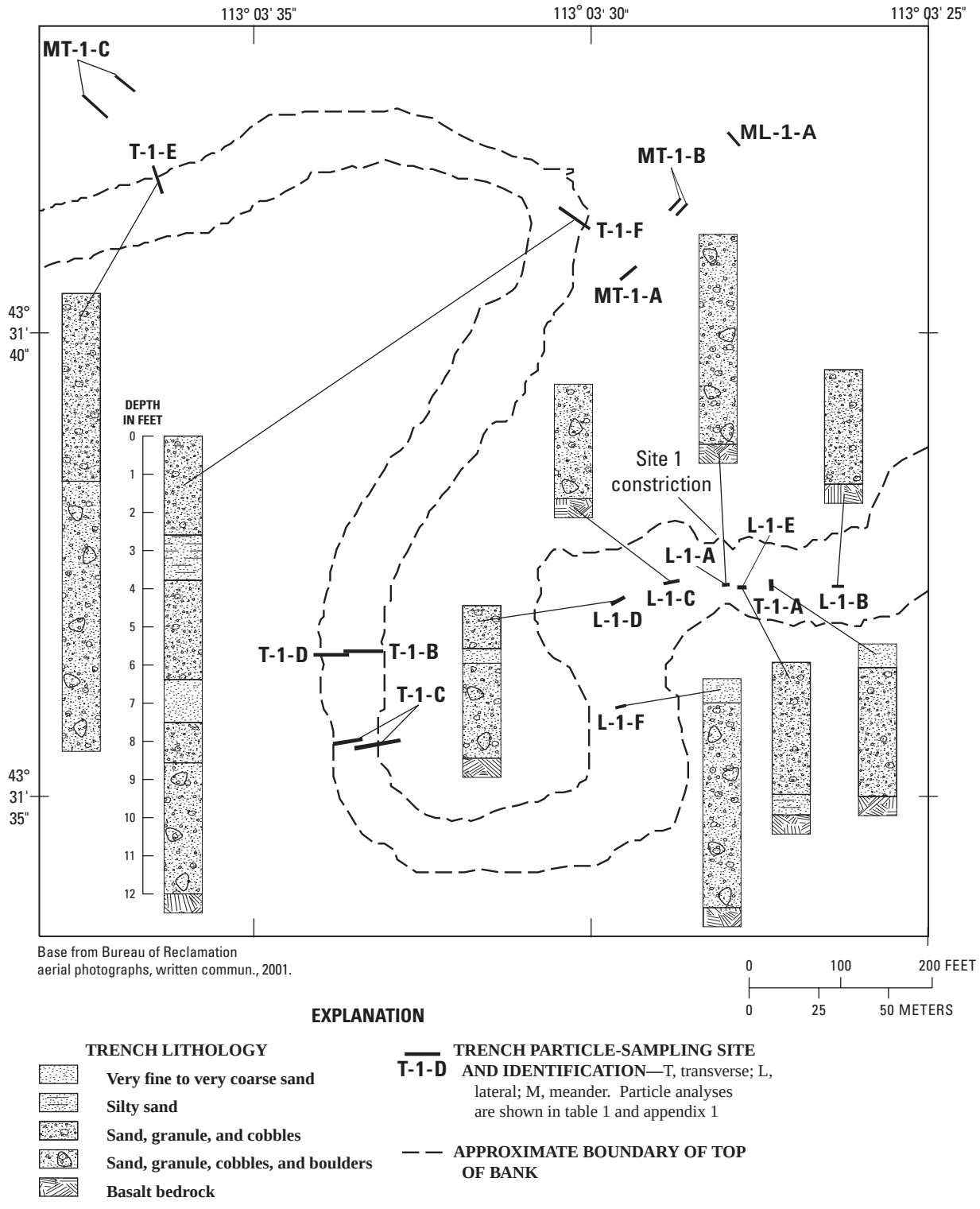

Figure 2–1. Lithology of selected trenches at site 1, Big Lost River, Idaho National Engineering and Environmental Laboratory, Idaho.

SIEVE ANALYSIS

Sample ID:	L-1-A1
Location:	Big Lost River (INEEL)
Date/Time:	August 25, 2000
Analyzed by:	BVT, AJW
Date/Time:	December 19, 2000
Gross weight:	30362.1 g
Tare weight:	1359.5 g
Net weight:	29002.6 g
Gravel weight:	5794.1 g
Sand weight:	1941.4 g
Portion analyzed:	7773.9 g
Remarks:	Sediments collected during trenching of the Big Lost River. ~1/4 of sample analyzed, used splitter. Poorly sorted sand to cobble-size sediment.

Sieve Size (mm)	Weight (g)	Percent Finer	Cumulative Percent Finer	Size Class	Remarks
8192					
4096				**Boulders**	
2048					
1024					
512					No of Particles
256	0.0	0.00	100.00		0
64	1990.7	25.63	74.37	**Cobble**	4
32	1262.1	16.25	58.12		9
16	1216.8	15.67	42.45	**Pebble**	68
8	831.6	10.71	31.75		>100
4	492.9	6.35	25.40		
2	464.7	5.98	19.42	**Very coarse sand**	30% consolidated sediment
1	425.6	5.48	13.94	**Granule**	45% consolidated sediment
0.5	391.2	5.04	8.90	**Coarse sand**	75% consolidated sediment
0.25	423.1	5.45	3.46	**Medium sand**	
0.125	182.1	2.34	1.11	**Fine sand**	
0.0625	54.7	0.70	0.41	**Very fine sand**	
<0.0625	31.6	0.41	0.00	**Silt & clays**	
TOTAL	7767.1				

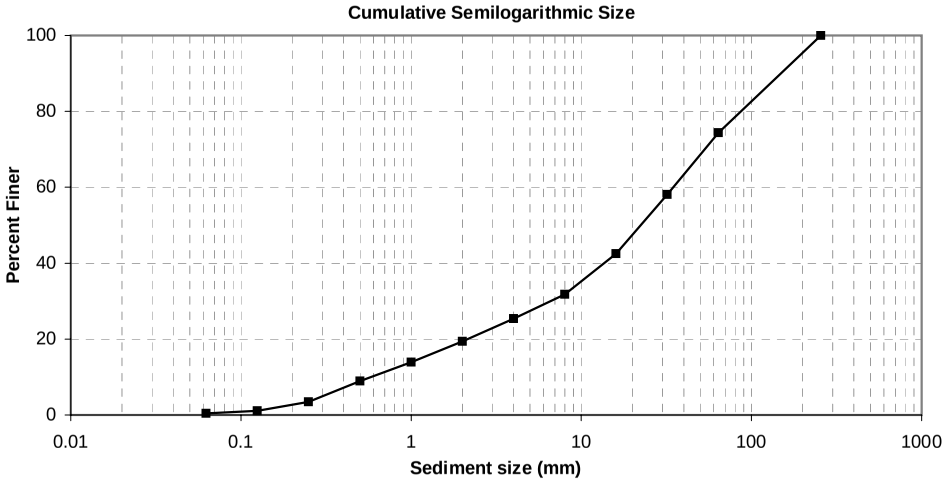

Particle Characteristics			
d_{90}	=	149	mm
$d_{84.1}$	=	108	mm
d_{65}	=	42.9	mm
d_{50}	=	22.3	mm
d_{35}	=	9.87	mm
$d_{15.9}$	=	1.28	mm
d_g	=	11.8	mm
σ_g	=	9.19	mm
G	=	2.36	

SIEVE ANALYSIS

Sample ID:	L-1-B1
Location:	Big Lost River (INEEL)
Date/Time:	August 25, 2000
Analyzed by:	BVT, AJW
Date/Time:	December 19, 2000
Gross weight:	28118.4 g
Tare weight:	808.4 g
Net weight:	27310.0 g
Gravel weight:	3751.9 g
Sand weight:	2436.2 g
Portion analyzed:	6200.2 g
Remarks:	Sediments collected during trenching of the Big Lost River. ~1/4 of sample analyzed, used splitter. Poorly sorted sand to pebble-size sediment.

Sieve Size (mm)	Weight (g)	Percent Finer	Cumulative Percent Finer	Size Class	Remarks
8192					
4096				Boulders	
2048					
1024					
512					
256					No. of Particles
64	0.0	0.00	100.00	Cobble	0
32	1107.9	17.88	82.12		9
16	1111.1	17.93	64.18	Pebble	65
8	965.9	15.59	48.59		>100
4	567.0	9.15	39.44		
2	436.0	7.04	32.41	Very coarse sand	
1	716.0	11.56	20.85	Granule	
0.5	793.3	12.80	8.05	Coarse sand	
0.25	356.8	5.76	2.29	Medium sand	
0.125	113.1	1.83	0.46	Fine sand	
0.0625	21.0	0.34	0.12	Very fine sand	
<0.0625	7.6	0.12	0.00	Silt & clays	
TOTAL	6195.7				

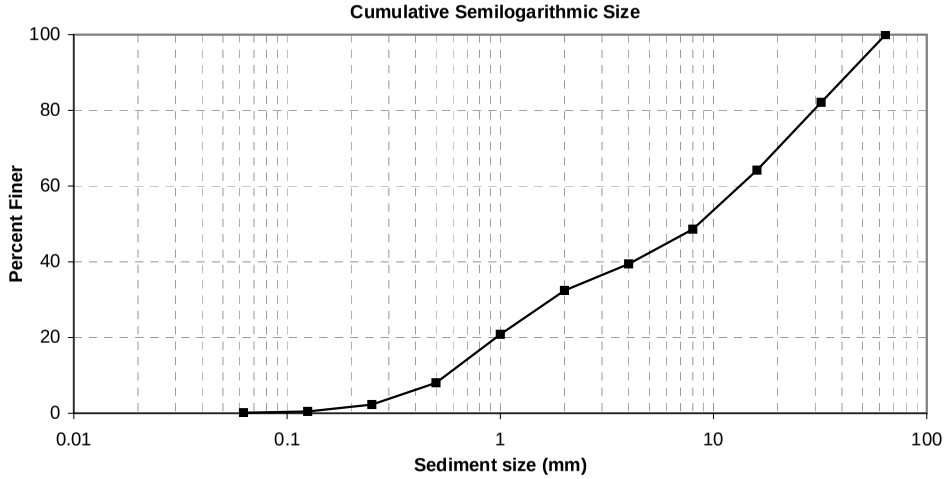

Particle Characteristics			
d_{90}	=	43.4	mm
$d_{84.1}$	=	34.6	mm
d_{65}	=	16.5	mm
d_{50}	=	8.52	mm
d_{35}	=	2.58	mm
$d_{15.9}$	=	0.76	mm
d_g	=	5.13	mm
σ_g	=	6.75	mm
G	=	1.95	

SIEVE ANALYSIS

Sample ID:	L-1-C1
Location:	Big Lost River (INEEL)
Date/Time:	August 25, 2000
Analyzed by:	BVT, AJW
Date/Time:	December 14, 2000
Gross weight:	28409.9 g
Tare weight:	808.4 g
Net weight:	27601.5 g
Gravel weight:	4880.5 g
Sand weight:	1697.5 g
Portion analyzed:	6586.1 g
Remarks:	Sediments collected during trenching of the Big Lost River. ~1/4 of sample analyzed, used splitter. Poorly sorted sand to pebble-size sediment.

Sieve Size (mm)	Weight (g)	Percent Finer	Cumulative Percent Finer	Size Class	Remarks
				Boulders	
8192					
4096					
2048					
1024					
512					
256					No of Particles
64	0.0	0.00	100.00	Cobble	0
32	2345.7	35.65	64.35	Pebble	18
16	1224.8	18.61	45.74		87
8	819.7	12.46	33.28		>100
4	490.3	7.45	25.83		
2	364.5	5.54	20.29	Very coarse sand	
1	305.2	4.64	15.66	Granule	
0.5	410.6	6.24	9.42	Coarse sand	
0.25	416.2	6.32	3.09	Medium sand	
0.125	168.7	2.56	0.53	Fine sand	
0.0625	32.3	0.49	0.04	Very fine sand	
<0.0625	2.5	0.04	0.00	Silt & clays	
TOTAL	6580.5				

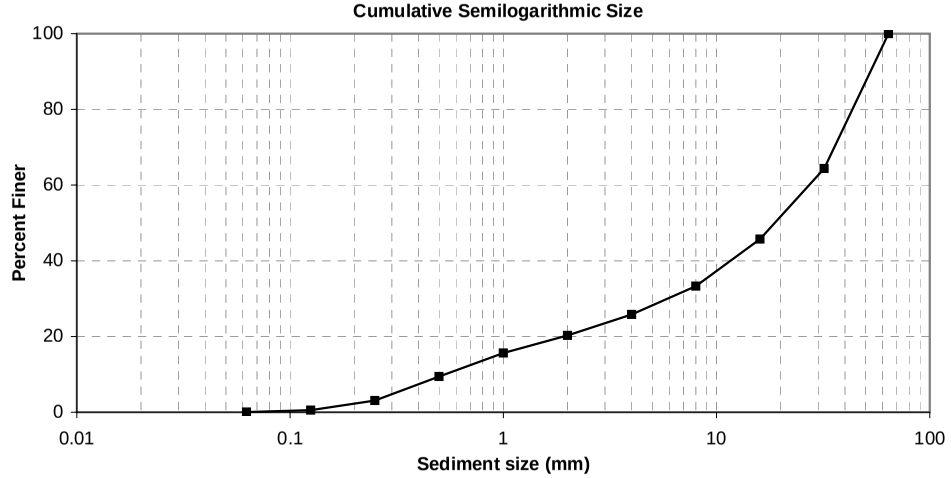

Particle Characteristics			
d_{90}	=	52.7	mm
$d_{84.1}$	=	47.0	mm
d_{65}	=	32.4	mm
d_{50}	=	18.7	mm
d_{35}	=	8.80	mm
$d_{15.9}$	=	1.04	mm
d_g	=	6.99	mm
σ_g	=	6.72	mm
G	=	2.26	

SIEVE ANALYSIS

Sample ID:	L-1-D1
Location:	BLR sediments
Date/Time:	August 25, 2000
Analyzed by:	BVT, AJW
Date/Time:	December 4, 2000
Gross weight:	5785.5 g
Tare weight:	164.2 g
Net weight:	5621.3 g
Gravel weight:	3380.1 g
Sand weight:	2183.9 g
Portion analyzed:	5621.3 g
Remarks:	Sediments collected during trenching of the Big Lost River. Poorly sorted sand to pebble-size sediment.

Sieve Size (mm)	Weight (g)	Percent Finer	Cumulative Percent Finer	Size Class	Remarks
				Boulders	
8192					
4096					
2048					
1024					
512					
256					No. of particles
64	0.0	0.00	100.00	Cobble	0
32	743.0	13.22	86.78	Pebble	7
16	1212.0	21.56	65.22		95
8	839.0	14.93	50.29		>100
4	586.1	10.43	39.87		
2	435.3	7.74	32.12	Very coarse sand	
1	382.3	6.80	25.32	Granule	
0.5	489.4	8.71	16.61	Coarse sand	
0.25	513.9	9.14	7.47	Medium sand	
0.125	273.1	4.86	2.61	Fine sand	
0.0625	89.9	1.60	1.01	Very fine sand	
<0.0625	57.0	1.01	0.00	Silt & clays	
TOTAL	5621.0				

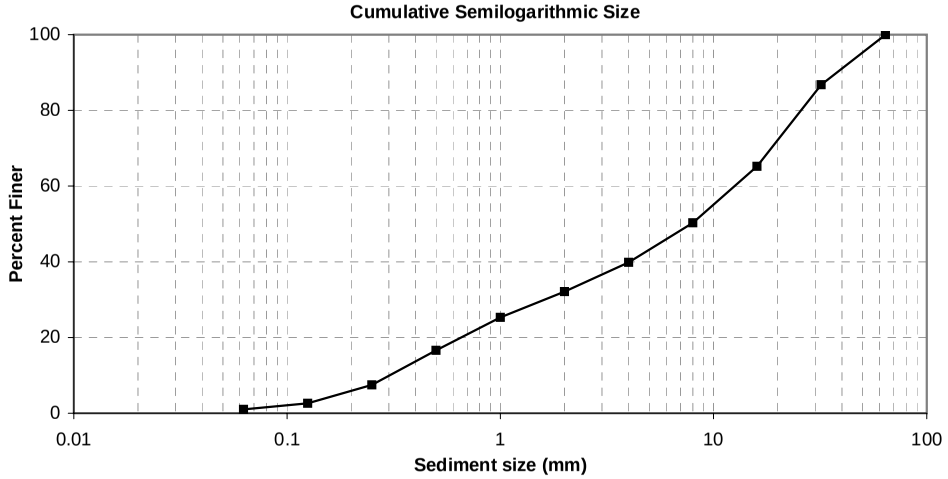

Particle Characteristics			
d_{90}	=	37.9	mm
$d_{84.1}$	=	29.4	mm
d_{65}	=	15.8	mm
d_{50}	=	7.85	mm
d_{35}	=	2.59	mm
$d_{15.9}$	=	0.47	mm
d_g	=	3.73	mm
σ_g	=	7.87	mm
G	=	2.25	

SIEVE ANALYSIS

Sample ID:	L-1-D2
Location:	BLR sediments
Date/Time:	August 25, 2000
Analyzed by:	BVT, AJW
Date/Time:	December 4, 2000
Gross weight:	1543.7 g
Tare weight:	110.7 g
Net weight:	1433.0 g
Gravel weight:	2.0 g
Sand weight:	1427.8 g
Portion analyzed:	1433.0 g
Remarks:	Sediments collected during trenching of the Big Lost River. Well-sorted coarse sand.

Sieve Size (mm)	Weight (g)	Percent Finer	Cumulative Percent Finer	Size Class	Remarks
8192					
4096				**Boulders**	
2048					
1024					
512					
256					
64				**Cobble**	
32					
16				**Pebble**	No. of particles
8	0.0	0.00	100.00		0
4	2.0	0.14	99.86		11
2	1.6	0.11	99.75	**Very coarse sand**	54
1	1.3	0.09	99.66	**Granule**	>100
0.5	10.8	0.75	98.90	**Coarse sand**	
0.25	1169.3	81.60	17.30	**Medium sand**	
0.125	213.7	14.91	2.39	**Fine sand**	
0.0625	31.1	2.17	0.22	**Very fine sand**	
<0.0625	3.1	0.22	0.00	**Silt & clays**	
TOTAL	1432.9				

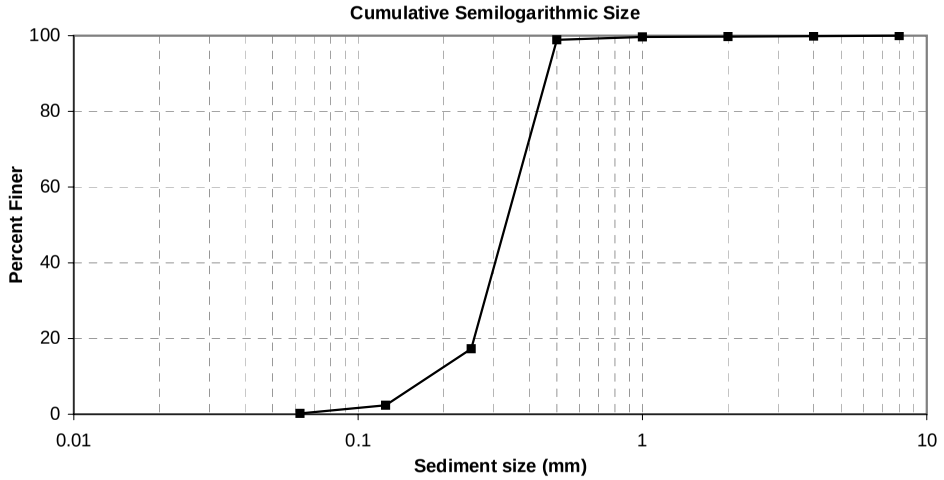

Particle Characteristics			
d_{90}	=	0.46	mm
$d_{84.1}$	=	0.44	mm
d_{65}	=	0.37	mm
d_{50}	=	0.33	mm
d_{35}	=	0.29	mm
$d_{15.9}$	=	0.23	mm
d_g	=	0.32	mm
σ_g	=	1.37	mm
G	=	0.83	

SIEVE ANALYSIS

Sample ID:	L-1-D3
Location:	BLR sediments
Date/Time:	August 25, 2000
Analyzed by:	BVT, AJW
Date/Time:	December 4, 2000
Gross weight:	11256.9 g
Tare weight:	275.1 g
Net weight:	10981.8 g
Gravel weight:	7232.9 g
Sand weight:	3735.5 g
Portion analyzed:	10981.8 g
Remarks:	Sediments collected during trenching of the Big Lost River. Poorly sorted sand to cobble-size sediment.

Sieve Size (mm)	Weight (g)	Percent Finer	Cumulative Percent Finer	Size Class	Remarks
				Boulders	
8192					
4096					
2048					
1024					
512					No. of particles
256	0.0	0.00	100.00		0
64	2348.0	21.38	78.62	Cobble	4
32	1776.6	16.18	62.44	Pebble	15
16	1260.4	11.48	50.96		74
8	963.5	8.78	42.18		>100
4	884.4	8.05	34.13		
2	1025.7	9.34	24.79	Very coarse sand	
1	1214.6	11.06	13.72	Granule	
0.5	900.2	8.20	5.52	Coarse sand	
0.25	436.6	3.98	1.55	Medium sand	
0.125	128.3	1.17	0.38	Fine sand	
0.0625	30.1	0.27	0.11	Very fine sand	
<0.0625	11.6	0.11	0.00	Silt & clays	
TOTAL	10980.0				

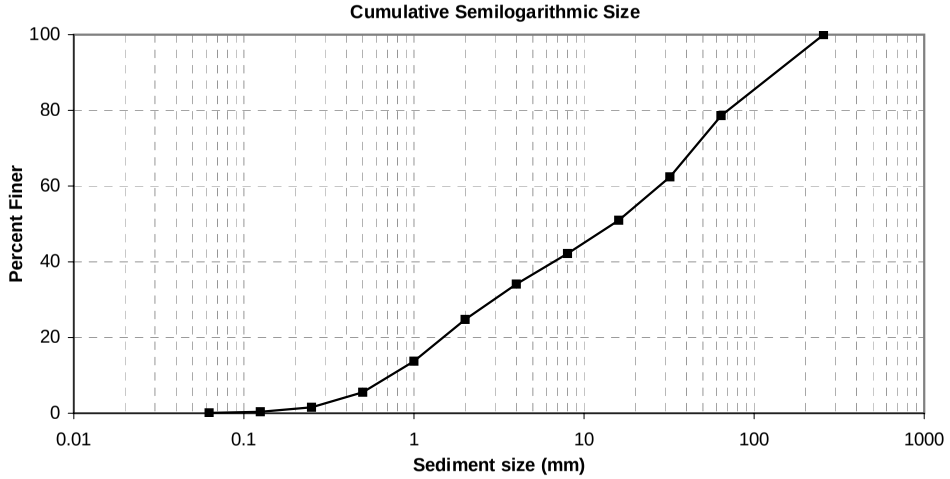

Particle Characteristics			
d_{90}	=	134	mm
$d_{84.1}$	=	91.3	mm
d_{65}	=	35.7	mm
d_{50}	=	14.8	mm
d_{35}	=	4.31	mm
$d_{15.9}$	=	1.15	mm
d_g	=	10.2	mm
σ_g	=	8.93	mm
G	=	2.19	

SIEVE ANALYSIS

Sample ID:	L-1-DC1
Location:	BLR sediments
Date/Time:	August 25, 2000
Analyzed by:	BVT, AJW
Date/Time:	December 4, 2000
Gross weight:	221.9 g
Tare weight:	122.8 g
Net weight:	99.1 g
Gravel weight:	1.1 g
Sand weight:	88.8 g
Portion analyzed:	99.1 g
Remarks:	Sediments collected during trenching of the Big Lost River. Fine sand to pebble-size sediment.

Sieve Size (mm)	Weight (g)	Percent Finer	Cumulative Percent Finer	Size Class	Remarks
8192					
4096				**Boulders**	
2048					
1024					
512					
256					
64				**Cobble**	
32					
16				**Pebble**	No. of particles
8	0.0	0.00	100.00		0
4	1.1	1.11	98.89		12
2	8.1	8.19	90.70	**Very coarse sand**	>100; 90% consol. clay
1	9.2	9.30	81.40	**Granule**	85% consol. clay
0.5	11.9	12.03	69.36	**Coarse sand**	90% consol. clay
0.25	10.6	10.72	58.65	**Medium sand**	
0.125	29.6	29.93	28.72	**Fine sand**	
0.0625	19.4	19.62	9.10	**Very fine sand**	
<0.0625	9.0	9.10	0.00	**Silt & clays**	
TOTAL	98.9				

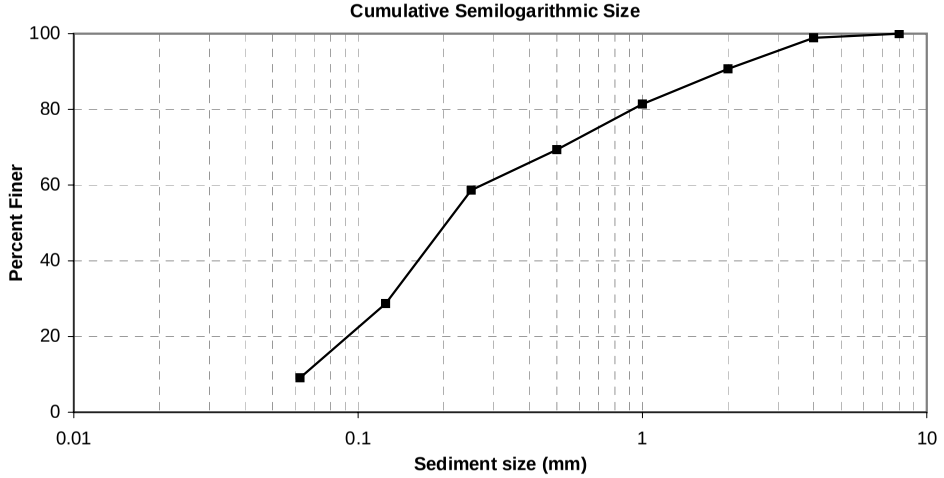

Particle Characteristics			
d_{90}	=	1.90	mm
$d_{84.1}$	=	1.22	mm
d_{65}	=	0.38	mm
d_{50}	=	0.20	mm
d_{35}	=	0.14	mm
$d_{15.9}$	=	0.08	mm
d_g	=	0.31	mm
σ_g	=	3.92	mm
G	=	1.46	

SIEVE ANALYSIS

Sample ID:	L-1-DC2	
Location:	BLR sediments	
Date/Time:	August 25, 2000	
Analyzed by:	BVT, AJW	
Date/Time:	December 4, 2000	
Gross weight:	410.7	g
Tare weight:	122.8	g
Net weight:	287.9	g
Gravel weight:	15.1	g
Sand weight:	232.4	g
Portion analyzed:	287.0	g
Remarks:	Sediments collected during trenching of the Big Lost River. Fine sand to pebble-size sediment.	

Sieve Size (mm)	Weight (g)	Percent Finer	Cumulative Percent Finer	Size Class	Remarks
8192					
4096				**Boulders**	
2048					
1024					
512					
256					
64				**Cobble**	
32					
16				**Pebble**	No. of particles
8	0.0	0.00	100.00		0
4	15.1	5.26	94.74		89; 25% consol. clay
2	44.3	15.44	79.30	**Very coarse sand**	>100; 20% consol. clay
1	50.2	17.49	61.81	**Granule**	90% consol. clay, silt
0.5	36.2	12.61	49.20	**Coarse sand**	85% consol. clay, silt
0.25	26.3	9.16	40.03	**Medium sand**	
0.125	26.8	9.34	30.70	**Fine sand**	
0.0625	48.6	16.93	13.76	**Very fine sand**	
<0.0625	39.5	13.76	0.00	**Silt & clays**	
TOTAL	287.0				

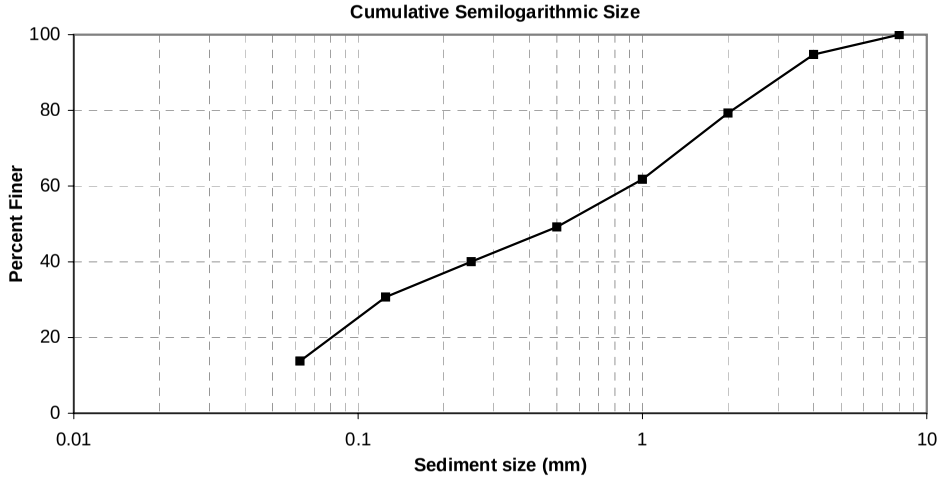

Particle Characteristics			
d_{90}	=	3.23	mm
$d_{84.1}$	=	2.48	mm
d_{65}	=	1.13	mm
d_{50}	=	0.52	mm
d_{35}	=	0.17	mm
$d_{15.9}$	=	0.07	mm
d_g	=	0.41	mm
σ_g	=	6.03	mm
G	=	1.76	

SIEVE ANALYSIS

Sample ID:	L-1-DC3
Location:	BLR sediments
Date/Time:	August 25, 2000
Analyzed by:	BVT, AJW
Date/Time:	December 4, 2000
Gross weight:	169.9 g
Tare weight:	116.2 g
Net weight:	53.7 g
Gravel weight:	9.2 g
Sand weight:	42.6 g
Portion analyzed:	53.7 g
Remarks:	Sediments collected during trenching of the Big Lost River. Poorly sorted fine sand to pebble-size sediment.

Sieve Size (mm)	Weight (g)	Percent Finer	Cumulative Percent Finer	Size Class	Remarks
8192					
4096				**Boulders**	
2048					
1024					
512					
256					
64				**Cobble**	
32					
16				**Pebble**	No. of particles
8	0.0	0.00	100.00		0
4	9.2	17.23	82.77		24
2	7.0	13.11	69.66	**Very coarse sand**	>100
1	9.3	17.42	52.25	**Granule**	60% consol. clay
0.5	8.7	16.29	35.96	**Coarse sand**	90% consol. clay
0.25	9.8	18.35	17.60	**Medium sand**	
0.125	5.5	10.30	7.30	**Fine sand**	
0.0625	2.3	4.31	3.00	**Very fine sand**	
<0.0625	1.6	3.00	0.00	**Silt & clays**	
TOTAL	53.4				

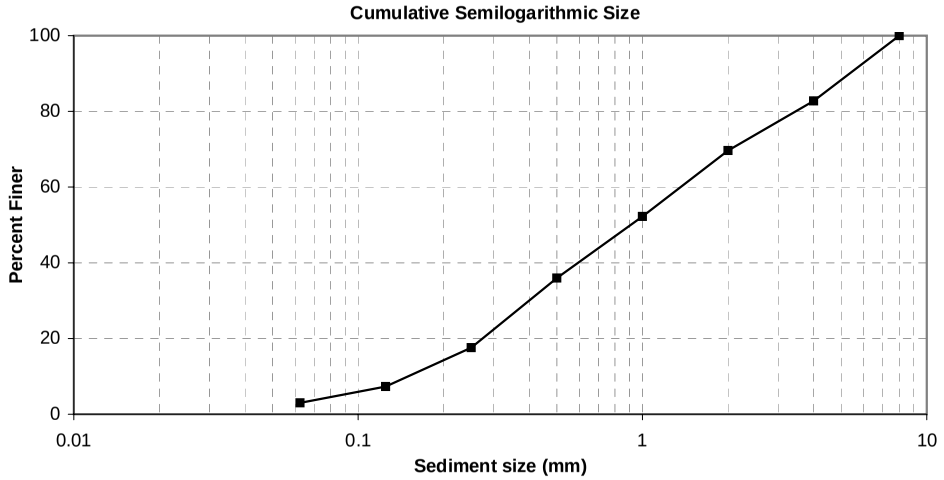

Particle Characteristics			
d_{90}	=	5.35	mm
$d_{84.1}$	=	4.22	mm
d_{65}	=	1.66	mm
d_{50}	=	0.91	mm
d_{35}	=	0.48	mm
$d_{15.9}$	=	0.22	mm
d_g	=	0.97	mm
σ_g	=	4.35	mm
G	=	1.48	

SIEVE ANALYSIS

Sample ID:	L-1-E1
Location:	Big Lost River (INEEL)
Date/Time:	August 25, 2000
Analyzed by:	BVT, AJW
Date/Time:	December 14, 2000
Gross weight:	4336.7 g
Tare weight:	113.8 g
Net weight:	4222.9 g
Gravel weight:	1489.2 g
Sand weight:	2605.1 g
Portion analyzed:	4222.9 g
Remarks:	Sediments collected during trenching of the Big Lost River. Poorly sorted fine sand to cobble-size sediment.

Sieve Size (mm)	Weight (g)	Percent Finer	Cumulative Percent Finer	Size Class	Remarks
8192					
4096				Boulders	
2048					
1024					
512					No of Particles
256	0.0	0.00	100.00		0
64	441.6	10.46	89.54	Cobble	1
32	177.7	4.21	85.33		1
16	228.5	5.41	79.92	Pebble	>100; 20% consol. sed
8	409.8	9.71	70.21		60% consol. sediment
4	231.6	5.49	64.72		20% consol. sediment
2	358.8	8.50	56.22	Very coarse sand	60% consol. sediment
1	397.7	9.42	46.80	Granule	80% consol. sediment
0.5	389.5	9.23	37.58	Coarse sand	80% consol. sediment
0.25	614.8	14.56	23.01	Medium sand	
0.125	557.8	13.21	9.80	Fine sand	
0.0625	286.5	6.79	3.01	Very fine sand	
<0.0625	127.2	3.01	0.00	Silt & clays	
TOTAL	4221.5				

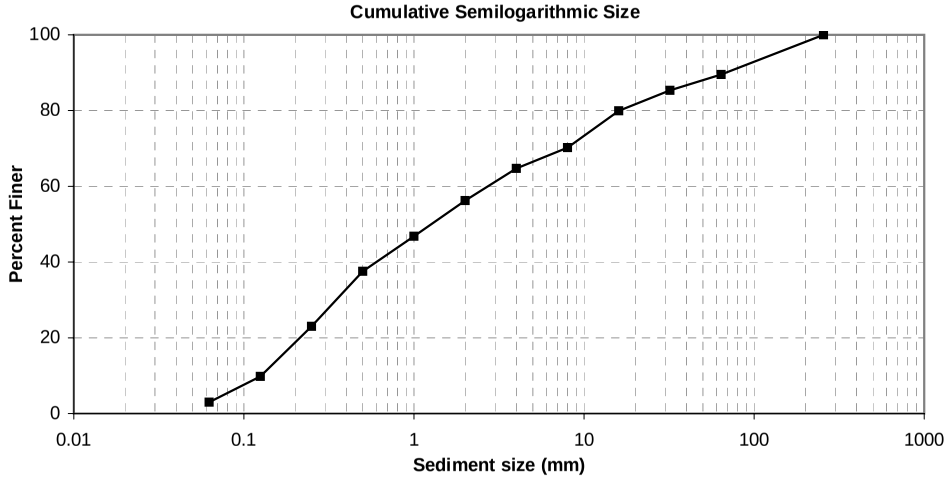

Particle Characteristics			
d_{90}	=	68	mm
$d_{84.1}$	=	27.3	mm
d_{65}	=	4.14	mm
d_{50}	=	1.27	mm
d_{35}	=	0.44	mm
$d_{15.9}$	=	0.17	mm
d_g	=	2.15	mm
σ_g	=	12.7	mm
G	=	2.69	

SIEVE ANALYSIS

Sample ID:	MT-1-A1
Location:	BLR sediments
Date/Time:	Augurst 26, 2000
Analyzed by:	BVT, AJW
Date/Time:	December 5, 2000
Gross weight:	1917.0 g
Tare weight:	116.5 g
Net weight:	1800.5 g
Gravel weight:	38.0 g
Sand weight:	739.8 g
Portion analyzed:	871.9 g
Remarks:	Sediments collected during trenching of the Big Lost River. Poorly sorted fine sand to pebble-size sediment.

Sieve Size (mm)	Weight (g)	Percent Finer	Cumulative Percent Finer	Size Class	Remarks
				Boulders	
8192					
4096					
2048					
1024					
512					
256					
64				Cobble	No. of Particles
32	0.0	0.00	100.00	Pebble	0
16	12.8	1.47	98.53		1
8	5.2	0.60	97.93		2
4	20.0	2.30	95.64		162
2	107.3	12.32	83.32	Very coarse sand	>100; 95% consol. clay
1	170.0	19.51	63.81	Granule	95% consol. clay
0.5	149.7	17.18	46.63	Coarse sand	95% consol. clay & organics
0.25	110.1	12.64	33.99	Medium sand	
0.125	76.7	8.80	25.18	Fine sand	
0.0625	126.0	14.46	10.72	Very fine sand	
<0.0625	93.4	10.72	0.00	Silt & clays	
TOTAL	871.2				

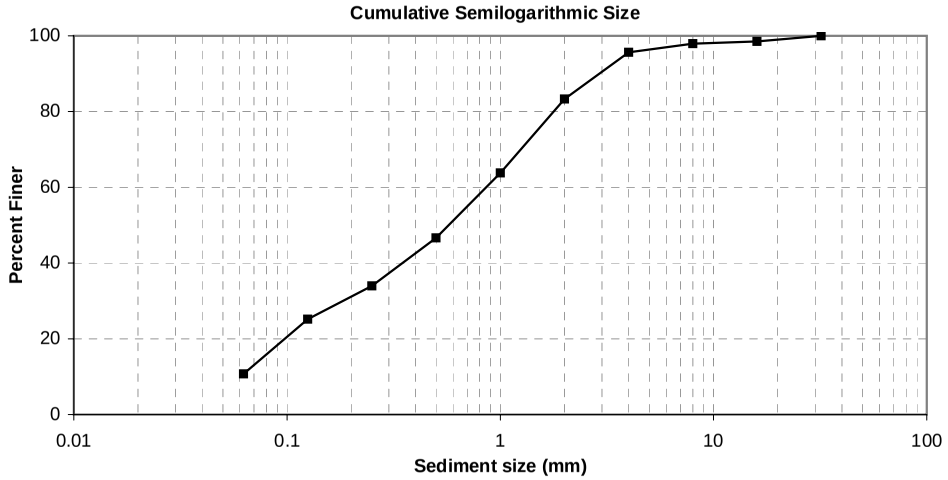

Particle Characteristics			
d_{90}	=	2.91	mm
$d_{84.1}$	=	2.09	mm
d_{65}	=	1.04	mm
d_{50}	=	0.57	mm
d_{35}	=	0.26	mm
$d_{15.9}$	=	0.08	mm
d_g	=	0.41	mm
σ_g	=	5.11	mm
G	=	1.64	

SIEVE ANALYSIS

Sample ID:	MT-1-B1
Location:	Big Lost River (INEEL)
Date/Time:	August 29, 2000
Analyzed by:	BVT, AJW
Date/Time:	December 12, 2000
Gross weight:	26458.0 g
Tare weight:	340.5 g
Net weight:	26117.5 g
Gravel weight:	1759.2 g
Sand weight:	4966.0 g
Portion analyzed:	6758.3 g
Remarks:	Sediments collected during trenching of the Big Lost River. ~1/4 of sample analyzed, used splitter. Poorly sorted fine sand to pebble-size sediment.

Sieve Size (mm)	Weight (g)	Percent Finer	Cumulative Percent Finer	Size Class	Remarks
8192					
4096				**Boulders**	
2048					
1024					
512					
256					
64				**Cobble**	No of Particles
32	0.0	0.00	100.00		0
16	347.9	5.15	94.85	**Pebble**	35
8	707.0	10.47	84.38		
4	704.3	10.43	73.95		
2	653.7	9.68	64.27	**Very coarse sand**	
1	557.6	8.26	56.01	**Granule**	
0.5	685.1	10.14	45.87	**Coarse sand**	
0.25	2187.9	32.40	13.47	**Medium sand**	
0.125	648.6	9.60	3.87	**Fine sand**	
0.0625	233.1	3.45	0.42	**Very fine sand**	
<0.0625	28.2	0.42	0.00	**Silt & clays**	
TOTAL	6753.4				

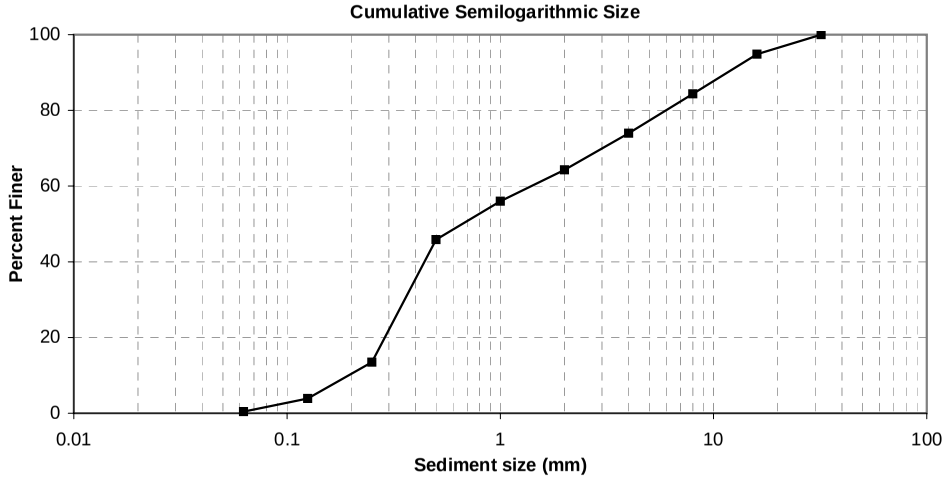

Particle Characteristics			
d_{90}	=	11.6	mm
$d_{84.1}$	=	7.85	mm
d_{65}	=	2.11	mm
d_{50}	=	0.66	mm
d_{35}	=	0.4	mm
$d_{15.9}$	=	0.26	mm
d_g	=	1.43	mm
σ_g	=	5.49	mm
G	=	1.90	

SIEVE ANALYSIS

Sample ID:	MT-1-B2
Location:	Big Lost River (INEEL)
Date/Time:	
Analyzed by:	BVT, AJW
Date/Time:	
Gross weight:	1775.4 g
Tare weight:	116.3 g
Net weight:	1659.1 g
Gravel weight:	27.7 g
Sand weight:	1569.1 g
Portion analyzed:	1659.1 g
Remarks:	Sediments collected during trenching of the Big Lost River. Moderately sorted medium sand with some pebbles present.

Sieve Size (mm)	Weight (g)	Percent Finer	Cumulative Percent Finer	Size Class	Remarks
				Boulders	
8192					
4096					
2048					
1024					
512					
256					
64				Cobble	
32				Pebble	
16					No. of Particles
8	0.0	0.00	100.00		0
4	27.7	1.68	98.32		>100; 95% consol clay & silt
2	60.8	3.68	94.64	Very coarse sand	95% consol. clay & silt
1	62.3	3.77	90.87	Granule	95% consol. clay & silt
0.5	72.5	4.39	86.48	Coarse sand	90% consol. clay & silt
0.25	478.9	28.99	57.50	Medium sand	
0.125	629.1	38.08	19.42	Fine sand	
0.0625	265.5	16.07	3.35	Very fine sand	
<0.0625	55.3	3.35	0.00	Silt & clays	
TOTAL	1652.1				

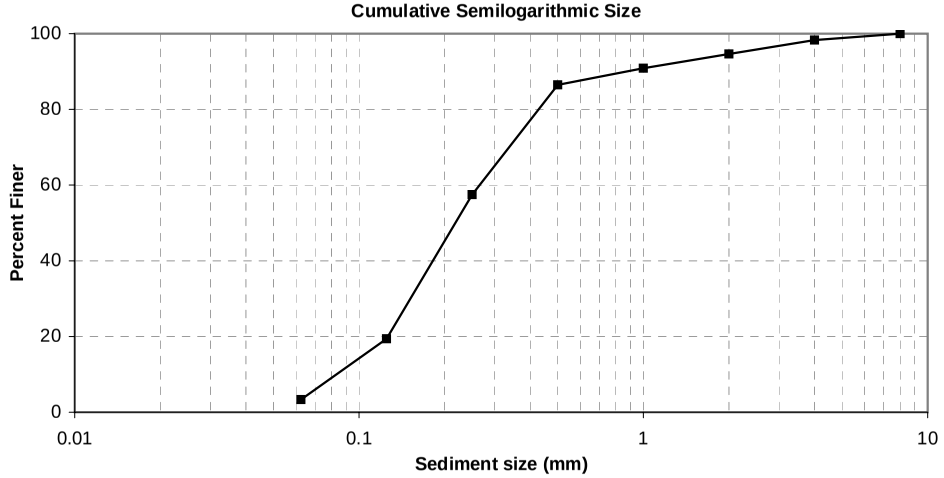

Particle Characteristics			
d_{90}	=	0.87	mm
$d_{84.1}$	=	0.47	mm
d_{65}	=	0.3	mm
d_{50}	=	0.22	mm
d_{35}	=	0.17	mm
$d_{15.9}$	=	0.11	mm
d_g	=	0.23	mm
σ_g	=	2.07	mm
G	=	1.02	

SIEVE ANALYSIS

Sample ID:	MT-1-B3	
Location:	Big Lost River (INEEL)	
Date/Time:		
Analyzed by:	BVT, AJW	
Date/Time:		
Gross weight:	27735.2	g
Tare weight:	876.7	g
Net weight:	26858.5	g
Gravel weight:	4244.1	g
Sand weight:	2893.2	g
Portion analyzed:	7147.0	g
Remarks:	Sediments collected during trenching of the Big Lost River. ~1/4 of sample analyzed, used splitter. Poorly sorted sand to pebble-size sediment.	

Sieve Size (mm)	Weight (g)	Percent Finer	Cumulative Percent Finer	Size Class	Remarks
8192					
4096				**Boulders**	
2048					
1024					
512					
256					No of Particles
64	0.0	0.00	100.00	**Cobble**	0
32	2508.1	35.12	64.88		18
16	1084.5	15.19	49.69	**Pebble**	71; 40% consol. sediment
8	395.4	5.54	44.16		>100; 40% consol. sediment
4	256.1	3.59	40.57		40% consol. sediment
2	279.8	3.92	36.65	**Very coarse sand**	40% consol. sediment
1	307.8	4.31	32.34	**Granule**	45% consol. sediment
0.5	909.8	12.74	19.60	**Coarse sand**	
0.25	1098.0	15.38	4.23	**Medium sand**	
0.125	230.6	3.23	1.00	**Fine sand**	
0.0625	67.2	0.94	0.06	**Very fine sand**	
<0.0625	4.1	0.06	0.00	**Silt & clays**	
TOTAL	7141.4				

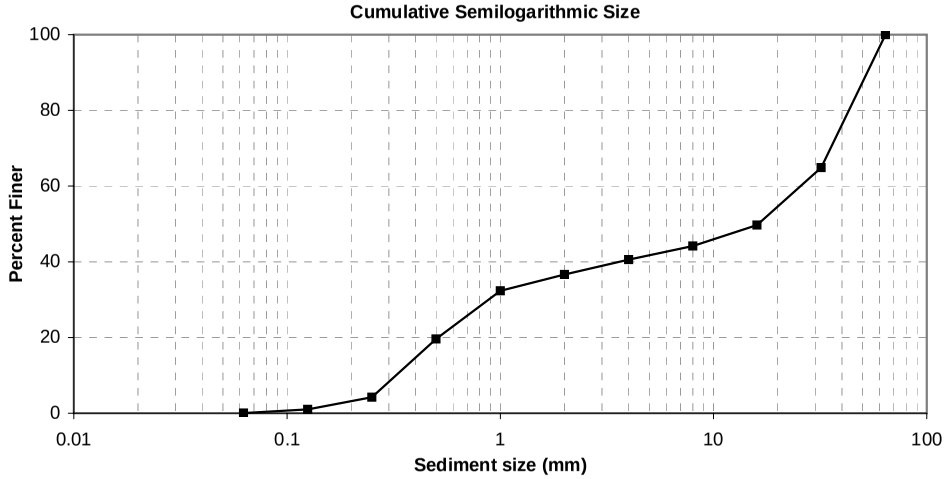

Particle Characteristics			
d_{90}	=	52.5	mm
$d_{84.1}$	=	46.8	mm
d_{65}	=	32.1	mm
d_{50}	=	16.2	mm
d_{35}	=	1.53	mm
$d_{15.9}$	=	0.42	mm
d_g	=	4.43	mm
σ_g	=	10.6	mm
G	=	3.22	

SIEVE ANALYSIS

Sample ID:	T-1-A1
Location:	Big Lost River (INEEL)
Date/Time:	August 25, 2000
Analyzed by:	BVT, AJW
Date/Time:	December 14, 2000
Gross weight:	2540.1 g
Tare weight:	113.2 g
Net weight:	2426.9 g
Gravel weight:	3.2 g
Sand weight:	2403.1 g
Portion analyzed:	2462.9 g
Remarks:	Sediments collected during trenching of the Big Lost River. Well-sorted coarse sand.

Sieve Size (mm)	Weight (g)	Percent Finer	Cumulative Percent Finer	Size Class	Remarks
				Boulders	
8192					
4096					
2048					
1024					
512					
256					
64				Cobble	
32				Pebble	
16					No. of Particles
8	0.0	0.00	100.00		0
4	3.2	0.13	99.87		16
2	4.8	0.20	99.67	Very coarse sand	>100
1	13.3	0.55	99.12	Granule	20% consol. sediments
0.5	36.9	1.52	97.60	Coarse sand	40% consol. sediments
0.25	1879.9	77.68	19.92	Medium sand	
0.125	402.3	16.62	3.29	Fine sand	
0.0625	65.9	2.72	0.57	Very fine sand	
<0.0625	13.8	0.57	0.00	Silt & clays	
TOTAL	2420.1				

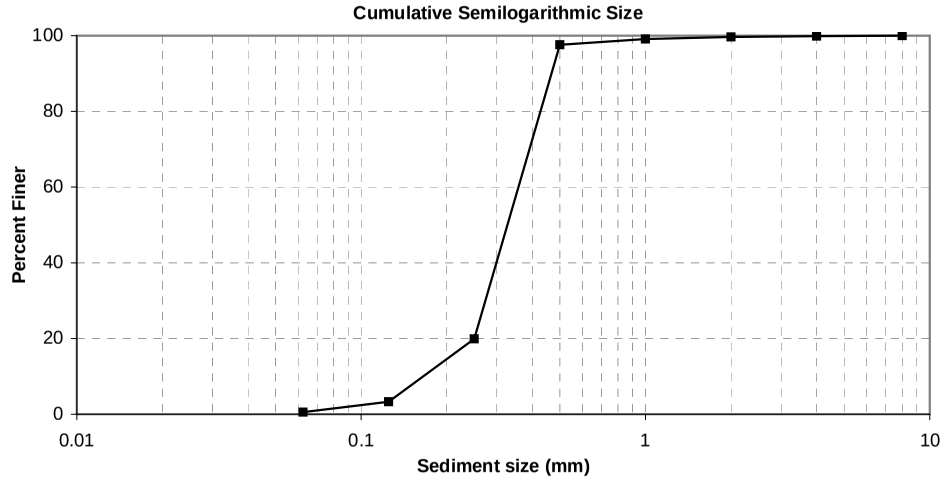

Particle Characteristics			
d_{90}	=	0.47	mm
$d_{84.1}$	=	0.44	mm
d_{65}	=	0.37	mm
d_{50}	=	0.33	mm
d_{35}	=	0.29	mm
$d_{15.9}$	=	0.21	mm
d_g	=	0.30	mm
σ_g	=	1.45	mm
G	=	0.85	

SIEVE ANALYSIS

Sample ID:	T-1-A2
Location:	Big Lost River (INEEL)
Date/Time:	August 25, 2000
Analyzed by:	BVT, AJW
Date/Time:	December 14, 2000
Gross weight:	31475.7 g
Tare weight:	876.8 g
Net weight:	30598.9 g
Gravel weight:	4740.5 g
Sand weight:	2625.1 g
Portion analyzed:	7402.1 g
Remarks:	Sediments collected during trenching of the Big Lost River. ~1/4 of sample analyzed, used splitter. Poorly sorted sand to pebble-size sediment.

Sieve Size (mm)	Weight (g)	Percent Finer	Cumulative Percent Finer	Size Class	Remarks
8192					
4096				Boulders	
2048					
1024					
512					
256					No. of Particles
64	0.0	0.00	100.00	Cobble	0
32	2133.8	28.84	71.16		17
16	1423.2	19.24	51.92	Pebble	83
8	678.3	9.17	42.75		>100
4	505.2	6.83	35.92		
2	479.3	6.48	29.45	Very coarse sand	
1	375.3	5.07	24.37	Granule	
0.5	605.5	8.18	16.19	Coarse sand	
0.25	788.5	10.66	5.53	Medium sand	
0.125	312.6	4.23	1.30	Fine sand	
0.0625	63.9	0.86	0.44	Very fine sand	
<0.0625	32.6	0.44	0.00	Silt & clays	
TOTAL	7398.2				

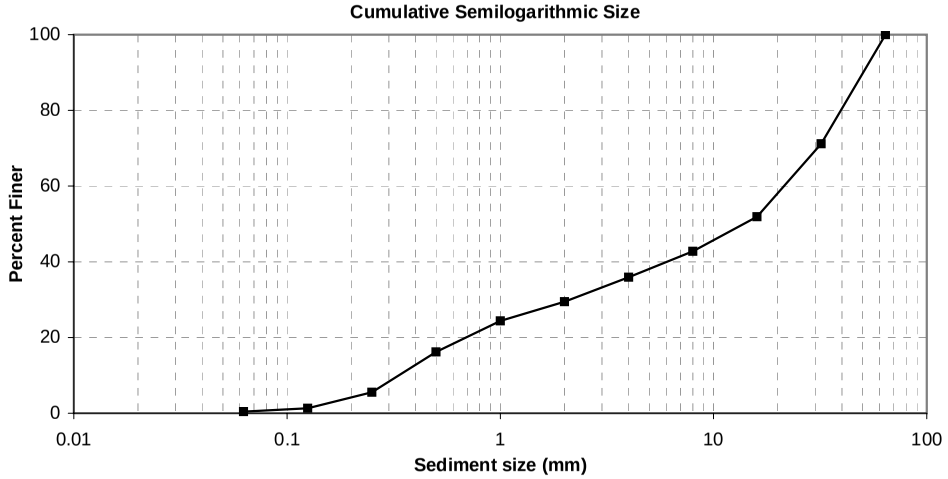

Particle Characteristics			
d_{90}	=	50.3	mm
$d_{84.1}$	=	43.7	mm
d_{65}	=	25.6	mm
d_{50}	=	13.8	mm
d_{35}	=	3.62	mm
$d_{15.9}$	=	0.49	mm
d_g	=	4.63	mm
σ_g	=	9.44	mm
G	=	2.80	

SIEVE ANALYSIS

Sample ID:	T-1-B1
Location:	BLR Sediments
Date/Time:	August 26, 2000
Analyzed by:	BVT, AJW
Date/Time:	November 27, 2000
Gross weight:	5314.1 g
Tare weight:	110.8 g
Net weight:	5203.3 g
Gravel weight:	4187.0 g
Sand weight:	999.1 g
Portion analyzed:	5203.3 g
Remarks:	Sediments collected during trenching of the Big Lost River. Poorly sorted sand to cobble-size sediment.

Sieve Size (mm)	Weight (g)	Percent Finer	Cumulative Percent Finer	Size Class	Remarks
				Boulders	
8192					
4096					
2048					
1024					
512					No of Particles
256	0.0	0.00	100.00		0
64	1317.4	25.34	74.66	Cobble	2
32	1417.9	27.28	47.38	Pebble	12
16	640.9	12.33	35.05		46
8	503.8	9.69	25.36		>100
4	307.0	5.91	19.45		>100
2	243.0	4.67	14.78	Very coarse sand	
1	243.4	4.68	10.09	Granule	
0.5	293.3	5.64	4.45	Coarse sand	
0.25	166.9	3.21	1.24	Medium sand	
0.125	38.1	0.73	0.51	Fine sand	
0.0625	14.4	0.28	0.23	Very fine sand	
<0.0625	12.0	0.23	0.00	Silt & clays	
TOTAL	5198.1				

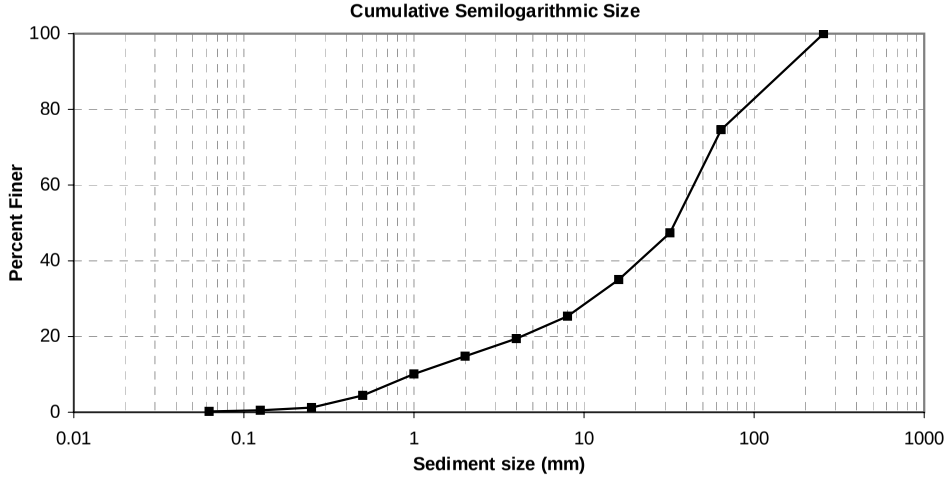

Particle Characteristics			
d_{90}	=	148	mm
$d_{84.1}$	=	107	mm
d_{65}	=	50.1	mm
d_{50}	=	34.2	mm
d_{35}	=	15.9	mm
$d_{15.9}$	=	2.36	mm
d_{g}	=	15.9	mm
σ_{g}	=	6.74	mm
G	=	2.10	

SIEVE ANALYSIS

Sample ID:	T-1-B2	
Location:	Big Lost River (INEEL)	
Date/Time:	August 26, 2000	
Analyzed by:	BVT, AJW	
Date/Time:	November 24, 2000	
Gross weight:	5659.6	g
Tare weight:	110.8	g
Net weight:	5548.8	g
Gravel weight:	28.9	g
Sand weight:	2317.9	g
Portion analyzed:	2361.1	g
Remarks:	Sediments collected during trenching of the Big Lost River. Moderately sorted granule.	

Sieve Size (mm)	Weight (g)	Percent Finer	Cumulative Percent Finer	Size Class	Remarks
				Boulders	
8192					
4096					
2048					
1024					
512					
256					
64				Cobble	
32				Pebble	No of Particles
16	0.0	0.00	100.00		0
8	12.7	0.54	99.46		10
4	16.2	0.69	98.77		79
2	45.8	1.94	96.83	Very coarse sand	>100
1	201.0	8.53	88.31	Granule	
0.5	1217.5	51.64	36.66	Coarse sand	
0.25	582.1	24.69	11.97	Medium sand	
0.125	223.6	9.48	2.49	Fine sand	
0.0625	47.9	2.03	0.46	Very fine sand	
<0.0625	10.8	0.46	0.00	Silt & clays	
TOTAL	2357.6				

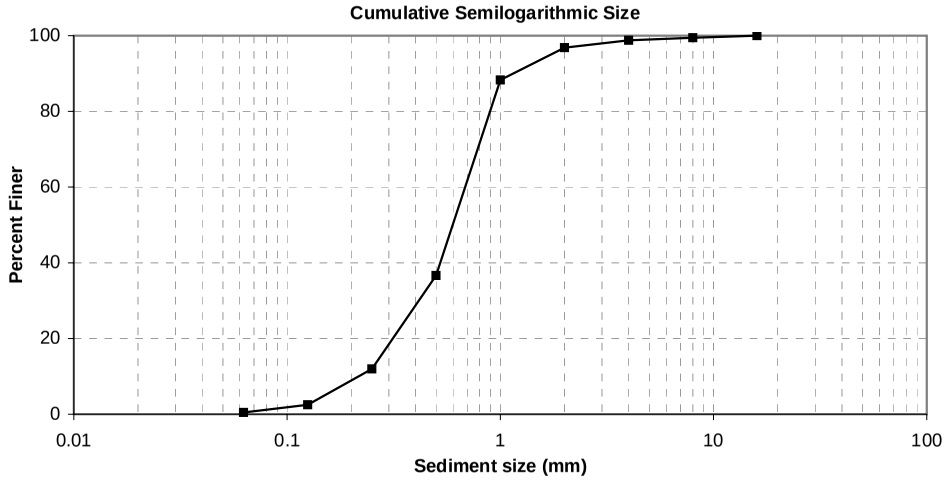

Particle Characteristics			
d_{90}	=	1.15	mm
$d_{84.1}$	=	0.95	mm
d_{65}	=	0.73	mm
d_{50}	=	0.60	mm
d_{35}	=	0.48	mm
$d_{15.9}$	=	0.28	mm
d_g	=	0.51	mm
σ_g	=	1.84	mm
G	=	0.96	

SIEVE ANALYSIS

Sample ID:	T-1-B3
Location:	Big Lost River (INEEL)
Date/Time:	August 26, 2000
Analyzed by:	BVT, AJW
Date/Time:	November 24, 2000
Gross weight:	3976.2 g
Tare weight:	110.8 g
Net weight:	3865.4 g
Gravel weight:	2576.7 g
Sand weight:	1282.9 g
Portion analyzed:	3865.4 g
Remarks:	Sediments collected during trenching of the Big Lost River. Poorly sorted sand to pebble-size sediment.

Sieve Size (mm)	Weight (g)	Percent Finer	Cumulative Percent Finer	Size Class	Remarks
				Boulders	
8192					
4096					
2048					
1024					
512					
256					No of Particles
64	0.0	0.00	100.00	Cobble	0
32	847.9	21.94	78.06	Pebble	5
16	1038.5	26.87	51.19		54
8	416.0	10.76	40.42		>100
4	274.3	7.10	33.32		
2	287.0	7.43	25.90	Very coarse sand	
1	338.9	8.77	17.13	Granule	
0.5	389.6	10.08	7.04	Coarse sand	
0.25	227.7	5.89	1.15	Medium sand	
0.125	32.9	0.85	0.30	Fine sand	
0.0625	6.8	0.18	0.12	Very fine sand	
<0.0625	4.8	0.12	0.00	Silt & clays	
TOTAL	3864.4				

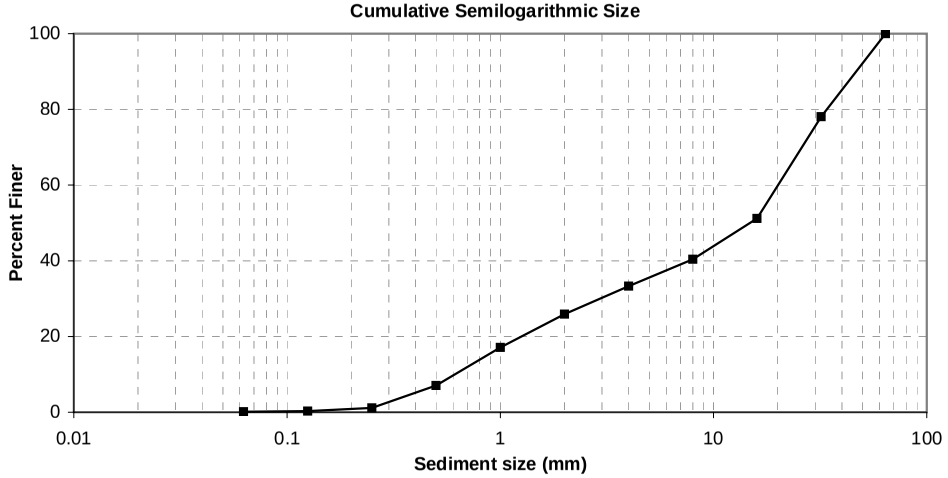

Particle Characteristics			
d_{90}	=	46.7	mm
$d_{84.1}$	=	38.7	mm
d_{65}	=	22.8	mm
d_{50}	=	14.8	mm
d_{35}	=	4.71	mm
$d_{15.9}$	=	0.92	mm
d_g	=	5.97	mm
σ_g	=	6.49	mm
G	=	2.16	

SIEVE ANALYSIS

Sample ID:	T-1-C1
Location:	BLR Sediments
Date/Time:	August 28, 2000
Analyzed by:	BVT, AJW
Date/Time:	December 4, 2000
Gross weight:	1394.7 g
Tare weight:	122.9 g
Net weight:	1271.8 g
Gravel weight:	22.2 g
Sand weight:	1123.5 g
Portion analyzed:	1271.8 g
Remarks:	Sediments collected during trenching of the Big Lost River. Fine sand to pebble-size sediment.

Sieve Size (mm)	Weight (g)	Percent Finer	Cumulative Percent Finer	Size Class	Remarks
				Boulders	
8192					
4096					
2048					
1024					
512					
256					
64				Cobble	
32				Pebble	
16					No. of Particles
8	0.0	0.00	100.00		0
4	22.2	1.75	98.25		>100; 90% consol. clay
2	123.5	9.71	88.54	Very coarse sand	95% consol. clay
1	182.0	14.31	74.23	Granule	95% consol. clay
0.5	181.8	14.30	59.93	Coarse sand	95% consol. clay
0.25	187.4	14.74	45.20	Medium sand	
0.125	193.5	15.22	29.98	Fine sand	
0.0625	255.3	20.08	9.90	Very fine sand	
<0.0625	125.9	9.90	0.00	Silt & clays	
TOTAL	1271.6				

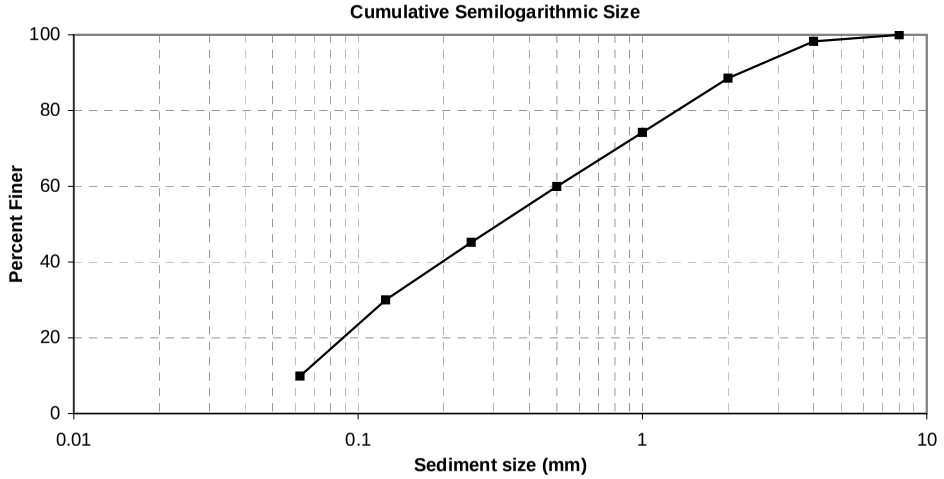

Particle Characteristics			
d_{90}	=	2.22	mm
$d_{84.1}$	=	1.61	mm
d_{65}	=	0.64	mm
d_{50}	=	0.31	mm
d_{35}	=	0.16	mm
$d_{15.9}$	=	0.08	mm
d_g	=	0.35	mm
σ_g	=	4.57	mm
G	=	1.52	

SIEVE ANALYSIS

Sample ID:	T-1-C2
Location:	BLR Sediments
Date/Time:	August 28, 2000
Analyzed by:	BVT, AJW
Date/Time:	December 4, 2000
Gross weight:	2399.7 g
Tare weight:	122.8 g
Net weight:	2276.9 g
Gravel weight:	0.0 g
Sand weight:	2273.4 g
Portion analyzed:	2276.9 g
Remarks:	Sediments collected during trenching of the Big Lost River. Sample collected outside of active channel. Well-sorted coarse sand.

Sieve Size (mm)	Weight (g)	Percent Finer	Cumulative Percent Finer	Size Class	Remarks
8192					
4096				**Boulders**	
2048					
1024					
512					
256					
64				**Cobble**	
32					
16				**Pebble**	
8					No. of Particles
4	0.0	0.00	100.00		0
2	0.9	0.04	99.96	**Very coarse sand**	27
1	5.4	0.24	99.72	**Granule**	>100
0.5	42.0	1.85	97.88	**Coarse sand**	
0.25	1975.6	86.79	11.08	**Medium sand**	
0.125	228.1	10.02	1.06	**Fine sand**	
0.0625	21.4	0.94	0.12	**Very fine sand**	
<0.0625	2.8	0.12	0.00	**Silt & clays**	
TOTAL	2276.2				

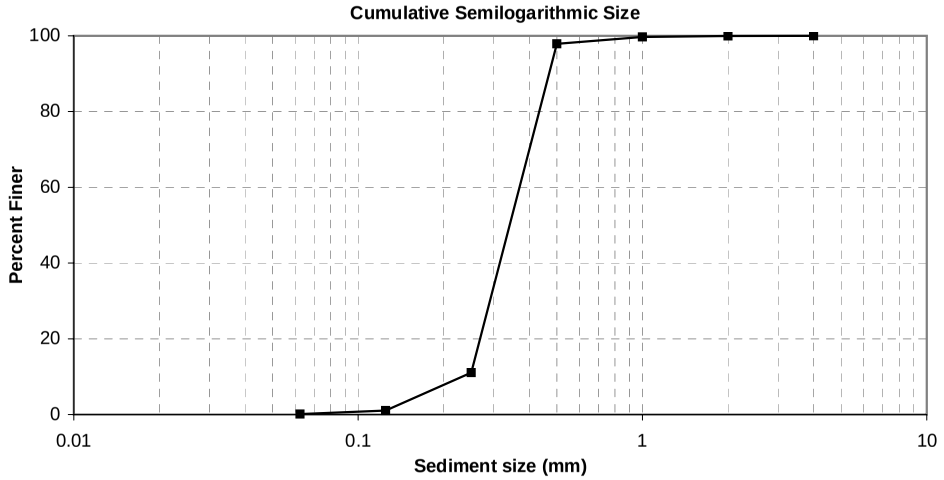

Particle Characteristics			
d_{90}	=	0.47	mm
$d_{84.1}$	=	0.45	mm
d_{65}	=	0.38	mm
d_{50}	=	0.34	mm
d_{35}	=	0.30	mm
$d_{15.9}$	=	0.26	mm
d_g	=	0.34	mm
σ_g	=	1.32	mm
G	=	0.81	

SIEVE ANALYSIS

Sample ID:	T-1-C3
Location:	BLR Sediments
Date/Time:	August 28, 2000
Analyzed by:	BVT, AJW
Date/Time:	December 4, 2000
Gross weight:	703.5 g
Tare weight:	116.5 g
Net weight:	587.0 g
Gravel weight:	2.7 g
Sand weight:	521.6 g
Portion analyzed:	587.0 g
Remarks:	Sediments collected during trenching of the Big Lost River. Well-sorted medium sand.

Sieve Size (mm)	Weight (g)	Percent Finer	Cumulative Percent Finer	Size Class	Remarks
8192					
4096				**Boulders**	
2048					
1024					
512					
256					
64				**Cobble**	
32					
16				**Pebble**	No. of Particles
8	0.0	0.00	100.00		0
4	2.7	0.46	99.54		8
2	3.1	0.53	99.01	**Very coarse sand**	>100; 95% consol. clay, silt
1	10.7	1.82	97.19	**Granule**	95% consol. clay, silt
0.5	19.1	3.25	93.93	**Coarse sand**	95% consol. clay, silt
0.25	45.1	7.69	86.25	**Medium sand**	
0.125	281.7	48.01	38.24	**Fine sand**	
0.0625	161.9	27.59	10.65	**Very fine sand**	
<0.0625	62.5	10.65	0.00	**Silt & clays**	
TOTAL	586.8				

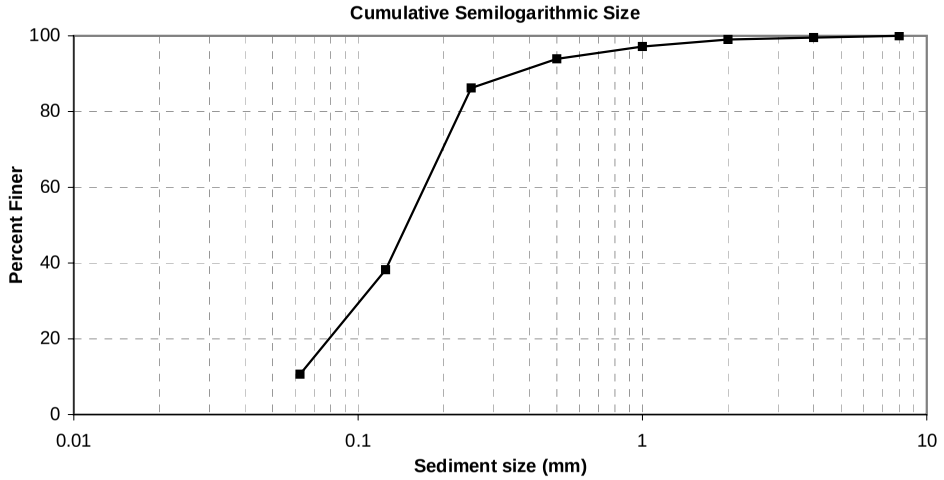

Particle Characteristics			
d_{90}	=	0.35	mm
$d_{84.1}$	=	0.24	mm
d_{65}	=	0.18	mm
d_{50}	=	0.15	mm
d_{35}	=	0.12	mm
$d_{15.9}$	=	0.07	mm
d_g	=	0.13	mm
σ_g	=	1.84	mm
G	=	0.96	

SIEVE ANALYSIS

Sample ID:	T-1-C4
Location:	BLR Sediments
Date/Time:	August 28, 2000
Analyzed by:	BVT, AJW
Date/Time:	December 5, 2000
Gross weight:	6899.4 g
Tare weight:	275.6 g
Net weight:	6623.8 g
Gravel weight:	5217.0 g
Sand weight:	1393.6 g
Portion analyzed:	6623.8 g
Remarks:	Sediments collected during trenching of the Big Lost River. Poorly sorted sand to pebble-size sediment.

Sieve Size (mm)	Weight (g)	Percent Finer	Cumulative Percent Finer	Size Class	Remarks
				Boulders	
8192					
4096					
2048					
1024					
512					
256					No. of Particles
64	0.0	0.00	100.00	Cobble	0
32	2853.0	43.08	56.92	Pebble	25
16	1592.8	24.05	32.87		82
8	554.9	8.38	24.49		194
4	216.3	3.27	21.22		>100
2	165.7	2.50	18.72	Very coarse sand	
1	125.0	1.89	16.83	Granule	
0.5	346.6	5.23	11.60	Coarse sand	
0.25	644.5	9.73	1.87	Medium sand	
0.125	95.5	1.44	0.43	Fine sand	
0.0625	16.3	0.25	0.18	Very fine sand	
<0.0625	11.9	0.18	0.00	Silt & clays	
TOTAL	6622.5				

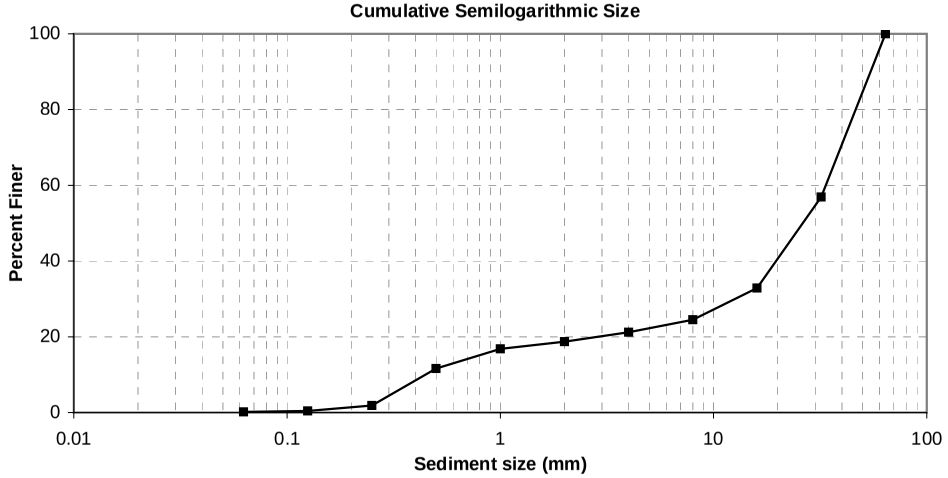

Particle Characteristics			
d_{90}	=	54.5	mm
$d_{84.1}$	=	49.6	mm
d_{65}	=	36.4	mm
d_{50}	=	26.2	mm
d_{35}	=	17.0	mm
$d_{15.9}$	=	0.88	mm
d_g	=	6.61	mm
σ_g	=	7.51	mm
G	=	2.81	

SIEVE ANALYSIS

Sample ID:	T-1-C5
Location:	BLR Sediments
Date/Time:	August 28, 2000
Analyzed by:	BVT, AJW
Date/Time:	December 5, 2000
Gross weight:	6158.4 g
Tare weight:	275.2 g
Net weight:	5883.2 g
Gravel weight:	4848.7 g
Sand weight:	1018.4 g
Portion analyzed:	5883.2 g
Remarks:	Sediments collected during trenching of the Big Lost River. Poorly sorted sand to cobble-size sediment.

Sieve Size (mm)	Weight (g)	Percent Finer	Cumulative Percent Finer	Size Class	Remarks
8192					
4096				Boulders	
2048					
1024					
512					No. of Particles
256	0.0	0.00	100.00		0
64	538.7	9.16	90.84	Cobble	1
32	2828.4	48.10	42.74		24
16	791.4	13.46	29.29	Pebble	42
8	389.5	6.62	22.66		166
4	300.7	5.11	17.55		>100
2	290.5	4.94	12.61	Very coarse sand	
1	328.3	5.58	7.03	Granule	
0.5	211.8	3.60	3.42	Coarse sand	
0.25	122.5	2.08	1.34	Medium sand	
0.125	50.5	0.86	0.48	Fine sand	
0.0625	14.8	0.25	0.23	Very fine sand	
<0.0625	13.6	0.23	0.00	Silt & clays	
TOTAL	5880.7				

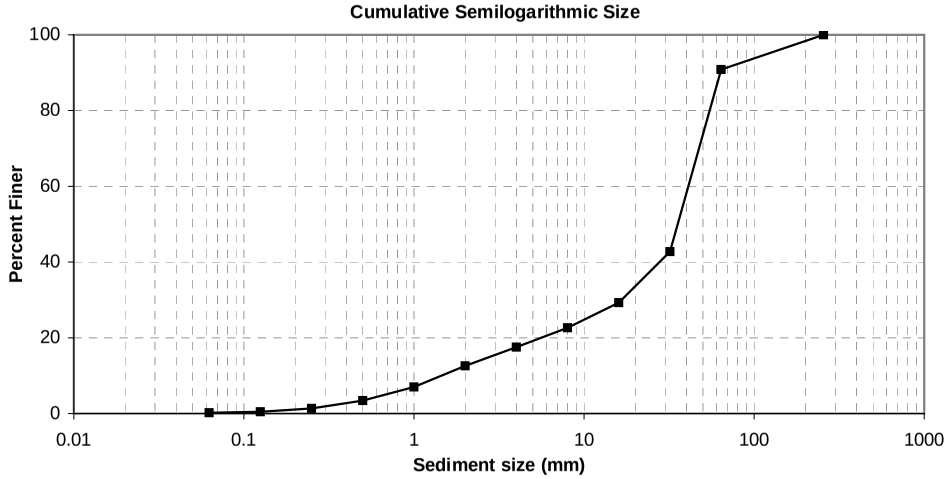

Particle Characteristics			
d_{90}	=	63.2	mm
$d_{84.1}$	=	58.1	mm
d_{65}	=	44.1	mm
d_{50}	=	35.5	mm
d_{35}	=	21.5	mm
$d_{15.9}$	=	3.17	mm
d_g	=	13.6	mm
σ_g	=	4.28	mm
G	=	1.79	

SIEVE ANALYSIS

Sample ID:	T-1-C6
Location:	BLR Sediments
Date/Time:	August 28, 2000
Analyzed by:	BVT, AJW
Date/Time:	December 5, 2000
Gross weight:	8641.8 g
Tare weight:	275.3 g
Net weight:	8366.5 g
Gravel weight:	6324.0 g
Sand weight:	2017.4 g
Portion analyzed:	8366.5 g
Remarks:	Sediments collected during trenching of the Big Lost River. Poorly sorted sand to pebble-size sediment.

Sieve Size (mm)	Weight (g)	Percent Finer	Cumulative Percent Finer	Size Class	Remarks
				Boulders	
8192					
4096					
2048					
1024					
512					
256					No. of Particles
64	0.0	0.00	100.00	Cobble	0
32	2696.9	32.25	67.75	Pebble	24
16	1348.0	16.12	51.63		105
8	1578.9	18.88	32.74		>100
4	700.2	8.37	24.37		
2	316.4	3.78	20.59	Very coarse sand	
1	173.7	2.08	18.51	Granule	
0.5	580.7	6.94	11.56	Coarse sand	
0.25	698.6	8.35	3.21	Medium sand	
0.125	200.9	2.40	0.81	Fine sand	
0.0625	47.1	0.56	0.24	Very fine sand	
<0.0625	20.4	0.24	0.00	Silt & clays	
TOTAL	8361.8				

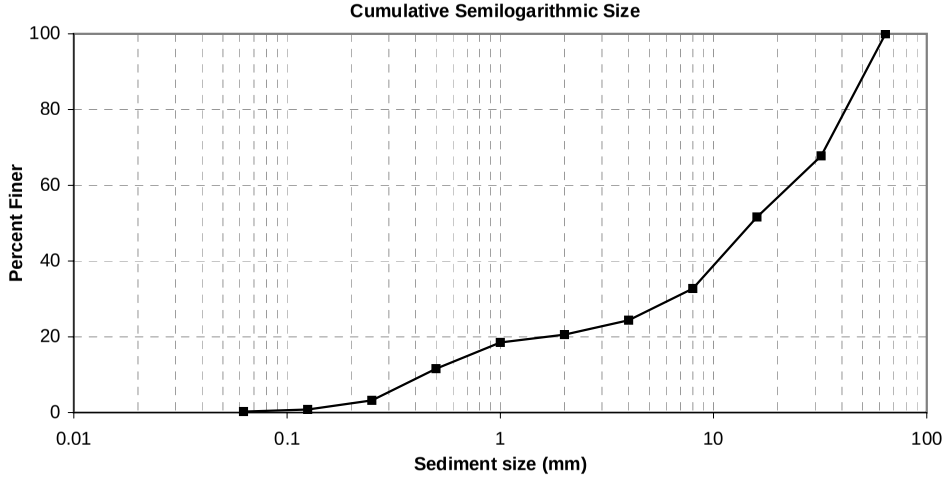

Particle Characteristics			
d_{90}	=	51.6	mm
$d_{84.1}$	=	45.5	mm
d_{65}	=	28.4	mm
d_{50}	=	15.1	mm
d_{35}	=	8.69	mm
$d_{15.9}$	=	0.77	mm
d_g	=	5.92	mm
σ_g	=	7.69	mm
G	=	2.38	

SIEVE ANALYSIS

Sample ID:	T-1-C7	
Location:	BLR Sediments	
Date/Time:	August 28, 2000	
Analyzed by:	BVT, AJW	
Date/Time:	December 5, 2000	
Gross weight:	1470.9	g
Tare weight:	122.8	g
Net weight:	1348.1	g
Gravel weight:	0.2	g
Sand weight:	1295.9	g
Portion analyzed:	1348.1	g
Remarks:	Sediments collected during trenching of the Big Lost River. Well-sorted medium sand.	

Sieve Size (mm)	Weight (g)	Percent Finer	Cumulative Percent Finer	Size Class	Remarks
8192					
4096				Boulders	
2048					
1024					
512					
256					
64				Cobble	
32					
16				Pebble	No. of Particles
8	0.0	0.00	100.00		0
4	0.2	0.01	99.99		4; 100% consol. sediment
2	2.9	0.22	99.77	Very coarse sand	90; 85% consol. sed. & org.
1	15.5	1.15	98.62	Granule	>100; 90% consol. sed. & org.
0.5	59.9	4.44	94.18	Coarse sand	90% consol. sed. & org.
0.25	458.8	34.03	60.14	Medium sand	Organics present
0.125	593.8	44.05	16.10	Fine sand	
0.0625	165.0	12.24	3.86	Very fine sand	
<0.0625	52.0	3.86	0.00	Silt & clays	
TOTAL	1348.1				

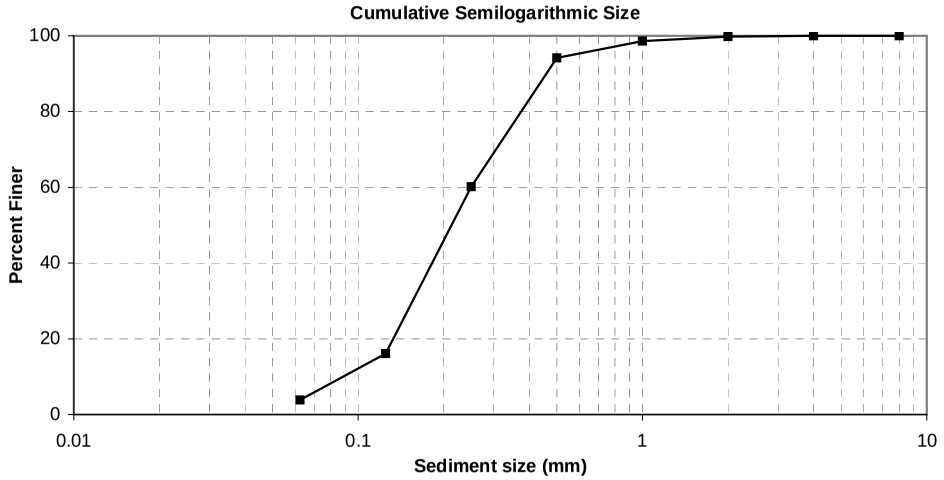

Particle Characteristics			
d_{90}	=	0.46	mm
$d_{84.1}$	=	0.41	mm
d_{65}	=	0.28	mm
d_{50}	=	0.21	mm
d_{35}	=	0.17	mm
$d_{15.9}$	=	0.12	mm
d_g	=	0.22	mm
σ_g	=	1.85	mm
G	=	0.96	

SIEVE ANALYSIS

Sample ID:	T-1-C8
Location:	BLR Sediments
Date/Time:	August 28, 2000
Analyzed by:	BVT, AJW
Date/Time:	December 5, 2000
Gross weight:	9426.6 g
Tare weight:	275.9 g
Net weight:	9150.7 g
Gravel weight:	6715.4 g
Sand weight:	2423.5 g
Portion analyzed:	9150.7 g
Remarks:	Sediments collected during trenching of the Big Lost River.
	Coarse sand, gravel, and cobble. Poorly sorted. Located near bottom of trench.

Sieve Size (mm)	Weight (g)	Percent Finer	Cumulative Percent Finer	Size Class	Remarks
8192					
4096				**Boulders**	
2048					
1024					
512					No. of Particles
256	0.0	0.00	100.00		0
64	434.7	4.75	95.25	**Cobble**	1
32	3966.2	43.37	51.88		34
16	682.6	7.46	44.41	**Pebble**	50
8	998.5	10.92	33.49		>100
4	633.4	6.93	26.57		
2	466.2	5.10	21.47	**Very coarse sand**	
1	375.2	4.10	17.37	**Granule**	
0.5	757.5	8.28	9.08	**Coarse sand**	
0.25	710.7	7.77	1.31	**Medium sand**	
0.125	99.8	1.09	0.22	**Fine sand**	
0.0625	14.1	0.15	0.07	**Very fine sand**	
<0.0625	6.0	0.07	0.00	**Silt & clays**	
TOTAL	9144.9				

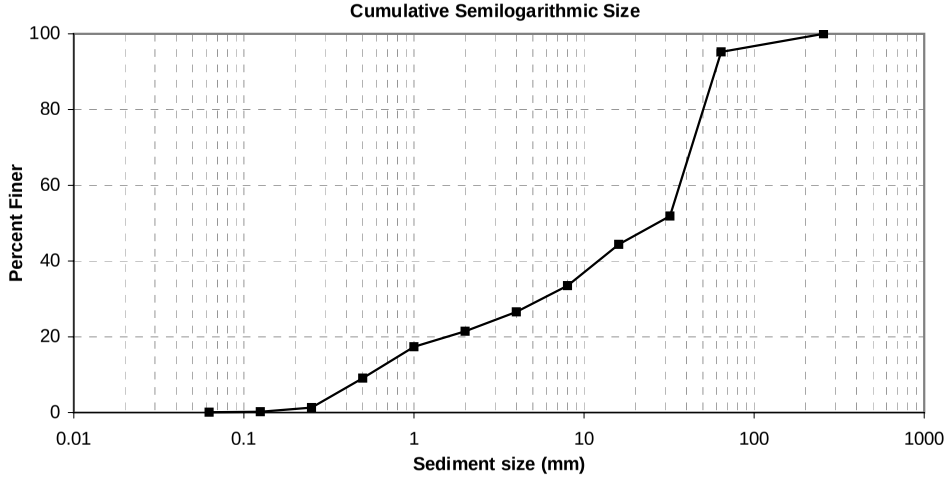

Particle Characteristics			
d_{90}	=	58.9	mm
$d_{84.1}$	=	53.6	mm
d_{65}	=	39.5	mm
d_{50}	=	26.9	mm
d_{35}	=	8.8	mm
$d_{15.9}$	=	0.88	mm
d_g	=	6.87	mm
σ_g	=	7.80	mm
G	=	2.85	

SIEVE ANALYSIS

Sample ID:	T-1-D1
Location:	BLR Channel
Date/Time:	August 28, 2000
Analyzed by:	BVT, AJW
Date/Time:	November 27, 2000
Gross weight:	5164.5 g
Tare weight:	110.8 g
Net weight:	5053.7 g
Gravel weight:	3473.7 g
Sand weight:	1557.1 g
Portion analyzed:	5053.7 g
Remarks:	Sediments collected during trenching of the Big Lost River. Poorly sorted sand to pebble-size sediment.

Sieve Size (mm)	Weight (g)	Percent Finer	Cumulative Percent Finer	Size Class	Remarks
8192					
4096				**Boulders**	
2048					
1024					
512					
256					No. of Particles
64	0.0	0.00	100.00	**Cobble**	0
32	1488.2	29.45	70.55		14
16	729.6	14.44	56.12	**Pebble**	46
8	760.5	15.05	41.07		>100
4	495.4	9.80	31.26		
2	475.4	9.41	21.86	**Very coarse sand**	
1	444.9	8.80	13.05	**Granule**	
0.5	305.0	6.04	7.02	**Coarse sand**	
0.25	183.5	3.63	3.39	**Medium sand**	
0.125	110.1	2.18	1.21	**Fine sand**	
0.0625	38.2	0.76	0.45	**Very fine sand**	
<0.0625	22.9	0.45	0.00	**Silt & clays**	
TOTAL	5053.7				

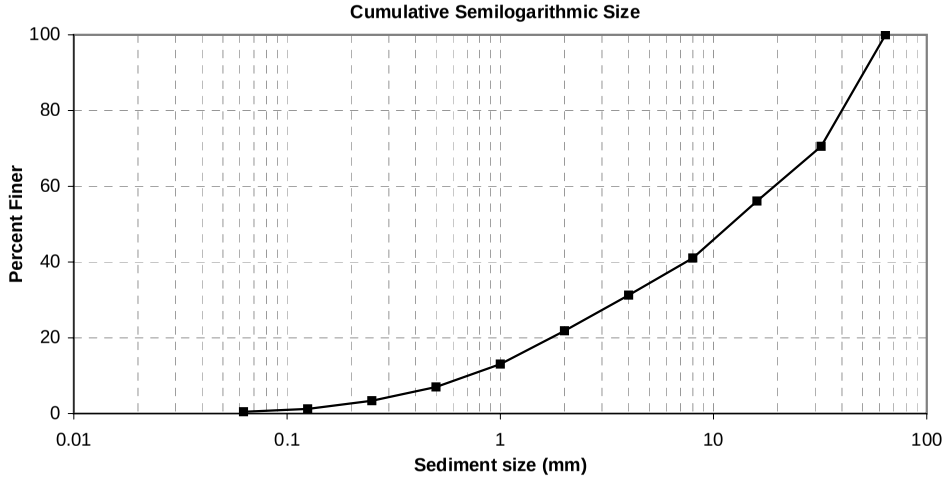

Particle Characteristics			
d_{90}	=	50.6	mm
$d_{84.1}$	=	44.0	mm
d_{65}	=	24.5	mm
d_{50}	=	12.1	mm
d_{35}	=	5.21	mm
$d_{15.9}$	=	1.25	mm
d_g	=	7.42	mm
σ_g	=	5.93	mm
G	=	1.82	

SIEVE ANALYSIS

Sample ID:	T-1-D2
Location:	BLR Channel
Date/Time:	August 28, 2000
Analyzed by:	BVT, AJW
Date/Time:	November 27, 2000
Gross weight:	3830.4 g
Tare weight:	110.8 g
Net weight:	3719.6 g
Gravel weight:	5.2 g
Sand weight:	3711.5 g
Portion analyzed:	3719.6 g
Remarks:	Sediments collected during trenching of the Big Lost River. Sieving required two runs in shaker. Bedded coarse sand and granule-size sediment.

Sieve Size (mm)	Weight (g)	Percent Finer	Cumulative Percent Finer	Size Class	Remarks
				Boulders	
8192					
4096					
2048					
1024					
512					
256					
64				Cobble	
32				Pebble	No. of Particles
16	0.0	0.00	100.00		0
8	2.9	0.08	99.92		1
4	2.3	0.06	99.86		16
2	8.7	0.23	99.63	Very coarse sand	>100
1	51.1	1.37	98.25	Granule	
0.5	2028.3	54.53	43.72	Coarse sand	
0.25	1372.0	36.89	6.84	Medium sand	
0.125	231.4	6.22	0.62	Fine sand	
0.0625	20.0	0.54	0.08	Very fine sand	
<0.0625	2.9	0.08	0.00	Silt & clays	
TOTAL	3719.6				

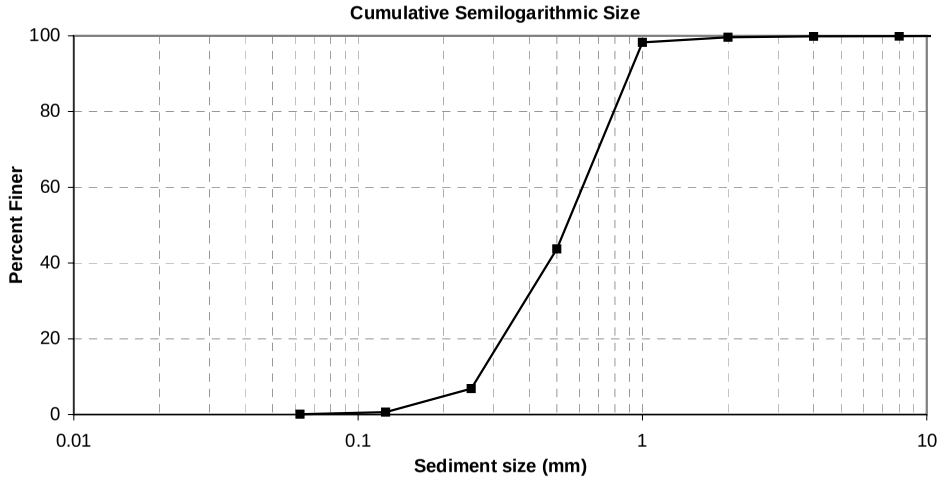

Particle Characteristics			
d_{90}	=	0.90	mm
$d_{84.1}$	=	0.84	mm
d_{65}	=	0.66	mm
d_{50}	=	0.54	mm
d_{35}	=	0.42	mm
$d_{15.9}$	=	0.30	mm
d_g	=	0.50	mm
σ_g	=	1.67	mm
G	=	0.92	

SIEVE ANALYSIS

Sample ID:	T-1-D3
Location:	BLR Channel
Date/Time:	August 28, 2000
Analyzed by:	BVT, AJW
Date/Time:	November 27, 2000
Gross weight:	5546.0 g
Tare weight:	110.8 g
Net weight:	5435.2 g
Gravel weight:	2027.0 g
Sand weight:	1088.1 g
Portion analyzed:	3128.0 g
Remarks:	Sediments collected during trenching of the Big Lost River. Well-sorted pebble layer.

Sieve Size (mm)	Weight (g)	Percent Finer	Cumulative Percent Finer	Size Class	Remarks
				Boulders	
8192					
4096					
2048					
1024					
512					
256					
64				Cobble	No. of Particles
32	0.0	0.00	100.00	Pebble	0
16	209.0	6.68	93.32		15
8	986.5	31.54	61.78		>100
4	831.5	26.58	35.20		
2	444.0	14.19	21.00	Very coarse sand	
1	166.8	5.33	15.67	Granule	
0.5	155.0	4.96	10.72	Coarse sand	
0.25	191.9	6.13	4.58	Medium sand	
0.125	102.6	3.28	1.30	Fine sand	
0.0625	27.8	0.89	0.41	Very fine sand	
<0.0625	12.9	0.41	0.00	Silt & clays	
TOTAL	3128.0				

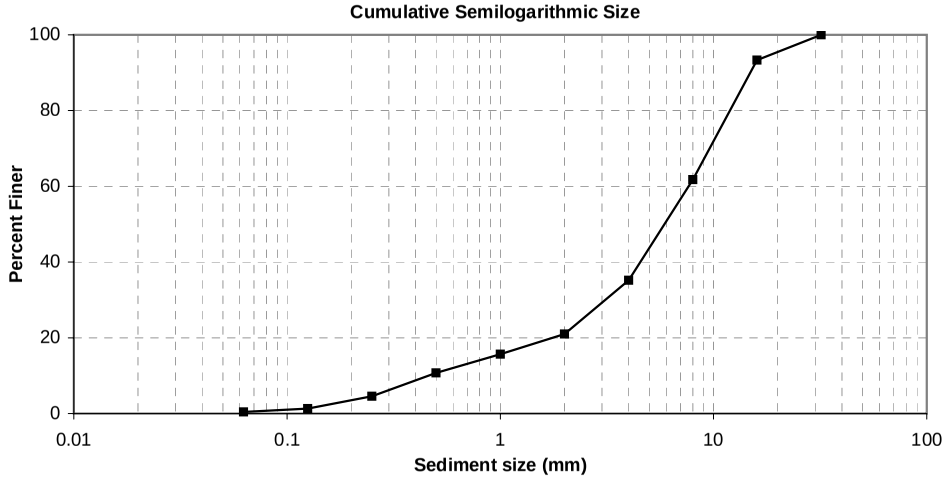

Particle Characteristics			
d_{90}	=	14.9	mm
$d_{84.1}$	=	13.1	mm
d_{65}	=	8.59	mm
d_{50}	=	5.88	mm
d_{35}	=	3.96	mm
$d_{15.9}$	=	1.03	mm
d_g	=	3.67	mm
σ_g	=	3.57	mm
G	=	1.41	

SIEVE ANALYSIS

Sample ID:	T-1-D4
Location:	BLR Channel
Date/Time:	August 28, 2000
Analyzed by:	BVT, AJW
Date/Time:	November 27, 2000
Gross weight:	5844.8 g
Tare weight:	110.8 g
Net weight:	5734.0 g
Gravel weight:	3904.4 g
Sand weight:	1796.2 g
Portion analyzed:	5734.0 g
Remarks:	Sediments collected during trenching of the Big Lost River.
	Poorly sorted sand to pebble-size sediment.

Sieve Size (mm)	Weight (g)	Percent Finer	Cumulative Percent Finer	Size Class	Remarks
8192					
4096				Boulders	
2048					
1024					
512					
256					No. of Particles
64	0.0	0.00	100.00	Cobble	0
32	1188.6	20.73	79.27		12
16	1345.9	23.47	55.80	Pebble	91
8	933.2	16.27	39.52		>100
4	436.7	7.62	31.91		>100
2	244.0	4.26	27.65	Very coarse sand	
1	342.3	5.97	21.68	Granule	
0.5	643.2	11.22	10.47	Coarse sand	
0.25	346.1	6.04	4.43	Medium sand	
0.125	158.4	2.76	1.67	Fine sand	
0.0625	62.2	1.08	0.58	Very fine sand	
<0.0625	33.4	0.58	0.00	Silt & clays	
TOTAL	5734.0				

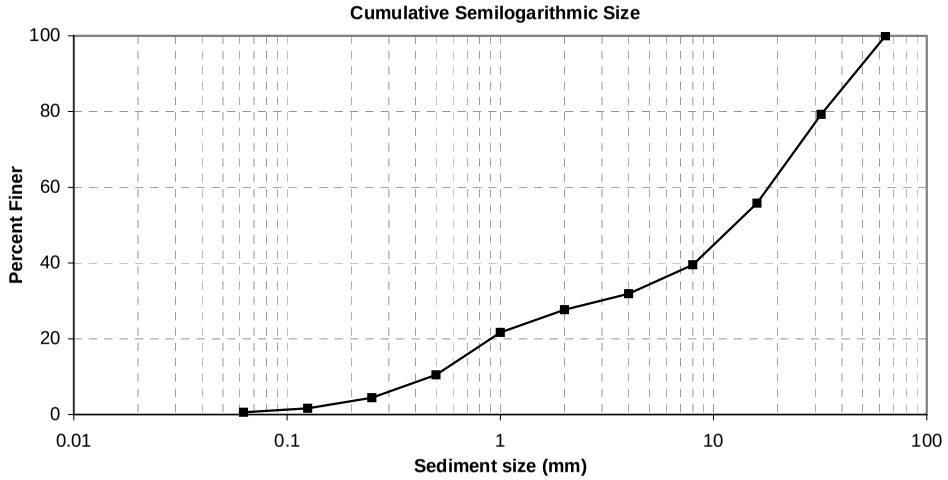

Particle Characteristics			
d_{90}	=	45.8	mm
$d_{84.1}$	=	37.6	mm
d_{65}	=	21.0	mm
d_{50}	=	12.5	mm
d_{35}	=	5.30	mm
$d_{15.9}$	=	0.70	mm
d_g	=	5.13	mm
σ_g	=	7.33	mm
G	=	2.28	

SIEVE ANALYSIS

Sample ID:	T-1-D5	
Location:	BLR Channel	
Date/Time:	August 28, 2000	
Analyzed by:	BVT, AJW	
Date/Time:	November 27, 2000	
Gross weight:	3388.2	g
Tare weight:	110.8	g
Net weight:	3277.4	g
Gravel weight:	0.6	g
Sand weight:	1748.0	g
Portion analyzed:	1753.0	g
Remarks:	Sediments collected during trenching of the Big Lost River. ~1/2 of sample analyzed, used splitter. Bedded coarse sand layer.	

Sieve Size (mm)	Weight (g)	Percent Finer	Cumulative Percent Finer	Size Class	Remarks
				Boulders	
8192					
4096					
2048					
1024					
512					
256					
64				Cobble	
32				Pebble	
16					No. of Particles
8	0.0	0.00	100.00		0
4	0.6	0.03	99.97		6
2	4.6	0.26	99.70	Very coarse sand	>100
1	45.5	2.60	97.11	Granule	
0.5	314.1	17.92	79.19	Coarse sand	
0.25	1142.3	65.16	14.03	Medium sand	
0.125	214.1	12.21	1.81	Fine sand	
0.0625	27.4	1.56	0.25	Very fine sand	
<0.0625	4.4	0.25	0.00	Silt & clays	
TOTAL	1753.0				

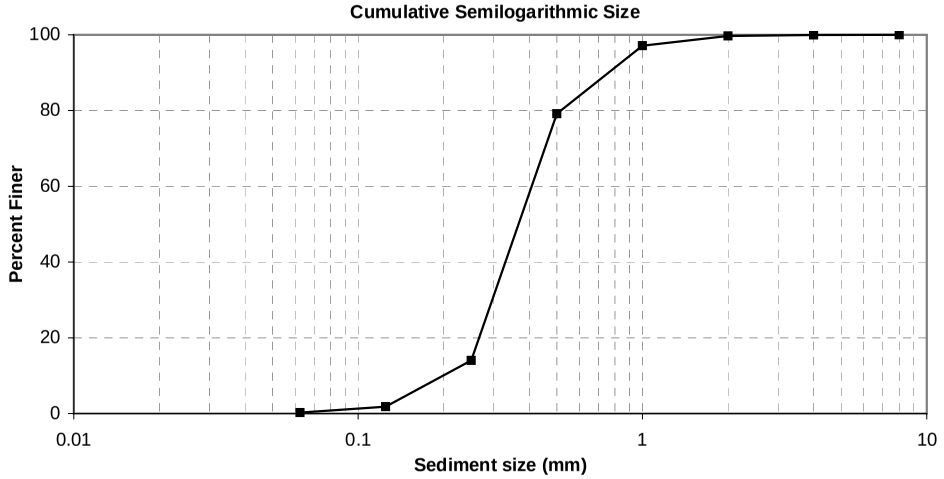

Particle Characteristics			
d_{90}	=	0.76	mm
$d_{84.1}$	=	0.60	mm
d_{65}	=	0.43	mm
d_{50}	=	0.37	mm
d_{35}	=	0.31	mm
$d_{15.9}$	=	0.26	mm
d_g	=	0.39	mm
σ_g	=	1.52	mm
G	=	0.87	

SIEVE ANALYSIS

Sample ID:	T-1-DCLAY2
Location:	BLR Channel
Date/Time:	August 28, 2000
Analyzed by:	BVT, AJW
Date/Time:	November 27, 2000
Gross weight:	464.7 g
Tare weight:	110.8 g
Net weight:	353.9 g
Gravel weight:	7.6 g
Sand weight:	98.5 g
Portion analyzed:	120.5 g
Remarks:	Sediments collected during trenching of Big Lost River. Poorly sorted sand to pebble-size sediment. Clay was described.

Sieve Size (mm)	Weight (g)	Percent Finer	Cumulative Percent Finer	Size Class	Remarks
8192					
4096				Boulders	
2048					
1024					
512					
256					
64				Cobble	
32					
16				Pebble	No. of Particles
8	0.0	0.00	100.00		0
4	7.6	6.31	93.69		36
2	12.1	10.04	83.65	Very coarse sand	>100
1	21.8	18.09	65.56	Granule	
0.5	20.3	16.85	48.71	Coarse sand	
0.25	18.8	15.60	33.11	Medium sand	
0.125	15.9	13.20	19.92	Fine sand	
0.0625	9.6	7.97	11.95	Very fine sand	
<0.0625	14.4	11.95	0.00	Silt & clays	
TOTAL	120.5				

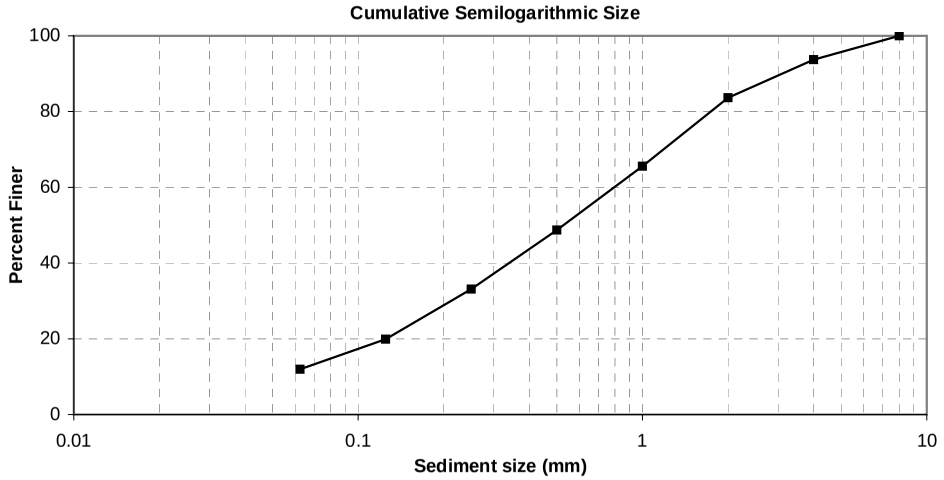

Particle Characteristics			
d_{90}	=	3.10	mm
$d_{84.1}$	=	2.06	mm
d_{65}	=	0.98	mm
d_{50}	=	0.53	mm
d_{35}	=	0.27	mm
$d_{15.9}$	=	0.09	mm
d_g	=	0.43	mm
σ_g	=	4.84	mm
G	=	1.57	

SIEVE ANALYSIS

Sample ID:	T-1-E1
Location:	Big Lost River (INEEL)
Date/Time:	August 29, 2000
Analyzed by:	BVT, AJW
Date/Time:	Decenber 19, 2000
Gross weight:	24767.8 g
Tare weight:	808.4 g
Net weight:	23959.4 g
Gravel weight:	3515.7 g
Sand weight:	1560.5 g
Portion analyzed:	5115.3 g
Remarks:	Sediments collected during trenching of the Big Lost River. ~1/4 of sample analyzed, used splitter. Poorly sorted sand to pebble-size sediment.

Sieve Size (mm)	Weight (g)	Percent Finer	Cumulative Percent Finer	Size Class	Remarks
				Boulders	
8192					
4096					
2048					
1024					
512					
256					No. of Particles
64	0.0	0.00	100.00	Cobble	0
32	974.8	19.06	80.94	Pebble	9
16	1086.1	21.24	59.70		70
8	883.7	17.28	42.42		>100
4	571.1	11.17	31.25		
2	406.6	7.95	23.30	Very coarse sand	20% consol. sediments
1	246.3	4.82	18.48	Granule	40% consol. sediments
0.5	207.3	4.05	14.42	Coarse sand	75% consol. sediments
0.25	398.4	7.79	6.63	Medium sand	
0.125	214.3	4.19	2.44	Fine sand	
0.0625	87.6	1.71	0.73	Very fine sand	
<0.0625	37.3	0.73	0.00	Silt & clays	
TOTAL	5113.5				

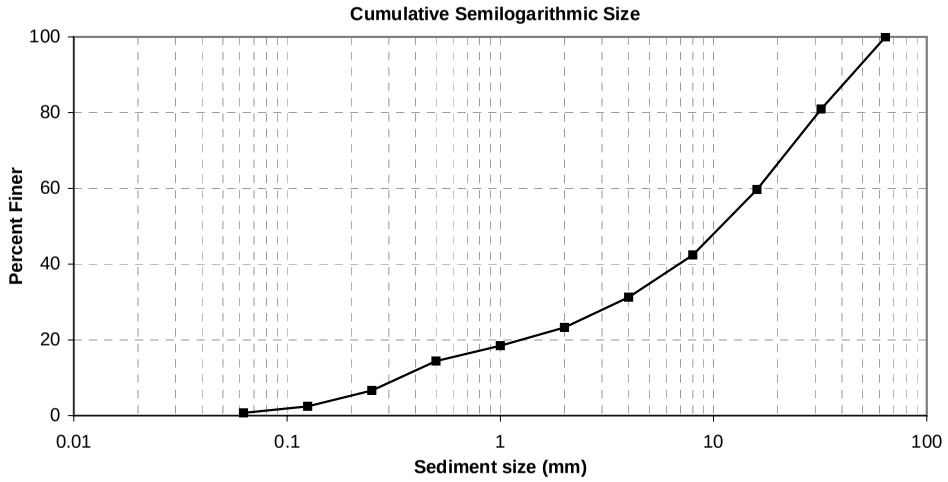

Particle Characteristics			
d_{90}	=	44.5	mm
$d_{84.1}$	=	35.9	mm
d_{65}	=	19.0	mm
d_{50}	=	10.8	mm
d_{35}	=	5.05	mm
$d_{15.9}$	=	0.64	mm
d_g	=	4.79	mm
σ_g	=	7.49	mm
G	=	2.25	

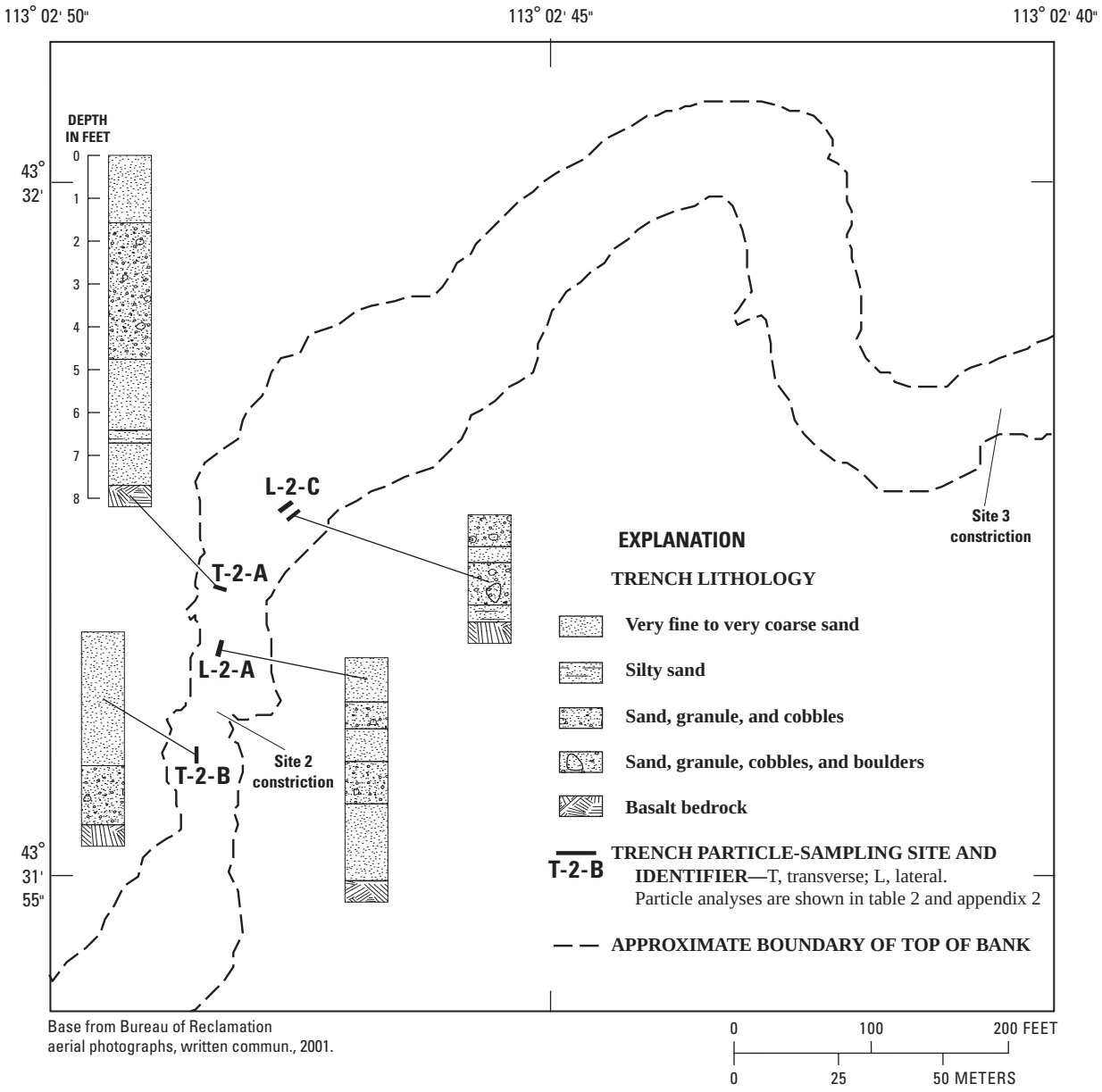

Figure 2–2. Lithology of selected trenches at site 2, Big Lost River upstream from Pioneer diversion structures, Idaho National Engineering and Environmental Laboratory, Idaho.

SIEVE ANALYSIS

Sample ID:	L-2-A1	
Location:	BLR Sediments	
Date/Time:	August 24, 2000	
Analyzed by:	BVT, AJW	
Date/Time:	November 27, 2000	
Gross weight:	2973.2	g
Tare weight:	110.8	g
Net weight:	2862.4	g
Gravel weight:	12.7	g
Sand weight:	1209.1	g
Portion analyzed:	1224.9	g
Remarks:	Sediments collected during trenching of the Big Lost River. Wood found in sample.	

Sieve Size (mm)	Weight (g)	Percent Finer	Cumulative Percent Finer	Size Class	Remarks
				Boulders	
8192					
4096					
2048					
1024					
512					
256					
64				Cobble	
32				Pebble	
16					No. of Particles
8	0.0	0.00	100.00		0
4	12.7	1.04	98.96		65; some wood--3 pieces
2	44.5	3.63	95.33	Very coarse sand	>100
1	87.4	7.14	88.19	Granule	
0.5	123.3	10.07	78.13	Coarse sand	
0.25	619.8	50.60	27.53	Medium sand	
0.125	310.4	25.34	2.19	Fine sand	
0.0625	23.7	1.93	0.25	Very fine sand	
<0.0625	3.1	0.25	0.00	Silt & clays	
TOTAL	1224.9				

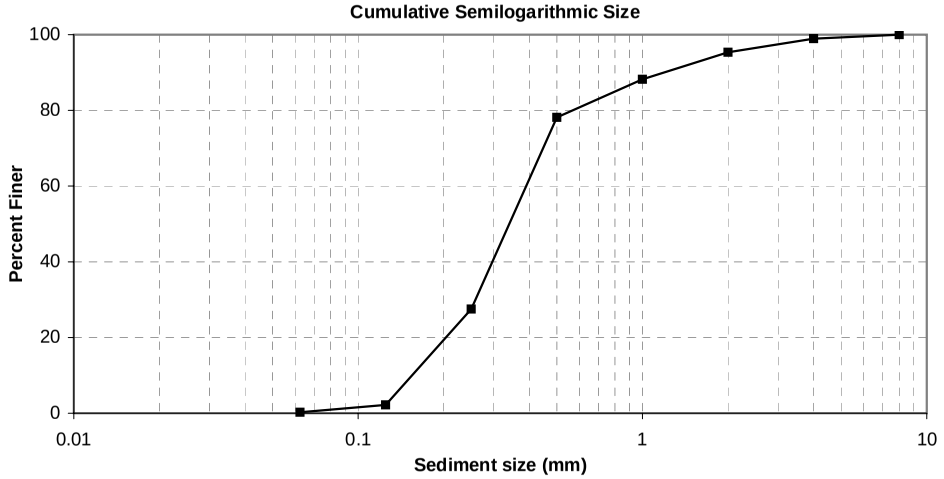

Particle Characteristics			
d_{90}	=	1.19	mm
$d_{84.1}$	=	0.75	mm
d_{65}	=	0.42	mm
d_{50}	=	0.34	mm
d_{35}	=	0.28	mm
$d_{15.9}$	=	0.18	mm
d_g	=	0.37	mm
σ_g	=	2.04	mm
G	=	1.01	

SIEVE ANALYSIS

Sample ID:	L-2-A2
Location:	BLR Sediments
Date/Time:	August 24, 2000
Analyzed by:	BVT, AJW
Date/Time:	November 27, 2000
Gross weight:	2604.3 g
Tare weight:	110.8 g
Net weight:	2493.5 g
Gravel weight:	408.3 g
Sand weight:	2083.9 g
Portion analyzed:	2493.5 g
Remarks:	Sediments collected during trenching of the Big Lost River. Moderately sorted, very coarse sand and pebble layer.

Sieve Size (mm)	Weight (g)	Percent Finer	Cumulative Percent Finer	Size Class	Remarks
8192					
4096				**Boulders**	
2048					
1024					
512					
256					
64				**Cobble**	
32					No. of Particles
16	0.0	0.00	100.00	**Pebble**	0
8	54.4	2.18	97.82		69
4	353.9	14.19	83.63		>100
2	814.2	32.65	50.97	**Very coarse sand**	
1	488.0	19.57	31.40	**Granule**	
0.5	282.2	11.32	20.08	**Coarse sand**	
0.25	305.9	12.27	7.82	**Medium sand**	
0.125	183.4	7.36	0.46	**Fine sand**	
0.0625	10.2	0.41	0.05	**Very fine sand**	
<0.0625	1.3	0.05	0.00	**Silt & clays**	
TOTAL	2493.5				

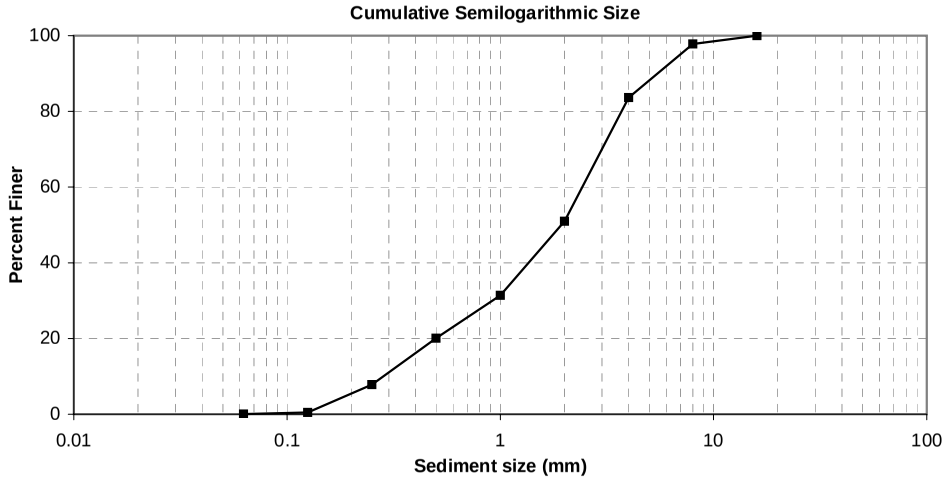

Particle Characteristics			
d_{90}	=	5.46	mm
$d_{84.1}$	=	4.09	mm
d_{65}	=	2.69	mm
d_{50}	=	1.93	mm
d_{35}	=	1.14	mm
$d_{15.9}$	=	0.39	mm
d_g	=	1.27	mm
σ_g		3.22	mm
G	=	1.32	

SIEVE ANALYSIS

Sample ID:	L-2-A3
Location:	BLR Sediments
Date/Time:	August 24, 2000
Analyzed by:	BVT, AJW
Date/Time:	November 27, 2000
Gross weight:	2426.2 g
Tare weight:	110.8 g
Net weight:	2315.4 g
Gravel weight:	18.7 g
Sand weight:	1350.4 g
Portion analyzed:	1369.9 g
Remarks:	Sediments collected during trenching of the Big Lost River. Wood fragments found during excavation; well-sorted granule layer.

Sieve Size (mm)	Weight (g)	Percent Finer	Cumulative Percent Finer	Size Class	Remarks
				Boulders	
8192					
4096					
2048					
1024					
512					
256					
64				Cobble	
32				Pebble	No. of Particles
16	0.0	0.00	100.00		0
8	5.0	0.36	99.64		3
4	13.7	1.00	98.63		79
2	39.8	2.91	95.73	Very coarse sand	>100
1	262.3	19.15	76.58	Granule	
0.5	850.9	62.11	14.47	Coarse sand	
0.25	153.6	11.21	3.26	Medium sand	
0.125	37.8	2.76	0.50	Fine sand	
0.0625	6.0	0.44	0.06	Very fine sand	
<0.0625	0.8	0.06	0.00	Silt & clays	
TOTAL	1369.9				

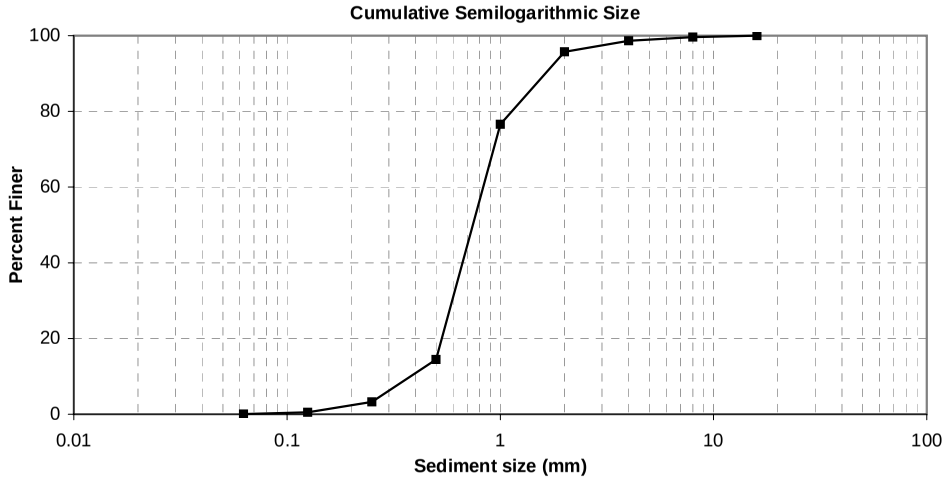

Particle Characteristics			
d_{90}	=	1.63	mm
$d_{84.1}$	=	1.31	mm
d_{65}	=	0.88	mm
d_{50}	=	0.74	mm
d_{35}	=	0.63	mm
$d_{15.9}$	=	0.51	mm
d_g	=	0.82	mm
σ_g	=	1.61	mm
G	=	0.90	

SIEVE ANALYSIS

Sample ID:	L-2-A4
Location:	BLR Sediments
Date/Time:	August 24, 2000
Analyzed by:	BVT, AJW
Date/Time:	November 27, 2000
Gross weight:	4979.9 g
Tare weight:	110.8 g
Net weight:	4869.1 g
Gravel weight:	746.9 g
Sand weight:	1964.9 g
Portion analyzed:	2737.0 g
Remarks:	Sediments collected during trenching of the Big Lost River. ~1/2 sample analyzed, used splitter. Poorly sorted sand to pebble-size sediment.

Sieve Size (mm)	Weight (g)	Percent Finer	Cumulative Percent Finer	Size Class	Remarks
				Boulders	
8192					
4096					
2048					
1024					
512					
256					
64				Cobble	No. of Particles
32	0.0	0.00	100.00	Pebble	0
16	148.5	5.46	94.54		13
8	288.4	10.60	83.94		143
4	310.0	11.39	72.55		>100
2	359.9	13.23	59.32	Very coarse sand	
1	292.7	10.76	48.56	Granule	
0.5	437.4	16.08	32.48	Coarse sand	
0.25	533.9	19.62	12.86	Medium sand	
0.125	300.0	11.03	1.83	Fine sand	
0.0625	41.0	1.51	0.33	Very fine sand	
<0.0625	8.9	0.33	0.00	Silt & clays	
TOTAL	2720.7				

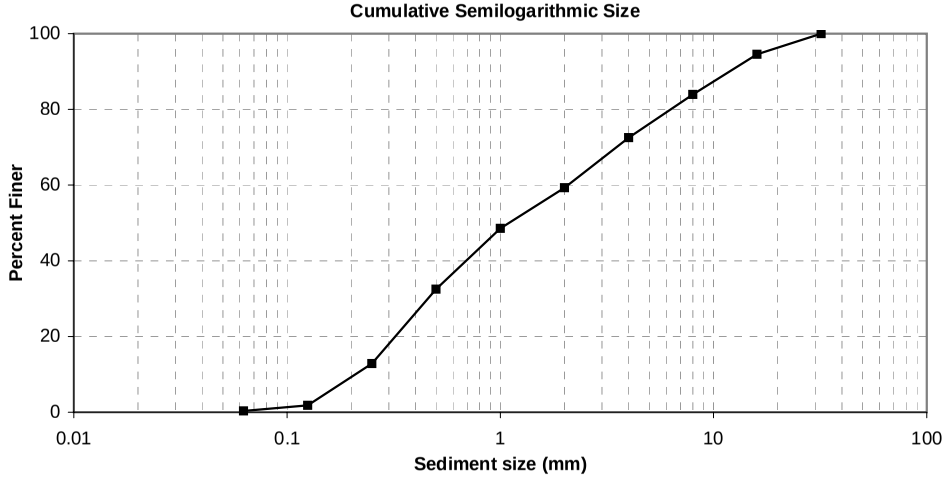

Particle Characteristics			
d_{90}	=	11.9	mm
$d_{84.1}$	=	8.08	mm
d_{65}	=	2.69	mm
d_{50}	=	1.10	mm
d_{35}	=	0.56	mm
$d_{15.9}$	=	0.28	mm
d_g	=	1.50	mm
σ_g		5.39	mm
G	=	1.68	

SIEVE ANALYSIS

Sample ID:	L-2-B1	
Location:	Big Lost River (INEEL)	
Date/Time:	August 25, 2000	
Analyzed by:	BVT, AJW	
Date/Time:	November 21, 2000	
Gross weight:	1747.6	g
Tare weight:	110.8	g
Net weight:	1636.8	g
Gravel weight:	10.0	g
Sand weight:	1596.1	g
Portion analyzed:	1636.8	g
Remarks:	Sediments collected during trenching of the Big Lost River.	
	Well-sorted coarse sand.	

Sieve Size (mm)	Weight (g)	Percent Finer	Cumulative Percent Finer	Size Class	Remarks
8192					
4096				Boulders	
2048					
1024					
512					
256					
64				Cobble	
32					
16				Pebble	No of particles
8	0.0	0.00	100.00		0
4	10.0	0.61	99.39		58
2	44.7	2.73	96.66	Very coarse sand	>100
1	71.3	4.36	92.30	Granule	
0.5	137.3	8.39	83.91	Coarse sand	
0.25	857.2	52.37	31.54	Medium sand	
0.125	399.8	24.43	7.12	Fine sand	
0.0625	85.8	5.24	1.88	Very fine sand	
<0.0625	30.7	1.88	0.00	Silt & clays	
TOTAL	1636.8				

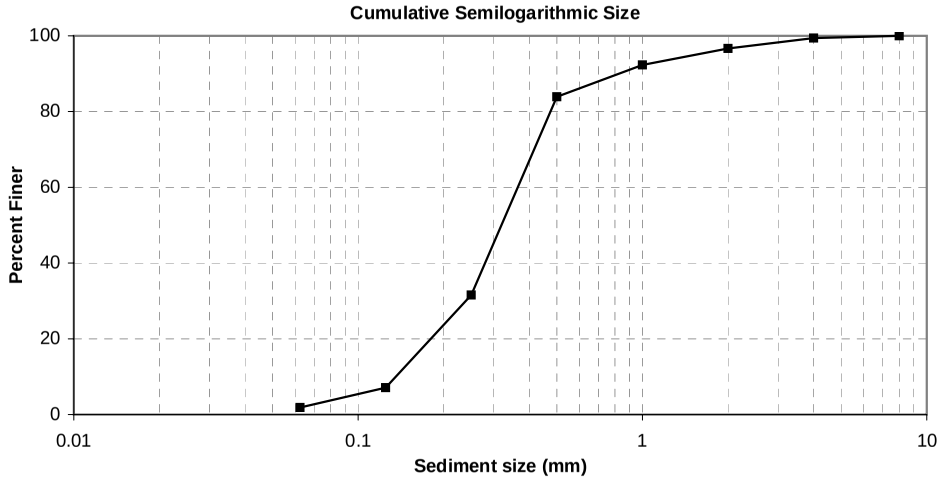

Particle Characteristics			
d_{90}	=	0.83	mm
$d_{84.1}$	=	0.51	mm
d_{65}	=	0.39	mm
d_{50}	=	0.32	mm
d_{35}	=	0.26	mm
$d_{15.9}$	=	0.16	mm
d_g	=	0.29	mm
σ_g		1.78	mm
G	=	0.95	

SIEVE ANALYSIS

Sample ID:	L-2-B2
Location:	Big Lost River (INEEL)
Date/Time:	August 25, 2000
Analyzed by:	BVT, AJW
Date/Time:	November 21, 2000
Gross weight:	3470.0 g
Tare weight:	110.8 g
Net weight:	3359.2 g
Gravel weight:	14.9 g
Sand weight:	3330.5 g
Portion analyzed:	3359.2 g
Remarks:	Sediments collected during trenching of the Big Lost River. Well-sorted coarse sand and granule layer.

Sieve Size (mm)	Weight (g)	Percent Finer	Cumulative Percent Finer	Size Class	Remarks
8192					
4096				**Boulders**	
2048					
1024					
512					
256					
64				**Cobble**	
32					
16				**Pebble**	No of particles
8	0.0	0.00	100.00		0
4	14.9	0.45	99.55		92
2	51.1	1.53	98.03	**Very coarse sand**	>100
1	102.3	3.06	94.97	**Granule**	
0.5	1571.7	46.96	48.02	**Coarse sand**	
0.25	1453.6	43.43	4.59	**Medium sand**	
0.125	143.1	4.28	0.31	**Fine sand**	
0.0625	8.7	0.26	0.05	**Very fine sand**	
<0.0625	1.8	0.05	0.00	**Silt & clays**	
TOTAL	3347.2				

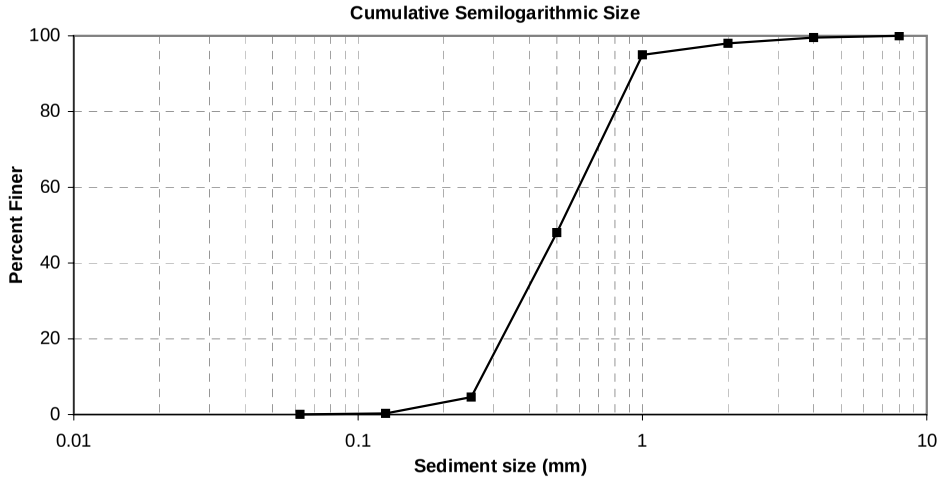

Particle Characteristics			
d_{90}	=	0.93	mm
$d_{84.1}$	=	0.85	mm
d_{65}	=	0.64	mm
d_{50}	=	0.51	mm
d_{35}	=	0.41	mm
$d_{15.9}$	=	0.30	mm
d_g	=	0.51	mm
σ_g		1.69	mm
G	=	0.92	

SIEVE ANALYSIS

Sample ID:	L-2-B3
Location:	Big Lost River (INEEL)
Date/Time:	August 24, 2000
Analyzed by:	BVT, AJW
Date/Time:	November 21, 2000
Gross weight:	4738.3 g
Tare weight:	110.8 g
Net weight:	4627.5 g
Gravel weight:	2353.0 g
Sand weight:	2266.1 g
Portion analyzed:	4627.5 g
Remarks:	Sediments collected during trenching of the Big Lost River. Poorly sorted sand to pebble-size sediment.

Sieve Size (mm)	Weight (g)	Percent Finer	Cumulative Percent Finer	Size Class	Remarks
				Boulders	
8192					
4096					
2048					
1024					
512					
256					No of particles
64	0.0	0.00	100.00	Cobble	0
32	546.6	11.81	88.19	Pebble	4
16	1037.3	22.42	65.77		63
8	329.5	7.12	58.65		188
4	439.6	9.50	49.15		>100
2	539.5	11.66	37.49	Very coarse sand	
1	583.3	12.61	24.88	Granule	
0.5	459.9	9.94	14.94	Coarse sand	
0.25	550.9	11.91	3.03	Medium sand	
0.125	113.3	2.45	0.59	Fine sand	
0.0625	19.2	0.41	0.17	Very fine sand	
<0.0625	7.9	0.17	0.00	Silt & clays	
TOTAL	4627.0				

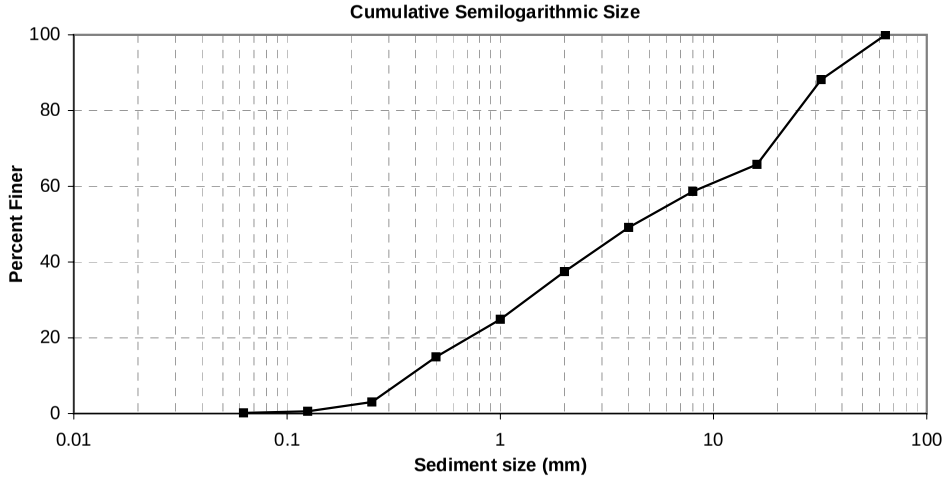

Particle Characteristics			
d_{90}	=	35.6	mm
$d_{84.1}$	=	28.2	mm
d_{65}	=	14.8	mm
d_{50}	=	4.26	mm
d_{35}	=	1.74	mm
$d_{15.9}$	=	0.53	mm
d_g	=	3.88	mm
σ_g		7.26	mm
G	=	1.91	

SIEVE ANALYSIS

Sample ID:	L-2-C1
Location:	BLR sediments
Date/Time:	August 24, 2000
Analyzed by:	BVT, AJW
Date/Time:	December 4, 2000
Gross weight:	7913.6 g
Tare weight:	275.9 g
Net weight:	7637.7 g
Gravel weight:	4858.4 g
Sand weight:	2756.7 g
Portion analyzed:	7637.7 g
Remarks:	Sediments collected during trenching of the Big Lost River. Poorly sorted sand to pebble-size sediment.

Sieve Size (mm)	Weight (g)	Percent Finer	Cumulative Percent Finer	Size Class	Remarks
8192					
4096				**Boulders**	
2048					
1024					
512					
256					No. of Particles
64	0.0	0.00	100.00	**Cobble**	0
32	206.9	2.71	97.29		3
16	747.4	9.79	87.50	**Pebble**	58
8	2490.2	32.62	54.88		>100
4	1413.9	18.52	36.37		
2	786.9	10.31	26.06	**Very coarse sand**	
1	506.4	6.63	19.43	**Granule**	
0.5	600.7	7.87	11.56	**Coarse sand**	
0.25	665.7	8.72	2.84	**Medium sand**	
0.125	157.9	2.07	0.77	**Fine sand**	
0.0625	39.1	0.51	0.26	**Very fine sand**	
<0.0625	19.8	0.26	0.00	**Silt & clays**	
TOTAL	7634.9				

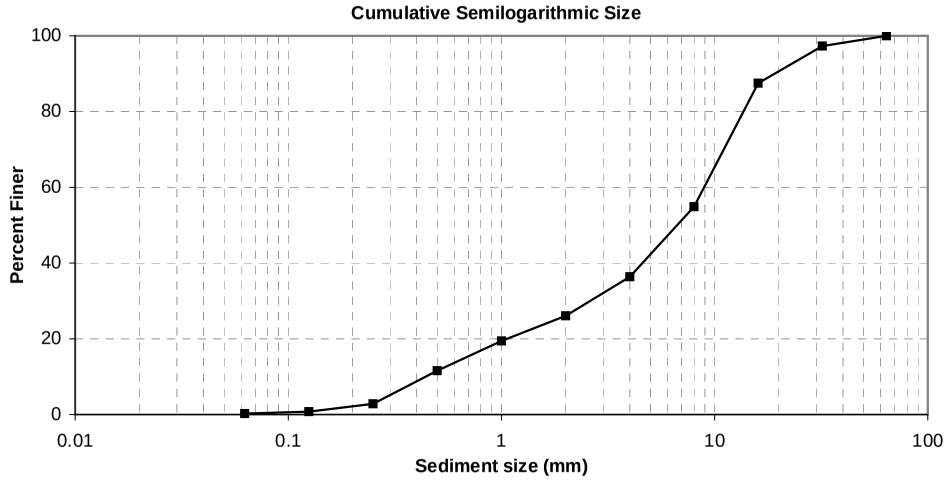

Particle Characteristics			
d_{90}	=	19.1	mm
$d_{84.1}$	=	14.9	mm
d_{65}	=	9.92	mm
d_{50}	=	6.66	mm
d_{35}	=	3.65	mm
$d_{15.9}$	=	0.73	mm
d_g	=	3.30	mm
σ_g		4.51	mm
G	=	1.68	

SIEVE ANALYSIS

Sample ID:	L-2-C2
Location:	BLR sediments
Date/Time:	August 24, 2000
Analyzed by:	BVT, AJW
Date/Time:	December 4, 2000
Gross weight:	3689.8 g
Tare weight:	113.6 g
Net weight:	3576.2 g
Gravel weight:	205.9 g
Sand weight:	3366.4 g
Portion analyzed:	3576.2 g
Remarks:	Sediments collected during trenching of the Big Lost River. Well-sorted granule layer.

Sieve Size (mm)	Weight (g)	Percent Finer	Cumulative Percent Finer	Size Class	Remarks
8192					
4096				**Boulders**	
2048					
1024					
512					
256					
64				**Cobble**	
32					
16				**Pebble**	No. of Particles
8	0.0	0.00	100.00		0
4	205.9	5.76	94.24		>100
2	249.8	6.99	87.25	**Very coarse sand**	
1	454.2	12.70	74.55	**Granule**	
0.5	1728.8	48.36	26.19	**Coarse sand**	
0.25	754.0	21.09	5.10	**Medium sand**	
0.125	165.7	4.63	0.47	**Fine sand**	
0.0625	13.9	0.39	0.08	**Very fine sand**	
<0.0625	2.9	0.08	0.00	**Silt & clays**	
TOTAL	3575.2				

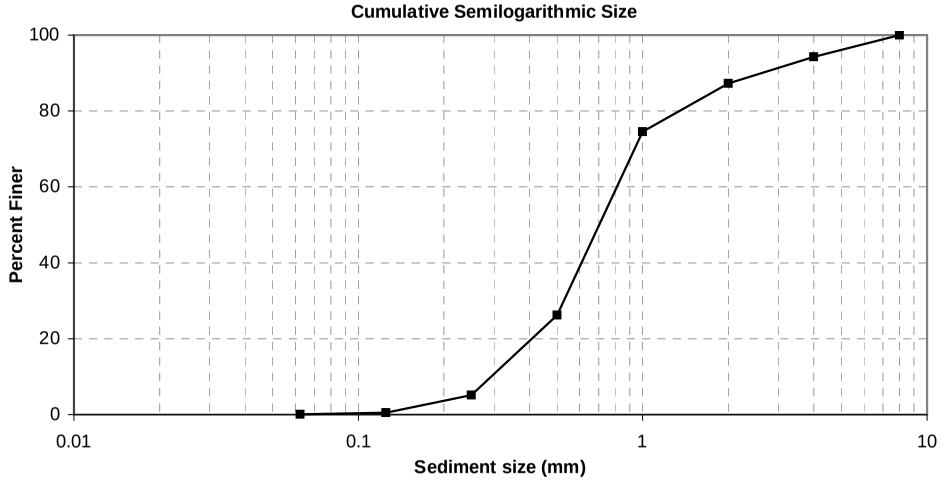

Particle Characteristics			
d_{90}	=	2.63	mm
$d_{84.1}$	=	1.68	mm
d_{65}	=	0.87	mm
d_{50}	=	0.70	mm
d_{35}	=	0.57	mm
$d_{15.9}$	=	0.36	mm
d_g	=	0.77	mm
σ_g		2.17	mm
G	=	1.04	

SIEVE ANALYSIS

Sample ID:	L-2-C4
Location:	BLR sediments
Date/Time:	August 24, 2000
Analyzed by:	BVT, AJW
Date/Time:	December 4, 2000
Gross weight:	1764.6 g
Tare weight:	122.8 g
Net weight:	1641.8 g
Gravel weight:	177.7 g
Sand weight:	545.8 g
Portion analyzed:	745.6 g
Remarks:	Sediments collected during trenching of the Big Lost River. Poor sample due to consolidated clay. Poorly sorted sand to pebble-size materials. Clay described in sample.

Sieve Size (mm)	Weight (g)	Percent Finer	Cumulative Percent Finer	Size Class	Remarks
8192					
4096				**Boulders**	
2048					
1024					
512					
256					
64				**Cobble**	
32					No. of Particles
16	0.0	0.00	100.00	**Pebble**	0
8	95.7	12.86	87.14		49; 60% consol. Clay
4	82.0	11.02	76.13		50% consol. clay
2	150.3	20.19	55.94	**Very coarse sand**	85% consol. clay
1	154.3	20.73	35.21	**Granule**	90% consol. clay
0.5	105.6	14.19	21.02	**Coarse sand**	90% consol. clay
0.25	74.0	9.94	11.08	**Medium sand**	
0.125	36.9	4.96	6.13	**Fine sand**	
0.0625	24.7	3.32	2.81	**Very fine sand**	
<0.0625	20.9	2.81	0.00	**Silt & clays**	
TOTAL	744.4				

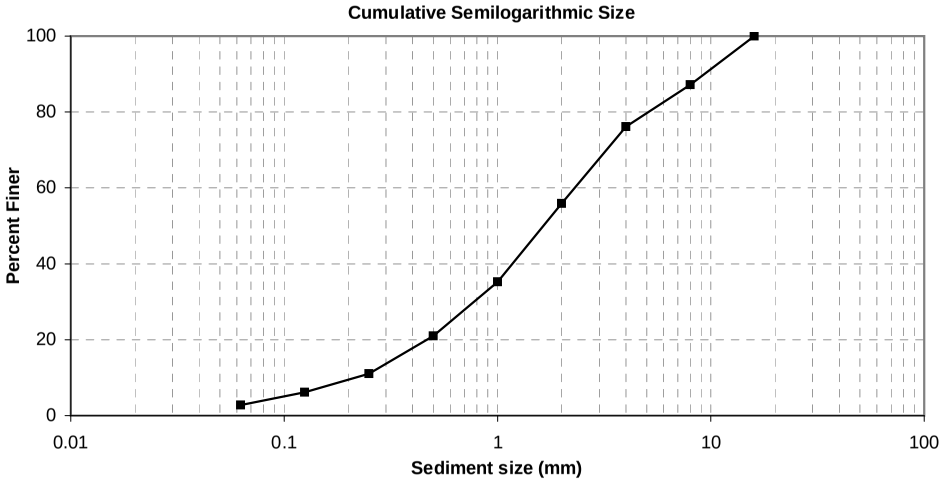

Particle Characteristics			
d_{90}	=	9.33	mm
$d_{84.1}$	=	6.61	mm
d_{65}	=	2.73	mm
d_{50}	=	1.64	mm
d_{35}	=	0.99	mm
$d_{15.9}$	=	0.35	mm
d_g	=	1.52	mm
σ_g		4.35	mm
G	=	1.48	

SIEVE ANALYSIS

Sample ID:	M-2-A1
Location:	Big Lost River (INEEL)
Date/Time:	August 29, 2000
Analyzed by:	BVT, AJW
Date/Time:	December 19, 2000
Gross weight:	26685.9 g
Tare weight:	808.4 g
Net weight:	25877.5 g
Gravel weight:	5274.9 g
Sand weight:	1413.9 g
Portion analyzed:	6724.8 g
Remarks:	Sediments collected during trenching of the Big Lost River. ~1/4 of sample analyzed, used splitter. Poorly sorted sand to cobble-size sediment.

Sieve Size (mm)	Weight (g)	Percent Finer	Cumulative Percent Finer	Size Class	Remarks
8192					
4096				Boulders	
2048					
1024					
512					No of Particles
256	0.0	0.00	100.00		0
64	504.3	7.50	92.50	Cobble	1
32	1277.1	19.00	73.50		14
16	1664.9	24.76	48.74	Pebble	104
8	1195.5	17.78	30.96		>100
4	633.1	9.42	21.54		
2	411.2	6.12	15.42	Very coarse sand	
1	291.2	4.33	11.09	Granule	
0.5	250.2	3.72	7.37	Coarse sand	
0.25	258.6	3.85	3.53	Medium sand	
0.125	153.5	2.28	1.24	Fine sand	
0.0625	49.2	0.73	0.51	Very fine sand	
<0.0625	34.3	0.51	0.00	Silt & clays	
TOTAL	6723.1				

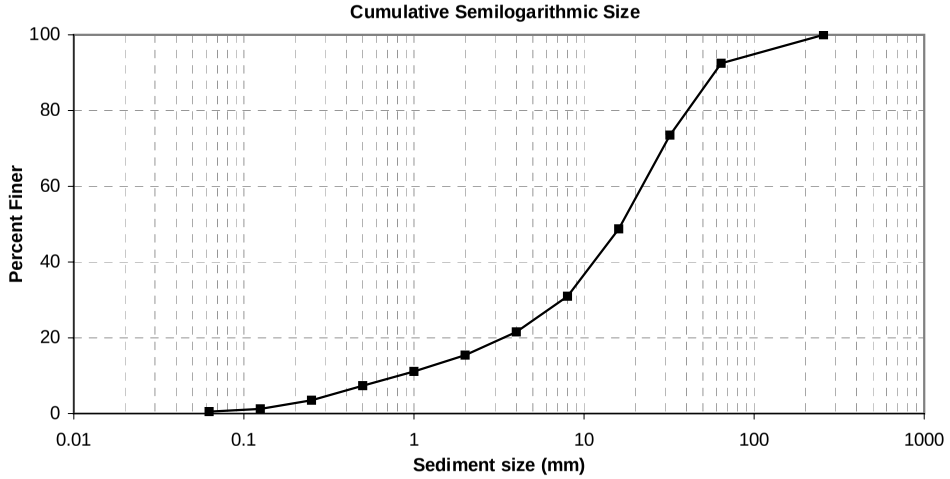

Particle Characteristics			
d_{90}	=	58.4	mm
$d_{84.1}$	=	47.1	mm
d_{65}	=	25.2	mm
d_{50}	=	16.6	mm
d_{35}	=	9.37	mm
$d_{15.9}$	=	2.11	mm
d_g	=	9.97	mm
σ_g		4.72	mm
G	=	1.64	

SIEVE ANALYSIS

Sample ID:	T-2-A1
Location:	Big Lost River (INEEL)
Date/Time:	August 24, 2000
Analyzed by:	BVT, AJW
Date/Time:	November 21, 2000
Gross weight:	2039.2 g
Tare weight:	110.8 g
Net weight:	1928.4 g
Gravel weight:	5.7 g
Sand weight:	1918.5 g
Portion analyzed:	1928.4 g
Remarks:	Sediments collected during trenching of the Big Lost River. Well-sorted coarse sand.

Sieve Size (mm)	Weight (g)	Percent Finer	Cumulative Percent Finer	Size Class	Remarks
8192					
4096				**Boulders**	
2048					
1024					
512					
256					
64				**Cobble**	
32					
16				**Pebble**	No of particles
8	0.0	0.00	100.00		0
4	5.7	0.30	99.70		31
2	26.2	1.36	98.35	**Very coarse sand**	>100
1	41.0	2.13	96.22	**Granule**	
0.5	81.2	4.21	92.01	**Coarse sand**	
0.25	1439.5	74.65	17.36	**Medium sand**	
0.125	286.3	14.85	2.52	**Fine sand**	
0.0625	44.3	2.30	0.22	**Very fine sand**	
<0.0625	4.2	0.22	0.00	**Silt & clays**	
TOTAL	1928.4				

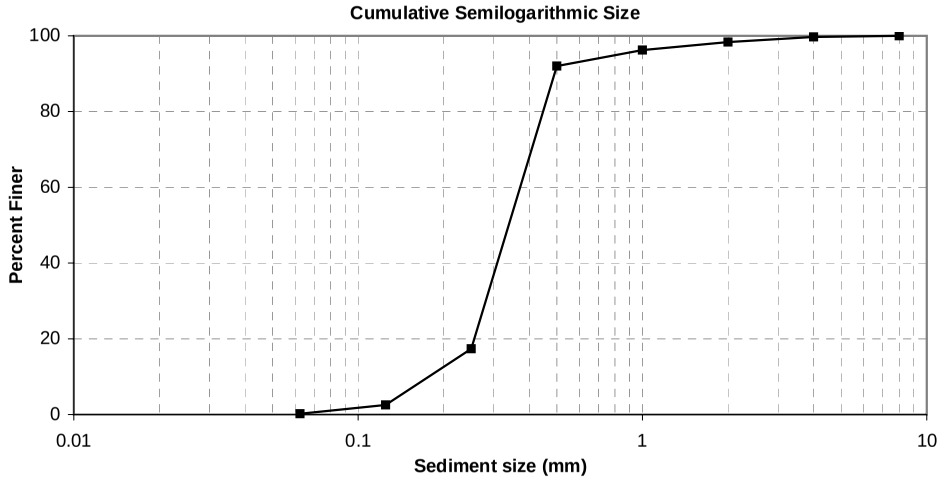

Particle Characteristics			
d_{90}	=	0.49	mm
$d_{84.1}$	=	0.46	mm
d_{65}	=	0.39	mm
d_{50}	=	0.34	mm
d_{35}	=	0.29	mm
$d_{15.9}$	=	0.23	mm
d_g	=	0.33	mm
σ_g		1.41	mm
G	=	0.84	

SIEVE ANALYSIS

Sample ID:	T-2-A2	
Location:	Big Lost River (INEEL)	
Date/Time:	August 24, 2000	
Analyzed by:	BVT, AJW	
Date/Time:	November 24, 2000	
Gross weight:	4058.2	g
Tare weight:	110.8	g
Net weight:	3947.4	g
Gravel weight:	19.3	g
Sand weight:	3921.3	g
Portion analyzed:	3947.4	g
Remarks:	Sediments collected during trenching of the Big Lost River.	
	Well-sorted coarse sand.	

Sieve Size (mm)	Weight (g)	Percent Finer	Cumulative Percent Finer	Size Class	Remarks
8192					
4096				Boulders	
2048					
1024					
512					
256					
64				Cobble	
32					
16				Pebble	No of particles
8	0.0	0.00	100.00		0
4	19.3	0.49	99.51		82
2	93.3	2.37	97.14	Very coarse sand	>100
1	265.7	6.74	90.40	Granule	
0.5	495.6	12.57	77.83	Coarse sand	
0.25	2876.9	72.97	4.86	Medium sand	
0.125	161.3	4.09	0.77	Fine sand	
0.0625	28.5	0.72	0.05	Very fine sand	
<0.0625	2.0	0.05	0.00	Silt & clays	
TOTAL	3942.6				

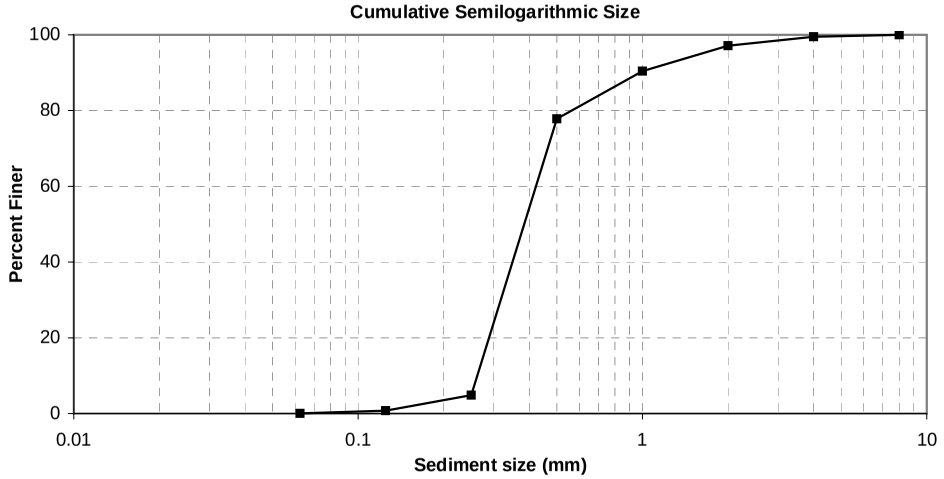

Particle Characteristics			
d_{90}	=	0.98	mm
$d_{84.1}$	=	0.71	mm
d_{65}	=	0.44	mm
d_{50}	=	0.38	mm
d_{35}	=	0.33	mm
$d_{15.9}$	=	0.28	mm
d_g	=	0.44	mm
σ_g		1.60	mm
G	=	0.90	

SIEVE ANALYSIS

Sample ID:	T-2-A3
Location:	Big Lost River (INEEL)
Date/Time:	August 24, 2000
Analyzed by:	BVT, AJW
Date/Time:	November 24, 2000
Gross weight:	4273.3 g
Tare weight:	110.8 g
Net weight:	4162.5 g
Gravel weight:	1590.9 g
Sand weight:	2561.8 g
Portion analyzed:	4162.5 g
Remarks:	Sediments collected during trenching of the Big Lost River. Poorly sorted sand to pebble-size sediment.

Sieve Size (mm)	Weight (g)	Percent Finer	Cumulative Percent Finer	Size Class	Remarks
				Boulders	
8192					
4096					
2048					
1024					
512					
256					No of particles
64	0.0	0.00	100.00	Cobble	0
32	249.1	5.99	94.01	Pebble	4
16	525.1	12.63	81.38		38
8	462.0	11.11	70.27		>100
4	354.7	8.53	61.74		
2	389.2	9.36	52.37	Very coarse sand	
1	570.8	13.73	38.64	Granule	
0.5	981.9	23.62	15.03	Coarse sand	
0.25	492.9	11.86	3.17	Medium sand	
0.125	109.6	2.64	0.54	Fine sand	
0.0625	17.4	0.42	0.12	Very fine sand	
<0.0625	4.9	0.12	0.00	Silt & clays	
TOTAL	4157.6				

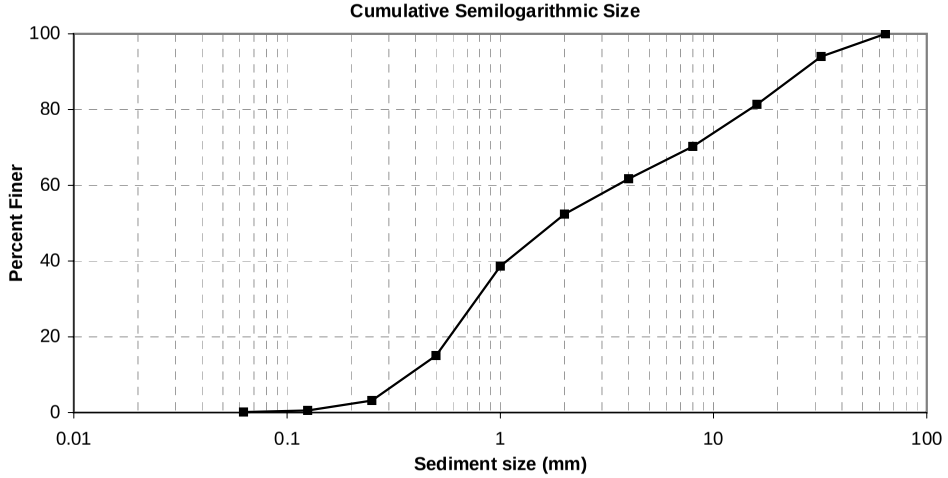

Particle Characteristics			
d_{90}	=	25.7	mm
$d_{84.1}$	=	18.6	mm
d_{65}	=	5.22	mm
d_{50}	=	1.77	mm
d_{35}	=	0.90	mm
$d_{15.9}$	=	0.51	mm
d_g	=	3.09	mm
σ_g		6.02	mm
G	=	1.87	

SIEVE ANALYSIS

Sample ID:	T-2-A4
Location:	Big Lost River (INEEL)
Date/Time:	August 25, 2000
Analyzed by:	BVT, AJW
Date/Time:	November 24, 2000
Gross weight:	8745.5 g
Tare weight:	275.5 g
Net weight:	8470.0 g
Gravel weight:	4433.8 g
Sand weight:	4025.1 g
Portion analyzed:	8470.0 g
Remarks:	Sediments collected during trenching of the Big Lost River. Moderately sorted granule and pebble sediment layer.

Sieve Size (mm)	Weight (g)	Percent Finer	Cumulative Percent Finer	Size Class	Remarks
8192					
4096				Boulders	
2048					
1024					
512					
256					No of particles
64	0.0	0.00	100.00	Cobble	0
32	1471.2	17.38	82.62		10
16	677.0	8.00	74.62	Pebble	48
8	1387.9	16.40	58.22		>100
4	897.7	10.61	47.62		
2	700.6	8.28	39.34	Very coarse sand	
1	751.8	8.88	30.46	Granule	
0.5	1608.1	19.00	11.46	Coarse sand	
0.25	786.1	9.29	2.17	Medium sand	
0.125	156.4	1.85	0.32	Fine sand	
0.0625	22.1	0.26	0.06	Very fine sand	
<0.0625	5.1	0.06	0.00	Silt & clays	
TOTAL	8464.0				

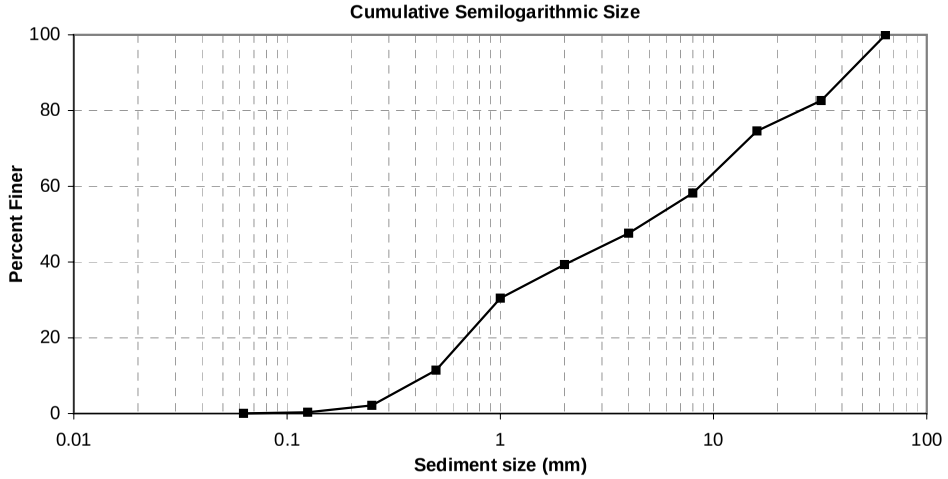

Particle Characteristics			
d_{90}	=	43.0	mm
$d_{84.1}$	=	33.9	mm
d_{65}	=	10.7	mm
d_{50}	=	4.67	mm
d_{35}	=	1.43	mm
$d_{15.9}$	=	0.59	mm
d_g	=	4.47	mm
σ_g		7.60	mm
G	=	1.95	

SIEVE ANALYSIS

Sample ID:	T-2-A5
Location:	Big Lost River (INEEL)
Date/Time:	August 25, 2000
Analyzed by:	BVT, AJW
Date/Time:	November 24, 2000
Gross weight:	1367.7 g
Tare weight:	110.8 g
Net weight:	1256.9 g
Gravel weight:	28.8 g
Sand weight:	1184.0 g
Portion analyzed:	1256.9 g
Remarks:	Sediments collected during trenching of the Big Lost River. Well-sorted coarse sand.

Sieve Size (mm)	Weight (g)	Percent Finer	Cumulative Percent Finer	Size Class	Remarks
				Boulders	
8192					
4096					
2048					
1024					
512					
256					
64				Cobble	
32				Pebble	No of particles
16	0.0	0.00	100.00		0
8	10.8	0.86	99.14		7
4	18.0	1.44	97.70		116
2	31.9	2.54	95.16	Very coarse sand	>100
1	72.3	5.77	89.39	Granule	
0.5	187.4	14.95	74.45	Coarse sand	
0.25	558.6	44.55	29.90	Medium sand	
0.125	250.9	20.01	9.89	Fine sand	
0.0625	82.9	6.61	3.28	Very fine sand	
<0.0625	41.1	3.28	0.00	Silt & clays	
TOTAL	1253.9				

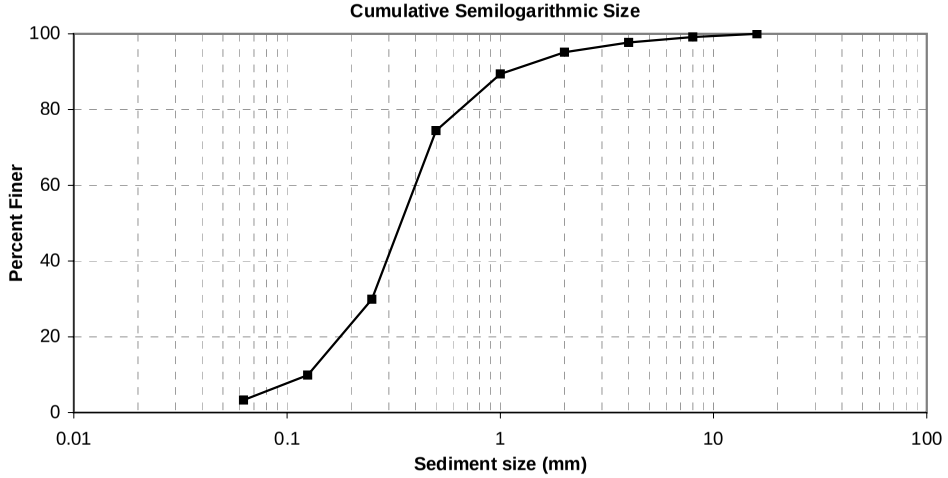

Particle Characteristics			
d_{90}	=	1.08	mm
$d_{84.1}$	=	0.78	mm
d_{65}	=	0.43	mm
d_{50}	=	0.34	mm
d_{35}	=	0.27	mm
$d_{15.9}$	=	0.15	mm
d_g	=	0.35	mm
σ_g		2.25	mm
G	=	1.06	

SIEVE ANALYSIS

Sample ID:	T-2-A6	
Location:	Big Lost River (INEEL)	
Date/Time:	August 25, 2000	
Analyzed by:	BVT, AJW	
Date/Time:	November 24, 2000	
Gross weight:	341.8	g
Tare weight:	110.8	g
Net weight:	231.0	g
Gravel weight:	0.0	g
Sand weight:	204.5	g
Portion analyzed:	231.0	g
Remarks:	Sediments collected during trenching of the Big Lost River. Well-sorted medium sand.	

Sieve Size (mm)	Weight (g)	Percent Finer	Cumulative Percent Finer	Size Class	Remarks
				Boulders	
8192					
4096					
2048					
1024					
512					
256					
64				Cobble	
32				Pebble	
16					
8					No of particles
4	0.0	0.00	100.00		0
2	1.9	0.83	99.17	Very coarse sand	99
1	5.7	2.48	96.69	Granule	>100
0.5	13.0	5.66	91.03	Coarse sand	
0.25	45.1	19.64	71.39	Medium sand	
0.125	86.3	37.59	33.80	Fine sand	
0.0625	52.5	22.87	10.93	Very fine sand	
<0.0625	25.1	10.93	0.00	Silt & clays	
TOTAL	229.6				

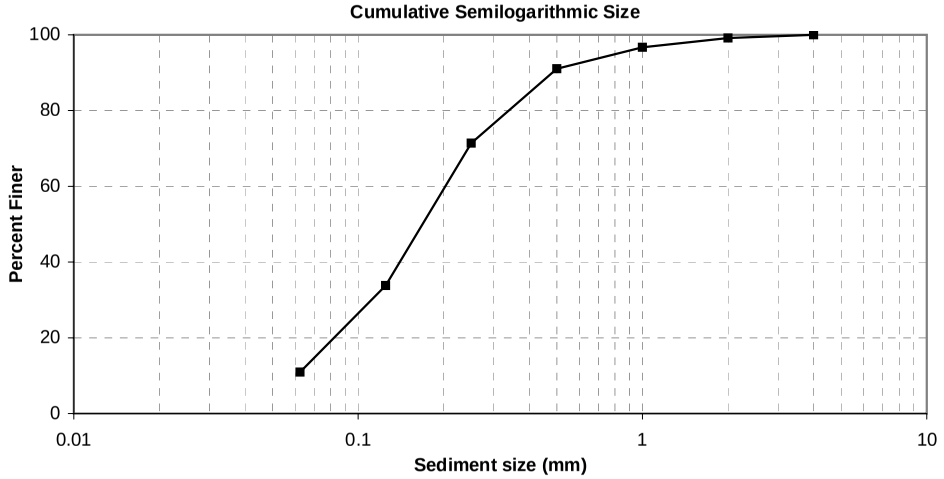

Particle Characteristics			
d_{90}	=	0.48	mm
$d_{84.1}$	=	0.39	mm
d_{65}	=	0.22	mm
d_{50}	=	0.17	mm
d_{35}	=	0.13	mm
$d_{15.9}$	=	0.07	mm
d_g	=	0.17	mm
σ_g		2.32	mm
G	=	1.08	

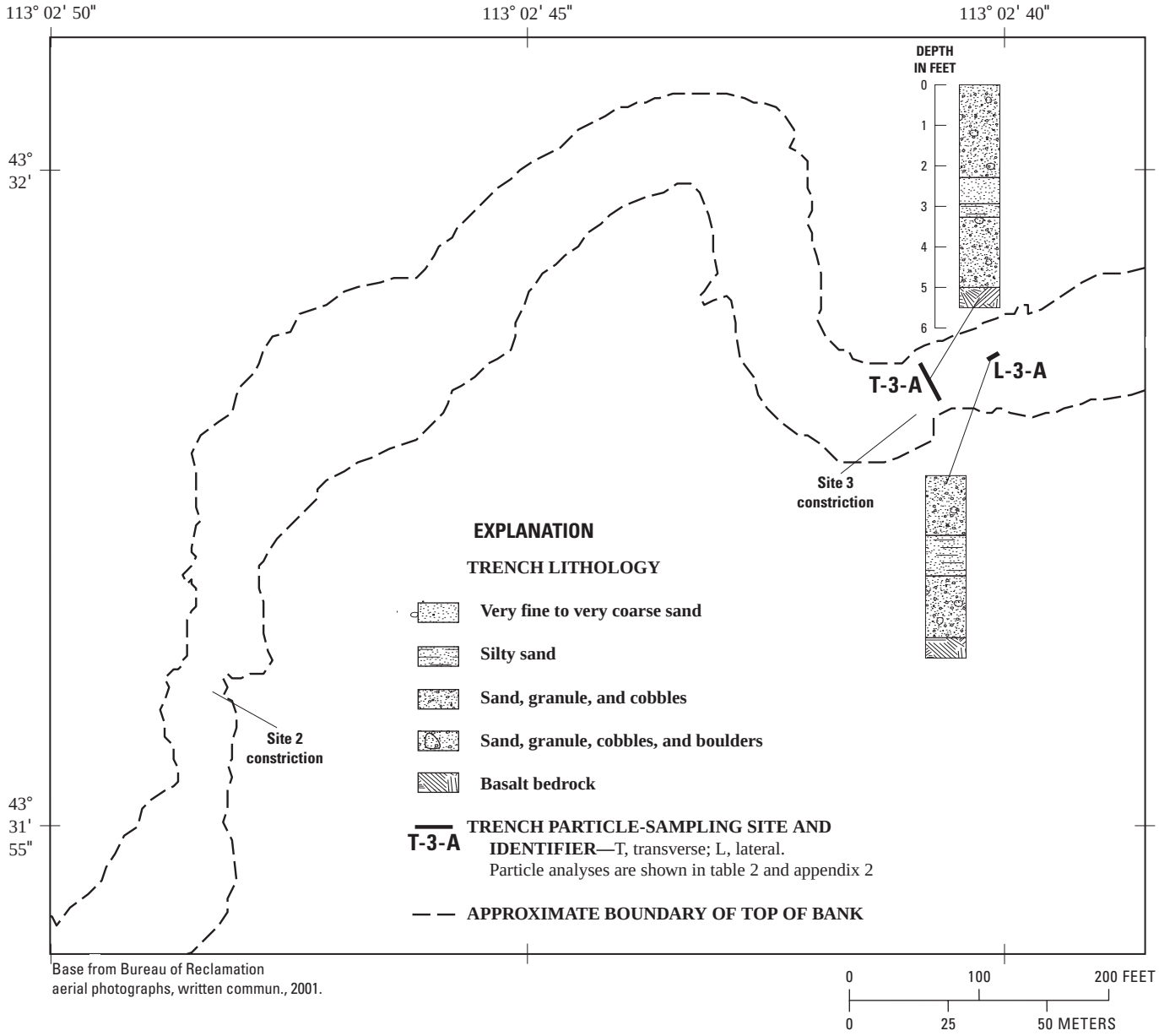

Figure 2–3. Lithology of selected trenches at site 3, Big Lost River upstream of Pioneer diversion structures, Idaho National Engineering and Environmental Laboratory, Idaho.

SIEVE ANALYSIS

Sample ID:	L-3-A1
Location:	BLR Sediments
Date/Time:	August 23, 2000
Analyzed by:	BVT, AJW
Date/Time:	November 29, 2000
Gross weight:	1893.1 g
Tare weight:	110.8 g
Net weight:	1782.3 g
Gravel weight:	3795.0 g
Sand weight:	1782.3 g
Portion analyzed:	5601.0 g
Remarks:	Sediments collected during trenching of the Big Lost River. Poorly sorted sand to pebble-size sediment layer.

Sieve Size (mm)	Weight (g)	Percent Finer	Cumulative Percent Finer	Size Class	Remarks
				Boulders	
8192					
4096					
2048					
1024					
512					
256					No of Particles
64	0.0	0.00	100.00	Cobble	0
32	461.0	8.24	91.76	Pebble	4
16	1428.9	25.53	66.23		103
8	1165.8	20.83	45.41		>100
4	739.3	13.21	32.20		
2	482.6	8.62	23.58	Very coarse sand	
1	262.3	4.69	18.89	Granule	
0.5	281.7	5.03	13.86	Coarse sand	
0.25	520.5	9.30	4.56	Medium sand	
0.125	192.9	3.45	1.11	Fine sand	
0.0625	42.3	0.76	0.36	Very fine sand	
<0.0625	19.9	0.36	0.00	Silt & clays	
TOTAL	5597.2				

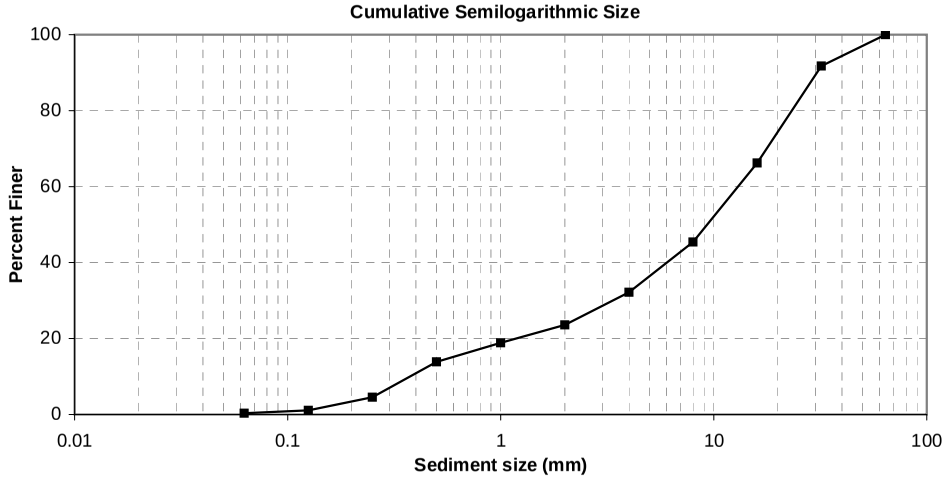

Particle Characteristics			
d_{90} =	30.5	mm
$d_{84.1}$ =	26.0	mm
d_{65} =	15.4	mm
d_{50} =	9.32	mm
d_{35} =	4.63	mm
$d_{15.9}$ =	0.66	mm
d_g =	4.15	mm
σ_g	6.26	mm
G =	2.05	

SIEVE ANALYSIS

Sample ID:	L-3-A2
Location:	BLR Sediments
Date/Time:	August 23, 2000
Analyzed by:	BVT, AJW
Date/Time:	November 29, 2000
Gross weight:	6829.3 g
Tare weight:	110.8 g
Net weight:	6718.5 g
Gravel weight:	4341.3 g
Sand weight:	2346.6 g
Portion analyzed:	6718.5 g
Remarks:	Sediments collected during trenching of the Big Lost River Poorly sorted sand to pebble-size sediment layer.

Sieve Size (mm)	Weight (g)	Percent Finer	Cumulative Percent Finer	Size Class	Remarks
8192					
4096				**Boulders**	
2048					
1024					
512					
256					No. of Particles
64	0.0	0.00	100.00	**Cobble**	0
32	588.0	8.75	91.25		5
16	1668.6	24.84	66.40	**Pebble**	135
8	1185.1	17.64	48.76		>100
4	899.6	13.39	35.36		>100
2	658.4	9.80	25.56	**Very coarse sand**	
1	447.6	6.66	18.90	**Granule**	
0.5	487.5	7.26	11.64	**Coarse sand**	
0.25	530.4	7.90	3.74	**Medium sand**	
0.125	172.4	2.57	1.18	**Fine sand**	
0.0625	50.3	0.75	0.43	**Very fine sand**	
<0.0625	28.7	0.43	0.00	**Silt & clays**	
TOTAL	6716.6				

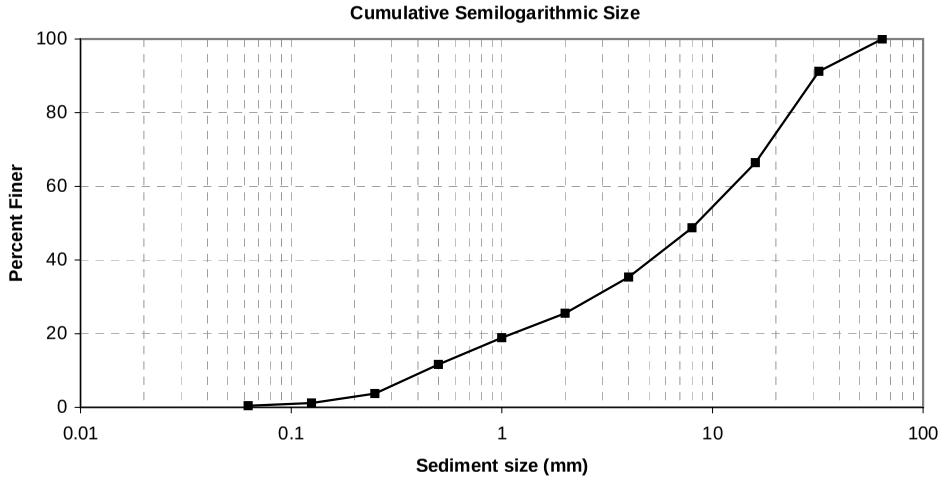

Particle Characteristics			
d_{90}	=	30.9	mm
$d_{84.1}$	=	26.2	mm
d_{65}	=	15.1	mm
d_{50}	=	8.40	mm
d_{35}	=	3.90	mm
$d_{15.9}$	=	0.75	mm
d_g	=	4.44	mm
σ_g		5.91	mm
G	=	1.89	

SIEVE ANALYSIS

Sample ID:	L-3-A3
Location:	BLR Sediments
Date/Time:	August 23, 2000
Analyzed by:	BVT, AJW
Date/Time:	November 29, 2000
Gross weight:	5271.5 g
Tare weight:	110.8 g
Net weight:	5160.7 g
Gravel weight:	3671.6 g
Sand weight:	1542.9 g
Portion analyzed:	5260.7 g
Remarks:	Sediments collected during trenching of the Big Lost River. Artillery shell fragments found in sample. Poorly sorted sand to pebble-size sediment layer.

Sieve Size (mm)	Weight (g)	Percent Finer	Cumulative Percent Finer	Size Class	Remarks
8192					
4096				Boulders	
2048					
1024					
512					
256					No. of Particles
64	0.0	0.00	100.00	Cobble	0
32	96.7	1.84	98.16		2
16	1001.5	19.04	79.12	Pebble	76
8	1550.4	29.47	49.65		>100
4	1023.0	19.45	30.20		
2	398.7	7.58	22.63	Very coarse sand	
1	286.0	5.44	17.19	Granule	
0.5	306.7	5.83	11.36	Coarse sand	
0.25	350.7	6.67	4.69	Medium sand	
0.125	134.8	2.56	2.13	Fine sand	
0.0625	66.0	1.25	0.87	Very fine sand	
<0.0625	46.0	0.87	0.00	Silt & clays	
TOTAL	5260.5				

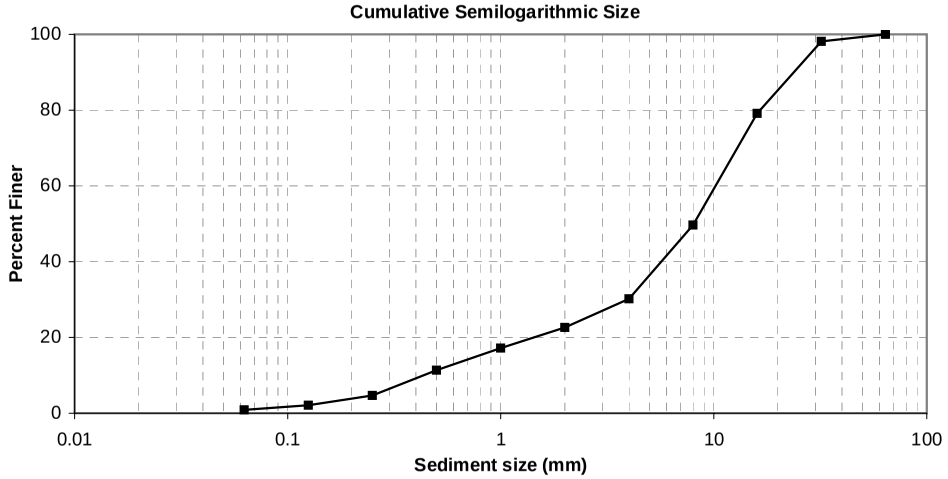

Particle Characteristics			
d_{90}	=	23.8	mm
$d_{84.1}$	=	19.2	mm
d_{65}	=	11.5	mm
d_{50}	=	8.07	mm
d_{35}	=	4.75	mm
$d_{15.9}$	=	0.86	mm
d_g	=	4.06	mm
σ_g		4.73	mm
G	=	1.72	

SIEVE ANALYSIS

Sample ID:	L-3-A4
Location:	BLR Sediments
Date/Time:	August 23, 2000
Analyzed by:	BVT, AJW
Date/Time:	November 29, 2000
Gross weight:	2431.2 g
Tare weight:	110.8 g
Net weight:	2320.4 g
Gravel weight:	783.1 g
Sand weight:	1461.3 g
Portion analyzed:	2320.4 g
Remarks:	Sediments collected during trenching of the Big Lost River. Artillery shell fragments found in sample. Poorly sorted sand to pebble-size sediment layer.

Sieve Size (mm)	Weight (g)	Percent Finer	Cumulative Percent Finer	Size Class	Remarks
8192					
4096				**Boulders**	
2048					
1024					
512					
256					
64				**Cobble**	No. of Particles
32	0.0	0.00	100.00		0
16	164.9	7.11	92.89	**Pebble**	13
8	320.1	13.80	79.10		218
4	298.1	12.85	66.25		>100
2	314.4	13.55	52.70	**Very coarse sand**	
1	282.3	12.17	40.53	**Granule**	
0.5	261.5	11.27	29.26	**Coarse sand**	
0.25	260.0	11.21	18.05	**Medium sand**	
0.125	188.5	8.12	9.93	**Fine sand**	
0.0625	154.6	6.66	3.27	**Very fine sand**	
<0.0625	75.8	3.27	0.00	**Silt & clays**	
TOTAL	2320.2				

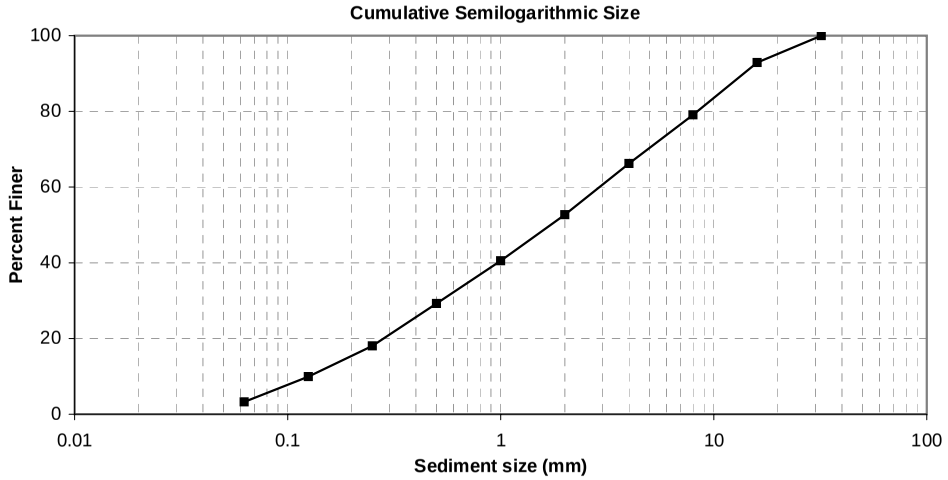

Particle Characteristics			
d_{90}	=	13.8	mm
$d_{84.1}$	=	10.3	mm
d_{65}	=	3.75	mm
d_{50}	=	1.72	mm
d_{35}	=	0.71	mm
$d_{15.9}$	=	0.21	mm
d_g	=	1.46	mm
σ_g		7.03	mm
G	=	1.89	

SIEVE ANALYSIS

Sample ID:	L-3-A5	
Location:	BLR Sediments	
Date/Time:	August 23, 2000	
Analyzed by:	BVT, AJW	
Date/Time:	November 29, 2000	
Gross weight:	3431.3	g
Tare weight:	110.8	g
Net weight:	3320.5	g
Gravel weight:	49.7	g
Sand weight:	1406.0	g
Portion analyzed:	1513.0	g
Remarks:	Sediments collected during trenching of the Big Lost River. ~1/2 sample analyzed, used splitter. Artillery shell fragments found in sample. Poorly sorted sand to pebble-size sediment layer.	

Sieve Size (mm)	Weight (g)	Percent Finer	Cumulative Percent Finer	Size Class	Remarks
				Boulders	
8192					
4096					
2048					
1024					
512					
256					
64				Cobble	
32				Pebble	No. of Particles
16	0.0	0.00	100.00		0
8	7.2	0.48	99.52		6
4	42.5	2.81	96.71		211
2	92.0	6.09	90.62	Very coarse sand	>100
1	125.8	8.32	82.30	Granule	
0.5	302.5	20.01	62.29	Coarse sand	
0.25	493.9	32.68	29.61	Medium sand	
0.125	281.7	18.64	10.97	Fine sand	
0.0625	110.1	7.28	3.69	Very fine sand	
<0.0625	55.7	3.69	0.00	Silt & clays	
TOTAL	1511.4				

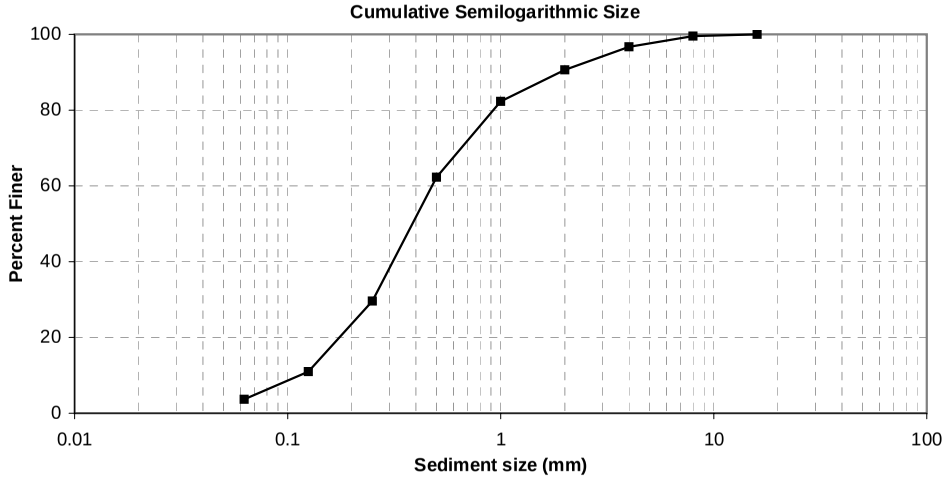

Particle Characteristics			
d_{90}	=	1.90	mm
$d_{84.1}$	=	1.16	mm
d_{65}	=	0.55	mm
d_{50}	=	0.39	mm
d_{35}	=	0.28	mm
$d_{15.9}$	=	0.15	mm
d_g	=	0.42	mm
σ_g		2.78	mm
G	=	1.18	

SIEVE ANALYSIS

Sample ID:	L-3-A6
Location:	BLR Sediments
Date/Time:	August 23, 2000
Analyzed by:	BVT, AJW
Date/Time:	November 29, 2000
Gross weight:	889.4 g
Tare weight:	110.8 g
Net weight:	778.6 g
Gravel weight:	78.3 g
Sand weight:	590.7 g
Portion analyzed:	778.6 g
Remarks:	Sediments collected during trenching of the Big Lost River. Carbonate present in fine-grained material.

Sieve Size (mm)	Weight (g)	Percent Finer	Cumulative Percent Finer	Size Class	Remarks
				Boulders	
8192					
4096					
2048					
1024					
512					
256					
64				Cobble	
32				Pebble	No. of Particles
16	0.0	0.00	100.00		0
8	1.2	0.15	99.85		1
4	77.1	9.92	89.93		>100
2	99.8	12.84	77.09	Very coarse sand	
1	73.4	9.44	67.65	Granule	
0.5	50.3	6.47	61.18	Coarse sand	
0.25	46.0	5.92	55.26	Medium sand	
0.125	117.8	15.15	40.11	Fine sand	
0.0625	203.4	26.16	13.94	Very fine sand	
<0.0625	108.4	13.94	0.00	Silt & clays	
TOTAL	777.4				

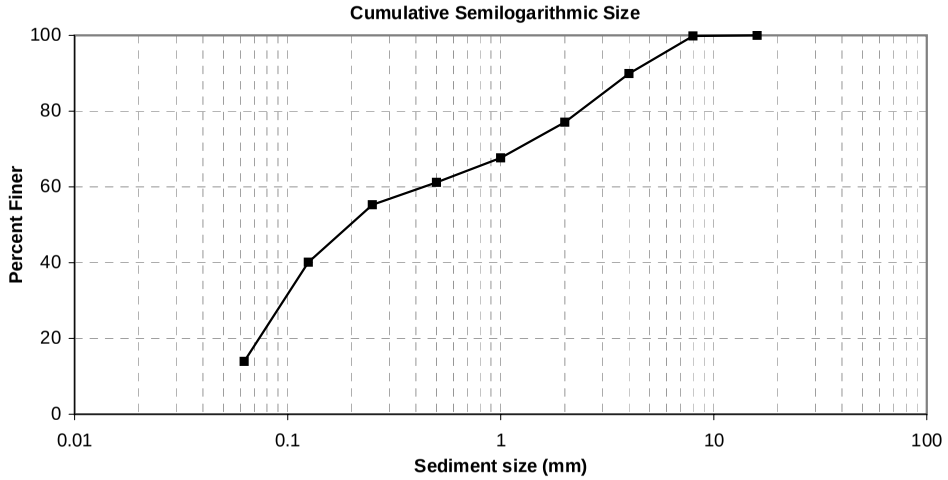

Particle Characteristics			
d_{90}	=	4.02	mm
$d_{84.1}$	=	2.92	mm
d_{65}	=	0.75	mm
d_{50}	=	0.20	mm
d_{35}	=	0.11	mm
$d_{15.9}$	=	0.07	mm
d_g	=	0.44	mm
σ_g		6.66	mm
G	=	2.11	

SIEVE ANALYSIS

Sample ID:	L-3-A7
Location:	BLR Sediments
Date/Time:	August 23, 2000
Analyzed by:	BVT, AJW
Date/Time:	November 29, 2000
Gross weight:	3968.5 g
Tare weight:	110.8 g
Net weight:	3857.7 g
Gravel weight:	114.0 g
Sand weight:	592.2 g
Portion analyzed:	762.6 g
Remarks:	Sediments collected during trenching of the Big Lost River. Artillery shell fragments found in sample. Poorly sorted sand to pebble-size sediment layer with some clay.

Sieve Size (mm)	Weight (g)	Percent Finer	Cumulative Percent Finer	Size Class	Remarks
8192					
4096				**Boulders**	
2048					
1024					
512					
256					
64				**Cobble**	
32					No. of Particles
16	0.0	0.00	100.00	**Pebble**	0
8	10.4	1.37	98.63		20
4	103.6	13.64	84.99		>100
2	126.5	16.66	68.33	**Very coarse sand**	
1	74.9	9.86	58.47	**Granule**	
0.5	57.6	7.58	50.88	**Coarse sand**	
0.25	161.6	21.28	29.60	**Medium sand**	
0.125	112.5	14.81	14.79	**Fine sand**	
0.0625	59.1	7.78	7.01	**Very fine sand**	
<0.0625	53.2	7.01	0.00	**Silt & clays**	
TOTAL	759.4				

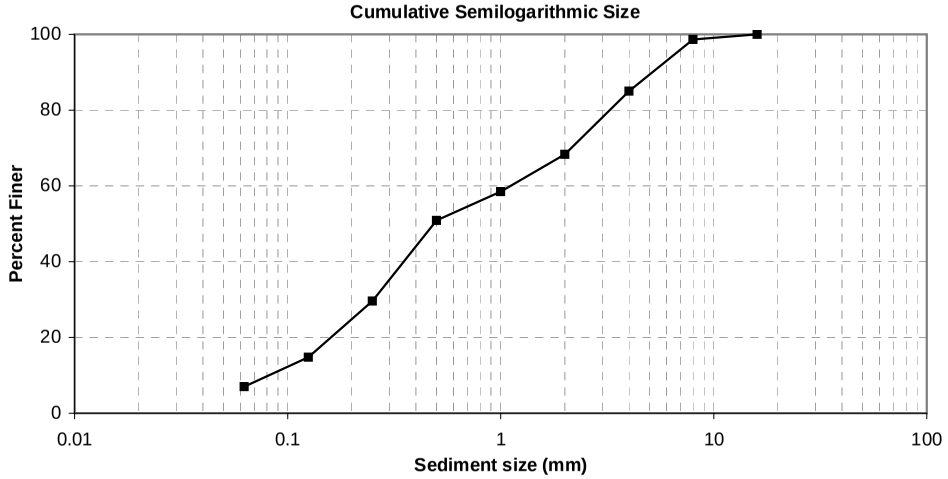

Particle Characteristics			
d_{90}	=	5.16	mm
$d_{84.1}$	=	3.85	mm
d_{65}	=	1.58	mm
d_{50}	=	0.49	mm
d_{35}	=	0.30	mm
$d_{15.9}$	=	0.13	mm
d_g	=	0.71	mm
σ_g		5.41	mm
G	=	1.70	

SIEVE ANALYSIS

Sample ID:	L-3-A8
Location:	BLR Sediments
Date/Time:	August 23, 2000
Analyzed by:	BVT, AJW
Date/Time:	November 29, 2000
Gross weight:	6161.0 g
Tare weight:	110.8 g
Net weight:	6050.2 g
Gravel weight:	750.9 g
Sand weight:	1721.3 g
Portion analyzed:	2480.8 g
Remarks:	Sediments collected during trenching of the Big Lost River. ~1/3 sample analyzed, used splitter Poorly sorted sand to pebble-size sediment layer.

Sieve Size (mm)	Weight (g)	Percent Finer	Cumulative Percent Finer	Size Class	Remarks
				Boulders	
8192					
4096					
2048					
1024					
512					
256					
64				Cobble	No. of Particles
32	0.0	0.00	100.00	Pebble	0
16	133.6	5.40	94.60		15
8	328.4	13.26	81.34		167 & piece of shell casing
4	288.9	11.67	69.67		>100
2	351.0	14.18	55.49	Very coarse sand	
1	504.7	20.39	35.11	Granule	
0.5	602.6	24.34	10.76	Coarse sand	
0.25	228.4	9.23	1.54	Medium sand	
0.125	29.6	1.20	0.34	Fine sand	
0.0625	5.0	0.20	0.14	Very fine sand	
<0.0625	3.5	0.14	0.00	Silt & clays	
TOTAL	2475.7				

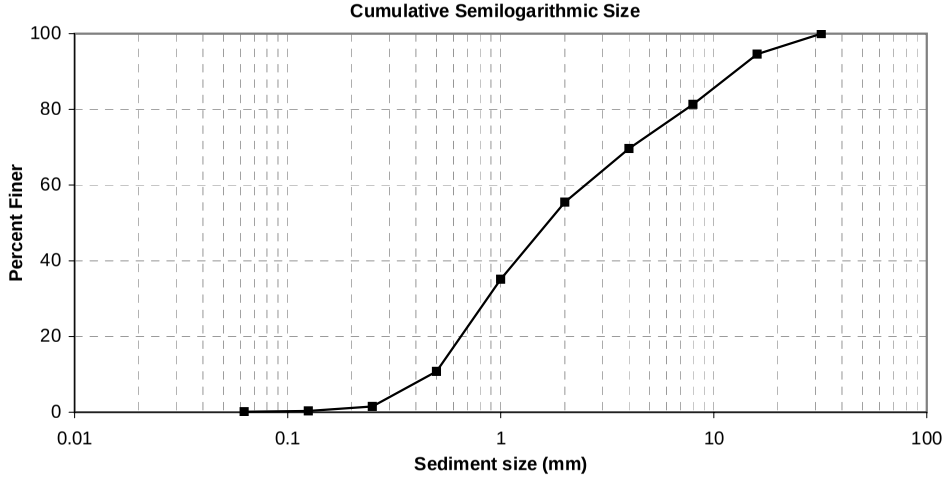

Particle Characteristics			
d_{90}	=	12.6	mm
$d_{84.1}$	=	9.24	mm
d_{65}	=	3.18	mm
d_{50}	=	1.66	mm
d_{35}	=	1.00	mm
$d_{15.9}$	=	0.58	mm
d_g	=	2.31	mm
σ_g		4.00	mm
G	=	1.45	

SIEVE ANALYSIS

Sample ID:	L-3-A9
Location:	BLR Sediments
Date/Time:	August 23, 2000
Analyzed by:	BVT, AJW
Date/Time:	November 29, 2000
Gross weight:	7243.5 g
Tare weight:	110.8 g
Net weight:	7132.7 g
Gravel weight:	1091.3 g
Sand weight:	1002.8 g
Portion analyzed:	2102.2 g
Remarks:	Sediments collected during trenching of the Big Lost River. ~1/4 sample analyzed; used splitter Poorly sorted sand to pebble-size sediment layer.

Sieve Size (mm)	Weight (g)	Percent Finer	Cumulative Percent Finer	Size Class	Remarks
8192					
4096				Boulders	
2048					
1024					
512					
256					No. of Particles
64	0.0	0.00	100.00	Cobble	0
32	68.2	3.25	96.75		1
16	229.5	10.95	85.80	Pebble	21
8	468.1	22.32	63.48		>100
4	325.5	15.52	47.95		
2	275.5	13.14	34.81	Very coarse sand	
1	265.3	12.65	22.16	Granule	
0.5	292.9	13.97	8.19	Coarse sand	
0.25	139.0	6.63	1.56	Medium sand	
0.125	25.7	1.23	0.34	Fine sand	
0.0625	4.4	0.21	0.13	Very fine sand	
<0.0625	2.7	0.13	0.00	Silt & clays	
TOTAL	2096.8				

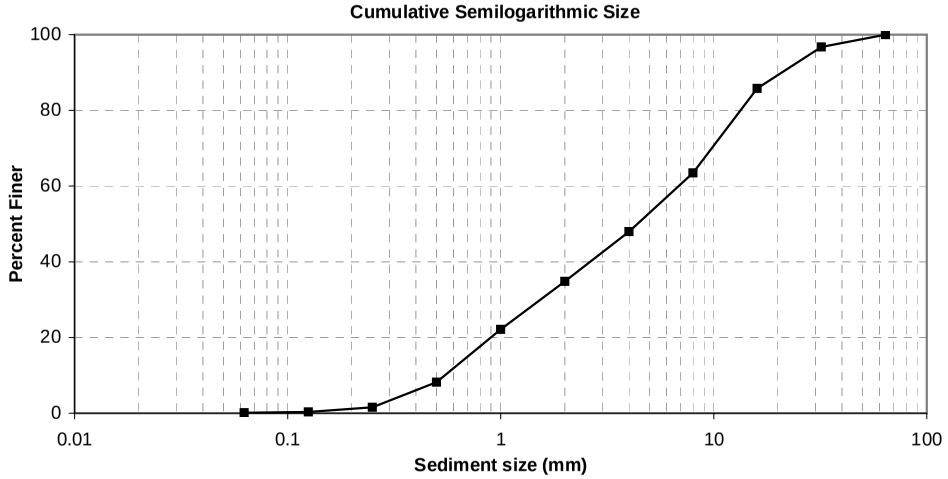

Particle Characteristics			
d_{90}	=	20.9	mm
$d_{84.1}$	=	15.2	mm
d_{65}	=	8.39	mm
d_{50}	=	4.38	mm
d_{35}	=	2.02	mm
$d_{15.9}$	=	0.73	mm
d_g	=	3.34	mm
σ_g		4.55	mm
G	=	1.54	

SIEVE ANALYSIS

Sample ID:	L-3-A11
Location:	BLR Sediments
Date/Time:	August 23, 2000
Analyzed by:	BVT, AJW
Date/Time:	November 29, 2000
Gross weight:	1825.3 g
Tare weight:	110.8 g
Net weight:	1714.5 g
Gravel weight:	19.6 g
Sand weight:	930.5 g
Portion analyzed:	997.9 g
Remarks:	Sediments collected during trenching of the Big Lost River. Organic matter present in sample. Well-sorted medium sand.

Sieve Size (mm)	Weight (g)	Percent Finer	Cumulative Percent Finer	Size Class	Remarks
8192					
4096				**Boulders**	
2048					
1024					
512					
256					
64				**Cobble**	
32					No. of Particles
16	0.0	0.00	100.00	**Pebble**	0
8	13.0	1.30	98.70		6
4	6.6	0.66	98.04		44
2	9.0	0.90	97.13	**Very coarse sand**	>100; lots of organics
1	12.8	1.28	95.85	**Granule**	Organic matter
0.5	62.9	6.30	89.55	**Coarse sand**	Organic matter
0.25	230.1	23.06	66.49	**Medium sand**	Organic matter
0.125	476.3	47.73	18.77	**Fine sand**	Organic matter
0.0625	139.4	13.97	4.80	**Very fine sand**	
<0.0625	47.9	4.80	0.00	**Silt & clays**	
TOTAL	998.0				

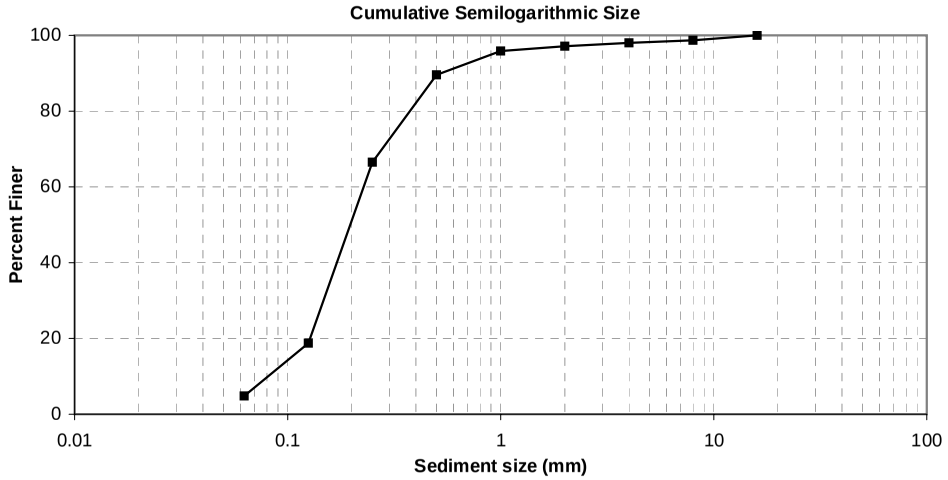

Particle Characteristics			
d_{90}	=	0.53	mm
$d_{84.1}$	=	0.42	mm
d_{65}	=	0.24	mm
d_{50}	=	0.20	mm
d_{35}	=	0.16	mm
$d_{15.9}$	=	0.11	mm
d_g	=	0.21	mm
σ_g		1.98	mm
G	=	1.00	

SIEVE ANALYSIS

Sample ID:	L-3-A12
Location:	BLR Sediments
Date/Time:	August 23, 2000
Analyzed by:	BVT, AJW
Date/Time:	November 29, 2000
Gross weight:	2799.2 g
Tare weight:	110.8 g
Net weight:	2688.4 g
Gravel weight:	1513.0 g
Sand weight:	1172.0 g
Portion analyzed:	2688.4 g
Remarks:	Sediments collected during trenching of the Big Lost River. Sediments are red in color -- iron staining Poorly sorted sand to pebble-size sediment layer.

Sieve Size (mm)	Weight (g)	Percent Finer	Cumulative Percent Finer	Size Class	Remarks
8192					
4096				**Boulders**	
2048					
1024					
512					
256					
64				**Cobble**	No. of particles
32	0.0	0.00	100.00		0
16	144.4	5.37	94.63	**Pebble**	12 -- Pieces of shell casing
8	714.5	26.59	68.04		>100
4	654.1	24.34	43.70		
2	559.0	20.80	22.90	**Very coarse sand**	
1	345.5	12.86	10.04	**Granule**	
0.5	194.1	7.22	2.82	**Coarse sand**	
0.25	59.8	2.23	0.60	**Medium sand**	
0.125	10.7	0.40	0.20	**Fine sand**	
0.0625	2.9	0.11	0.09	**Very fine sand**	
<0.0625	2.4	0.09	0.00	**Silt & clays**	
TOTAL	2687.4				

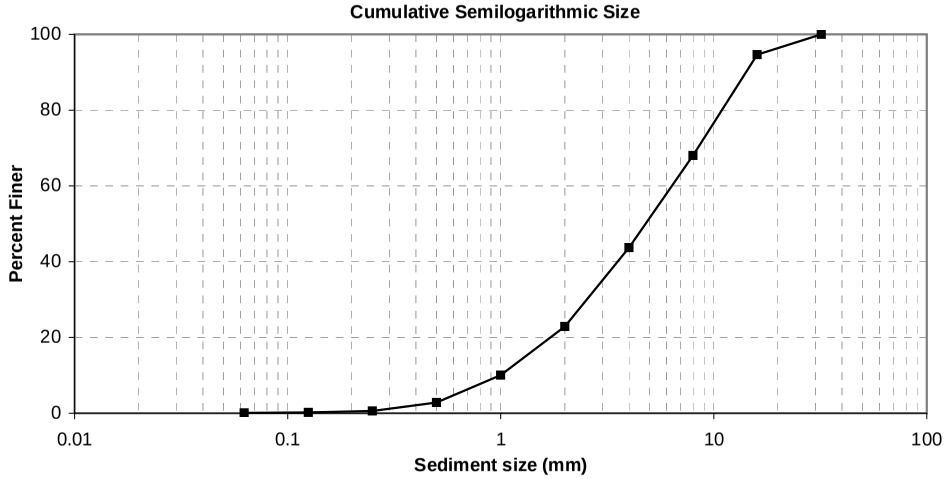

Particle Characteristics			
d_{90}	=	14.2	mm
$d_{84.1}$	=	12.2	mm
d_{65}	=	7.34	mm
d_{50}	=	4.79	mm
d_{35}	=	2.99	mm
$d_{15.9}$	=	1.37	mm
d_g	=	4.08	mm
σ_g		2.98	mm
G	=	1.23	

SIEVE ANALYSIS

Sample ID:	T-3-A1
Location:	BLG Sediments
Date/Time:	August 23, 2000
Analyzed by:	BVT, AJW
Date/Time:	November 29, 2000
Gross weight:	4183.2 g
Tare weight:	110.8 g
Net weight:	4072.4 g
Gravel weight:	25.4 g
Sand weight:	1952.0 g
Portion analyzed:	1983.2 g
Remarks:	Sediments collected during trenching of the Big Lost River. ~1/2 of sample analyzed; used splitter. Well-sorted granule layer.

Sieve Size (mm)	Weight (g)	Percent Finer	Cumulative Percent Finer	Size Class	Remarks
				Boulders	
8192					
4096					
2048					
1024					
512					
256					
64				Cobble	
32				Pebble	No. of particles
16	0.0	0.00	100.00		0
8	4.3	0.22	99.78		3
4	21.1	1.07	98.72		123
2	138.2	6.99	91.73	Very coarse sand	>100
1	604.4	30.55	61.18	Granule	
0.5	1003.6	50.73	10.44	Coarse sand	
0.25	187.8	9.49	0.95	Medium sand	
0.125	15.3	0.77	0.18	Fine sand	
0.0625	2.7	0.14	0.04	Very fine sand	
<0.0625	0.8	0.04	0.00	Silt & clays	
TOTAL	1978.2				

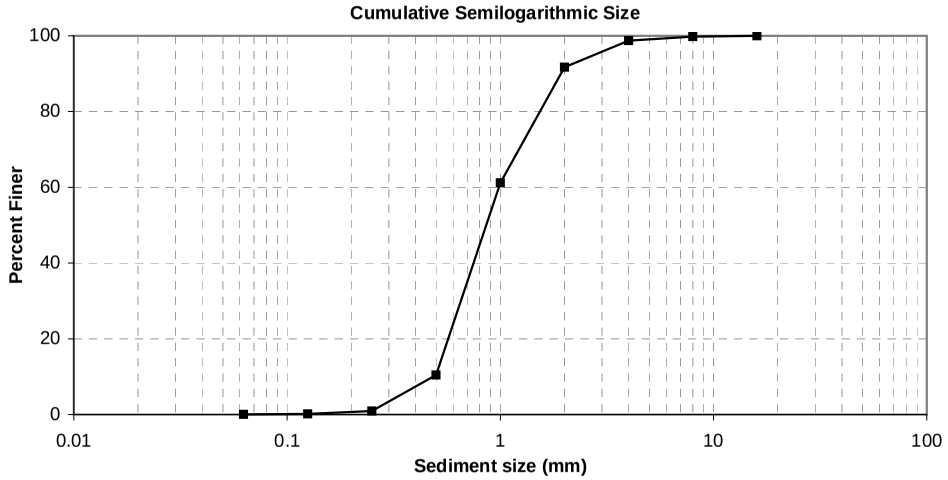

Particle Characteristics			
d_{90}	=	1.92	mm
$d_{84.1}$	=	1.68	mm
d_{65}	=	1.09	mm
d_{50}	=	0.86	mm
d_{35}	=	0.70	mm
$d_{15.9}$	=	0.54	mm
d_g	=	0.95	mm
σ_g		1.77	mm
G	=	0.94	

SIEVE ANALYSIS

Sample ID:	T-3-A2	
Location:	BLR Sediments	
Date/Time:	August 23, 2000	
Analyzed by:	BVT, AJW	
Date/Time:	November 29, 2000	
Gross weight:	2003.6	g
Tare weight:	110.8	g
Net weight:	1892.8	g
Gravel weight:	48.6	g
Sand weight:	1841.7	g
Portion analyzed:	1892.8	g
Remarks:	Sediments collected during trenching of the Big Lost River. Well-sorted coarse sand layer.	

Sieve Size (mm)	Weight (g)	Percent Finer	Cumulative Percent Finer	Size Class	Remarks
8192					
4096				**Boulders**	
2048					
1024					
512					
256					
64				**Cobble**	No. of Particles
32	0.0	0.00	100.00		0
16	37.7	1.99	98.01	**Pebble**	1
8	8.4	0.44	97.56		4
4	2.5	0.13	97.43		12
2	5.5	0.29	97.14	**Very coarse sand**	>100
1	18.2	0.96	96.18	**Granule**	
0.5	260.7	13.78	82.40	**Coarse sand**	
0.25	1320.3	69.76	12.64	**Medium sand**	
0.125	209.9	11.09	1.55	**Fine sand**	
0.0625	27.1	1.43	0.12	**Very fine sand**	
<0.0625	2.2	0.12	0.00	**Silt & clays**	
TOTAL	1892.5				

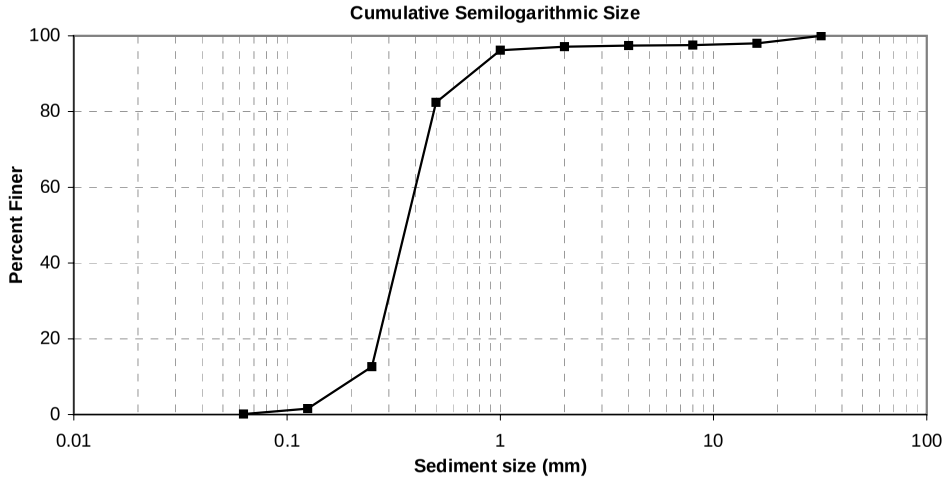

Particle Characteristics			
d_{90}	=	0.73	mm
$d_{84.1}$	=	0.54	mm
d_{65}	=	0.42	mm
d_{50}	=	0.36	mm
d_{35}	=	0.31	mm
$d_{15.9}$	=	0.26	mm
d_g	=	0.37	mm
σ_g		1.45	mm
G	=	0.85	

SIEVE ANALYSIS

Sample ID:	T-3-A3
Location:	BLR sediments
Date/Time:	August 23, 2000
Analyzed by:	BVT, AJW
Date/Time:	November 29, 2000
Gross weight:	8187.2 g
Tare weight:	110.8 g
Net weight:	8076.4 g
Gravel weight:	896.6 g
Sand weight:	1404.6 g
Portion analyzed:	2313.3 g
Remarks:	Sediments collected during trenching of the Big Lost River. ~1/4 of sample analyzed; used splitter. Poorly sorted sand to pebble-size sediment layer.

Sieve Size (mm)	Weight (g)	Percent Finer	Cumulative Percent Finer	Size Class	Remarks
				Boulders	
8192					
4096					
2048					
1024					
512					
256					
64				Cobble	No. of Particles
32	0.0	0.00	100.00	Pebble	0
16	246.7	10.70	89.30		14
8	334.8	14.52	74.78		194
4	315.1	13.67	61.11		>100
2	412.5	17.89	43.22	Very coarse sand	
1	459.2	19.92	23.30	Granule	
0.5	215.1	9.33	13.97	Coarse sand	
0.25	222.5	9.65	4.32	Medium sand	
0.125	84.4	3.66	0.66	Fine sand	
0.0625	10.9	0.47	0.19	Very fine sand	
<0.0625	4.3	0.19	0.00	Silt & clays	
TOTAL	2305.5				

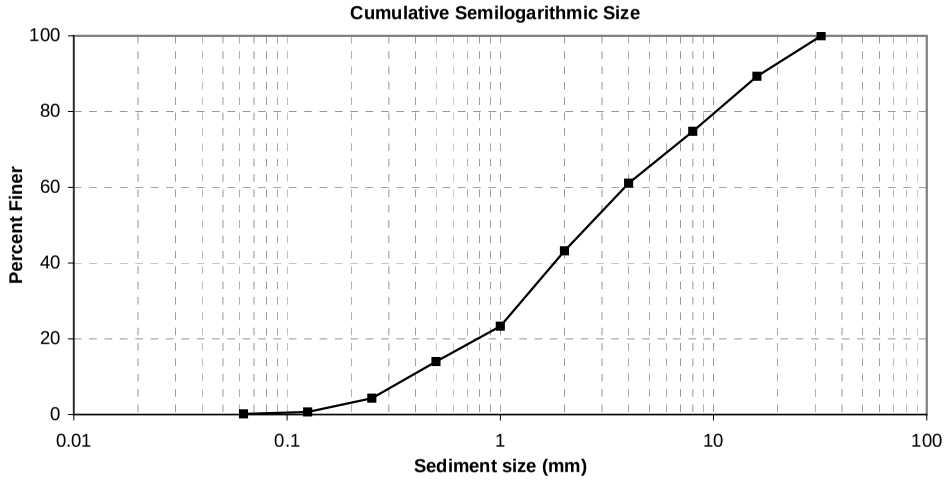

Particle Characteristics			
d_{90}	=	16.7	mm
$d_{84.1}$	=	12.5	mm
d_{65}	=	4.87	mm
d_{50}	=	2.60	mm
d_{35}	=	1.50	mm
$d_{15.9}$	=	0.58	mm
d_g	=	2.68	mm
σ_g	=	4.65	mm
G	=	1.53	

SIEVE ANALYSIS

Sample ID:	T-3-A4
Location:	BLR Sediments
Date/Time:	August 23, 2000
Analyzed by:	BVT, AJW
Date/Time:	November 29, 2000
Gross weight:	9421.5 g
Tare weight:	110.8 g
Net weight:	9310.7 g
Gravel weight:	1889.4 g
Sand weight:	1743.7 g
Portion analyzed:	3668.4 g
Remarks:	Sediments collected during trenching of the Big Lost River. ~1/2 of sample analyzed. Poorly sorted sand to pebble-size sediment layer.

Sieve Size (mm)	Weight (g)	Percent Finer	Cumulative Percent Finer	Size Class	Remarks
8192					
4096				Boulders	
2048					
1024					
512					
256					No. of Particles
64	0.0	0.00	100.00	Cobble	0
32	178.1	4.86	95.14		3
16	268.3	7.32	87.82	Pebble	22
8	787.8	21.50	66.31		>100
4	655.2	17.88	48.43		
2	481.9	13.15	35.28	Very coarse sand	
1	285.9	7.80	27.47	Granule	
0.5	229.8	6.27	21.20	Coarse sand	
0.25	487.7	13.31	7.89	Medium sand	
0.125	205.1	5.60	2.29	Fine sand	
0.0625	53.3	1.45	0.84	Very fine sand	
<0.0625	30.7	0.84	0.00	Silt & clays	
TOTAL	3663.8				

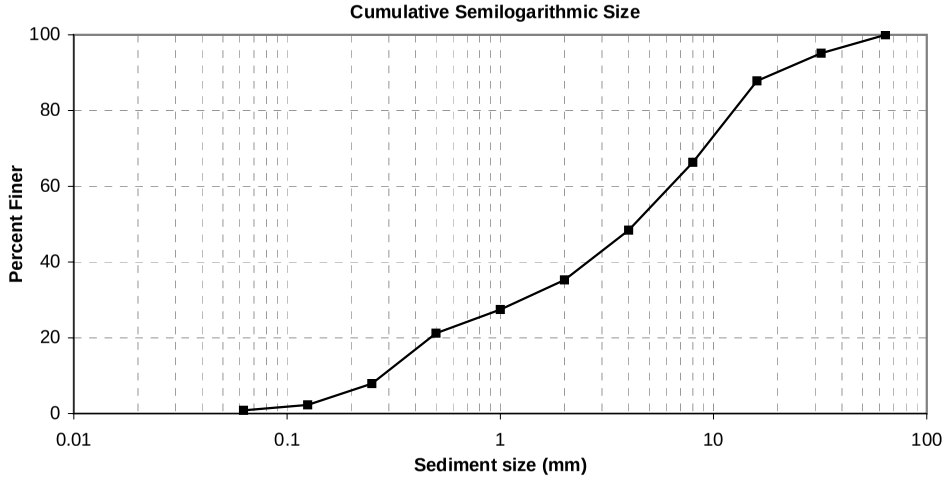

Particle Characteristics			
d_{90}	=	19.7	mm
$d_{84.1}$	=	14.2	mm
d_{65}	=	7.60	mm
d_{50}	=	4.25	mm
d_{35}	=	1.95	mm
$d_{15.9}$	=	0.38	mm
d_g	=	2.32	mm
σ_g		6.12	mm
G	=	1.91	

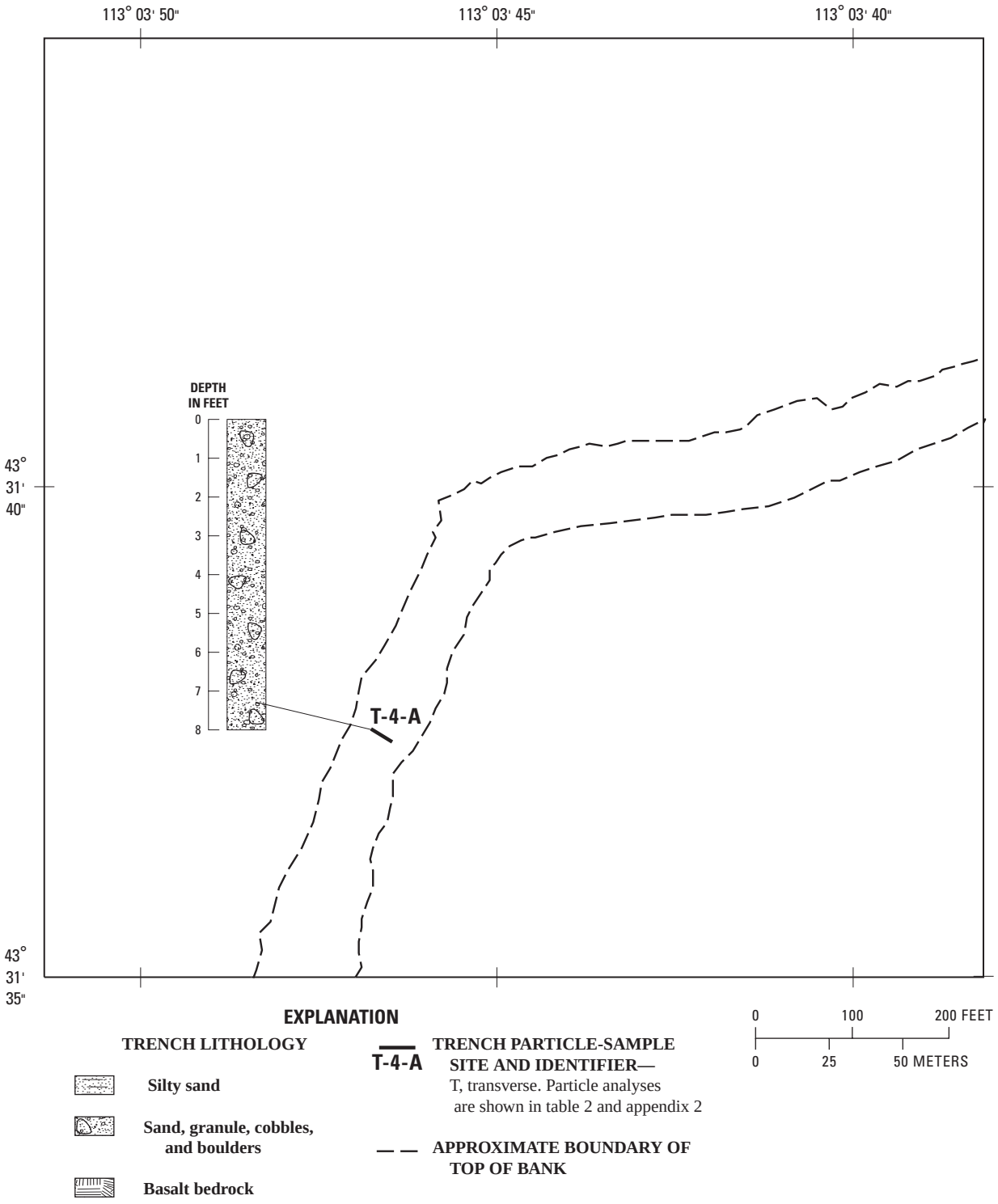

Figure 2–4. Lithology of selected trenches at site 4, Big Lost River upstream of Pioneer diversion structures, Idaho National Engineering and Environmental Laboratory, Idaho.

SIEVE ANALYSIS

Sample ID:	T-4-A1
Location:	BLR Sediments
Date/Time:	June 21, 2001
Analyzed by:	BVT, AJW
Date/Time:	June 26, 2001
Gross weight:	30452.2 g
Tare weight:	795.5 g
Net weight:	29656.7 g
Gravel weight:	5620.3 g
Sand weight:	2251.3 g
Portion analyzed:	7895.8 g
Remarks:	Sediments collected during trenching of the Big Lost River. ~1/4 of sample analyzed. Poorly sorted sand to cobble-size sediment layer.

Sieve Size (mm)	Weight (g)	Percent Finer	Cumulative Percent Finer	Size Class	Remarks
8192					
4096				**Boulders**	
2048					
1024					
512					No. of Particles
256	0.0	0.00	100.00		0
64	1615.6	20.48	79.52	**Cobble**	2
32	898.4	11.39	68.13		5
16	1208.5	15.32	52.81	**Pebble**	83
8	1106.6	14.03	38.78		>100
4	791.2	10.03	28.75		
2	601.5	7.63	21.13	**Very coarse sand**	
1	556.6	7.06	14.07	**Granule**	
0.5	689.7	8.74	5.33	**Coarse sand**	
0.25	304.1	3.86	1.47	**Medium sand**	
0.125	74.8	0.95	0.52	**Fine sand**	
0.0625	24.6	0.31	0.21	**Very fine sand**	
<0.0625	16.8	0.21	0.00	**Silt & clays**	
TOTAL	7888.4				

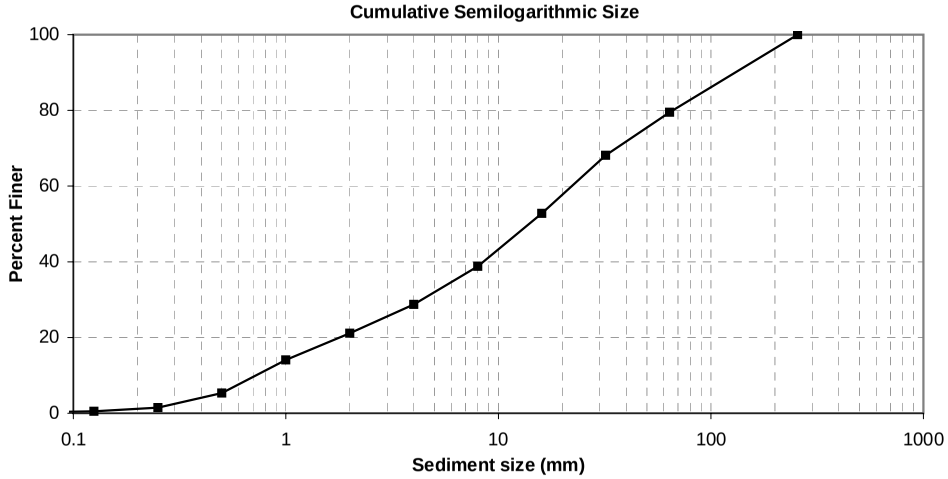

Particle Characteristics			
d_{90}	=	130	mm
$d_{84.1}$	=	87.3	mm
d_{65}	=	27.8	mm
d_{50}	=	13.9	mm
d_{35}	=	6.16	mm
$d_{15.9}$	=	1.20	mm
d_g	=	10.2	mm
σ_g	=	8.53	mm
G	=	2.11	

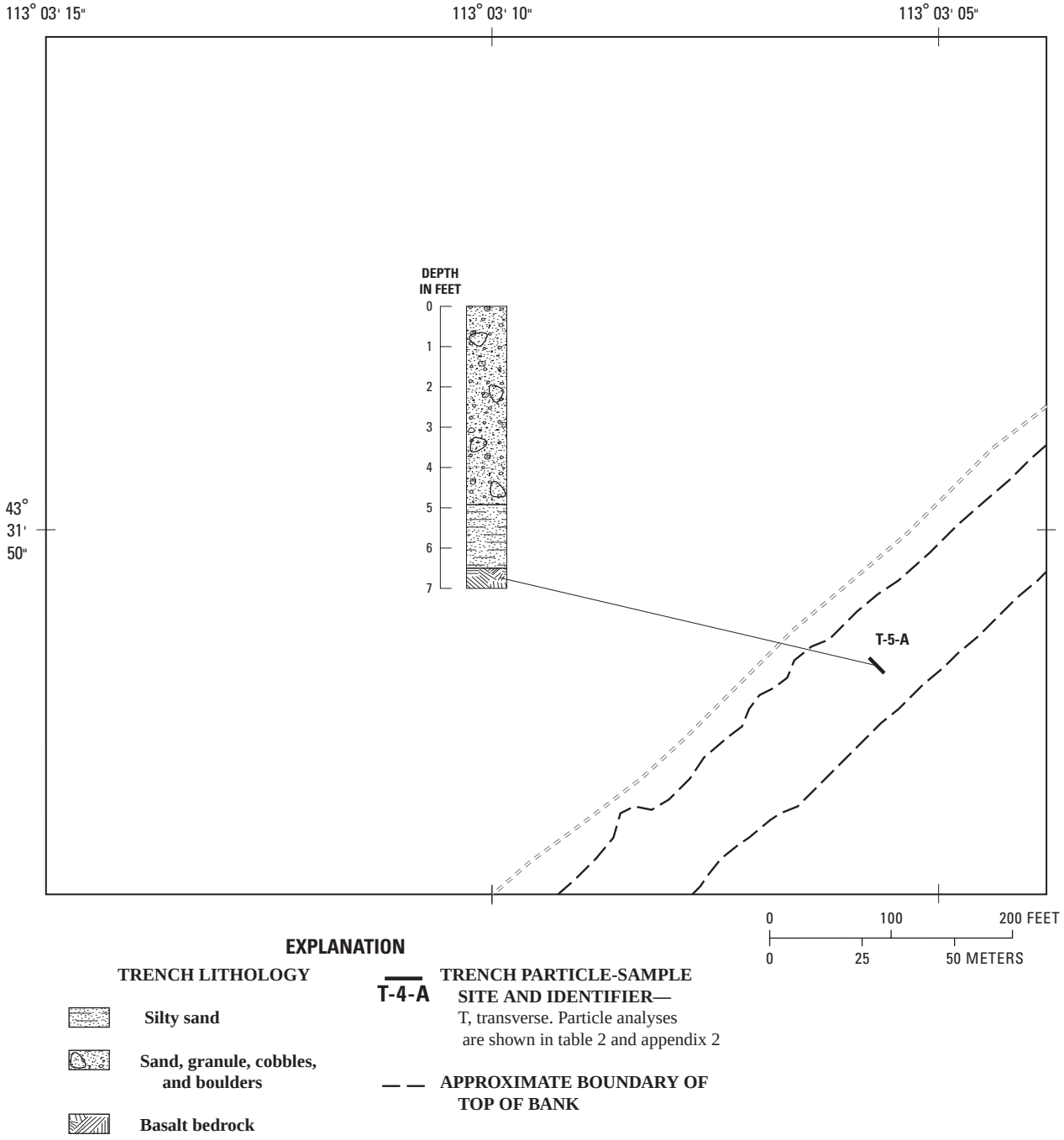

Figure 2–5. Lithology of selected trenches at site 4, Big Lost River upstream of Pioneer diversion structures, Idaho National Engineering and Environmental Laboratory, Idaho.

SIEVE ANALYSIS

Sample ID:	T-5-A1	
Location:	BLR Sediments	
Date/Time:	June 21, 2001	
Analyzed by:	BVT, AJW	
Date/Time:	June 26, 2001	
Gross weight:	34634.3	g
Tare weight:	929.8	g
Net weight:	33704.5	g
Gravel weight:	6187.2	g
Sand weight:	2715.3	g
Portion analyzed:	8919.0	g
Remarks:	Sediments collected during trenching of the Big Lost River. ~1/4 of sample analyzed. Poorly sorted sand to pebble-size sediment layer.	

Sieve Size (mm)	Weight (g)	Percent Finer	Cumulative Percent Finer	Size Class	Remarks
8192					
4096				**Boulders**	
2048					
1024					
512					
256					No. of particles
64	0.0	0.00	100.00	**Cobble**	0
32	2382.7	26.74	73.26		15
16	1562.3	17.53	55.73	**Pebble**	97
8	1344.4	15.09	40.64		>100
4	897.8	10.08	30.56		
2	629.5	7.06	23.50	**Very coarse sand**	
1	570.1	6.40	17.10	**Granule**	
0.5	957.9	10.75	6.35	**Coarse sand**	
0.25	463.2	5.20	1.15	**Medium sand**	
0.125	78.4	0.88	0.27	**Fine sand**	
0.0625	16.2	0.18	0.09	**Very fine sand**	
<0.0625	8.1	0.09	0.00	**Silt & clays**	
TOTAL	8910.6				

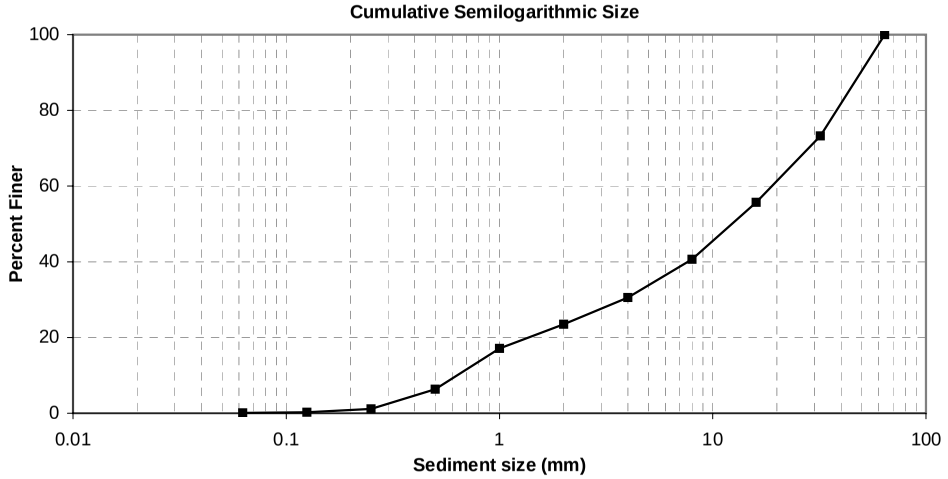

Particle Characteristics			
d_{90}	=	49.4	mm
$d_{84.1}$	=	42.4	mm
d_{65}	=	23.1	mm
d_{50}	=	12.3	mm
d_{35}	=	5.43	mm
$d_{15.9}$	=	0.93	mm
d_g	=	6.28	mm
σ_g	=	6.75	mm
G	=	2.04	

SIEVE ANALYSIS

Sample ID:	T-5-A2
Location:	BLR Sediments
Date/Time:	June 21, 2001
Analyzed by:	BVT, AJW
Date/Time:	June 26, 2001
Gross weight:	1868.8 g
Tare weight:	110.2 g
Net weight:	1758.6 g
Gravel weight:	12.6 g
Sand weight:	528.0 g
Portion analyzed:	575.9 g
Remarks:	Sediments collected during trenching of the Big Lost River. Poorly sorted sand to pebble-size sediiment layer.

Sieve Size (mm)	Weight (g)	Percent Finer	Cumulative Percent Finer	Size Class	Remarks
8192					
4096				**Boulders**	
2048					
1024					
512					
256					
64				**Cobble**	
32					
16				**Pebble**	No. of particles
8	0.0	0.00	100.00		0
4	12.6	2.19	97.81		60 (30% consolidated clay)
2	24.5	4.26	93.55	**Very coarse sand**	>100 (50% consolidated clay
1	60.7	10.55	82.99	**Granule**	60% consolidated clay & silt
0.5	97.9	17.02	65.97	**Coarse sand**	80% consolidated clay & silt
0.25	133.0	23.13	42.84	**Medium sand**	
0.125	121.2	21.07	21.77	**Fine sand**	
0.0625	90.7	15.77	6.00	**Very fine sand**	
<0.0625	34.5	6.00	0.00	**Silt & clays**	
TOTAL	575.1				

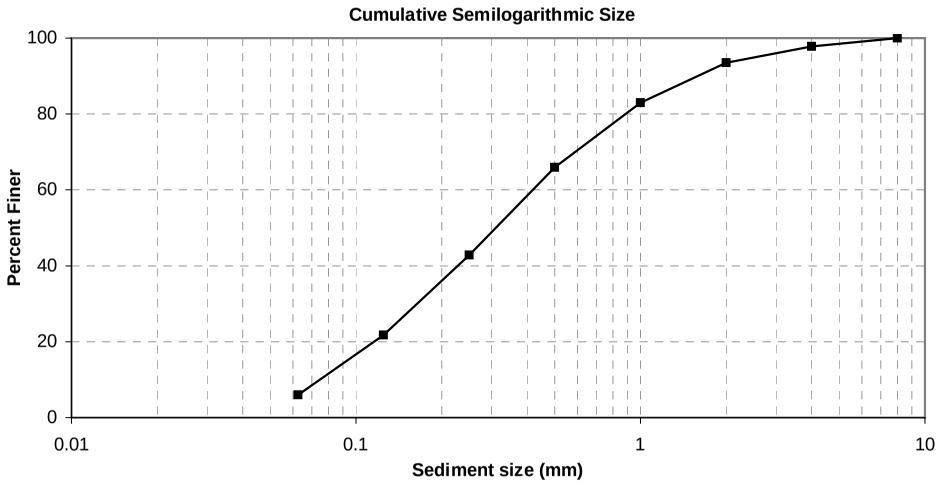

Particle Characteristics			
d_{90}	=	1.58	mm
$d_{84.1}$	=	1.08	mm
d_{65}	=	0.49	mm
d_{50}	=	0.31	mm
d_{35}	=	0.19	mm
$d_{15.9}$	=	0.097	mm
d_g	=	0.32	mm
σ_g	=	3.34	mm
G	=	1.29	

This page intentionally left blank.

Appendix 3

Field-Surveyed Map of the Saddle Area at Site 1 on the Big Lost River Upstream of the Pioneer Diversion Structures, Idaho National Engineering and Environmental Laboratory

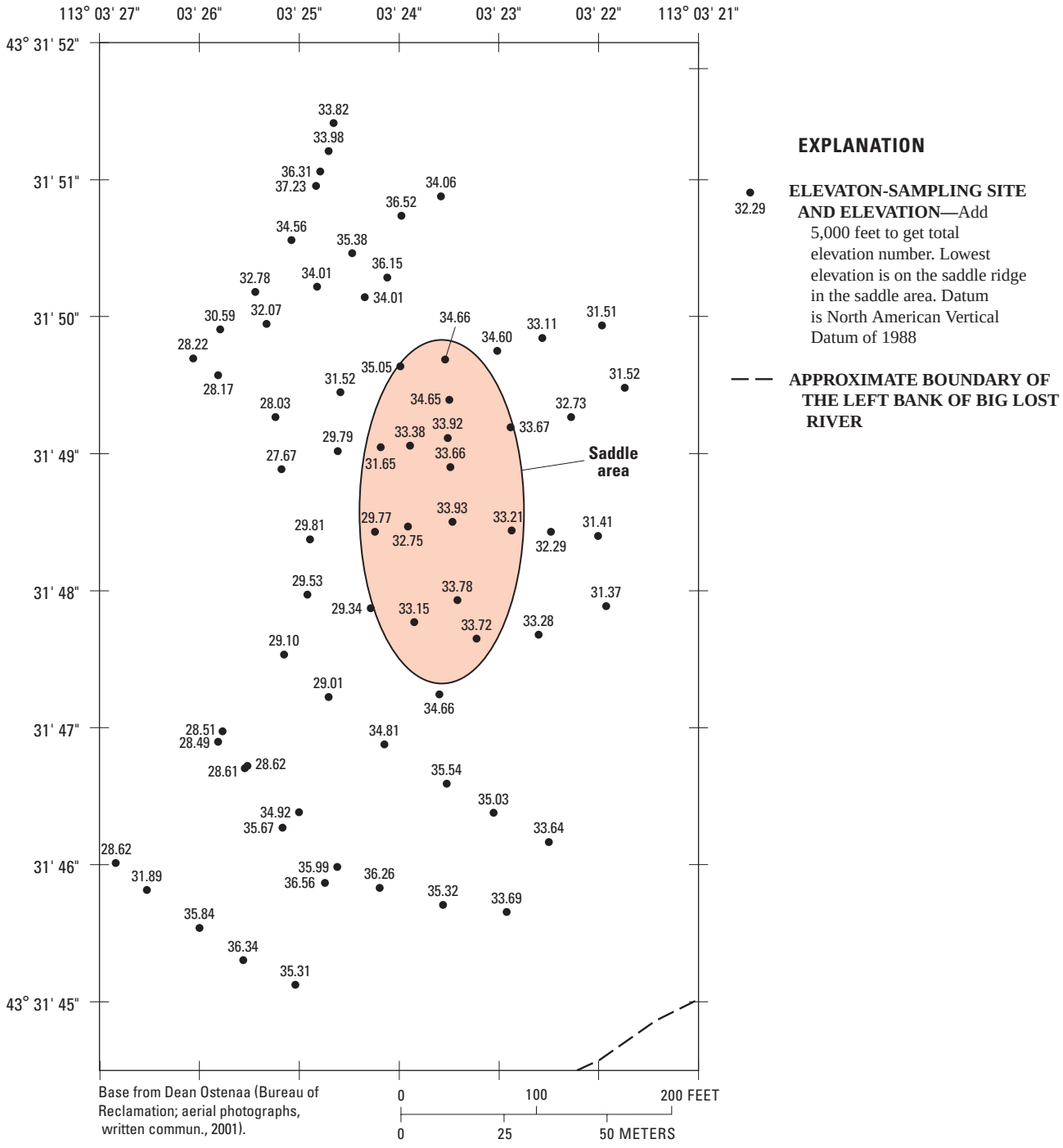

Figure 3–1. Location of the saddle area elevation-sampling sites at site 1 on the Big Lost River upstream of Pioneer diversion structures, Idaho National Engineering and Environmental Laboratory, Idaho.

Land-surface points GPSed in the Saddle area of the INEEL (Shaded points denote points within Saddle area). See previous figure for location of points and saddle area. See appendix figure 3-1 for location of saddle area to the study area.

[Latitude and longitude, in degrees (º), minutes (’), and seconds (”), are based on the North American Datum of 1983; land-surface elevations are based on the North American Vertical Datum of 1988]

Field no.	Latitude	Longitude	Land-surface elevation (feet)
1	43º 31’ 44.390520”	113º 03’ 23.499555”	5,034.65
2	43º 31’ 43.901199”	113º 03’ 23.486698”	5,033.66
3	43º 31’ 43.496611”	113º 03’ 23.465170”	5,033.93
4	43º 31’ 42.929625”	113º 03’ 23.414791”	5,033.78
5	43º 31’ 42.240115”	113º 03’ 23.601051”	5,034.66
6	43 º 31’ 43.462634”	113 º 03’ 23.914255”	5,032.75
7	43 º 31’ 43.437876”	113 º 03’ 22.874606”	5,033.21
1402	43º 31’ 41.892714”	113º 03’ 25.817010”	5,028.49
1403	43º 31’ 41.700719”	113º 03’ 25.546928”	5,028.61
1404	43º 31’ 41.381800”	113º 03’ 25.007009”	5,034.92
1405	43º 31’ 40.979651”	113º 03’ 24.623281”	5,035.99
1406	43º 31’ 40.826262”	113º 03’ 24.198113”	5,036.26
1407	43º 31’ 40.702427”	113º 03’ 23.562208”	5,035.32
1408	43º 31’ 40.650549”	113º 03’ 22.917951”	5,033.69
1409	43º 31’ 41.163888”	113º 03’ 22.498980”	5,033.64
1410	43º 31’ 41.376313”	113º 03’ 23.051822”	5,035.03
1411	43º 31’ 41.587658”	113º 03’ 23.524103”	5,035.54
1412	43º 31’ 41.871904”	113º 03’ 24.150855”	5,034.81
1413	43º 31’ 42.220892”	113º 03’ 24.708473”	5,029.01
1414	43º 31’ 42.532173”	113º 03’ 25.152051”	5,029.11
1415	43º 31’ 42.967764”	113º 03’ 24.924155”	5,029.53
1416	43º 31’ 42.869201”	113º 03’ 24.289355”	5,029.34
1417	43º 31’ 42.766289”	113º 03’ 23.849702”	5,033.15
1418	43º 31’ 42.645601”	113º 03’ 23.223508”	5,033.72
1419	43º 31’ 42.675940”	113º 03’ 22.600929”	5,033.28
1420	43º 31’ 42.882702”	113º 03’ 21.925800”	5,031.37
1421	43º 31’ 43.395043”	113º 03’ 22.008337”	5,031.41
1422	43º 31’ 43.425152”	113º 03’ 22.480975”	5,032.29
1423	43º 31’ 43.426917”	113º 03’ 24.245954”	5,029.77
1424	43º 31’ 43.374137”	113º 03’ 24.895574”	5,029.81
1425	43º 31’ 43.885301”	113º 03’ 25.177827”	5,027.67
1426	43º 31’ 44.015599”	113º 03’ 24.615400”	5,029.79
1427	43º 31’ 44.044086”	113º 03’ 24.186861”	5,031.65
1428	43º 31’ 44.056980”	113º 03’ 23.893684”	5,033.38
1429	43º 31’ 44.112055”	113º 03’ 23.512476”	5,033.92
1430	43º 31’ 44.189928”	113º 03’ 22.884283”	5,033.67
1431	43º 31’ 44.265052”	113º 03’ 22.275899”	5,032.73
1432	43º 31’ 44.477261”	113º 03’ 21.738004”	5,031.52
1433	43º 31’ 44.932760”	113º 03’ 21.963346”	5,031.51

1434	43° 31’ 44.840983”	113° 03’ 22.563704”	5,033.11
1435	43° 31’ 44.748063”	113° 03’ 23.016536”	5,034.60
1436	43° 31’ 44.683994”	113° 03’ 23.542476”	5,034.66
1437	43° 31’ 44.632239”	113° 03’ 23.986205”	5,035.05
1438	43° 31’ 44.446866”	113° 03’ 24.593131”	5,031.52
1439	43° 31’ 44.264159”	113° 03’ 25.243131”	5,028.03
1440	43° 31’ 44.568154”	113° 03’ 25.816542”	5,028.17
1441	43° 31’ 44.942268”	113° 03’ 25.331705”	5,032.07
1442	43° 31’ 45.215596”	113° 03’ 24.824076”	5,034.01
1443	43° 31’ 45.457830”	113° 03’ 24.472409”	5,035.38
1444	43° 31’ 45.733164”	113° 03’ 23.979734”	5,036.52
1445	43° 31’ 45.877906”	113° 03’ 23.582829”	5,034.06
1446	43° 31’ 45.284955”	113° 03’ 24.118903”	5,036.52
1447	43° 31’ 45.137956”	113° 03’ 24.343990”	5,036.15
1448	43° 31’ 46.412314”	113° 03’ 24.659299”	5,033.82
1449	43° 31’ 46.203697”	113° 03’ 24.708019”	5,033.98
1450	43° 31’ 46.055273”	113° 03’ 24.793510”	5,036.31
1451	43° 31’ 45.951375”	113° 03’ 24.833764”	5,037.23
1452	43° 31’ 45.554673”	113° 03’ 25.079404”	5,034.56
1453	43° 31’ 45.175142”	113° 03’ 25.445438”	5,032.78
1454	43° 31’ 44.903310”	113° 03’ 25.796107”	5,030.59
1455	43° 31’ 44.692546”	113° 03’ 26.066813”	5,028.22
1456	43° 31’ 41.967825”	113° 03’ 25.771712”	5,028.51
1457	43° 31’ 41.716390”	113° 03’ 25.523144”	5,028.62
1458	43° 31’ 41.264079”	113° 03’ 25.168218”	5,035.67
1459	43° 31’ 40.865486”	113° 03’ 24.744063”	5,036.56
1460	43° 31’ 40.117261”	113° 03’ 25.043463”	5,035.31
1461	43° 31’ 40.299931”	113° 03’ 25.564767”	5,036.34
1462	43° 31’ 40.534201”	113° 03’ 26.004518”	5,035.84

Appendix 4

HEC-RAS, HEC-6, and TRIM2D Model Results for a Peak Flow of 100 Cubic Meters per Second on the Big Lost River Upstream of the Pioneer Diversion Structures, Idaho National Engineering and Environmental Laboratory

Appendix 4–1. HEC-RAS simulation at a flow of 100 cubic meters per second

[**Abbreviations:** W.S. elev, water-surface elevation; Vel chnl, average flow velocity in channel; ft, foot; ft/s, foot per second; W/m^2, watt per squared meter]

Cross section	W.S. elev (ft)	Thalweg (ft)	Flow depth (ft)	Vel chnl (ft)	Stream power (W/m^2)
108	5,033.4	5,025.8	7.6	4.06	13.0
107	5,033.0	5,025.4	7.6	4.21	15.4
106	5,032.8	5,024.5	8.3	4.12	15.6
105	5,032.6	5,023.5	9.1	4.10	16.2
104	5,032.1	5,022.9	9.2	4.60	20.8
103	5,031.7	5,023.4	8.3	5.12	18.7
102	5,031.7	5,023.3	8.4	4.04	10.0
101	5,031.7	5,023.8	7.8	3.16	5.5
100	5,031.6	5,023.7	7.9	3.19	4.2
99	5,031.5	5,022.1	9.4	2.91	6.4
98	5,031.5	5,022.9	8.6	2.57	4.5
97	5,031.5	5,022.1	9.4	2.08	3.6
96	5,031.4	5,021.6	9.8	2.97	7.8
95	5,030.8	5,021.9	8.9	5.41	19.7
93	5,030.0	5,020.9	9.1	3.25	14.7
90	5,029.1	5,020.5	8.6	4.28	30.0
86	5,028.5	5,018.1	10.4	4.05	20.1
85	5,028.4	5,017.3	11.1	4.66	23.8
84	5,026.7	5,015.2	11.5	10.77	193.3
83	5,027.1	5,015.0	12.1	8.64	90.8
82	5,027.3	5,017.3	10.0	7.09	49.7
81	5,027.1	5,017.3	9.8	7.67	108.6
80	5,027.2	5,017.9	9.3	5.81	26.3
79	5,027.1	5,016.5	10.6	6.04	30.0
78	5,027.1	5,015.6	11.5	5.76	26.9
77	5,026.8	5,016.7	10.1	6.07	31.9
76.5	5,026.4	5,016.7	9.7	7.51	60.3
76	5,026.2	5,016.1	10.1	7.10	50.8
75	5,026.2	5,015.9	10.3	5.48	24.0
74	5,026.3	5,014.7	11.6	3.95	15.6
73	5,026.2	5,015.3	10.9	3.81	7.8
72	5,026.0	5,014.7	11.3	4.56	12.6
71	5,025.6	5,015.2	10.4	5.94	30.3
70.5	5,025.1	5,014.5	10.6	6.95	50.7
70	5,024.5	5,014.0	10.5	7.50	62.4
69	5,024.0	5,013.9	10.1	7.02	85.0
68	5,024.2	5,012.1	12.1	4.57	26.0
67	5,024.3	5,012.6	11.7	3.38	5.9
66	5,024.2	5,010.8	13.4	3.96	8.7
65	5,024.2	5,010.9	13.3	3.59	6.3
64	5,024.1	5,013.4	10.7	4.30	11.3
63	5,023.9	5,012.3	11.6	5.06	31.8
62	5,023.9	5,013.0	10.9	3.93	9.8
61	5,023.9	5,012.3	11.6	3.49	6.1
60.5	5,023.9	5,012.1	11.8	2.75	4.8
60	5,023.8	5,011.6	12.2	4.01	8.2
59	5,023.8	5,007.8	16.0	3.45	6.5
58	5,023.7	5,009.3	14.4	4.34	10.1
57	5,023.7	5,010.4	13.3	3.84	12.3
56	5,023.6	5,008.8	14.8	5.04	26.5
55	5,023.6	5,008.3	15.3	5.00	14.6
54	5,023.4	5,006.2	17.2	5.96	46.1
53	5,022.8	5,005.5	17.3	8.49	142.5
52.5	5,021.8	5,005.7	16.1	11.28	340.8
52	5,018.6	5,005.9	12.7	17.50	1,384.3
51.75	5,015.1	5,006.9	8.2	22.31	3,008.6
51.5	5,020.7	5,007.9	12.8	9.12	179.7
51.25	5,020.9	5,008.8	12.1	7.61	103.3
51	5,021.1	5,009.7	11.4	6.74	72.8
50.5	5,020.8	5,009.4	11.4	7.74	114.1
50	5,019.5	5,009.2	10.3	11.77	608.1
49.5	5,019.7	5,009.3	10.4	9.55	234.2
49	5,019.9	5,009.4	10.5	7.82	126.7
48	5,020.0	5,009.4	10.6	7.16	88.8
47	5,020.1	5,011.0	9.1	5.58	40.7
46	5,020.1	5,010.5	9.6	5.05	30.2
45	5,020.1	5,010.3	9.8	4.61	24.2
44	5,019.8	5,009.6	10.2	5.65	42.9
43	5,018.9	5,009.9	9.0	8.02	163.9
42	5,018.6	5,009.3	9.3	7.40	132.8
41	5,018.5	5,009.1	9.4	6.45	88.5
40	5,018.6	5,009.7	8.9	5.04	39.0
36	5,018.6	5,008.7	9.9	4.30	22.6
35	5,018.6	5,008.4	10.2	3.80	15.0
34	5,018.3	5,007.9	10.4	5.26	41.5
33	5,018.1	5,007.2	10.9	6.72	82.4
32	5,017.9	5,007.7	10.2	6.79	69.4
31	5,018.0	5,006.6	11.4	5.12	20.9
30	5,017.8	5,007.2	10.6	5.74	26.0
29	5,017.4	5,007.7	9.7	7.09	43.5
28	5,017.2	5,007.4	9.8	7.62	54.5
26	5,017.0	5,007.4	9.6	7.71	55.1
23	5,016.7	5,006.6	10.1	7.02	54.3
20	5,016.1	5,006.2	9.9	7.21	44.2
13	5,015.9	5,005.5	10.4	6.35	25.9
8	5,015.7	5,004.9	10.8	4.65	137.1
3	5,014.1	5,002.0	12.1	8.36	175.7
1	5,011.4	4,998.7	12.7	13.22	636.7

Appendix 4–2. HEC-6 simulation at a flow of 100 cubic meters per second

[**Abbreviations:** W.S. elev, water-surface elevation; Vel chnl, average flow velocity in channel; ft, foot; ft/s, foot per second; W/m^2, watt per squared meter]

Cross section	W.S. elev (ft)	Thalweg (ft)	Flow depth (ft)	Vel chnl (ft)	Stream power (W/m^2)
108	5,034.20	5,027.90	6.30	2.89	
107	5,033.70	5,024.60	9.10	2.75	
106	5,033.30	5,024.30	9.00	2.97	
105	5,033.20	5,023.00	10.20	3.01	
104	5,032.60	5,022.10	10.50	3.18	
103	5,032.10	5,022.30	9.80	3.60	
102	5,031.50	5,024.10	7.40	4.47	
101	5,031.30	5,025.50	5.80	3.97	
100	5,031.30	5,026.00	5.30	2.85	
99	5,031.30	5,022.20	9.10	2.57	
98	5,031.30	5,023.10	8.20	2.28	5
97	5,031.30	5,022.10	9.20	2.38	
96	5,031.20	5,021.40	9.80	2.91	
95	5,030.90	5,020.90	10.00	3.98	
93	5,030.10	5,019.10	11.00	2.73	
90	5,028.40	5,020.00	8.40	5.48	
86	5,027.50	5,017.00	10.50	4.32	
85	5,027.30	5,016.70	10.60	5.08	
84	5,026.50	5,011.10	15.40	8.25	339
83	5,026.60	5,010.50	16.10	7.49	
82	5,026.50	5,015.40	11.10	7.52	
81	5,026.30	5,015.00	11.30	7.20	
80	5,026.60	5,014.10	12.50	4.90	
79	5,026.00	5,016.60	9.40	6.97	
78	5,026.10	5,012.40	13.70	6.00	
77	5,025.90	5,014.50	11.40	5.60	
76.5	5,025.80	5,013.10	12.70	6.44	
76	5,025.70	5,012.70	13.00	6.08	46
75	5,025.20	5,017.00	8.20	6.92	
74	5,025.50	5,011.60	13.90	4.03	
73	5,025.00	5,018.70	6.30	5.91	
72	5,025.00	5,012.10	12.90	4.89	24
71	5,024.50	5,013.00	11.50	6.53	
70.5	5,024.20	5,010.90	13.30	6.29	
70	5,023.70	5,011.90	11.80	7.51	
69	5,023.50	5,011.60	11.90	6.47	
68	5,023.30	5,015.30	8.00	6.27	
67	5,023.50	5,012.60	10.90	3.96	
66	5,023.20	5,012.10	11.10	5.57	
65	5,023.30	5,010.90	12.40	4.11	
64	5,022.90	5,015.00	7.90	6.22	
63	5,022.80	5,010.60	12.20	5.83	
62	5,022.70	5,013.00	9.70	5.72	
61	5,022.60	5,014.00	8.60	5.48	
60.5	5,022.50	5,016.70	5.80	4.49	
60	5,022.50	5,010.40	12.10	4.86	
59	5,022.30	5,009.00	13.30	5.57	
58	5,022.30	5,008.90	13.40	5.36	
57	5,022.30	5,011.30	11.00	5.73	
56	5,022.10	5,008.40	13.70	6.23	54
55	5,022.00	5,007.10	14.90	6.23	
54	5,021.90	5,003.10	18.80	6.50	
53	5,021.60	5,002.10	19.50	9.82	
52.5	5,020.90	5,001.10	19.80	11.39	
52	5,020.30	5,001.60	18.70	12.46	3,440
51.75	5,019.80	5,002.10	17.70	9.33	
51.5	5,020.50	5,003.30	17.20	7.24	
51.25	5,020.90	5,004.50	16.40	6.17	
51	5,021.00	5,005.70	15.30	5.21	
50.5	5,021.20	5,006.90	14.30	6.59	
50	5,020.90	5,007.50	13.40	8.81	
49.5	5,020.30	5,008.10	12.20	6.25	
49	5,020.60	5,006.30	14.30	5.36	
48	5,020.70	5,004.50	16.20	6.34	
47	5,020.50	5,009.40	11.10	3.91	
46	5,020.80	5,007.20	13.60	5.42	
45	5,020.50	5,011.50	9.00	4.21	
44	5,020.60	5,010.30	10.30	5.07	
43	5,020.40	5,008.70	11.70	6.13	
42	5,020.00	5,008.90	11.10	5.15	40
41	5,020.00	5,008.30	11.70	4.85	
40	5,020.00	5,009.10	10.90	5.78	
36	5,019.90	5,012.80	7.10	8.08	
35	5,019.50	5,012.90	6.60	3.90	
34	5,019.70	5,013.90	5.80	5.40	
33	5,019.50	5,013.10	6.40	5.39	41
32	5,019.50	5,007.10	12.40	4.60	
31	5,019.40	5,007.80	11.60	3.61	
30	5,019.40	5,005.40	14.00	4.17	
29	5,019.20	5,006.40	12.80	5.55	
28	5,019.00	5,007.90	11.10	5.68	
26	5,018.90	5,006.70	12.20	4.76	
23	5,019.00	5,006.10	12.90	5.75	
20	5,018.50	5,005.00	13.50	5.08	64
13	5,017.60	5,005.60	12.00	4.10	
8	5,017.10	5,007.10	10.00	6.83	
3	5,015.80	5,003.80	12.00	6.63	
1	5,014.90	5,000.30	14.60	13.23	

Appendix 4–3. TRIM2D simulation at a flow of 100 cubic meters per second

[**Abbreviations:** W.S. elev, water-surface elevation; ft, foot; ft/s, foot per second; W/m^2, watt per squared meter]

Cross section	W.S. elev (ft)	Thalweg (ft)	Flow depth (ft)	Velocity (ft/s)				Stream power (W/m^2)				Remarks
				Thalweg	Channel	Overbank	Used	Thalweg	Channel	Overbank	Used	
108	5,032.94	5,027.49	5.45	5.96	6.61	–	5.96	111.5	–	–	111.5	
107	5,032.94	5,025.49	7.45	5.15	5.68	–	5.15	43.3	57.5	58.0	57.5	Left bank
106	5,032.64	5,025.49	7.15	4.36	–	6.59	4.36	88.5	–	–	88.5	Meander (left bank)
105	5,032.02	5,025.49	6.53	5.43	–	8.49	5.43	100.4	195.1	–	195.1	Meander (left bank)
104	5,031.79	5,025.49	6.30	8.16	–	8.44	8.16	153.8	196.3	–	196.3	Meander (left bank)
103	5,031.33	5,023.49	7.84	5.48	7.58	–	5.48	55.8	130.4	–	130.4	
102	5,031.43	5,023.49	7.94	5.99	6.83	–	5.99	65.8	110.9	–	110.9	
101	5,031.30	5,025.49	5.81	5.85	6.13	–	5.85	66.2	76.6	–	76.6	
100	5,031.20	5,023.72	7.48	5.01	5.04	–	5.01	38.4	47.1	87.1	47.1	Right bank
99	5,031.13	5,023.49	7.64	2.83	–	5.03	2.83	6.9	30.2	51.3	30.2	Right bank
98	5,031.20	5,023.49	7.71	2.14	–	4.10	2.14	3.0	9.5	26.5	9.5	Right bank
97	5,031.23	5,023.49	7.74	0.82	–	3.85	0.82	0.2	8.1	20.7	8.1	Right bank
96	5,031.16	5,023.49	7.67	1.90	–	3.87	1.90	2.9	14.4	20.8	14.4	Right bank
95	5,030.84	5,023.49	7.35	4.42	–	5.52	4.42	31.1	51.6	–	51.6	Right bank
93	5,030.34	5,023.49	6.85	4.83	6.24	–	4.83	35.4	98.8	–	98.8	Right bank
90	5,030.25	5,021.49	8.76	3.19	–	5.07	3.19	9.4	10.6	72.8	10.6	Left bank
86	5,029.43	5,021.49	7.94	5.58	–	9.41	5.58	52.0	417.8	–	417.8	Right bank
85	5,028.90	5,018.24	10.66	7.86	8.01	–	7.86	132.5	147.3	–	147.3	
84	5,028.41	5,017.48	10.93	8.91	9.04	–	8.91	189.8	258.8	–	258.8	
83	5,028.34	5,017.48	10.86	8.88	9.12	–	8.88	188.6	229.4	–	229.4	
82	5,028.31	5,017.48	10.83	8.31	8.57	–	8.31	154.6	185.2	–	185.2	
81	5,027.85	5,019.48	8.37	9.45	–	10.66	9.45	247.3	425.5	–	425.5	Left bank
80	5,028.04	5,019.48	8.56	7.63	7.73	–	7.63	128.9	134.6	–	134.6	
79	5,027.62	5,019.48	8.14	8.69	–	–	8.69	195.0	202.0	–	202.0	
78	5,027.65	5,017.48	10.17	7.15	8.05	–	7.15	112.4	149.8	–	149.8	
77	5,027.36	5,017.48	9.88	7.09	7.41	–	7.09	99.1	112.8	–	112.8	
76	5,027.36	5,017.48	9.88	5.85	7.22	–	5.85	55.5	104.6	–	104.6	
76.5	5,027.39	5,017.48	9.91	5.23	6.67	–	5.23	39.8	82.3	–	82.3	
75	5,027.33	5,015.48	11.85	5.89	6.07	–	5.89	53.5	58.4	–	58.4	
74	5,027.33	5,015.47	11.86	5.68	5.88	–	5.68	51.0	56.5	–	56.5	
73	5,027.46	5,015.48	11.98	3.84	4.52	–	3.84	14.8	25.4	–	25.4	
72	5,027.42	5,017.48	9.94	2.54	4.29	–	2.54	4.5	21.9	–	21.9	
71	5,027.29	5,015.48	11.81	4.19	4.42	–	4.19	19.2	23.1	42.6	23.1	Right bank
70.5	5,026.67	5,017.48	9.19	7.13	7.14	–	7.13	103.3	–	124.8	103.3	Right bank
70	5,025.55	5,017.48	8.07	9.39	9.90	–	9.39	258.8	289.3	–	289.3	
69	5,025.09	5,015.68	9.41	8.77	–	10.37	8.77	237.3	336.9	–	336.9	Right bank
68	5,024.41	5,014.27	10.14	8.55	–	10.79	8.55	170.1	448.8	–	448.8	Left bank
67	5,024.18	5,015.48	8.70	8.08	–	10.09	8.08	152.7	381.9	–	381.9	Left bank
66	5,024.34	5,013.55	10.79	8.50	8.74	–	8.50	180.6	212.2	–	212.2	
65	5,024.41	5,013.15	11.26	8.03	8.10	–	8.03	138.4	139.7	–	139.7	
64	5,024.37	5,014.07	10.30	7.07	7.20	–	7.07	97.1	101.3	–	101.3	
63	5,023.81	5,015.48	8.33	8.09	–	–	8.09	155.7	–	–	155.7	
62	5,023.91	5,015.48	8.43	7.00	7.20	–	7.00	101.0	115.2	–	115.2	
61	5,023.95	5,015.48	8.47	6.28	7.11	–	6.28	72.6	105.4	–	105.4	
60.5	5,024.01	5,015.48	8.53	5.86	6.13	–	5.86	58.7	67.1	–	67.1	
60	5,023.91	5,013.51	10.40	5.58	6.38	–	5.58	49.4	71.3	–	71.3	
59	5,023.75	5,011.48	12.27	6.48	6.49	–	6.48	70.3	87.2	–	87.2	
58	5,023.78	5,011.48	12.30	6.21	–	–	6.21	62.9	–	–	62.9	
57	5,023.85	5,011.64	12.21	4.46	5.70	–	4.46	20.3	50.3	53.3	50.3	Left bank
56	5,023.65	5,013.48	10.17	6.59	6.83	–	6.59	78.9	91.6	–	91.6	

Appendix 4–3. TRIM2D simulation at a flow of 100 cubic meters per second—Continued

[**Abbreviations:** W.S. elev, water-surface elevation; ft, foot; ft/s, foot per second; W/m^2, watt per squared meter]

Cross section	W.S. elev (ft)	Thalweg (ft)	Flow depth (ft)	Velocity (ft/s)				Stream power (W/m^2)				
				Thalweg	Channel	Overbank	Used	Thalweg	Channel	Overbank	Used	Remarks
55	5,023.39	5,013.48	9.91	7.44	–	–	7.44	138.1	–	–	138.1	
54	5,022.73	5,011.71	11.02	10.70	–	12.76	10.70	326.4	–	–	326.4	Right bank
53	5,022.31	5,011.60	10.71	12.71	–	13.69	12.71	558.5	–	–	558.5	Left bank
52.5	5,021.75	5,011.48	10.27	12.14	–	–	12.14	389.9	407.4	–	407.4	
52	5,021.75	5,011.48	10.27	10.03	–	15.52	10.03	327.1	–	1,841.0	327.1	Right bank
51.75	5,021.68	5,011.48	10.20	9.56	11.67	–	9.56	241.1	302.5	1,038.0	302.5	Right bank
51.5	5,021.72	5,011.48	10.24	9.73	10.48	–	9.73	316.0	–	–	316.0	
51.25	5,021.85	5,011.48	10.37	10.57	10.62	–	10.57	323.2	–	–	323.2	
51	5,021.94	5,011.48	10.46	10.63	–	–	10.63	327.7	–	–	327.7	
50.5	5,021.91	5,011.48	10.43	10.78	–	–	10.78	342.1	–	–	342.1	
50	5,021.81	5,011.48	10.33	11.23	11.53	–	11.23	387.8	425.0	–	425.0	
49.5	5,021.81	5,011.54	10.27	10.83	–	–	10.83	351.9	–	–	351.9	
49	5,021.75	5,011.48	10.27	10.36	10.66	–	10.36	307.7	333.9	–	333.9	
48	5,021.85	5,011.48	10.37	10.15	10.19	–	10.15	287.4	291.6	–	291.6	
47	5,021.94	5,011.51	10.43	9.10	9.79	–	9.10	211.3	260.3	–	260.3	
46	5,021.98	5,011.51	10.47	8.61	–	–	8.61	176.5	–	–	176.5	
45	5,022.01	5,011.64	10.37	8.32	–	–	8.32	164.1	–	–	164.1	
44	5,021.91	5,013.48	8.43	6.86	7.21	–	6.86	94.5	110.1	–	110.1	
43	5,021.72	5,011.58	10.14	4.56	–	7.67	4.56	26.8	136.5	149.0	136.5	Right bank
42	5,021.49	5,011.48	10.01	2.54	–	8.26	2.54	9.1	146.7	226.6	146.7	Right bank
41	5,021.55	5,011.48	10.07	5.59	–	8.03	5.59	48.2	115.1	226.9	115.1	Right bank
40	5,020.99	5,011.48	9.51	1.02	–	8.26	1.02	0.3	20.1	201.0	20.1	Left bank
36	5,020.96	5,011.48	9.48	0.94	–	8.36	0.94	0.2	16.7	217.4	16.7	Left bank
35	5,020.99	5,011.48	9.51	0.91	–	8.75	0.91	0.2	40.3	252.4	40.3	Left bank
34	5,020.93	5,010.89	10.04	5.81	–	9.13	5.81	56.0	120.3	299.9	120.3	Left bank
33	5,020.83	5,009.90	10.93	5.35	–	9.15	5.35	41.1	101.6	288.8	101.6	Left bank
32	5,020.93	5,009.48	11.45	4.39	–	8.74	4.39	22.5	88.7	238.4	88.7	Left bank
31	5,020.67	5,009.48	11.19	3.33	–	6.38	3.33	9.9	54.9	75.8	54.9	Right bank
30	5,020.14	5,010.69	9.45	5.48	–	7.48	5.48	50.1	114.9	–	114.9	Right bank
29	5,020.21	5,011.18	9.03	6.34	7.49	–	6.34	72.1	121.7	–	121.7	
28	5,019.98	5,011.48	8.50	6.21	–	7.95	6.21	69.8	97.8	146.0	97.8	Right bank
26	5,019.58	5,011.48	8.10	7.97	–	8.57	7.97	154.1	173.5	187.0	173.5	Right bank
23	5,019.02	5,010.30	8.72	6.69	–	8.57	6.69	102.2	181.7	–	181.7	Right bank
20	5,018.70	5,009.48	9.22	2.50	–	7.98	2.50	7.9	139.2	144.7	139.2	Right bank
13	5,018.30	5,011.50	6.80	3.67	–	8.25	3.67	20.7	109.5	189.4	109.5	Right bank
8	5,018.04	5,007.48	10.56	4.10	–	6.77	4.10	33.2	43.8	103.9	43.8	Right bank
3	5,016.10	5,007.57	8.53	5.30	–	11.41	5.30	68.8	367.6	484.3	367.6	Right bank
1	5,013.02	5,005.90	7.12	2.66	–	23.59	2.66	38.4	–	4,141.2	38.4	Right bank

Calculation of TRIM2D inflow into model reach (upstream of HEC-RAS model reach)

Simulated Q = 100 m^3/s)

Variables
- v1 = x coordinate in meters
- v2 = y coordinate in meters
- v3 = Z
- v4 = eta
- v5 = u
- v6 = v
- v7 = H in meters
- p = Power W/m^2
- z = land-surface elevation in feet
- eta = water-surface elevation in feet
- distance= distance across the section

										Distance	
v1	v2	v3	v4	v5	v6	v7	p	z	eta	(m)	(ft)
511.4702	286.4551	16.76	16.75045	0.018004	-0.000228	0	0.000208	5045.987	5045.956	0	0
512.4077	286.4551	16.69681	16.62902	0.022545	0	0	0.00035	5045.779	5045.557	1.875095	6.151886
513.4234	286.4551	16.48934	16.43947	0.045106	0.239418	0.080441	1.999636	5045.099	5044.935	3.906448	12.81643
514.5172	286.4212	16.05373	16.4	0.13455	1.043353	0.647896	26.21276	5043.67	5044.806	6.09511	19.99708
515.5329	286.4551	15.28002	16.39467	0.215758	1.671069	1.595308	59.34823	5041.131	5044.788	8.127595	26.66534
516.4704	286.4551	14.40399	16.39	0.237214	2.011067	2.348394	89.96438	5038.257	5044.773	10.00269	32.81722
517.6423	286.4551	13.7969	16.38358	0.239038	2.333467	2.67	132.428	5036.265	5044.752	12.34656	40.50708
518.5018	286.4551	13.72	16.38	0.239054	2.426898	2.664983	148.2068	5036.013	5044.74	14.0654	46.14631
519.5174	286.4551	13.72	16.37772	0.235516	2.41587	2.66	146.2806	5036.013	5044.733	16.09675	52.81085
520.6894	286.4551	13.72	16.37545	0.229295	2.29332	2.66	125.43	5036.013	5044.725	18.44062	60.50071
521.5488	286.4551	13.72	16.37226	0.221469	2.164889	2.657705	105.8115	5036.013	5044.715	20.15945	66.13994
522.5645	286.4551	13.72	16.37	0.210522	1.973558	2.655449	80.66249	5036.013	5044.708	22.19081	72.80448
523.502	286.4551	13.72274	16.37	0.199754	1.702833	2.655449	53.2092	5036.022	5044.708	24.0659	78.95637
524.4396	286.4551	13.81116	16.37	0.181513	1.353796	2.642262	27.65988	5036.312	5044.708	25.941	85.10826
525.6115	286.4551	14.1708	16.37	0.138915	0.965811	2.408734	10.32994	5037.492	5044.708	28.28487	92.79812
526.549	286.4551	14.84374	16.37	0.087012	0.753209	1.95302	5.160195	5039.7	5044.708	30.15996	98.95
527.4085	286.4551	15.72286	16.37	0.038812	0.416177	1.211738	2.1002	5042.584	5044.708	31.8788	104.5892
528.6585	286.4551	16.82465	16.69058	0.003586	0.019635	0.177569	0.004607	5046.199	5045.759	34.37892	112.7917
529.5961	286.4212	17.06936	16.87953	0	0	0	0	5047.002	5046.379	36.25525	118.9477
530.5336	286.4551	16.93272	16.82425	0	0	0	0	5046.554	5046.198	38.13157	125.1036
531.393	286.4551	16.82465	16.78376	0	0	0	0	5046.199	5046.065	39.8504	130.7428

Resultant velocity

(m/s)	(ft/s)	Depth (ft)	Area (ft^2)	Qi (ft^3/s)
0	0	0	0	0
0	0	0	0	0
0	0	0	0	0
1.051993	3.45142	1.135869	4.078137	7.037683
1.68494	5.528018	3.656923	15.97978	71.74474
2.025009	6.64373	6.515812	40.08453	243.9494
2.345678	7.695795	8.486485	65.25986	467.8977
2.438643	8.000798	8.727051	48.53554	380.9213
2.427323	7.963657	8.719606	58.18662	464.4588
2.304755	7.561532	8.712161	67.02391	520.2794
2.176188	7.139724	8.701717	49.15932	361.3519
1.984755	6.511662	8.694336	58.01756	396.0101
1.714509	5.62503	8.685357	53.51418	324.7426
1.36591	4.481333	8.395348	54.32338	274.5059
0.97575	3.201279	7.215447	69.09567	265.4176
0.758219	2.487594	5.007543	37.59722	106.9429
0.417983	1.371334	2.123261	8.132564	15.69149
0	0	0	0	0
0	0	0	0	0
0	0	0	0	0
0	0	0	0	0

Calculated Q = 3901.0 ft^3/s

Calculated Q = 110.5 m^3/s

Simulated Q = 100 m^3/s

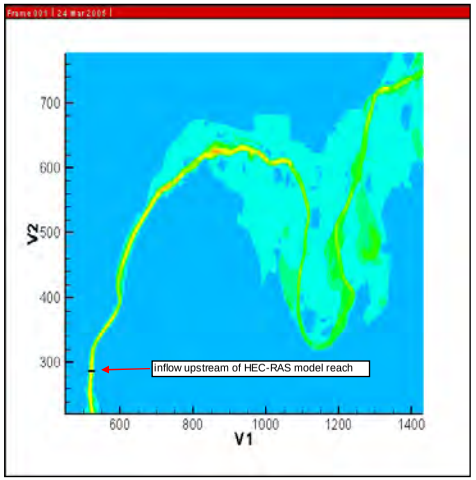

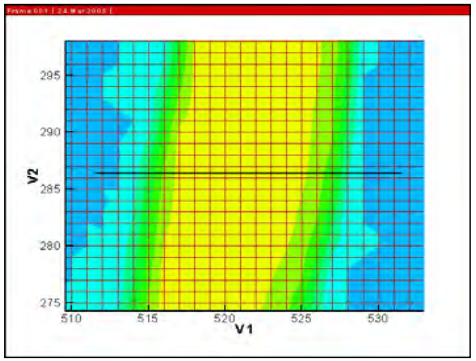

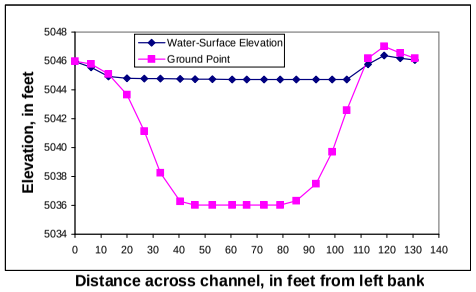

Distance across channel, in feet from left bank

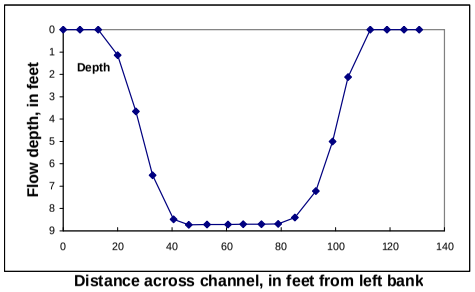

Distance across channel, in feet from left bank

Calculation of TRIM2D flow—middle of model reach (near cross section 80)

Simulated Q = 100 m^3/s

Variables
- v1 = x coordinate in meters
- v2 = y corrdinate in meters
- v3 = Z
- v4 = eta
- v5 = u
- v6 = v
- v7 = H in meters
- p = Power W/m^2
- z = land-surface elevation in feet
- eta = water-surface elevation in feet

distance= distance across the section

										Distance	
v1	v2	v3	v4	v5	v6	v7	p	z	eta	(m)	(ft)
1530.547	681.6219	11.089	10.99486	0	0	0	0	5027.381	5027.072	0	0
1530.572	680.6237	10.87899	10.7577	0	0	0	0	5026.692	5026.294	2.242113	7.356014
1530.547	679.5008	10.60095	10.4546	0	0	0	0	5025.78	5025.3	4.226937	13.8679
1530.572	678.565	10.30723	10.27101	0.480899	0.015113	0.13705	12.28244	5024.816	5024.698	5.975453	19.6045
1530.547	677.4421	9.881496	10.22907	1.657691	0.053287	0.56652	92.07049	5023.42	5024.56	8.20838	26.93038
1530.521	676.5063	9.472222	10.23212	2.254965	0.063444	0.984821	165.152	5022.077	5024.57	9.956896	32.66698
1530.547	675.321	8.936058	10.23746	2.55312	0.06108	1.550563	204.6111	5020.318	5024.587	12.19901	40.02299
1530.547	674.51	8.521597	10.23907	2.707104	0.036609	2.010474	223.5495	5018.958	5024.593	13.94752	45.75959
1530.521	673.5118	7.97755	10.23958	2.889425	-0.01744	2.467123	253.4349	5017.173	5024.594	15.93235	52.27148
1530.521	672.4513	7.656103	10.23958	3.010137	-0.06149	2.619584	280.5051	5016.118	5024.594	17.91717	58.78337
1530.521	671.5155	7.62	10.23958	3.014464	-0.08458	2.619584	281.84	5016	5024.594	20.15929	66.13939
1530.521	670.3926	7.62	10.23958	2.931194	-0.1118	2.619584	259.5844	5016	5024.594	22.14411	72.65128
1530.521	669.3944	7.62282	10.23958	2.741389	-0.13481	2.619584	213.7015	5016.009	5024.594	24.12893	79.16317
1530.495	668.3963	7.83676	10.2401	2.379577	-0.13841	2.601689	142.8296	5016.711	5024.596	26.11376	85.67506
1530.469	667.4605	8.360832	10.24061	1.840288	-0.10865	2.223052	73.36879	5018.431	5024.598	28.10891	92.22083
1530.495	666.4623	9.069747	10.2401	1.385882	-0.04137	1.530253	33.39891	5020.757	5024.596	30.34184	99.54671
1530.521	665.4641	9.745418	10.23958	1.185995	0.009009	0.81213	26.10439	5022.973	5024.594	32.09035	105.2833
1530.521	664.5284	10.2075	10.24194	0.591862	0.008833	0.256316	13.4717	5024.489	5024.602	34.08551	111.8291
1530.495	663.5302	10.5001	10.38129	0	-0.00189	0.005401	2.82E-06	5025.449	5025.059	36.31843	119.155
1530.469	662.532	10.68947	10.61179	0	0	0	0	5026.07	5025.816	38.30326	125.6669
1530.469	661.5963	10.81134	10.74805	0	0	0	0	5026.47	5026.263	39.79187	130.5508
1530.469	660.5357	10.93032	10.87032	0	0	0	0	5026.861	5026.664	42.0248	137.8766

Resultant velocity				
(m/s)	(ft/s)	Depth (ft)	Area (ft^2)	Qi (ft^3/s)
0	0	0	0	0
0	0	0	0	0
0	0	0	0	0
0	0	0	0	0
1.658547	5.441428	1.140392	4.177185	11.36493
2.255857	7.401105	2.493192	10.42221	66.9238
2.553851	8.378775	4.269789	24.87429	196.2567
2.707352	8.882389	5.634856	28.40949	245.1905
2.889478	9.479915	7.42138	42.51038	390.2943
3.010765	9.877838	8.475901	51.76067	500.9851
3.01565	9.893866	8.594342	62.78447	620.678
2.933326	9.623771	8.594342	55.9654	546.1562
2.744702	9.004928	8.585117	55.99544	521.5611
2.383599	7.820208	7.884834	58.18541	489.4887
1.843493	6.048205	6.167106	57.23429	396.8744
1.386499	4.548881	3.839516	53.70527	284.5597
1.186029	3.891171	1.621096	6.363094	26.85242
0	0	0	0	0
0	0	0	0	0
0	0	0	0	0
0	0	0	0	0
0	0	0	0	0

Calculated Q = 4297.2 ft^3/s

Calculated Q = 121.7 m^3/s

Simulated Q = 100 m^3/s

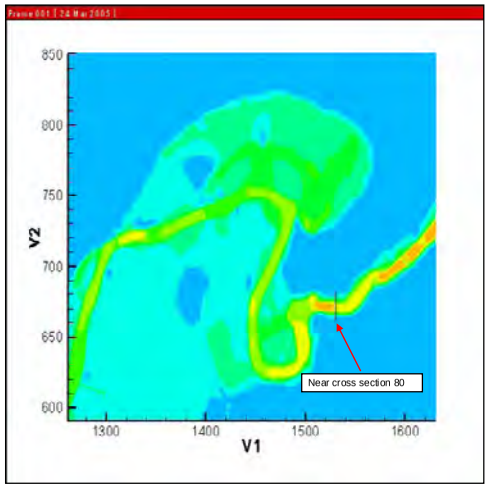

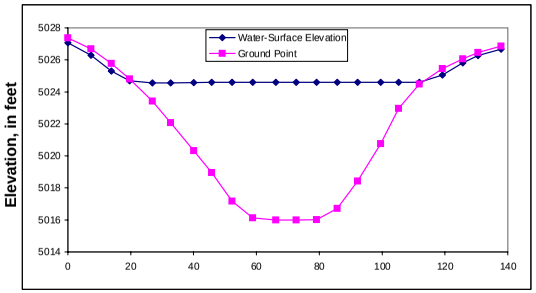

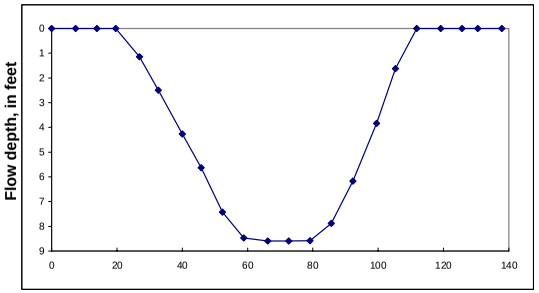

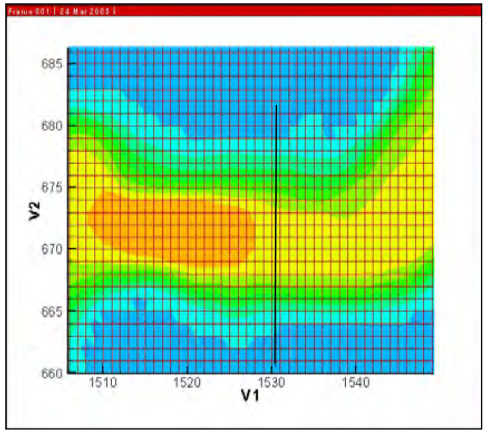

Calculation of TRIM2D outflow (near cross section 23)

Simulated Q = 100 m^3/s

Variables
- v1 = x coordinate in meters
- v2 = y corrdinate in meters
- v3 = Z
- v4 = eta
- v5 = u
- v6 = v
- v7 = H in meters
- p = Power W/m^2
- z = land-surface elevation in feet
- eta = water-surface elevation in feet
- distance= distance across the section

v1	v2	v3	v4	v5	v6	v7	p	z	eta	Distance (m)	Distance (ft)
2221.593	1038.478	8.23	8.23	0	0	0	0	5018.001	5018.001	0	0
2221.492	1037.362	8.23	8.23	0	0	0	0	5018.001	5018.001	2.242113	7.356014
2221.492	1036.369	8.23	8.23	0	0	0	0	5018.001	5018.001	4.226937	13.8679
2221.593	1035.501	8.23	8.23	0	0	0	0	5018.001	5018.001	5.975453	19.6045
2221.593	1034.384	8.172436	8.065903	0	0	0	0	5017.813	5017.463	8.20838	26.93038
2221.492	1033.516	7.946122	7.727882	0	0	-0.02662	0	5017.07	5016.354	9.956896	32.66698
2221.593	1032.399	7.483761	7.457913	0.627909	-0.03954	0.191941	15.2552	5015.553	5015.468	12.19901	40.02299
2221.492	1031.531	7.089612	7.449605	1.428496	-0.087	0.595841	56.36017	5014.26	5015.441	13.94752	45.75959
2221.492	1030.539	6.556287	7.457222	2.015771	-0.11247	1.241667	111.873	5012.51	5015.466	15.93235	52.27148
2221.492	1029.546	5.862433	7.46	2.446219	-0.07258	1.946273	168.2894	5010.234	5015.475	17.91717	58.78337
2221.39	1028.43	5.286687	7.463751	2.728532	-0.04032	2.28	219.2011	5008.345	5015.487	20.15929	66.13939
2221.39	1027.437	5.18	7.462423	2.824468	-0.06925	2.28	242.89	5007.995	5015.483	22.14411	72.65128
2221.39	1026.445	5.172196	7.46	2.867292	-0.10175	2.295608	253.6663	5007.969	5015.475	24.12893	79.16317
2221.39	1025.453	5.132739	7.46	2.829389	-0.10263	2.361244	241.8677	5007.84	5015.475	26.11376	85.67506
2221.492	1024.46	5.108664	7.462615	2.684148	-0.0918	2.403132	205.7177	5007.761	5015.484	28.10891	92.22083
2221.492	1023.344	5.376297	7.471479	2.452614	-0.09352	2.330764	158.8329	5008.639	5015.513	30.34184	99.54671
2221.39	1022.475	5.65861	7.4811	2.276483	-0.08876	1.983002	133.8724	5009.565	5015.544	32.09035	105.2833
2221.492	1021.483	5.802843	7.502843	1.993507	-0.08154	1.710173	96.49072	5010.038	5015.616	34.08551	111.8291
2221.492	1020.366	5.941625	7.521251	1.54129	-0.09016	1.682156	46.21441	5010.493	5015.676	36.31843	119.155
2221.492	1019.374	6.187307	7.524916	1.281187	-0.08481	1.481518	26.50743	5011.3	5015.688	38.30326	125.6669
2221.492	1018.63	6.379032	7.523065	1.180978	-0.06773	1.271241	21.7365	5011.929	5015.682	39.79187	130.5508
2221.492	1017.513	6.63255	7.52	1.071838	-0.02489	0.992534	17.58768	5012.76	5015.672	42.0248	137.8766
2221.492	1016.521	6.833769	7.512813	0.736127	-0.00611	0.779336	8.985763	5013.421	5015.648	44.00963	144.3885
2221.39	1015.528	7.02732	7.503902	0.071074	-0.00436	0.567151	1.049939	5014.055	5015.619	46.00478	150.9343
2221.39	1014.536	7.201315	7.503902	-0.35598	0.01703	0.387227	0.980474	5014.626	5015.619	47.9896	157.4462
2221.39	1013.544	7.367412	7.506515	-0.33085	0.041048	0.224539	0.957161	5015.171	5015.628	49.97443	163.9581
2221.39	1012.551	7.534588	7.522099	-0.14842	0.020917	0.07395	0.315316	5015.72	5015.679	51.95925	170.47
2221.492	1011.311	7.742434	7.652434	0	0.000466	0	4.26E-08	5016.402	5016.106	54.44855	178.637
2221.39	1010.442	7.898673	7.808673	0	0	0	0	5016.914	5016.619	56.19707	184.3736
2221.39	1009.326	8.092895	8.002895	0	0	0	0	5017.551	5017.256	58.42999	191.6995
2221.39	1008.333	8.266036	8.176036	0	0	0	0	5018.12	5017.824	60.41482	198.2113
2221.39	1007.465	8.420674	8.334072	0	0	0	0	5018.627	5018.343	62.15154	203.9092
2221.39	1006.473	8.60263	8.515406	0	0	0	0	5019.224	5018.938	64.13636	210.4211

Resultant velocity (m/s)	(ft/s)	Depth (ft)	Area (ft^2)	Qi (ft^3/s)
0	0	0	0	0
0	0	0	0	0
0	0	0	0	0
0	0	0	0	0
0	0	0	0	0
0	0	0	0	0
0.629153	2.06415	0	0	0
1.431143	4.69535	1.181236	3.388141	11.45107
2.018906	6.623708	2.955847	13.47012	76.23451
2.447295	8.029184	5.24132	26.68952	195.5393
2.72883	8.952854	7.142646	45.54831	386.7516
2.825317	9.269414	7.488395	47.63786	434.0349
2.869097	9.413047	7.506096	48.82123	456.0504
2.83125	9.288878	7.635541	49.30033	461.0056
2.685718	8.81141	7.722998	50.26678	454.9216
2.454396	8.052481	6.87392	53.4676	450.8359
2.278213	7.474452	5.979224	36.86668	286.2132
1.995174	6.545846	5.577397	37.82353	265.1486
1.543925	5.065371	5.18251	39.41287	228.8157
1.283992	4.212571	4.388443	25.99162	120.5744
1.182918	3.880966	3.753341	16.78011	67.90524
1.072127	3.517476	2.911488	18.24554	67.49428
0.736152	2.415198	2.227855	12.28168	36.4316
0.071207	0.233618	1.563771	8.062626	10.67821
0.356384	1.169239	0.992839	4.606337	3.231016
0.333384	1.093779	0.456453	1.225927	1.387148
0.149884	0.491746	0	0	0
0.000466	0.001529	0	0	0
0	0	0	0	0
0	0	0	0	0
0	0	0	0	0
0	0	0	0	0
0	0	0	0	0

Calculated Q = 4014.7 ft^3/s

Calculated Q = 113.7 m^3/s

Simulated Q = 100 m^3/s

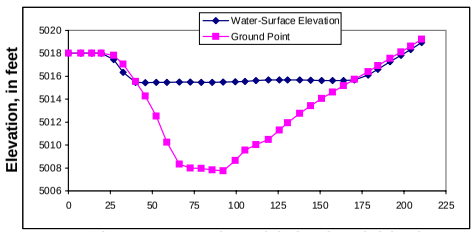

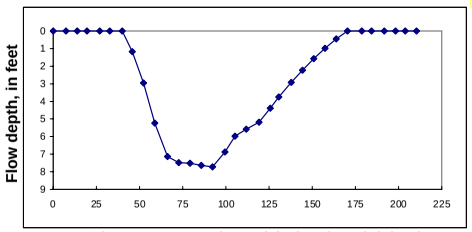

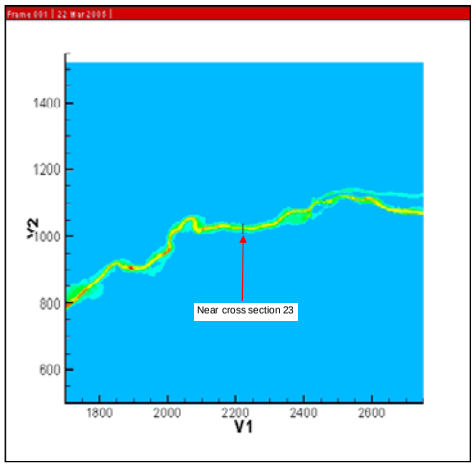

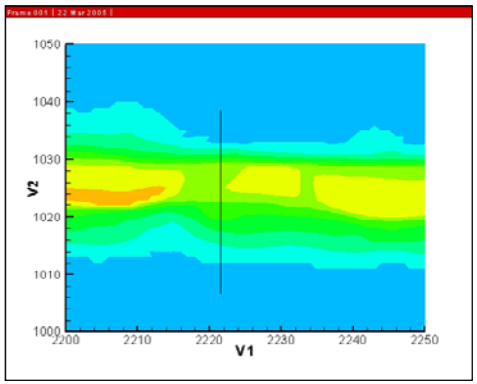

Manuscript approved for publication, May 2, 2007
Prepared by the USGS Publishing Network
Robert Crist
Linda Rogers
Sharon Wahlstrom
For more information concerning the research in this report, contact the
Director, Idaho Water Science Center
230 Collins Road
Boise, Idaho 83702-4520
http://id.water.usgs.gov